Cellular and Molecular Characterisation of Novel Lipopeptides with Anti-Myeloma Activities

Dissertation

zur Erlangung des Doktorgrades
der Fakultät für Chemie und Pharmazie
der Ludwig-Maximilians-Universität München

Amparo Hausherr-Bohn

Wiesbaden
2009

Erklärung

Diese Dissertation wurde im Sinne von §13 Abs.4 der Promotionsordnung vom 29. Januar 1998 von PD Dr. Haralabos Zorbas betreut.

Ehrenwörtliche Versicherung

Diese Dissertation wurde selbständig, ohne unerlaubte Hilfe erarbeitet.

München,

Amparo Hausherr-Bohn

Dissertation eingereicht:	16.07.2009
Tag der mündlichen Prüfung:	24.08.2009
1. Gutachter:	Prof. Dr. Michael Hallek
2. Gutachter:	PD Dr. Haralabos Zorbas

Acknowledgments

Die vorliegende Arbeit entstand in den Jahren 2003 bis 2007 während meiner Tätigkeit als wissenschaftliche Mitarbeiterin der LMU München, des Universitätsklinikums zu Köln und seit 2006 als Stipendiatin der Deutschen José Carreras Stiftung am Hämatologikum des Helmholtz Zentrums München.

Mein besonderer Dank gilt Herrn Prof. Dr. Michael Hallek für die Förderung der Arbeit und sein Vertrauen in mich, diese Arbeit auch nach dem Umzug der Arbeitsgruppe nach Köln selbständig in München abzuschließen. Herrn Prof. Dr. Haralabos Zorbas danke ich für die Vertretung der Arbeit vor der Fakultät für Chemie und Pharmazie. Bei Herrn Dr. Günter Krause bedanke ich mich für die Betreuung der Arbeit und besonders für die große wissenschaftliche Freiheit, die er mir in meiner Arbeit gelassen hat. Besonderer Dank gilt auch Frau PD. Dr. Irmela Jeremias für die herzliche Aufnahme in Ihr Team und die großzügige Bereitstellung der notwendigen Laborinfrastruktur zur Fertigstellung der Arbeit.

Allen Mitglieder der *AGV-Apoptose* danke ich für die sehr angenehme Arbeitsatmosphäre als Teil dieser kleinen, feinen Forscherfamilie hatte ich sehr viel Spaß. Bei Michaela Grunert, Sibylle Gündisch, Ines Höfig, Liliana Mura, Katja Schneider, Dr. Nadia Terziyska, Agniezka Toloczko und Frau Dr. Michaela Patz, möchte ich mich für die wissenschaftliche und persönliche Unterstützung bedanken. Bei Frau Dr. Rosario Tavares-Krause möchte ich mich für die praktischen Arbeiten zu diesem Projekt und Ihr anhaltende moralische Unterstützung im Hintergrund bedanken. Den Mitglieder der ehemaligen *KKG-Gentherapie*, des *Labors für präklinische Arzneimitteltestung* und der *KKG-Leukämie* danke ich die gute Zusammenarbeit und Hilfsbereitschaft.

Meinem Mann Marc danke ich dafür, dass er immer für mich da ist und mir besonders in der Endphase der Arbeit und bei der Vorbereitung auf die Prüfung den Rücken freigehalten hat. Unserem Sohn Leopold danke ich dafür, dass er die Wochen mit einer gestressten Mama gut überstanden hat. Meinen Eltern danke ich dafür, dass Sie mir das Studium ermöglicht haben. Besonders meiner Mutter danke ich dafür, dass Sie immer an mich geglaubt und mich unterstützt hat.

München, 2009

Amparo Hausherr-Bohn

Contents

1. Introduction

1.1. Protein kinases

1.1.1. Protein phosporylation and protein kinases

During evolution, cells acquired diverse and complex systems to continuously sense changes occurring in their environment. Protein phosphorylation is one of the major posttranslational modifications to regulate the function and activity of proteins. The interplay between protein kinases and protein phosphatases regulates major aspects of cellular processes in eukaryots e.g. proliferation, cell cycle progression, metabolism, transcription, cell movement, differentiation and apoptosis. Kinases play an essential role in many kinds of signal transduction processes. They are involved in the transmission of signals from the outside to the inside of the cell. Inside the cell, kinase cascades lead to activation and inactivation of proteins. Eventually, as a response to the external stimulus, the cascade results in changes in gene expression. In multicellular organisms, kinases are essential for intercellular communication during development, in the function of the immune and the nervous system, in physiolocial responses as well as in homeostasis [229; 278]. The phenomenon of protein phosphorylation was discovered a century ago [207]. Kinases catalyze the addition of the γ-phosphate group of adenosine tri-phosphate (ATP) to the hydroxyl groups of the amino acids tyrosine, serine and threonine in substrate proteins. Regarding substrate specificity, kinases can be divided in Ser/Thr specific kinases, in Tyr specific kinases and in dual specific kinases. Burnett and Co-workers were among the first to describe protein kinase activities in extracts from rat liver mitochondria [36].

1.1.2. Protein tyrosine kinases

The human kinome consists of 518 Kinases. Protein kinases are one of the largest gene families in the eukaryotic genome, they comprise 1.7 % of the human genome [229; 230]. Approximately 100 belong to the group of protein tyrosine kinases

(PTKs). Because tyrosine kinases are found exclusively in metazoans, it is suggested that they evolved to regulate multicellular development and communication. Genetic alterations which perturb the tight regulation of PTK activity result in deregulation of kinase activity and can lead to malignant transformation. They are one large group among the known dominant oncogenes [22]. PTKs can roughly be divided into receptor tyrosine kinases (RTKs) and non-RTKs. To manage the complex functional requirements, the activity of PTKs is tightly regulated. In RTKs, the intrinsic kinase activity of the receptor is activated by binding of an external ligand. Ligand-induced receptor dimerisation and autophosphorylation of the receptor subsequently lead to recruitment and/or activation of key regulatory proteins which are part of a signal transduction cascade to the plasmamembrane. While RTK activation is controlled by ligand binding, the activation and substrate specificity of non-RTKs is regulated by the non-catalytic domains of the proteins which are involved in sophisticated mechanisms of intra- and intermolecular interactions accompanied by protein tyrosine phosphorylation. The intracellular signals generated from RTKs and non-RTKs have a wide spectrum of functions including regulation of proliferation, differentiation, promotion of cell survival and modulation of cellular metabolism [22].

1.2. Src family kinases (SFKs)

Src-Family-Kinases (SFKs) belong to the 32 non-RTKs discovered in the human genome which can be divided into 10 different families [22; 302]. A century ago Peyton Rous found that injection of cell free extracts from chicken sarcomas into healthy animals could cause sarcomas in chicken. He described this as a "transmissable avian neoplasm". The origin for these chicken sarcomas turned out to be the first described oncogenic virus, the Rous sarcoma virus (RSV), [311]. Rous received the Nobel price in 1966 for his work on oncogenic viruses. In the 1970s a 60 kDAa protein from RSV was identified to be responsible for the development of sarcomas in chicken: v-Src [33; 55; 125; 208; 233]. At the same time it was proven that the viral gene has a normal cellular counterpart: c-Src. Thus c-Src was the first cellular homolog of a viral oncoprotein [57; 65; 179; 266; 363] and it was the first protein tyrosine kinase [56; 85; 156; 157; 208; 209]. The major differences between c-Src and v-Src turned out to be a truncation at the C-terminus of v-Src, which is responsible for the transforming potential of v-Src and some point mutations [338]. Since that time SFKs have been implicated in a variety of cancers [7; 95; 399].

1.2.1. Structure and activation of SFKs

1.2.1.1. Structure of SFKs

The domain organisation of SFKs shares a common concept. It consists of a myristoylated and or palmitoylated N-terminus, followed by a unique, non-conserved region, the Src homology 3 (SH3) and Src homology 2 (SH2) domains, a catalytic domain (SH1) and a short C-terminal tail [32; 373] and (Figure 1.1a). The SH2 and SH3 domains are the major protein-protein interaction domains of SFKs [276]. SH2 and SH3 domains are present in a variety of different proteins involved in signal transduction processes [277]. SH2 domains bind to specific sequences in proteins containing phosphotyrosine [8; 84; 248; 390; 391]. SH3 domains bind to sequences that contain a PXXP-motive which forms a type II polyproline helix [235; 417; 418]. Apart from the SH2 and SH3 domains, SFKs contain two important sites of protein-tyrosine-phosphorylation with opposing regulatory effects. Tyr 416[1] is located in the activation loop and its phosphorylation leads to activation of the kinase while the phosphorylation of Tyr 527 at the C-terminal tail, by the C-terminal Src kinase (CSK) [265] or its homologs CSK-homologous kinase (CHKs) [72], lead to inactivation of the enzyme [32; 63; 154; 309].

The differences between the crystal structures of the inactive SFKs, Hck (Hematopoetic cell kinase) [345] or c-Src [408] and of the active kinase domain of Lck [410], demonstrate the tight structural regulation of the kinase activity. In the inactive enzyme, the SH2 domain is sequestered in an intramolecular interaction with the phosphorylated Tyr 527 at the C-terminal tail. In this closed conformation the linker region between SH2- and kinase domain forms a type II polyproline helix which interacts with the SH3 domain and by this sequesters it (Figure 1.1b). In the catalytic inactive molecule the two major protein-protein interaction domains are kept "dormant" by intramolecular interactions [344; 345; 407; 408]. The enzymatic cleft is located between the N-terminal region, the N-lobe and the C-terminal region, the C-lobe of the kinase. Structural analysis using inhibitors that bind in the ATP binding pocket like PP1 (4-Amino-5-(4-methylphenyl)-7-(t-butyl)pyrazolo[3,4-d]- pyrimidine) revealed that the ATP-binding pocket is accessible in the inactive conformation while the substrate binding pocket is blocked by the unphosphorylated activation loop of the kinase, "which occludes the mouth of the catalytic domain" [328] (Figures 1.1 and 1.2). Mutational analysis combined with molecular dynamic (MD) simulations showed that the activity state of the catalytic domain is structurally and functionally coupled to these protein-protein interaction domains and vice versa. Structural changes which are induced by dephosphorylation of Tyr 527 or intermolecular ligation of SH3 and SH2 domain

[1] The chicken Src numbering is used within this thesis.

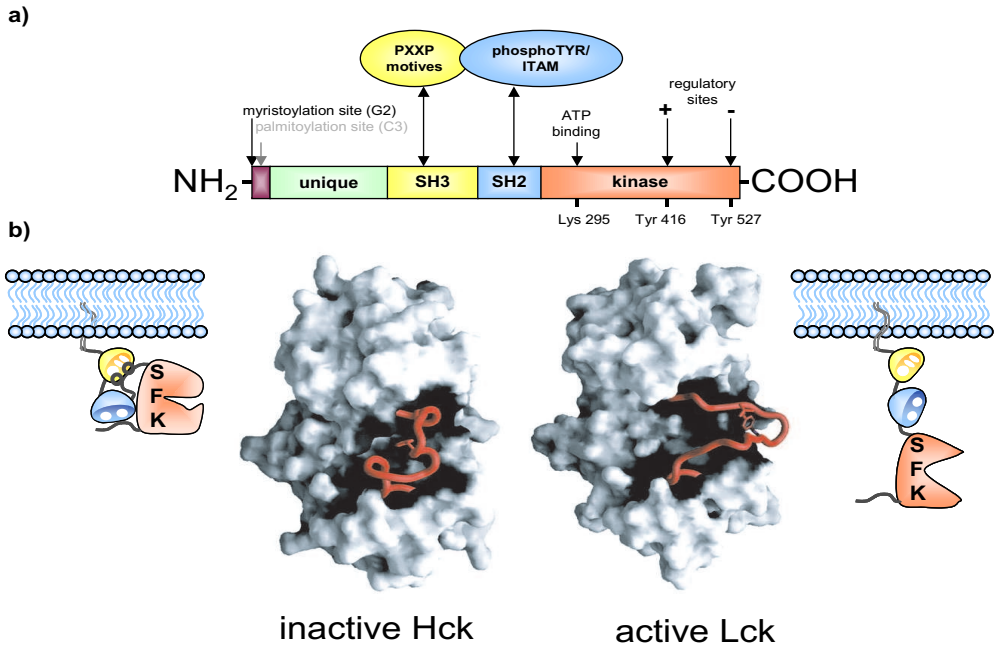

Figure 1.1. | **Schematic Structure of SFKs.** a.) Modular structure of SFKs. b.) Schematic representation of the inactive (left) or active enzyme (right). The catalytic domains of inactive Hck and active Lck with characteristic conformations of the activation loop (middle) The molecular surfaces are represented in grey, the activation loop segment is shown in red. Surface models are taken from [286; 328].

interacting proteins are transmitted to the inactive catalytic domain (CD) leading to a higher probability of conformational changes, which allow peptide substrate entry and catalysis. In a concerted reaction these changes lead to (1) opening of the activation loop, (2) inward movement of the αC-Helix, (3) reorientation of N- and C-lobes and (4) autophosphorylation of Tyr 416 [155; 241; 328].

The key structural changes in the catalytic domain during activation The conversion of an inactive kinase to an active kinase results from conformational changes in the regulatory domains. In the catalytic domain these changes lead to (1) the proper assembly of substrate binding and catalytic groups to enable effective catalysis and (2) the relief of sterical constraints to permit access of the substrate to its binding pocket. Two adjacent regions in the center of the kinase domain are important for catalysis and regulation of kinase activity: the catalytic segment and the activation segment. Residues of the catalytic segment are conserved among all kinases. They are crucial for ATP binding and orientation as well as binding of Mg^{2+}-ions (for SFKs). The activation segment is defined as the

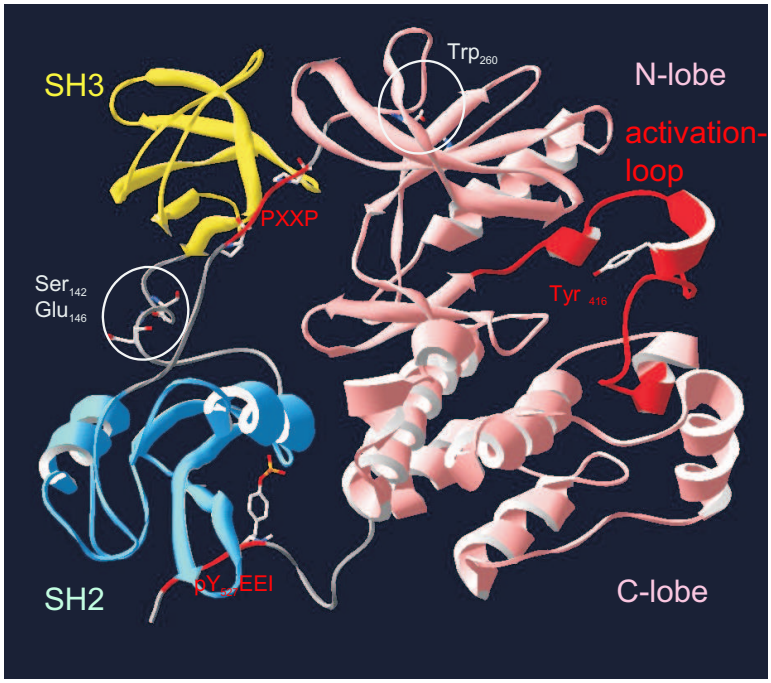

Figure 1.2. | **Ribbon presentation of Hck structure.** Based on PDB code 1QCF [84], generated using Swiss-PdbViewer.

region spanning the conserved sequence DFG and APE, residues 404-432 in c-Src. This sequence is divergent and in many kinases contains one or more phosphorylation sites which control catalytic activity. In c-Src Tyr 416 is located in the activation loop [344].

Comparison of the crystal structures of inactive Hck [345] and active Lck [410] reveals two critical structural differences. In the active enzyme Glu 310 forms a salt bridge with Lys 295 which coordinates the α- and β-phosphates of ATP. In PKA it was shown, that this interaction (Lys 72 and Glu 91) is necessary for efficient catalysis although Glu 91 does not directly participate in catalysis [169]. Glu 310 is part of the αC helix. Both residues as well as the αC helix are highly conserved among Ser/Thr and Tyr kinase. The mutation of Lys 295 to Arg generates kinase-dead mutants of SFKs and other kinases [176; 303]. In the inactive conformation the αC helix is rotated in an outward position and Glu 310 is moved out of the active site into the solvent. In this conformation Glu 310 is incapable to coordinate the phosphate-groups of ATP [345]. At the same time the activation loop forms a compact structure that occludes substrate entry. The outward position of the αC Helix sterically prevents the activation loop to fold out. The conformations of activation loop and αC Helix are structurally coupled. When

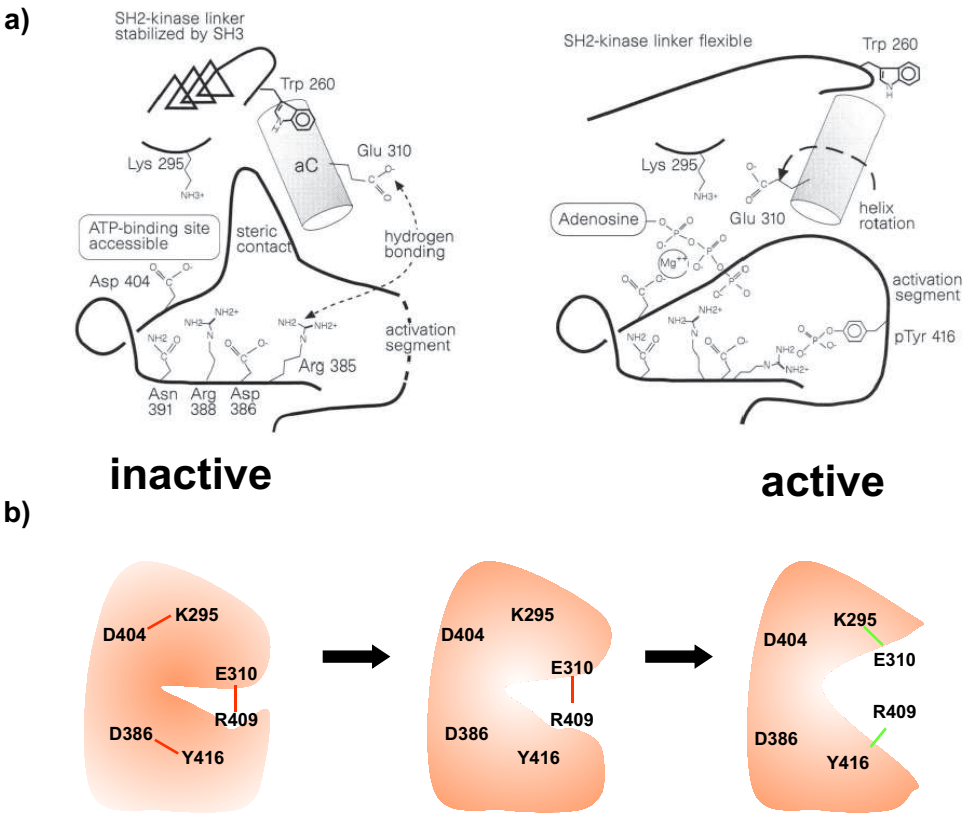

Figure 1.3. | **Electrostatical network changes during the activation cycle of SFK.** a.) Major changes in the activation loop, the SH2-kinase linker and the αC helix during activation of the kinase [345]. b.) A three way electrostatical network changes to a two way network during activation. Modified from [270].

one is in, the other one is out (Figure 1.3a). Based on structural calculations, models for SFK activation were proposed in which the conformational transition is driven by a switched electrostatical network comprising charged residues conserved among kinases. Two models based on the Hck cyrstal structure [344] or on MD simulations for Lyn [270] are largely compatible with each other, but differ by participation of Arg 409 or Arg 385. In the inactive conformation there is a three way network consisting of salt bridges between Asp 404 and Lys 295, Glu 310 and Arg 409 and between Asp 386 and Tyr 416. These interactions change to a two way network during activation. Salt bridges are formed between Lys 295 and Glu 310 as well as Arg 409 and Tyr 416 (Figure 1.3b). Asp 404 is free to coordinate Mg^{2+}-ions and Asp 386 serves as the catalytic base to remove the proton from the protein substrate hydroxyl group [169]. Factors which prevent the inward rotation

of the αC Helix also prevent the formation of the open, activated conformation of the activation loop and by doing so prevent peptide entry and catalysis [328]. Intramolecular binding of the SH3 domain to the SH2-kinase domain linker and SH2 domain binding to the tyrosine-phosphorylated C-terminal tail may be regarded as such factors. For instance, when the SH3 domain is bound to the type II polyprolyl helix, Thr 260 is positioned in a way that inward movement of the αC helix is not possible [246; 345] and (Figure 1.3a). Moreover in the inactive molecule the N- and C-lobes of the kinase domain are closer to each other which can prevent accessibility of Tyr 416 for phosphorylation [407]. The inactive structures of Hck or c-Src resemble the inactive structure of cyclin-dependent-kinase (CDKs), while the active structure of Lck is similar to the active structure of PKA. Interestingly both, PKA and Cdks are Ser/Thr specific kinases [328].

1.2.2. Regulation of SFK activity

Common cellular mechanisms to regulate the activity of SFKs like posttranslational modifications, spatiotemporal organisation, protein-protein interactions as well as cleavage and degradation are described in the following section.

1.2.2.1. Regulation by phosphorylation

The inhibitory tyrosine Tyr 527 is phosphorylated by CSK and its homolog CHK. CSK is ubiquitously expressed in mammalian tissue, whereas the expression of CHK is predominantly in neurons and hematopoetic cells [51; 265]. CSK is structurally related to SFKs. It consists of SH3, SH2 and kinase domains but lacks the myristoylation signal and the two regulatory phosphorylation sites [253]. Embryos from CSK knock out mice (CSK -/-) die between day 9 and 10 with defects in many tissues [160; 253].

The activation loop tyrosine Tyr 416 becomes phosphorylated by autophosphorylation. Intramolecular as well as trans-phosphorylation are described [32]. However, more recent reports suggest that other kinases are also able to phosphorylate Tyr 416 in trans [50].

Several Protein tyrosine phosphatases (PTP) are able to dephosphorylate Tyr 527 of SFK. PTP-α is a receptor like PTP which is ubiquitously expressed. Overexpression of PTP-α leads to dephosphorylation and activation of c-Src, Yes and Fyn in a variety of cell types [21]. Rat embryo fibroblast overexpressing PTP-α exhibit a transformed phenotype. In these cells, PTP-α also dephosphorylated Tyr 416 [423]. Two receptor PTPs CD45 and PTP-γ are able to dephosphorylate SFKs. In

lymphocytes CD45 is required for activation of SFKs. Absence of CD45 raises the steady state level of C-terminally phosphorylated Lck and decreases the cellular response to stimulation of the antigene receptors. There is evidence, that dephosphorylation of the C-terminal tyrosine may be necessary to put the SFKs Lck and Fyn into a signalling competent state. In this "primed" state, they may not be able to transmit a signal unless the antigen receptor is stimulated [32]. The SFK activity seems to be regulated by the opposing actions of CD45 and Cpb/PAG (Csk binding protein/ predominantly associated with glucolipid enriched membranes (GEMs)) associated CSK. Upon stimulation CD45 shuttles into lipid rafts where it dephosphorylates the C-terminal tyrosine in the SFK, leading to the activation of the enzyme. Subsequently the adapter protein Cbp/PAG becomes phosphorylated, allowing association of CSK, which will rephosphorylate the C-terminal tail of the kinase and inactivate it [180; 218; 409]and (Figure 1.4). In the same line of evidence it is described, that the proliferative response of multiple myeloma cells to the cytokine IL-6 dependents on CD45-induced activation of SFKs [165; 166]. Moreover the cytoplasmatic PTP SH2 domain-containing PTPs, SHP-1 and SHP-2, which are primarily expressed in hematopoetic cells can interact with SFKs and dephosphorylate Tyr 527 as well as to a lesser extent Tyr 416 [32].

Phosphorylation of Ser/Thr and Tyr residues in the SH3, SH2 and unique domains of some SFKs was shown to modulate their kinase activity in a particular cellular context. Generally these phosphorylation events are thought to reduce the affinity of SH2 and SH3 domains for their ligands. However, this change can be interpreted either as reduced affinity for intermolecular protein-protein interactions or as preference of the activated state of the kinase [21; 32].

1.2.2.2. Spatiotemporal organisation

Localisation by posttranslational acylation SFKs are associated with both, with the plasma membrane and intracellular membranes [295]. The inactive enzyme is localized in the perinuclear region of the cell, while the active enzyme is present at the plasma membrane [316]. Membrane association is achieved by myristoylation of the N-terminal Gly residues (G2) of all SFKs [38; 212; 281; 295; 346]. During translation the start methionine is removed and myristate is fused to G2 [169]. Besides myritoylation, SFKs, except Src and Blk, posses one or two Cys residues in the vicinity of G2 which can be reversibly palmitoylated. While myristoylation occurs during protein synthesis, palmitoylation is thought to occur at the membrane. Palmitoylation may be a mechanism to relocalize SFKs. For instance less than 30 % of unpalmitoylated Hck molecules are membrane-associated [5; 41]. Moreover palmitoylated SFKs are preferentially localized in glycosphin-

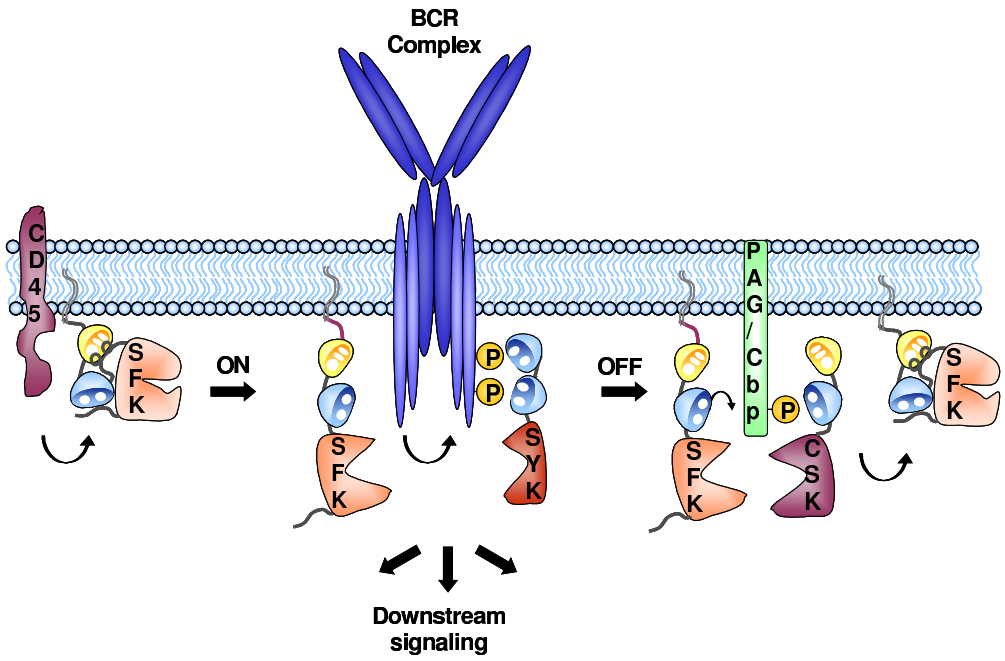

Figure 1.4. | **Model for the activation of SFKs in lymphocytes.** CD45 phosphorylates and activates the kinase. The active SFK phosphorylates target proteins like the BCR complex and induces downstream signalling cascades. Phosphorylation of Cpb/PAG recruits CSK to the membrane, which in turn inactivates the SFK by phosphorylation of Tyr 527.

golipid rich regions of the plasma membrane, so-called caveolae. Many cell surface receptors are known to be associated with caveolae while they are transducing signals [211; 301; 341; 342]. Acylation of SFKs can serve as a mechanism to take the kinases in proximity to their potential substrates [32]. Membrane localisation is essential for the transforming potential of v-Src [175] and for proper signal transduction. However several lines of evidence indicate that some SFKs are also present in the nucleus [219; 373] and that they play a role in cell cycle progression. G1/S transition is blocked by microinjection of antibodies directed against c-Src, Yes and Fyn. Injection during G2-Phase prevents the G2/M transition [305; 306]. Several mitotic substrates, e.g. Sam68, an RNA-binding protein [226] or Trask (transmembrane and associated with src kinases) were discovered recently [18].

Substrate specificity and substrate recognition The specificity of protein tyrosine kinases for tyrosine rather than serine or threonine residues is due to hydrophobic interactions between a conserved proline residue, Pro 425 and the phenylring of the substrate tyrosine [32]. Consensus substrate sequences for tyrosine kinases

were identified in peptide libraries by phosphorylation assays. The libraries consist of chemically synthesised peptides with random residues around the tyrosine, which are reacted with purified kinase preparations in the presence of e.g. radioactively labeled ATP. The peptides are subsequently analyzed for differential tyrosine phosphorylation.

These assays revealed EEI**Y**GEF [355; 357], YI**Y**GSF [200], GI**Y**WHHY [217] or Ac-EDAI**Y** [255] as the consensus substrate sequences for the catalytic domain of SFKs. The preference of SFKs for such selected substrate sequences, however, does not appear to be very strong, since the sequences of the actual phosphorylation sites found in known SFK substrate proteins often considerably differ, e.g. KVEKIGEGT**Y**GVVYK, aa 6-20 in cdc2 [48] or VPSGASTGI**Y**EALELR in rabbit muscle enolase [62]. At the same time the preferred phosphorylation sequences of different PTKs are quite similar [241], so that signalling specificity is not due to substrate selection by the participating kinases but to other mechanisms, e.g. compartmentation and protein-protein interactions.

As described above, structural changes which are induced either by phosphorylation or by intermolecular ligation of SH2 or SH3 domain interacting proteins are transmitted to the inactive molecule and lead to the activation of the enzyme (Figure 1.5). Potential ligands for the SH2 and SH3 domain interactions need to meet several requirements to push the equilibrium of active and inactive conformations towards the active forms. SH2 and SH3 domain need to have a higer affinity for their external ligand than for the the internal interaction regions. A prerequisite for such an mechanism of regulation and activation is that the internal interaction regions must posses sub-optimal binding sequences for their SH2 and SH3 domains to ensure that the enzyme can be activated by intermolecular binding of SH2 and SH3 domain ligands. The SH2 domain binding sequence in the SFK Hck is pYQQQP, while the "optimal" high affinity SH2 domain binding sequence was determined by combinatorial peptide library screening to be pYEEI [356]. The SH3 domain binding sequence of c-Src is PQKP and shows only little similarity with the optimal RXXPXXP sequence [32].

Compared to external interactions of SH2 and SH3 domains with their external ligands, the corresponding intramolecular interactions are energetically favoured by the entropy contribution because the interaction takes place in the same molecule. Consequently the external ligands require higher binding enthalpies and affinities than intramolecular SH2- and SH3-binding sequences to compensate for this entropy factor. This concept is confirmed by comparison of the binding enthalpies of known internal and external SH2 and SH3 ligands.

The observed in vivo specificity of tyrosine kinases is achieved by the intrinsic specificity of the catalytic domain and by the spatial and temporal organization of

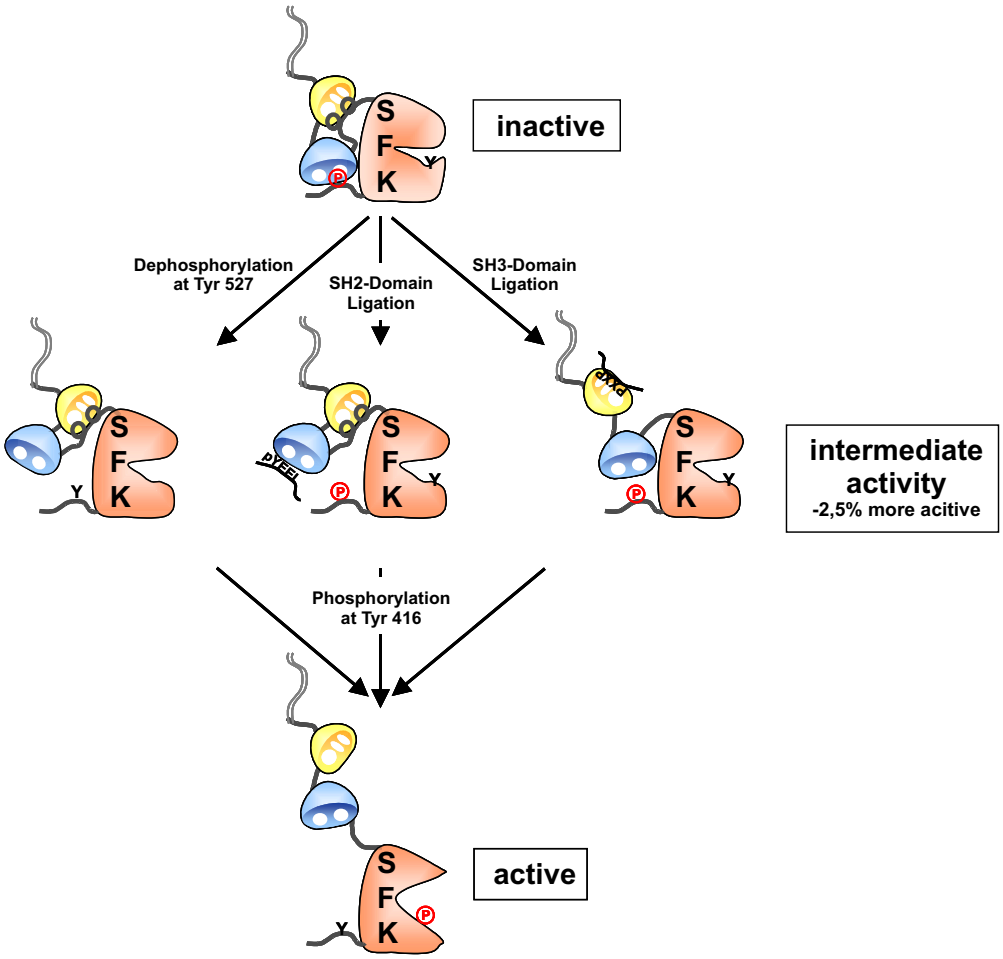

Figure 1.5. | **Different ways to activate SFKs.** Based on [241] and [345].

the kinase signalling pathway. In SFKs the non catalytic SH2 and SH3 domains are responsible for the recognition of cellular substrates, i. e. substitution of the Abl SH2 domain with heterologous SH2 domains results in the phosphorylation of alternative substrates in vivo [234]. Binding of substrates by SH2 and SH3 domains targets SFKs to potential substrates and concomitantly activates the catalytic domain. This mechanism ensures that SFKs are only active when they are in the correct cellular environment [241]. Evidence for such a model emerged from studies of different SFK substrates which possess SH2 or SH3 domain binding sites [4; 115; 279; 286; 372].

1.2.2.3. Regulation by cleavage and degradation

Fyn, Lyn, Hck and Lck are cleaved during Fas-mediated apoptosis in T- and B-cell lines. Caspase 3 cleaves Fyn and Lyn in their N-terminal unique region. The cleaved forms relocalize from the membrane to the cytosol. The activity of the cleaved cytosolic kinase is higher than that of the wild type kinase. It is speculated that SFKs could be involved in a feedback mechanism which blocks apoptotic signals [224; 298].

The E-3 ubiquitin ligase c-Cbl (Casitas B-lineage lymphoma) is involved in degradation of SFKs. C-Cbl is a known interaction partner for SFKs [317; 318]. All SFKs except Blk are supposed to interact with the TKB-domain (Tyrosine Kinase Binding domain) of c-Cbl. The TKB recognizes a motive comprising the activation loop with phosporylated Tyr 416. SFKs which are phosphorylated at Tyr 416 are preferred substrates for ubiquitinylation by c-Cbl and subsequent degradation by the proteasome or lysosome [414]. Because active SFKs are preferentially labeled with ubiquitin for degradation, this is likely to be a mechanism to terminate a specific signal [120; 127]. The overexpression of c-Cbl in v-Src transformed fibroblasts suppresses anchorage-independent growth, specifically reduces the levels of v-Src protein and causes reversion of the morphology of v-Src transformed cells. Moreover Src activates ubiquitin ligase activity of c-Cbl by phosphorylation at Tyr 371 [182]. In addition to the findings with v-Src transformed cells, c-Cbl is also able to suppress Hck-induced cellular transformation [151].

1.2.3. Functions of SFKs

The fate of "new born" cells in multicellular organism is ultimately dependent on the communication of the cell with its environment. Incoming information have to be properly integrated by the cell, leading to an appropriate response. In a still growing number of integration circuits SFKs are involved (Figure 1.6). Constitutively activated SFKs are transforming in tissue culture and transgenic models [116; 172; 400]. V-Src, v-yes and v-fgr are hyperactive viral homologes of their cellular counterparts that lack the negative regulatory Tyrosine Tyr 527 at the C-terminus of the molecule. The viral oncogenes are known to be responsible for the generation of tumors in animals. An elevated expression and activity of SFKs is found in colon cancer, breast cancer, lung cancer, sarcomas and melanomas [7; 42; 95; 164; 269; 308; 399]. In some of the tumors gain-of-function mutations of SFKs are found [163; 231; 364]. Because of the essential role of SFKs in B- and T-cell development (Section 1.2.3.1), SFK dysfunction is thought to be involved in the pathogenesis of different hematopoetic malignancies [191; 399]. Looking

at the growing list of SFKs substrates and interaction partner, SFKs seem to be involved in virtually all important aspects of a cell's lifetime: mitogenesis, proliferation, survival, differentiation, adhesion, migration and apoptosis. Because the deregulation of one or usually more of these processes leads to the development and progression of cancer, SFKs are in the focus of cancer researchers for decades.

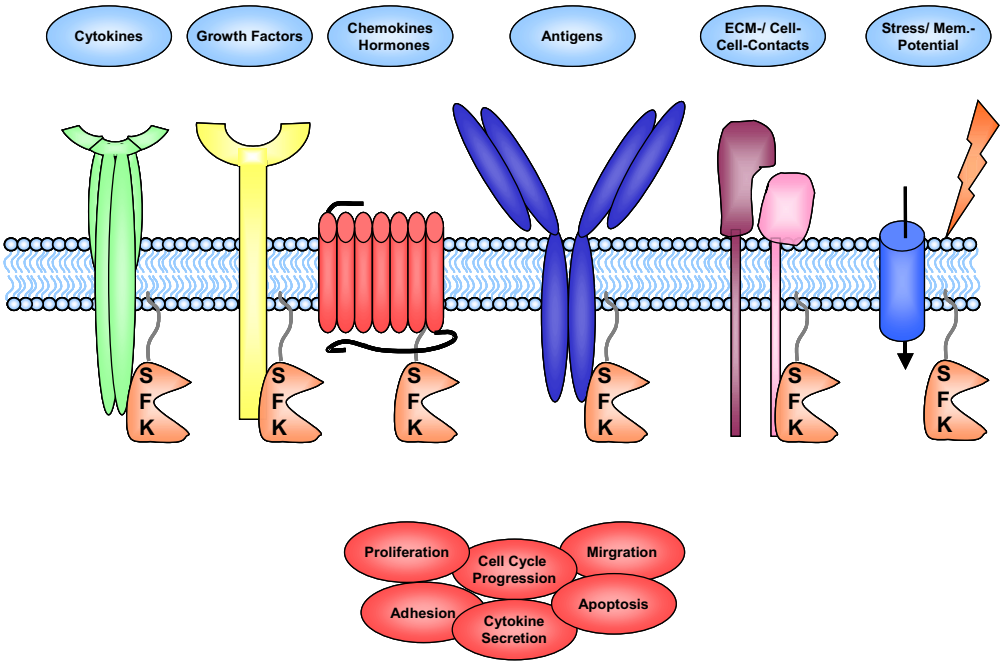

Figure 1.6. | **SFK interaction partners.**

The expression of SFKs The expression pattern of the nine different SFKs can be divided into the ubiquitously expressed kinases c-Src (celluar homolog of Avian sarcoma (Schmidt Ruppin A-2) viral oncogene), c-Yes (cellular homolog of Yamaguchi sarcoma viral oncogene), Fyn (Src/yes related novel gene), Yrk (Yes-related kinase) and the kinases which are predominantly expressed in hematopoetic cells: Blk (B lymphoid tyrosine kinase), Fgr (Feline Gardner Rasheed viral oncogene homolog), Hck, Lck (Lymphocyte specific protein tyrosine kinase) and Lyn (Yamaguchi sarcoma viral (v-yes-1) homolog) [25]. Some SFKs are expressed in different isoforms. Alternative splicing of exon 3 is responsible for the generation of two neuronal specific isoforms of c-Src, with an insertion of six additional amino acids in the SH3 domain. Exon 7 of the Fyn gene, containing the kinase domain, is alternative spliced to give the T-cell specific Fyn(T) form and a second isoform, Fyn(B), is expressed in other tissue, mainly the brain. Alternative splicing results in two coexpressed isoforms of Lyn, one of these isoforms contain 31 additional

amino acids in the unique region. Alternative translation initiation is responsible for the expression of two different isoforms of Hck, the larger isoform possesses 21 amino acids more at the N-terminus of the protein [218; 220].

1.2.3.1. Functions of SFKs in the hematopoetic System

Mature blood cells are generally short-lived and have to be replaced continuously. The development of specialized hematopoetic cells from a population of multi-potential self-renewing hematopoetic stem cells is termed hematopoesis. Hematopoetic stem cells become committed to differentiate along the erythroid, megakaryocytic, granulocytic, monocytic and lymphocytic lineages. This process is achieved through an intricate network of complex and finely tuned regulatory pathways. Hematopoetic cell proliferation and differentiation is controlled by cytokines and growth factors, including interleukins, interferons, colony-stimulation factors and erythropoetin. However, the precise mechanisms which are involved in the regulation of critical events of differentiation commitment and cellular maturation are fields of intensive research [40; 262; 275; 426].

SFKs in T-and B-cell development As shown in (Table 1.1), the knockout of a single SFK shows relative mild phenotypes in contrast to the knock out of CSK which is lethal already at the embryonic stage [254]. These less severe phenotypes can be explain by the fact that usually more than one kinase is expressed in the cells and that these kinases are, with exceptions, functionally redundant [218; 221].

In B-cells, the genetic knockout of the most abundant SFKs Blk, Lyn and Fyn results in a block in B-cell development. The block occurs in the maturation step from pro- to pre-B-cells. There is evidence that in these mice, the pre-BCR-mediated NF-κB activation was abrogated [315]. T-cells derived from mice lacking Lck and Fyn exhibit a block in T-cell development at the pre-TCRβ selection stage [382]. In both B- and T-cell precursors, cells with deleted SFKs fail to transduce signals from functionally rearranged antigen receptors. For the maturation of T-cells, surface expression of a productive chromosomally rearranged TCRβ (T-cell receptor-β) is required to produce a TCR-like signal [271]. In the development of B-cells, the signalling from a rearranged IgH-chain (Immunoglobulin heavy chain) locus is necessary for the transition of the checkpoint [195; 315]. These signals are responsible for the rescue of cells from apoptosis, the induction of differentiation, entry into cell cycle and allelic exclusion. Cells which are unable to signal properly from their pre-TCR or pre-BCR are arrested and die [218; 271].

Kinase	Tissue Expression	Phenotype of Knockout
Src[1,2]	ubiquitous, highest in brain, platelets and osteoclasts	Osteopetrosis
Fyn[1,2,3]	brain isoform: brain, fibroblasts, endothelial cells and keratinocytes; thymocyte form: T-cells and B-cells	abnormal hippocampal development, defect in Thymocyte signalling
Yes[1,2]	ubiquitous, highest in brain, fibroblasts, endothelial cells, T-cells and platelets	normal
Lyn[1,2,3]	brain, B-cells and myeloid cells	impaired B-cell function, autoimmunity
Hck[1,2]	myeloid cells, B-cells	normal
Fgr[1,2]	myeloid cells, B-cells	normal
Blk[1,2]	B-cells	normal
Lck[1,2]	T-cells, NK-cell	partial block in T-cell development, impaired TCR-signalling
Src/Yes[1]		lethal
Hck/Fgr[1,4,5]		compromised host defense
Lck/Fyn[6,7,8,9]		total block in T-cell development
Fyn/Lyn[3]		impaired B-cell function, autoimmunity
Hck/Fgr/Lyn[10]		impaired B-cell function, autoimmunity
Blk/Fyn/Lyn[11]		defect in B-cell development
Src/Yes/Fyn[12]		embryonic lethal, E 9,5

Table 1.1. | **Role of SFKs in differentiation and development.** Based on [64][1]; [220][2]; [150][3]; [219][4]; [221][5]; [112][6]; [271][7]; [381][8]; [382][9];[218][10]; [315][11];[186][12].

Underlying signal transduction pathways The immunoreceptor tyrosine-based activation motive (ITAM)-dependent signalling is used by the family of immunoreceptors such as the T-and B-lymphocyte antigen receptors TCR/CD3 and BCR-, Fcγ- and Fcϵ-receptors, NK (natural killer) cell activating receptors as well as the platelet receptor GPVI (Glycoprotein VI). Immunoreceptors are composed of multiple subunits which are involved in interactions with extracellular ligands and/or coupling with intracellular signaltransduction. The intracellular signal transducing subunit usually contain ITAM motives. Examples for signal transducing subunits containing ITAMs include TCRζ and CD3γ,δ,ϵ in T-cells, Ig-α and -β chains of the BCR in B-cells, the FcRγ chain of Fc receptors in myeloid cells or DAP12 in NK-cells [218].

Ligand binding induces clustering of the immunoreceptors and the regulatory C-terminal tyrosine of SFKs becomes dephosphorylated by the phosphatase CD45. Active SFKs phosphorylate the ITAM motives in the receptor subunits at the D/EXYXXLX(6-8)YXXL sites [296]. Spleen tyrosine kinase (Syk) or 70 kDa zeta-associated protein (Zap-70) are then able to interact via their tandem SH2 domains with the phosphorylated ITAM motives [203] and (Figure 1.4). This interaction leads to activation of these kinases which in turn leads to the phosphorylation and activation of a whole set of adapter molecules e.g. the linker for activation of T-cells (LAT), SH2 domain-containing leukocyte protein of 76 kDa (SLP-76), B-cell linker protein (BLNK) and others. They transduce the signal to activate the rat sarcoma viral oncogene homolog (Ras)-pathway, ras homologue (Rho)-GTPase signalling and lipid second messengers via growth factor receptor-bound protein 2 (Grb2), the guanine nucleotide exchange factor Vav and phospho-inositol-3-kinase (PI3K), respectively. Finally the pathways lead to transcriptional activation of different sets of genes, which has functional consequences e.g. induction of proliferation, cytokine secretion, differentiation, antibody secretion by lymphocytes or phagocytosis/degranulation by myeloid cells [218; 271].

Immunoreceptor tyrosine-based inhibitory motive (ITIM)-dependent signalling-pathways negatively regulate immunoreceptor function as well as cytokine and integrin induced signalling. Examples for surface receptors which contain ITIM motives are CD22, FcγRII, paired Ig-like receptor B (PIR-B) and signal regulatory protein 1-α (SIRP-1α). The consensus sequence of ITIMs is V/IxYXXL/V [348]. Following tyrosine phosphorylation these ITIM containing molecules recruit tyrosine phosphatases like SH2-containing inositol 5-phosphatase (SHIP-1), SHP-1 and SHP-2, which turn of the activation signalling by dephosphorylation of receptors and other signalling intermediate [291].

The phenotype of Lyn -/- mice reveals a role of SFKs in the negative regulation of immunoreceptor signalling. Lyn knock out mice have hyper-responsive B-cells, in-

creased immunoglobuline levels and autoimmunity (immune complex nephritis). In these mice the negative regulation of the ligand-induced immunoreceptor signalling is impaired [139], leading to the conclusion that SFKs are involved in positive and negative regulation of ligand induced immunoreceptor signalling [43; 44; 75]. Apart from participating in immunoreceptor signalling, studies with Lyn-deficient mice reveal a negative regulatory role of Lyn in cytokine-induced signalling in myeloid cells. Myeloid cells derived from Lyn-deficient mice show a hyper proliferative response to stimulation with myeloid growth factors like GM-CSF (Granulocyte-macrophage-colony stimulation factor) and G-CSF (Granulocyte-colony stimulation factor) which results in phenotypes with expanded myeloid cell compartment in contrast to wild-type mice [126]. Because the phenotypes of most single SFK knock-outs are relatively mild, their roles in signalling were suggested to consist in modulation rather than cell fate decisions. In line with this concept, expression of constitutively activated Lyn after genetic knock-in results in a similar phenotype as Lyn deletion [138; 218]. Abolishment of SFK signalling by knock-out of CSK or simultaneous knock-out of several SFKs, however, have much more severe effects on T- and B-cell development, which is completely blocked in CSK-/- mice [373]. Blk / Fyn / Lyn or Lck / Fyn deficiencies block early B- or T- cell development, respectively [112; 315; 382].

1.2.3.2. SFKs in RTK signalling

The family of RTKs is a diverse group of transmembrane receptors with intrinsic kinase activity. The receptor is activated by ligand binding. Ligand-induced receptor dimerisation followed by autophosphorylation of the receptor subsequently leads to the recruitment of key regulatory proteins to the plasmamembrane sometimes concomitantly with their activation. Among those downstream molecules participating in RTK signalling are SFKs [22]. SFKs promote mitogenic signalling from growth factor receptors by (1) inducing signalling pathways involved in DNA synthesis (2) control of receptor turnover, (3) actin cytoskeleton rearrangements and motility and (4) promotion of cellular survival. Conversely, SFKs can activate RTKs [29]. First evidence for the involvement of SFKs in RTK signalling came from studies with quiescent fibroblasts. Their stimulation with platelet derived growth factor (PDGF) led to two to five fold increase of SFK activity [288]. Subsequently SFKs were shown to be involved in signalling from the majority of known RTKs (Table 1.2).

From analyses with the PDGFR it is well established that SFKs interact via their SH2 domains with phosphotyrosine residues of activated RTKs. By association of the SFKs with RTKs, the intramolecular interaction between the SH2 domain and

Receptor	SFK	Reference
PDGFRα/β	Src, Fyn, Yes	[29; 373]
EGFR	Src, Fyn, Yes	[29; 373]
FGFR	Src	[29; 373]
CSF-1R	Src, Fyn, Yes	[29; 373]
NGFR	Src	[29; 373]
HGFR	Src	[29; 373]
IR	Fyn	[29; 373]
Neu (ErbB2)	Src	[373]
MuSK	Src, Fyn	[247]
SCFR/c-kit	Src, Fyn Yes	[29; 205]
Axl/Sky	Src, Fyn Yes	[29; 375]
Ret	Src	[88]
EPHR	Src, Fyn Yes	[87; 187; 425]
Flt3	Hck	[243]

Table 1.2. | **SFKs in receptor tyrosine kinase signalling.**

the C-terminal tail of the SFKs is released and, as described in section 1.2.1.1, the SFKs acquire the catalytically active conformation [6]. However there is evidence for an additional mechanism of SFK activation involving the tyrosine phosphatase SHP-2. In murine fibroblasts, stimulation with epidermal growth factor (EGF), fibroblast growth factor (FGF) or PDGF leads to an activation cycle which has similarities with the activation cycle described in immune cells (Figure 1.4). In fibroblasts SHP-2 takes the role of CD45 in immune cells [422].

Role of SFK in growth factor induced DNA-synthesis Increasing evidence suggest, that SFKs after activation by RTKs positively regulate DNA synthesis by the stabilisation of myc (Avian myelocytomatosis viral oncogene homolog) mRNA which leads to the increased production of the transcription factor Myc. A set of effector-molecules like Vav, Shc, Stat, Abl and Rac are responsible for the transduction of the SFK mediated DNA synthesis. Moreover SFKs were shown

to oppose the negative effects of the tumor suppressor p53 [29]. The well described Ras/Raf/Mek/MAPK-pathway also promotes growth factor induced DNA synthesis, presumably by stabilizing the Myc protein [336; 337].

Upside down signalling Stimulation of the receptors for EGF, PDGF and SCF was shown to lead to SFK activation. SFKs phosphorylate tyrosine residues in the cytoplasmatic tail of the receptors that are not phosphorylated by the intrinsic kinase activity of the receptors [29], e.g. in EGFR Tyr 745 is exclusively phosphorylated by SFKs. Cells transfected with a mutant receptor Y745F display impaired DNA synthesis in response to EGF stimulation compared to cells which were transfected with the wild-type receptor [19; 20; 374].

RTK Turnover is regulated by SFKs RTK signalling is attenuated by endocytosis of the receptors. In SYF cells (c-Src, Yes and Fyn knockout fibroblasts) or cells treated with PP1, the internalization of EGFR is impaired. While in cells that overexpress Src, the internalization of EGFR is increased [398]. The phosphorylation of clathrin as well as dynamin by SFKs is discussed to play an essential role in receptor endocytosis [3; 403]. The surface localisation of RTKs is regulated by ubiquitination [77].

1.2.3.3. SFK in cytokine signalling

Like growth factors, cytokines are essential for the communication between a cell and its extracellular environment. Cytokines bind to their cognate receptors and mediate cellular signal transduction, leading to changes in gene expression. Cytokines are involved in the regulation of cellular proliferation, differentiation, maturation and apoptosis. Structurally, cytokine receptors consist of multiple subunits. The receptors are composed of a unique and specific ligand binding complex and a signal transducing subunit, which can be structurally similar to other members of the cytokine receptor superfamily. As in RTK signalling, tyrosine phosphorylation is induced upon receptor engagement.

In contrast to RTKs the signal transducing subunits of cytokine receptors lack intrinsic tyrosine kinase activity. However, for receptor phosphorylation and induction of downstream signalling non-receptor PTKs like Janus Kinases (JAKs), Syk, Zap-70 and SFKs have been shown to be involved as the most upstream kinases which become activated after cytokine stimulation [158; 159; 184]. An acidic region of the IL-2Rβ subunit was found to be responsible for the interaction with the SFK p56lck [128]. Parts of the kinase domains of Lyn and Fyn bind to IL-2Rβ,

Cytokine	Shared Receptor	SFK	Reference
IL-2, IL-4, IL-7, IL-9, IL-15, IL-21	γc	Fyn, Lck, Hck, Lyn	[128; 162; 188; 373]
IL-3, IL-5, GM-CSF	βc	Lyn, Hck	[1; 37; 162; 373]
IL-6, IL-11, CNTFR, CT-1, LIF, OSM, CLC, LIF, NPN, IL-27, IL-31	gp130	Hck, Lyn, Fyn	[89; 123; 162; 323; 373]
INFα/β	INFRα	Lck	[162]
INFγ	INFRγ	Hck, Lyn	[162]
IL-12, IL-23	IL-12Rβ	Lck	[373]
Epo	EpoR	Lyn	[162; 373]
G-CSF	G-CSFR	Lyn	[64]
GH	GHR	Src kinases	[162]
PRL	PRLR	Src	[162]

Table 1.3. | **SFKs in cytokine signalling.**

which induces activation of the SFKs. [188]. Hck, Lyn and Fyn become activated by IL-3 stimulation. Hck and Fyn associate with the common signal transducing subunit, the IL-3 receptor β-subunit (βc), in a phosphorylation dependent and independent way. The SH2-domain of SFKs is one of the motives involved in the phosphorylation dependent association of the kinase with the receptor [37]. For Lyn the interaction domain was mapped to amino acids 457 to 465 of the IL-3 receptor β-subunit [1]. The Src family kinases Hck [89; 123] and Lyn are associated with gp130 [123]. Stimulation of multiple myeloma cells with IL-6 leads to activation of the SFKs Hck, Lyn and Fyn [123]. Recently, the Hck binding region of gp130 was mapped to positions 771-811 [323]. SFKs are activated by cytokine stimulation of the receptors, they are associate with. Moreover, they phosphorylate the receptor and interact with it and phosphorylate downstream signalling molecules in response to cytokine stimulation.

1.3. Interleukin-6

Interleukin-6 (IL-6) is a pleiotropic cytokine that is involved in the modulation of all major physiological cellular processes. As inflammatory cytokine it plays critical roles in the immune and hematopoetic system. It is involved in the differentiation and growth of hematopoetic precursor cells, B-cells, T-cells, keratinocytes and endothelial cells, having effects on bone metabolism, the nervous and the endocrine system. During inflammation, IL-6 induces the hepatic acute phase response by modulating the transcription of several liver-specific genes [173; 174].

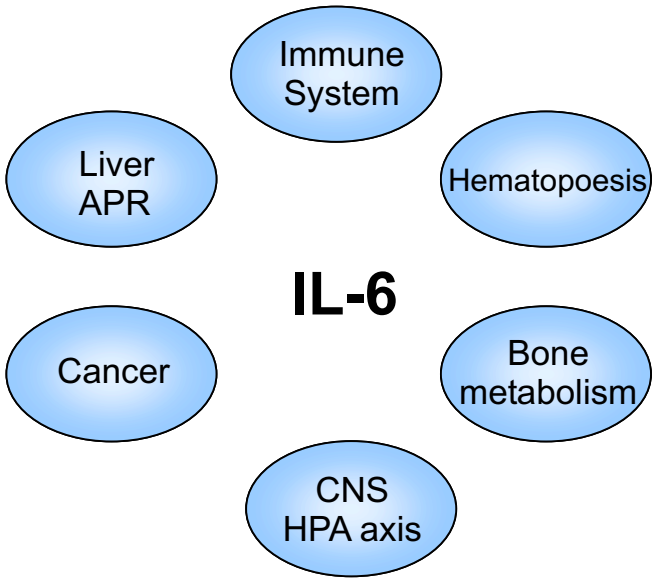

Figure 1.7. | **The pleiotropy of IL-6.** Adopted from [174].

1.3.1. History

IL-6 was discovered in the early 1980s by different groups as a factor which was able to induce B-cell growth and differentiation [146]. Human fibroblasts were found to produce this cytokine after stimulation by polyinosinic-polycytidylic acid (poly I:C) or IL-1 [60; 401]. IL-6 was identified as a factor inducing immunogobulin (Ig) production in B-cells [144; 145; 369], as a growth factor for mouse hybridoma and plasmacytoma [10; 383] and as a factor regulating the synthesis of acute-phase proteins in the liver [98]. In the late 1980s the IL-6 gene was cloned and the comparison of cDNA sequences revealed that the multiple functions ascribed to several growth factors all pertained to only one protein. Depending on the

organism the size of IL-6 varies between 22-26 kDa. Finally it was given the common designation "interleukin-6". For a historical overview see [174].

1.3.2. Role of IL-6 in various diseases

Malfunction of the IL-6 signalling system is associated with a growing number of chronic inflammatory diseases, autoimmune and malignant diseases, summarized in (Figure 1.8 and Table 1.4).

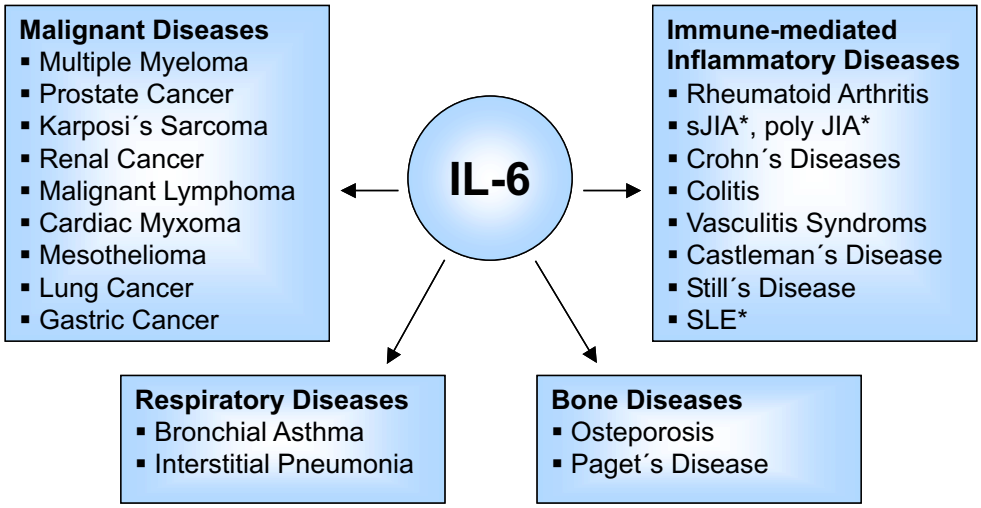

Figure 1.8. | **Role of IL-6 in various diseases.** Modified from [259]. * sJIA, systemic juvenile idiopathic arthritis; poly JIA, polyarticular juvenile ideopathic arthritis; SLE, systemic lupus erythematosus.

Disease	(+/-) Role of IL-6	Molecular Evidence	Molecular Therapies
Malignant diseases			
Multiple Myeloma	(+) Growth and survival factor	KO mice do not develop induced PC, Dependence of PC development on expression of IL-6 and IL-6R in KO and transgenic mice[1,2]	Anti-IL-6R-antibody, Tocilizumab, Phases I, II[3,4]
Prostate Cancer	(+) Growth and survival factor[1,2]		
Karposi's Sarcoma	(+) Promotion of hematopoesis, plasmocytosis and angiogenesis	Viral IL-6 is expressed from HHV8[1,2]	
Multicentric Castleman's Disease	(+) Promotion of hematopoesis, plasmocytosis and angiogenesis	Viral IL-6 is expressed from HHV8[1,2]	Anti-IL-6R-antibody, Tocilizumab (approved in Japan 2005)[3,4]
Primary Effusion Lymphomas	(+) Promotion of hematopoesis, plasmocytosis and angiogenesis	Viral IL-6 is expressed from HHV8[1,2]	
Breast Cancer	(-) Growth inhibition of estrogen receptor-positive cell[1]		
Melanoma	(-) Induction of an immune response against melanoma cells[1]		Vaccination with Hyper-IL-6[1]
Renal cancer	(+) Promotion of proliferation[1]		
Immune mediated inflammatory diseases			
Inflammatory Bowl Diseases (Crohn´s Disease, Ulcerative Colitis)	(+) Overproduction of IL-6 and sIL-6R by T-cells, increased STAT3 phosphorylation, apoptosis resistance of cytotoxic T-cells	Reduced development of experimentally induced colitis in IL-6 KO mice [2,3]	Anti-IL-6R-antibody, Tocilizumab, Phases I, II[3,4]
Rheumatoid Arthritis, sJIA, Still´s Disease	(+) Overproduction of TNF, IL-1 and IL-6 in inflamed synovium	Resistance of IL-6 KO mice to experimentally induced arthritis[1,2,3]	Anti-IL-6R-antibody, Tocilizumab, Phases I, II and III[3,4]

Disease	(+/-) Role of IL-6	Molecular Evidence	Molecular Therapies
Mesangial-proliferative Glomerulonephritis	(+) Increased proliferation of mesangial cells caused by constitutive secretion of IL-6		
Autoimmune diseases			
Multiple Seclerosis (MS)	(+) Upregulation of VCAM-I and ICAM-I	Resistance of IL-6 KO mice to the induction of the disease in an MS mouse model [1,3]	
Myasthenia gravis (MG)	(+) Involved in regulation of the anti-AChR levels	Resistance of IL-6 KO mice to the induction of the disease in an MG mouse model[3]	
Bone diseases			
Osteoporosis	(+) Promotion of osteoclastogenesis	IL-6 KO mice are protected from osteoporosis after ovaryectomy. Sex steroids down regulate the expression of IL-6R and gp130[1]	
Respiratory diseases			
Bronchial Asthma	(-)	IL-6 KO in a model for bronchial asthma show exaggerated symptoms[1,3]	

Table 1.4. | **Positive and negative roles of IL-6 in various diseases**. (+) disease promoted by IL-6, (-) disease due to IL-6 deficiency. (KO) knock out, (PC) plasmacytoma, (HHV8) human herpes virus 8, (AChR) acethylcholine receptor. Based on [173][1]; [325][2]; [174][3]; [259][4].

1.3.3. Structure of IL-6 and the IL-6 signalling complex

IL-6 has a molecular weight of 26 kDa and belongs to the family of the tall four-helix bundle cytokines, consisting of two pairs of antiparallel α-helices with an up-up-down-down topology [353]. Growth hormone (GH), erythropoietin (EPO) and granulocyte colony-stimulation factor (G-CSF) also belong to this family of cytokines. A similar topology is not found in other proteins [111; 174]. On the membrane of a target cell, IL-6 first interacts with a specific membrane-bound IL-6-receptor (IL-6R, IL-6Rα, gp80 or CD 126). The resulting ligand-receptor-complex subsequently associates with the signal-transducing transmembrane receptor, gp130 (IL-6Rβ or CD130). Binding of the IL-6-IL-6R complex promotes dimerization of gp130 which ultimately results in the formation of the signalling-competent hexameric complex [273; 396; 397].

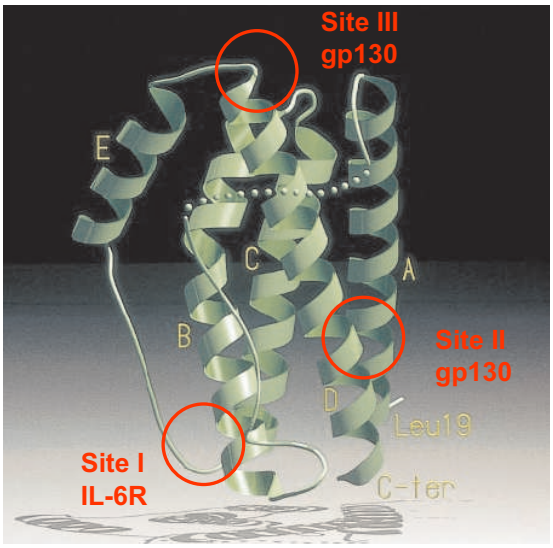

Figure 1.9. | **Ribbon representation of the IL-6 crystal structure.** The crystal structure shows three interaction sites with the receptor complex. The proposed binding sites are labeled site I-III. Site I is the site of IL-6-IL-6R interactions. Site II is the region where IL-6 interacts with gp130 in the trimer. Site III is the site of IL-6-gp130 interactions between trimers. Modified from [353].

1.3.3.1. The gp130 cytokine family

IL-6 is a member of a family of 10 cytokines, which all act via receptor complexes containing at least one molecule of the cytokine receptor subunit gp130.

Apart from IL-6, IL-11, ciliary neurotrophic factor (CNTF), cardiotrophin-1 (CT-1), cardiotrophin-like cytokine (CLC), leukemia inhibitory factor (LIF), neuropoietin (NPN), and oncostatin M (OSM) and the more recently characterized cytokines IL-27 and IL-31 are hitherto known members of the family. The receptors for the IL-6-type cytokines can be subdivided into non-signalling receptors, the α-receptors (IL-6R, IL-11R and CNTFR) and into the signal transducing receptors (gp130, OSMR and LIFR). To generate signalling-competent receptor complexes the cytokines within the family follow different strategies: IL-6 and IL-11 bind to their specific α-receptors before they associate with a homodimer of gp130, while CNTF, CLC, and NPN bind to CNTFR before they associate with a heterodimer of gp130 and LIF-R. A glycosylphosphatidylinositol-anchored α-receptor has been postulated for CT-1 as well. LIF and OSM signal via heterodimers of gp130 and the LIF-R. Human OSM can transduce a signal either via the gp130/LIF-R heterodimer or an alternative OSMRβ-R/gp130 heterodimer. IL-31 in complex with IL-31 binding protein signals via OSMRβ-receptor/gp130 heterodimer [134; 307; 325].

1.3.3.2. The extracellular domains of cytokine receptors

IL-6R and gp130 both belong to the family of type I transmembrane proteins, which span the plasma membran with a single transmembrane domain having the N-terminus at the extracellular and the C-terminus at the intracellular side of the membrane. Both receptors are members of the family of cytokine receptors, characterized by certain structural domains present in their extracelluar domain. They share characteristics such as an array of fibronectin type III (FNIII)-like and Ig-like domains. At least one cytokine-binding module (CBM) or cytokine homology region (CHR) that comprises two FNIII-domains is present in each receptor. Structurally conserved features of the CBM include a distinct pattern of cysteine residues in the N-terminal domain and a WSXWS motive at the C-terminal domain. N-terminal to the membrane-proximal CBM each receptor contains an Ig-like domain. Gp130 has three additional membrane-proximal FNIII regions [111; 134]. IL-6 binds gp130 via three conserved epitopes, site I, II and III. Site III is unique to gp130 cytokines. IL-6 forms a complex with IL-6R via site I. The binary complex of IL-6 with IL-6R forms two newly composed epitopes which interact with the CBM (site II) and the Ig-like domain (site III) of gp130 (Figure 1.9). Dimerization of two complexes of IL-6/IL-6R/gp130 has been postulated that constitute a signalling competent hexameric receptor complex with a (2:2:2) stoichiometry [27; 52; 249]. The hexameric structure of the receptor is supported by data from crystal structures of the IL-6/IL-6R/gp130 complex [27]. Recent data generated by single-particle electron-microscopy (EM) confirmed this hexameric

architecture of the complex [349]. In contrast, a tetrameric model (IL-6)-(IL-6R)-$(gp130)_2$ with a (1:1:2) stoichiometry is also applicable [104; 111; 136; 282; 332] and (Figure 1.10).

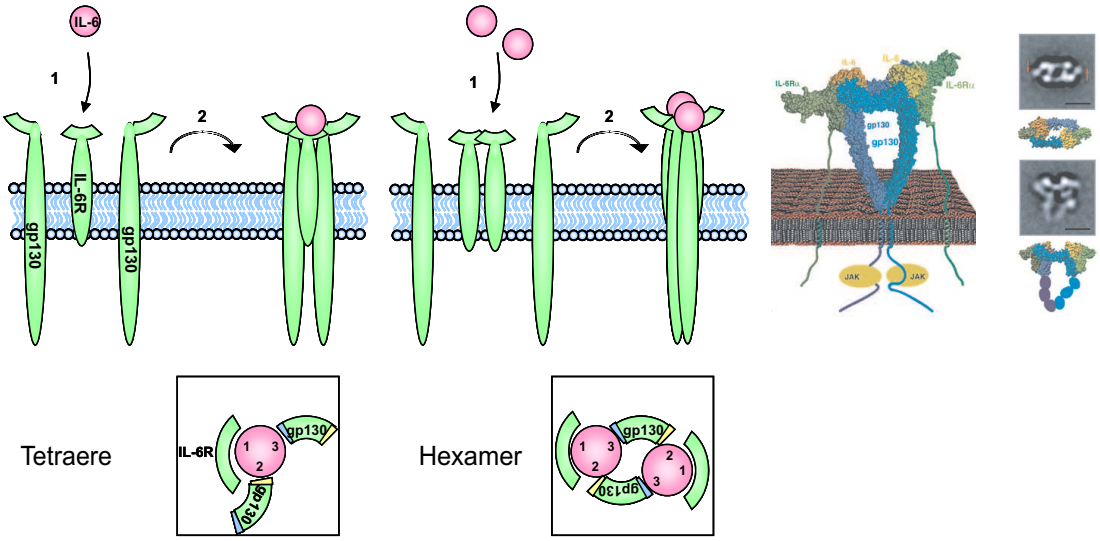

Figure 1.10. | **The IL-6 receptor complex: Tetramer or hexamer?** Models of the association of receptor components (green, turquoise) and ligand (red, yellow) as tetrameric (left) or hexameric complexes (middle). Derivation from the three-dimensional structures obtained from X-ray crystallography or the electron microscopic appearance of the extracellular parts (right, taken from [349]).

1.3.3.3. Soluble receptors

In addition to the general model of IL-6 signalling in ligand/receptor complexes, alternative mechanisms exist to modulate IL-6 signalling. The two transmembrane receptors involved in signalling are IL-6R and gp130. While gp130 is ubiquitously expressed, the presence of IL-6R is limiting for IL-6 stimulation in most target cells. On the other hand, soluble variants of both transmembrane receptor subunits exist. Soluble IL-6R (sIL-6R) is the product of alternative splicing or proteolytic cleavage (shedding) of the membrane-bound form, whereas soluble gp130 (sgp130) exclusively results from alternative splicing. Soluble IL-6R forms a complex with IL-6. This complex interacts with membrane bound gp130 and induces IL-6 signalling in cells which do not express the membrane bound IL-6R. The sIL-6R together with IL-6 acts as an agonist for IL-6 signalling. As a consequence, cells which express only gp130 and do not express IL-6R can signal in response to IL-6,

in case sIL-6R is shedded from surrounding cells which express IL-6R. This mechanism was termed 'trans-signalling' [173; 325; 326] and (Figure 1.11). Soluble gp130 has been detected in human serum in concentrations of 100-300 ng/ml and was found to inhibit membrane-bound gp130 signalling [257]. Using a fusion protein composed of the the extracellular part of gp130 and the Fc moiety of human IgG to mimic sgp130, sgp130 was shown to antagonize trans-signalling but not the classical signalling pathway [171]. The role of these naturally occurring soluble forms is still controversial. Especially sIL-6 induced trans-signalling appears to play pivotal roles in a growing number of diseases [173; 325; 326]. In general the existence of these two additional signalling components can be seen as a buffer system which modulates the response to IL-6 [250].

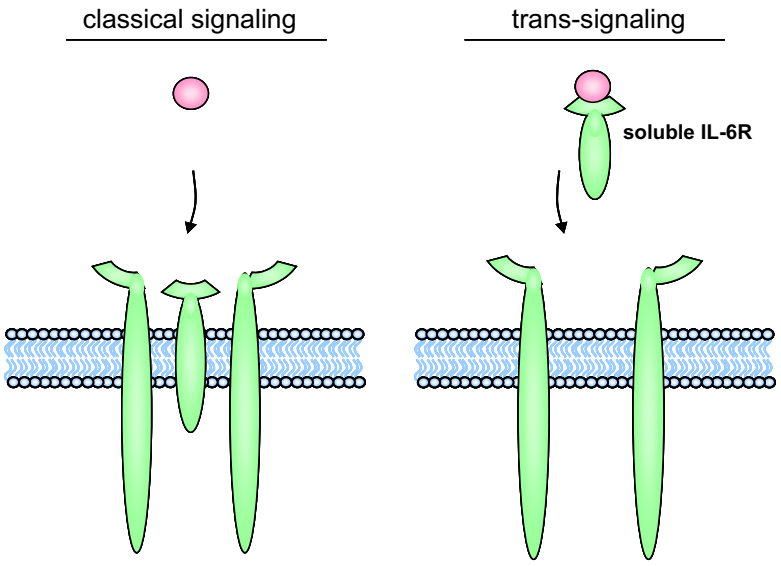

Figure 1.11. | **Classical vs. trans-signalling.**

IL-6 has been reported recently to be involved in the transition from innate to acquired immune responses during inflammation. Soluble IL-6R is thought to be responsive for the decreased attraction of neutrophils and the increased recruitment of mononuclear cells. Disruption of this immunological switch has been suggested to distort the immune response and to affect the onset of chronic inflammatory and autoimmune diseases [147; 170]. In many of the IL-6 related diseases a local or systemic increase of IL-6 and sIL-6R can be observed [173]. Soluble IL-6R is suggested to mediated the transition from the acute to the chronic phase of the disease.

1.3.3.4. The intracellular domain of gp130

Structural features of the intracellular domain of g130 are the membrane proximal box1 and box2 motives which are conserved among cytokine receptors [251]. Box1 (aa 651-658 of human gp130) is a proline rich 8 amino acid stretch, box2 (aa 691-712) is a cluster of hydrophobic amino acids followed by positively charged residues. Both motives are responsible for the interaction of the receptor with Janus Kinases (JAKs). Six tyrosine residues become phosphorylated after activation and serve as docking sites for downstream molecules. A dileucine motive with an adjacent phosphorylated Ser residue is responsible for receptor internalization [78; 103]. The basolateral sorting signal [79] overlaps with the internalization domain and the acidic domain (AD) which forms a docking site for Src-Family kinases [323].

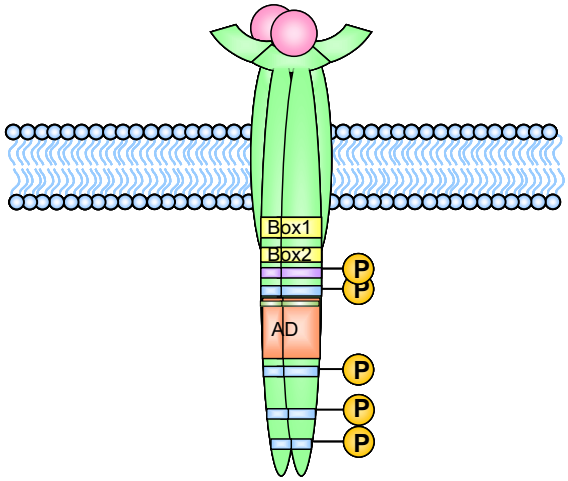

641 FNKRDLIKKH IWPNVPDPSK SHIAQWSPHT PPRHNFNSKD QMYSDGNFTD VSVVEIEAND

701 KKPFPEDLKS LDLFKKEKIN TEGHSSGIGG SSCMSSSRPS ISSSDENESS QNTSSTVQYS

761 TVVHSGYRHQ VPSVQVFSRS ESTQPLLDSE ERPEDLQLVD HVDGGDGILP RQQYFKQNCS

821 QHESSPDISH FERSKQVSSV NEEDFVRLKQ QISDHISQSC GSGQMKMFQE VSAADAFGPG

881 TEGQVERFET VGMEAATDEG MPKSYLPQTV RQGGYMPQ

Figure 1.12. | **Domain structure of the cytoplasmatic domain of gp130**. Box1 and box2 motives (yellow), SHP-2 binding site (violett), STAT binding sites (blue), acidic domain (red) and internalization motive (green) with dileucine motive (yellow). Phosphorylated residues are marked with an asterix.

1.3.4. Activation of downstream signals-The "ON" signals

The information of successful ligand binding to the extracellular part has to be transmitted to the intracellular signal-transducing subunit of the receptor complex. A paradigm of receptor activation is that the signal transducing subunits need to dimerize to acquire a signalling-competent conformational state. Evidence suggests the presence of pre-dimerized, signalling-incompetent receptors at the plasma membrane for some receptor complexes. In the case of the EPO receptor, ligand binding induces a conformational change in the pre-associated receptors, which stabilizes the active form of the receptor [216]. For gp130 as the signal tranducing subunit of at least 10 different cytokines, a pre-association with different α- and/or β-subunits is not intuitive because of the various possible combinations (Table 1.3). To transfer the ligand-adjusted conformation from the outside to the inside of the cells, a rigid α-helical structure of the transmembrane and juxtamembrane domain of gp130 is conceivable. In a recent study it was show that the introduction of one to four alanine residues in the juxtamembrane region of gp130 changed the ability to activate the receptor dependent on the number of introduced residues. While mutants with one, two or four additional alanines were less effective in the induction of downstream target genes, the mutant carrying three alanines was again signalling competent. The introduction of three amino acids into an α-helical structure results in a 330° twist which brings the receptor close to its native position [110]. In the EpoR a hydrophobic motive (LXXKW) in the juxtamembrane region has to be precisely orientated to allow signalling. Interestingly this motive is conserved among several cytokine receptors [59].

1.3.4.1. JAK/STAT pathway

While RTK posses an intrinsic tyrosine kinase activity, cytokine receptors lack intrinsic catalytic activity but are intimately associated with tyrosine kinases. The family of Janus Kinases (JAK) is well known to be one of the apical kinases, which become activated after effective ligand binding. Ligand-induced conformational changes bring JAK molecules, which are associated with the receptor-monomers, into close proximity to each other. This leads to activation of the kinase and in turn to trans-phosphorylation of the receptor-associated JAKs. Subsequently the six tyrosine residues in the cytoplasmatic tail of gp130 become phosphorylated to generate docking sites for downstream signalling molecules. Monomers of Signal Transducer and Activator of Transcription (STAT)-3 and -1 molecules associate with the phosphorylated YXXQ motives of gp130. STAT3 binds to (p)Y767RHQ, (p)Y814FKQ, (p)Y905LPQ and (p)Y915MPQ, while STAT1 is recruited to (p)Y905LPQ and (p)Y915MPQ in gp130. Receptor-bound JAKs phos-

phorylate STAT3 at Tyr 705 and STAT1 at Tyr 701. By SH2 domain-mediated interaction, phosphorylated STATs form STAT1-STAT1, STAT1-STAT3 and STAT3-STAT3 dimers and translocate to the nucleus, where they bind to specific DNA sequences to modulate the expression of target genes [90; 134; 135] and (Figure 1.13).

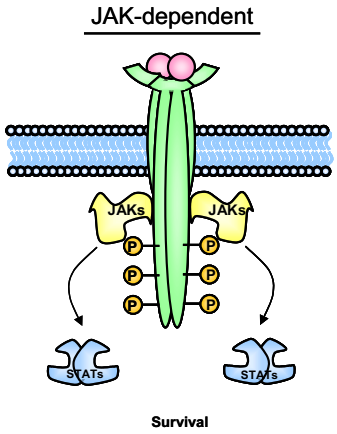

Figure 1.13. | **The JAK/STAT pathway.**

The Janus Kinases (JAKs) The family comprises four members, JAK1, JAK2, JAK3 and TYK2. Gp130, LIFR and OSM are known to interact with JAK1, JAK2 and TYK2 [222; 359], while JAK3 interacts exclusively with the common γ-chain [267]. The membrane proximal parts of the receptor comprising box1 and box2 regions are involved in the tight association of the receptors with JAKs [117; 251]. Recent evidence suggests that the exclusive membrane localisation of JAKs is a consequence of the tight association with the receptor. JAK1 and gp130 are hardly dissociable. Fluorescence recovery after photobleaching (FRAP) experiments show the same diffusion dynamics for the two molecules [14]. Thus the cytokine receptor/JAK complex may be comparable to a RTK [118].

The characteristic architecture of JAKs is composed of functionally distinct domains: An N-terminal FERM domain (Four-point-one, Ezrin, Radixin, Moesin homology domain), a SH2-like region, a pseudokinase domain, and a C-terminal kinase domain. The FERM domain mediates association with the box1 and box2 motive of the cytoplasmic region of cytokine receptors and may also participate in catalytic regulation. The crystal structure of the JAK3 kinase domain was recently solved [24]. JAK3 mutation is the source of ~7-14 % of the human severe combined immunodeficiencies (SCID) [268]. The somatic mutation of valine 617

to phenylalanine in JAK2 was recently found to be a recurring oncogenic mutation in myeloproliferative disorders [190; 280].

The Signal transducer and activator of transcription (STATS) Seven different molecules belong to the family of STATs STAT1,-2,-3,-4,-5a,-5b and -6. The conserved modular structure of STATs is, from N- to C-terminus: An oligomerisation domain (coiled-coil domain), the DNA-binding domain, the SH2 domain and the transactivation domain. Crystal structures exist of STAT1,-3 and -4 [13; 47; 386]. The SH2 domains of STATs are required for the interaction with the (p)YXXQ motives of cytokine receptors. The classical way of STAT activation, described above, is challenged by several recent findings: (i) STATs exist in higher molecular mass multimeres prior to stimulation [119; 361], (ii) tyrosine phosphorylation is not necessarily required for nuclear translocation of the dimers and [30; 242] (iii) dephosphorylation is not needed for nuclear export of STATs [238; 239; 419].

1.3.4.2. The SFK pathway

In addition to JAKs, SFKs are upstream kinases which are associated with cytokine receptors (Section 1.2.3.3) and Table 1.3. The SFK Hck interacts with positions 771-811 of gp130 [323]. This region was termed acidic domain (AD) owing to its high content of acidic residues, in analogy with the acidic region of the IL-2Rβ subunit for interaction with the SFK p56Lck [128]. In gp130 dependent signalling SFK activation by IL-6 leads to the downstream activation of Erk1/2 in a signalling cascade, which has not yet been fully characterized. There is, however, evidence, that it involves dephosphorylation by SHP-2 of the negative regulatory tyrosines of SFKs after IL-6-stimulation [323]. Adapter proteins like the scaffolding molecules Gab1/2 [284] or the kinase Pyk-2 were shown to be part of the cascade. In multiple myeloma cells, the transmembrane phosphatase CD45 plays a crucial role in IL-6 induced SFK activation [227]. CD45 is recruited to membrane lipid-rafts in response to IL-6 stimulation. In the rafts it can associate with SFKs bound to gp130 and activate them. The activation of SFKs by CD45 leads to the activation of PLCγ_2, Ca^{2+}-release from the ER and the activation of PKC-β. This pathway was shown to be independent of JAK/STAT and SHP-2/Erk1/2 signalling [165; 167]. In response to oxidative stress, SFKs are involved in the transduction of pro-apoptotic signals in CD45-positive myeloma cells [215]. Figure 1.14 summarizes the participation of SFK in multiple downstream signalling pathways.

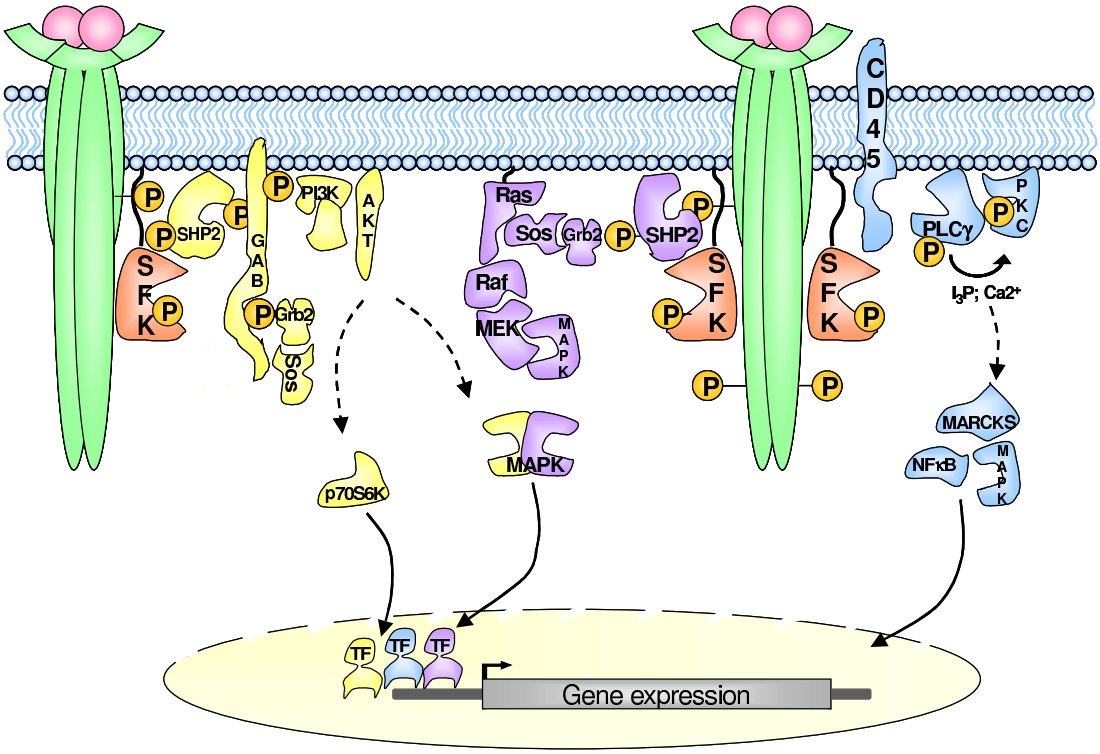

Figure 1.14. | **SFKs in IL-6 signalling.**

1.3.4.3. Crosstalk: JAK/STAT and SFK pathways

The ability of SFKs to activate STATs was shown in different model systems. Initially STAT activation was shown in v-Src transformed fibroblasts [416]. Evidence accumulated that SFKs play a role in STAT activation in several cytokine-, oncogene- and growth factor-induced signalling pathways. In the context of signalling from βc, the common signal transducing subunit of the IL-3/IL-5 and GM-CSF receptors, c-Src, is able to phosphorylate and induce nuclear translocation of STAT molecules following IL-3 stimulation [293]. A similar situation is observed in Epo receptor and in Bcr-Abl signalling [162; 185]. Experiments performed in fibroblast show that the SFK Hck directly interacts with STAT3 via its SH3 domain [331]. Based on these finding different model pathways are applicable to explain the cross talk between the JAK/STAT and the SFK pathways. Some data support a progressive or sequential model: JAKs are the most upstream kinases, they become activated by ligand-induced receptor dimerization and phosphorylate the receptor and activate SFKs by phosphorylation of Tyr 416. In a second step JAK activated SFKs phosphorylate and activate STATs [64]. A second possibility is the co-operative function of JAKs and SFKs. Both kinases become activated by

ligand-induced receptor phosphorylation and both kinases activate STATs [289]. The third possibility consists in JAK independent activation of STATs by SFKs [347]. In figure 1.15 the three models are visualised. In a murine cell culture model of gp130 signalling, STAT signalling was shown to be SFK independent [323]. Figure 1.16 shows a model for SFK and JAK dependent IL-6 signalling. Crosstalk between JAK/STAT and SFK pathways is a concept summarizing different cell type and cytokine specific phenomena.

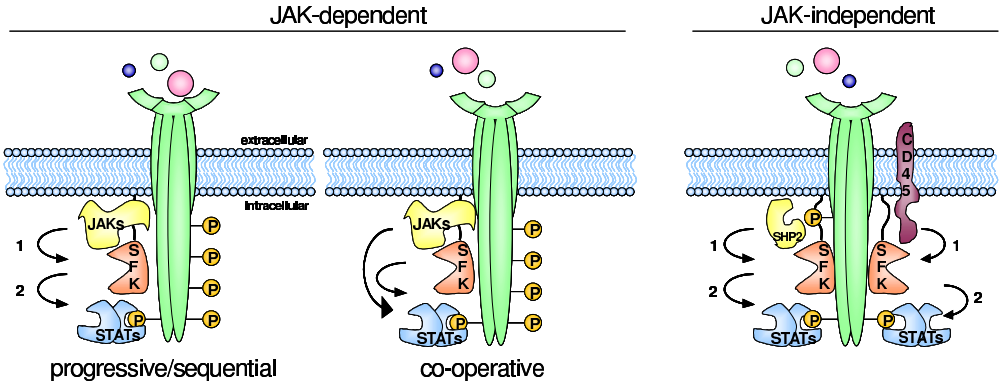

Figure 1.15. | **Crosstalk between SFK and JAK/STAT pathway.**

1.3.4.4. SHP-2/MAPK Pathway

Phosphorylation of Tyr 759 in gp130 leads to the recruitment and phosphorylation of SH2-domain-containing tryrosine phospatase-2 [28; 360]. Receptor-bound SHP-2 becomes phosphoryated [324] and forms a complex with adapter molecules like the complex of Grb2-SOS (Son of Sevenless) and Grb2-associated binder-1 (Gab1) [114; 327]. These interactions lead to the activation of the Ras-Raf-MAPK-Cascade, resulting in Erk1/2 phosphorylation [91; 134]. The MAPK Erk1/Erk2 are mainly associated with the maintenance of cellular survival and proliferation. While the other two members of the family p38 and JNK are known to be stress-activated. Upon IL-6 treatment Erk1/2 as well as p38 are activated. The scaffolding adapter proteins Gab1 and Gab2 contain binding sites for SHP-2, PI3K, phospholipase Cγ, Crk and c-Met. Gab1/2 are targeted to the plasma membran via a plecstrin-homology (PH)-domain [113]. After IL-6 stimulation Gab1 and Gab2 become phosphorylated at tyrosine residues and interact subsequently with SHP-2, Hck and PI3K. This links receptor activation to the third major pathway downstream of IL-6 stimulation, the phosphoinositid-3-kinase (PI3K)-pathway [284; 366].

1.3.4.5. PI3K/Akt pathway

IL-6 stimulation leads to activation of phosphoinositol-3-kinase (PI3K). By phosphorylating phosphoinositides in the inner leaflet of the plasma membrane PI3K recruits the Ser/Thr- kinase Akt (derived from oncogene carrying retrovirus AKT8/ protein kinase B) by its PH domain to the membrane. At the membrane phosphoinositide-dependent kinase-1 (PKD1) activates Akt by phosphorylation. Downstream targets of Akt are e.g. BAD (Bcl-2/Bcl-xL-antagonist, causing cell death), phosphorylation of which is associated with increased cell survival and proliferation, the family of forkhead transcription factors and Erk1/2 [134; 142].

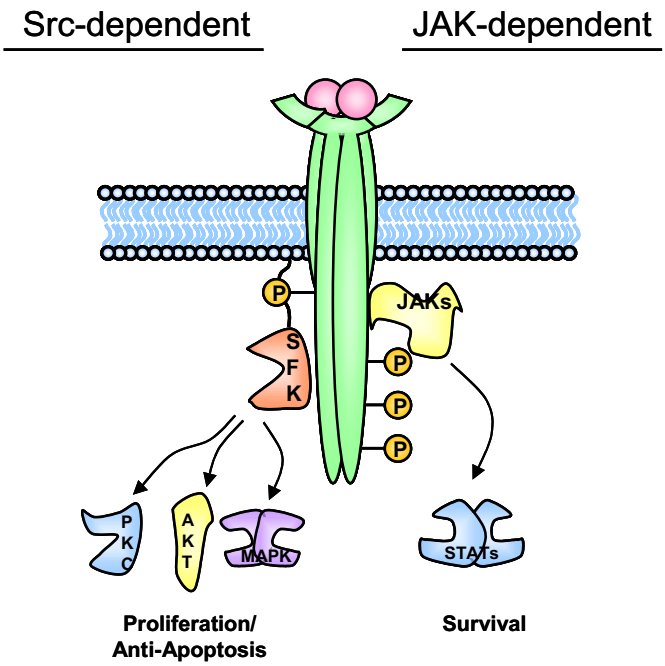

Figure 1.16. | **SFKs and JAKs in IL-6 signalling.**

1.3.5. Inactivation of downstream signalling

Positive signalling events are controlled and turned off by different negative feedback mechanism to guarantee a signalling system which stays excitable and which can be modulated by different stimuli.

1.3.5.1. Phosphatases

Dephosphorylation of the activated receptor and the involved downstream molecules is accomplished by various phosphatases e.g. SHP-2, PTPϵ, PTPϵC, PTP1B, CD45 and SHP-1 [134]. Among these, the role of SHP-2 in the down-regulation of signalling is characterized best. SHP-2 is a cytoplasmatic ubiquitously expressed tyrosine phosphatase which contains two N-terminal SH2 domains and a catalytic domain at the C-terminal parts of the molecule. The crystal structure implies autoregulation of the phosphatase. In the inactive conformation one SH2 domain occupies the active center of the enzyme and inhibits substrate binding. The enzyme can either be activated by the interaction of the SH2 domains with phosphorylated SH2 domain binding-motives [148] or by phosphorylation of Tyr 542 and Tyr 580 [223]. SHP-2 binds gp130 via its N-terminal SH2 domain [28; 360].

1.3.5.2. The SOCS family

Suppressor of cytokine signalling (SOCS) proteins act as classical feedback inhibitors. IL-6 stimulation rapidly induces the expression of SOCS proteins via the JAK/STAT pathway. SOCS proteins induce proteasomal degradation of the ligand-occupied receptor complex components which shuts down the signalling. The family comprises eight members SOCS1-SOCS7 and cytokine-inducible SH2 protein (CIS). All SOCS proteins contain a SH2 domain and a C-terminal SOCS-box [15; 34; 192; 362]. For the IL-6 signalling pathway SOCS1 and SOCS3 are most relevant. Both molecules inactivate JAKs. SOCS1 binds directly to tyrosine phosphorylated JAKs and blocks substrate binding. SOCS3 binds to Tyr 759 in gp130 but can also bind to activated JAKs [256; 258; 320; 329; 412]. Apart from inhibition of JAKs by direct interactions, there is evidence that SOCS proteins are parts of E3-ubiquitin ligases [34; 177; 421] and are responsible for the degradation of several signalling molecules such as JAK2 [379], SFKs [354] or Vav [74]. SFKs are involved in the tyrosine phosphorylation at 204 and Tyr 221 of SOCS3 after IL-6 stimulation [354]. Phosphorylated Tyr 759 in gp130 is differentially involved in the tranduction of positive and negative downstream signals. On the one hand SHP-2 binding triggers a cascade leading to the activation of the pro-survival and pro-proliferative MAPK-pathway. On the other hand two distinct modes of negative regulation result from the interaction of different molecules with phosphorylated Tyr 759: along with JAKs, STATs and the receptor, SHP-2 also dephosphorylates the negative feed back regulator SOCS3, which competes with SHP-2 for binding to (p)Tyr 759 of gp130 [204]. Transgenic mice which express a mutated gp130Y757F show reduced SHP-2/Erk1/2-activation and increased JAK/STAT signalling. The phenotype of these mice is characterized by

splenomegaly, lymphadenopathy, enhanced acute phase reaction and autoimmune arthritis [90]. These findings underscore the negative regulatory role of SHP-2 in IL-6 signalling [11; 264].

1.3.5.3. The PIAS family

The DNA binding activity of STAT1 and STAT3 is inhibited by protein inhibitors of activated STAT (PIAS) [53; 213]. PIAS1, PIAS3, PIASxα, PIASxβ and PIASγ are the five mammalian members of the family. While PIAS1 inhibits STAT1-mediated transcription, PIAS3 inhibits STAT3-mediated transcription. PIAS proteins were found in the cytoplasm and in specific nuclear bodies [90; 134]. Some PIAS proteins can regulate gene expression by their E3-SUMO (small ubiquitin-related-modifer)-ligase activity [189; 314].

1.3.6. Endocytosis and sorting of the receptor complex

Belonging to the class of N-glycosylated transmembrane proteins, cytokine receptors are synthesized and N-glycosylated at membrane-bound polysomes in the endoplasmatic reticulum (ER), transported via the trans golgi network to the golgi apparatus, where the N-linked-oligosaccharids are processed and finally the properly folded and N-glycosylated receptors are translocated to the plasma membrane. After IL-6 binding and activation the receptors gets internalized via clathrin-coated vesicles. The di-leucine motive in the cytoplasmatic tail of gp130 at positions Leu786 and Leu878 with the adjacent Ser782 is responsible for the internalization [78; 103; 371]. Either all components of the internalized receptor complex become degraded by lysosomes or IL-6 and IL-6R are separated from g130 and get degraded, while gp130 is recycled to the cell surface [377; 395].

Some IL-6 target cells are polarized cells, for instance hepatocytes or endometrial cells. Localization of the receptors at cytokine contact sites is essential for these cells. Assuming the blood stream as a potential source for IL-6, cytokine recpetors should be located at the side of the cell that faces the internal milileu, i.e. the basolateral side of hepatocytes. In a model system for polarized epithelial cells, Madin-Darby canine kidney (MDCK) cells, requirement of the cytoplasmic regions of gp130 and IL-6R for basolateral sorting was shown [232]. More recently, amino acids 782-792 of gp130, ecompassing the di-leucine motif for receptor internalization described above, was shown to be responsible for proper basolateral sorting of gp130 [79]. This region significantly overlaps with the acidic, SFK-binding domain [129; 323].

1.4. Multiple myeloma

Multiple myeloma (MM) is a clonal B-cell neoplasm. The disease is characterized by the accumulation of terminally differentiated, monoclonal, antibody producing plasma cells in the bone marrow. MM is associated with anemia, lytic bone lesions and increased immunoglobulin levels (M-protein) in blood and urine. The high blood concentration of immunoglobulin leads to increased blood viscosity that can cause renal failure and immunodeficiencies. [244; 411]. Despite conventional and high dose chemotherapies with combinations of alkylating agents, antracyclines and corticosteroids or the combination of high dose therapy with autologous transplantation, as well as novel biological therapeutics, the disease remains incurable.

1.4.1. Epidemiology and etiology

The median survival time after diagnosis of MM is 3-5 years [140]. Multiple myeloma is the 2nd most commonly diagnosed hematological malignancy in the western world [244]. It accounts for 20 % of all deaths caused by hematopoetic malignancies and for 2 % of all cancer deaths. The annual incidence of MM is approximately 3.8 per 100 000 population (~ 27 500 new cases of MM/year in the USA) and approximately 1.5 per 100 000 in Europe [197]. MM is 1.5 times more common in male versus female with a median age of 71 years. It is almost twice as common in the African versus Caucasian population and less common in the Asian population [31]. The five-years survival is 28 % and did not change since the 1970ies in the European Union (EU) [300; 319]. One reason for the increased incidence of MM in African-Americans could, at least in part, be related to elevated serum cholesterol levels, since cholesterol is an essential component of MM cell membranes [240]. Increased serum cholesterol has been implicated in myeloma pathogenesis, and is associated with higher mortality in African versus Caucasian men [321]. Independently of the genetic background of the population, a prospectively studied cohort of more than 900,000 US adults showed that increased body weight is associated with increased death rates from cancers, including MM [71; 109; 193; 283]. Novel therapeutics include thalidomide and its immunomodulatory derivatives (IMiD) e.g. lenalidomide/relimid^{TM} and the proteasome inhibitor bortezomib/velcade^{TM} show promising results in the clinic even in relapsed refractory MM [131; 140; 141; 299; 304]. The etiology of the disease is still unclear, but is associated with contact to organic solvents, other chemicals and ionizing irradiation [67; 161].

1.4.2. Development and pathophysiology

Normal B-cell development is characterized by the differentiation from a stem cell via different intermediate selection stages of pro- and pre-B-cells to terminally differentiated plasma cells. Ig VDJ rearrangement, somatic hypermutation and Ig class switching are the major steps of this process. During maturation, immature B-cells migrate to the lymph node where antigen recognition occurs. During the primary immune response, germinal centers are generated. Antigen-activated lymphoblasts that enter a germinal center are subjected to multiple rounds of somatic hypermutation of IgH and IgL V(D)J sequences and antigen selection. Cells that express high-affinity antigen receptors are selected for survival, with subsequent differentiation to memory B cells or post-germinal-center plasma cells. After productive IgH switch recombination, the cells home to the bone marrow, where they reside as terminally differentiated, nonproliferating, long-lived plasma cells for >30 days to years. Sequence analysis of Ig variable (VH) regions from MM tumors have shown that these cells are post-germinal center with mutated homogenous clonal sequences. Nearly 80 % of B-cell tumors arise from germinal-center or post-germinal-center B-cells, indicating that the intrinsic genetic instability of B-cells which is unleashed in the germinal center is important for their development. [122; 140; 193; 194].

The pathophysiology of MM can be divided into multiple evolutionary stages, from monoclonal gammopathy of undetermined significance (MGUS) via smouldering (asymptomatic) MM, intramedullary (symptomatic) MM to extramedullary MM or plasma cell leukemia (PCL). MGUS, is present in 1 % of individuals over the age of 50 years. With a ~ 1 % annual risk it can progress to MM or other plasma cell dyscrasias [196]. MGUS and smoldering MM lack MM-related symptoms. Smoldering MM progresses after variable periods of time to symptomatic myeloma.

1.4.3. Diagnosis and treatment

Diagnosis of MM is based on the detection of M-proteins in serum and/or urine, osteolysis shown by x-ray analysis and a percentage of plasma cells in the bone marrow above 10 %. Prognostic factors such β2-microglobuline, myelomatype and cytogenetic aberrations can be determined in addition [252].

The average survival time of a patient with newly diagnosed disease is between 6 and 12 month without therapy. Today's first line therapy is autologous stem cell transplantation in combination with high dose chemotherapy [197; 350]. Chemotherapy with mephalan or cyclophosphamide and prednisolone show response rates of 50 % but complete remission is rare [350]. (A reduction of M-proteins to 50

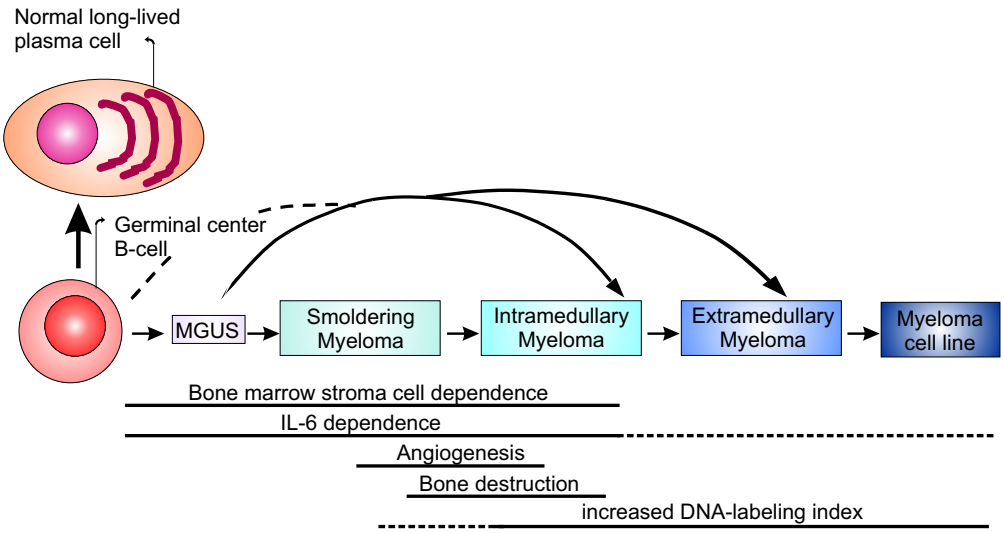

Figure 1.17. | **Disease stages.** Modified from [193].

% or less in response to chemotherapy is defined as positive response). Further options are treatments with high dose corticosteroids (dexamethasone) or combination therapies of vinc-alcaloids (vincristine), anthracyclines (doxorubicine) and corticosteroids (dexamethasone). In this VAD combination, the dexamethason component is estimated to account for 85 % of the effects. Novel biological treatments with thalidomide or IMiDs and bortezomib are approved for the treatment of relapsed refractory MM [83; 350].

1.4.4. Cytogenetics

MM lacks pathogenomic genetic lesions that could be either per se or in a concerted way be responsible for the disease. Using fluorescence in-situ hybridization (FISH) 90 % of the patients were shown to have genetic alterations. 45 % of these changes, involved chromsome 13 [197]. Nevertheless, the genetic background of MM patients is extremely heterogenic. MM cells can have either (1) hyperdiploid karyotypes with infrequent translocations (<30 %) or other structural chromosomal abnormalities or (2) non hyperdiploid karyotypes with high prevalence of translocations (>85 %) of Ig genes. These translocations are diverse but not random. They juxtapose potent enhancers of the IgH switch region on chromosome 14q32 next to oncogene-harboring partner loci. Five partners for IgH translocations in MGUS and MM are well-defined and recurrent, they account for ~ 40 % of the cases which have IgH translocations. They comprise cyclin D1 (11q13) cyclin D3 (6p21) fibroblast growth factor receptor 3 (FGFR3) and multiple myeloma

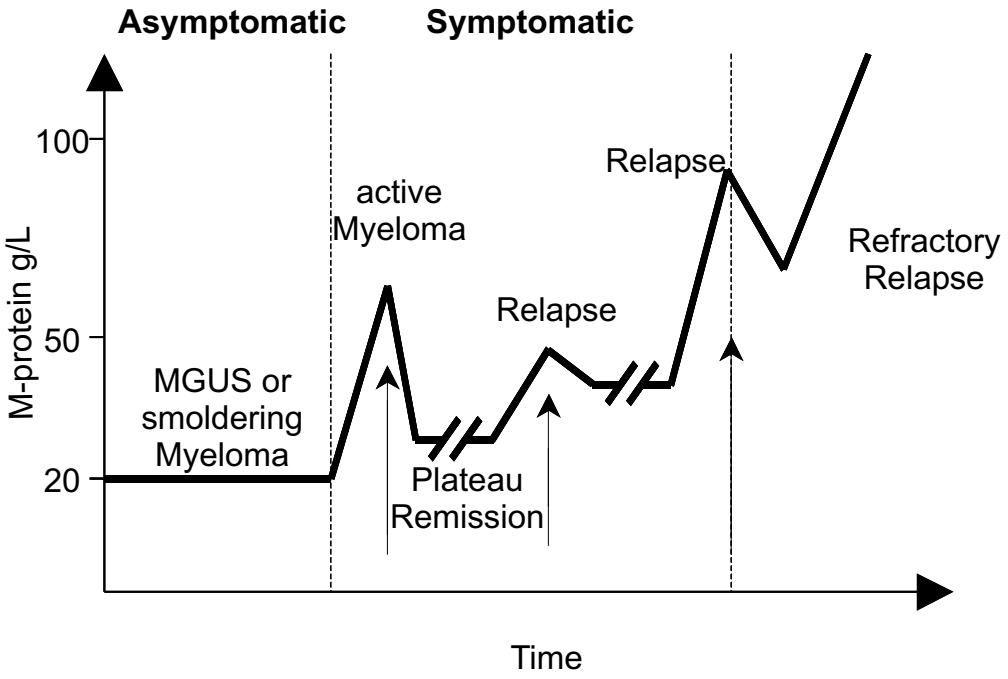

Figure 1.18. | **Normal progress of the disease.** Arrows indicate the onset of phases of chemotherapy, which are followed by declining M-protein levels. In the symptomatic stages, increasing M-protein levels are due to relapse. Modified from [83].

SET domain (MMSET) (4p16), c-maf (16q23) and mafB (20q11). Among these genes, FGFR3 on der(14) and MMSET on der(3) may be dysregulated by t(4;14) translocations. For instance FGFR3 is deleted or not expressed in 20 % of the cases carrying the t(4;14) translocation. Patients with a c-maf or mafB translocation have an extremely poor prognosis [141]. So far, there are no known markers that can distinguish MGUS from MM [94]. However a multitude of additional genetic changes, which are absent or rare in MGUS are being indentified in intramedullary and extramedullary MM [73]. It is conceivable that they contribute to further progression of the disease to its more aggressive stages. These secondary genetic mutations comprise: translocations involving c-myc, mutations and/or monoallelic p53 deletions, Rb or p18INK4c inactivation, activating mutations of K- or N-Ras [17] or FGFR3 in the case of the t(4;14) translocation [49] or deletion and inactivation mutations of PTEN [343]. The upregulation of cyclin D genes is proposed to render the plasma cells more susceptible to proliferative stimuli from BM-derived cytokines e.g. IL-6. This leads to an expansion of this population which is thought to be more susceptible to additional genetic events.

While MGUS and MM plasma cells can be distinguished from normal plasma cells by gene expression profiling of patient mRNA, they are difficult to differentiate

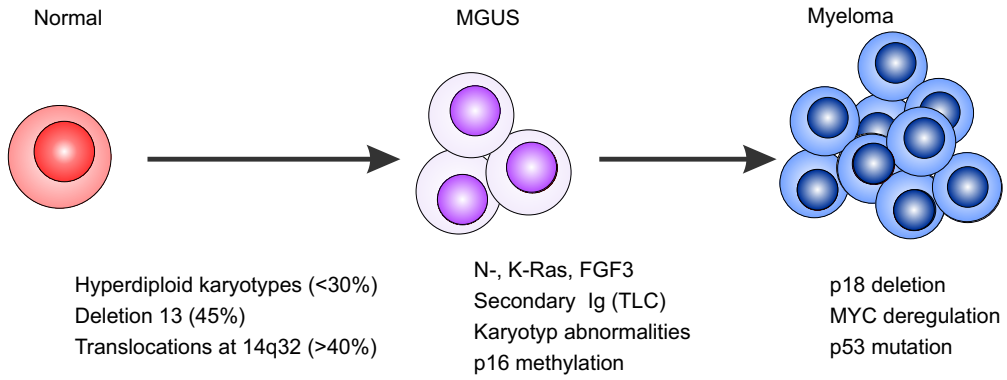

Figure 1.19. | **Genetic events in disease progession.**

from each other [73; 76; 420]. This suggests that changes in the bone marrow microenvironment in addition to genetic changes in plasma cells account for the malignant changes.

1.4.5. Microenvironment and cytokines

The biological behavior and the clinical response to therapeutic treatments is not exclusively determined by the genetic background, but in addition by the bone marrow (BM) microenvironment. The micromilieu surrounding the MM cell in the BM comprises hematopoetic stem cells, immune cells (e.g. T-cell, macrophages and natural killer cells), erythrocytes, bone marrow stromal cells (BMSCs), bone marrow endothelial cells (BMECs), osteoblasts and osteoclasts which are involved in bone homeostasis, extra cellular matrix (ECM) components and secreted growth factors [141; 411]. MM cells home to the BM by the interaction with various adhesion molecules on the surface of BMSC and to ECM proteins. On human MM cells, β1-Integrins, e.g. integrin $\alpha 4\beta 1$ (very late antigen-4 (VLA-4)) and syndecan-1 (CD138) were shown to interact with the ECM proteins fibronectin and type I collagen, respectively. Lymphocyte function-associated antigen-1 (LFA-1, CD18/CD11A or integrin $\alpha L/\beta 2$) and VLA-4 bind to intracellular adhesion molecule-1 (ICAM) and to vascular cell adhesion molecule-1 (VCAM-1, CD106) on BMSCs, respectively [297]. The interactions of MM cells with its microenvironment have complex bidirectional effects on the MM cells themselves as well as the surrounding cells. In MM cells a cascade of different pro-proliferative/anti-apoptotic signalling pathways is induced: The Ras/Raf/MAPK pathway, the PI3K/Akt pathway, the SFK pathway, the I kappa B kinase (IKK) nuclear factor kappa-B (NFκB) pathway and the JAK/STAT pathway. Further downstream these pathways lead for example to upregulation of anti-apoptotic

proteins of the Bcl-2 family, upregulation of cyclin D and cytoplasmatic sequestration of Forkhead transcription factors. The molecular events in the MM cell are either triggered directly via cell adhesion molecule-mediated interactions of MM cells with BMSC, osteoblast, BMECs, the ECM or other components of the BM microenvironment, or indirectly via cytokines and growth factors released by BMSCs and/ or MM cells. The number of factors that have a positive effect on MM cell survival and proliferation is still growing. Interleukin-6 (IL-6), insulin-like growth factors (IGFs), vascular endothelial growth factor (VEGF), serum derived factor-1 (SDF-1), TNF-α and transforming growth factor-b (TGF-β) are among the best studied factors [131; 140; 141; 244; 411]. Apart from their effects on MM cells the circulating factors have additional pleiotropic effects on cells of BM microenvironment, these effects can indirectly influence the fate of the MM cells. For example, TNF-α induces the activation of NFκB in BMSC. This leads to the upregulation of adhesion molecules on the surface and the secretion of IL-6 by the BMSC. In addition, adhesion of MM cells to BMSCs induces NFκB activation and IL-6 secretion [46; 143]. Secreted factors like IL-6, IL-1, macrophage inflammatory protein-1a (MIP-1α), SDF-1a and VEGF stimulate osteoclastogenesis which disturbes normal bone homeostasis and is one of the reason for the typical osteolytic bone lesions seen in MM patients [9; 124]. VEGF and basic fibroblast growth factor (bFGF) are at least in part responsible for the increased angiogenesis in MM [297]. The interaction of integrins expressed on the surface of MM cells with the ECM protein fibronectin leads to upregulation of p27Kip1 and c-FLIP which confers drug resistance [132; 133; 201].

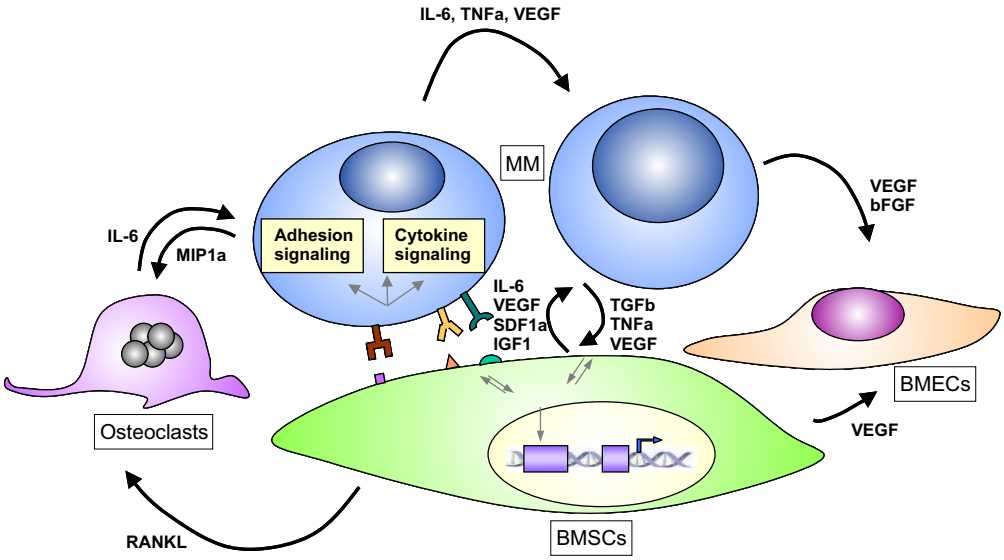

Figure 1.20. | **Interplay between myeloma and BMSC cells.**

1.4.6. IL-6 in multiple myeloma

IL-6 is one of the major growth factors for IL-6 in vivo and in vitro. IL-6 is produced in an autocrine fashion by the MM cells themselves or in a paracrine fashion by the surrounding BMSCs. The secretion of TNF-α [143], VEGF [68] and TGF-β [380] by the MM cells induces the production and secretion of IL-6 by the BMSCs. Apart from IL-6, IGF-1 [100] and IL-10 stimulate the proliferation of MM cells [82]. Clinically, serum IL-6 and IL-6 receptor (IL-6R) levels are the most important prognostic factors to determine the proliferative fraction of the MM cells and the tumor mass within the patient [12]. On the membrane of a target cell, binding of the IL-6-IL-6R complex promotes dimerization of gp130 and subsequent initiation of intracellular signalling (see section 1.3).

IL-6 based treatment strategies include monoclonal antibodies against IL-6 [310; 376] or IL-6R [415] and the superantagonist Sant7 [368]. All three strategies are designed to antagonize the downstream signalling from the IL-6 receptor complex. In clinical trails using antibodies against IL-6 or the IL-6R a transient response to the treatment is shown [310; 376; 411].

1.4.6.1. IL-6 dependence

In the progress of the disease MM cells can acquire secondary mutations (c-myc, p16, ras, p53 and others), which makes them independent of growth factors like IL-6. The isolation and cultivation of cell lines is difficult and generally more successful from late disease stages [193]. Currently, out of 112 described MM cell lines only 27 (~ 25 %), are IL-6-dependent [82]. IL-6 has a positive effect on the proliferation of IL-6-independent cells, in which the fraction of cells in the S-phase of the cell cycle is increased by IL-6 stimulation.

1.4.6.2. IL-6 downstream pathways in myeloma

IL-6 influences proliferation and survival of MM cells via different signalling pathways: (1) The activation of the JAK/STAT pathway leads to the up-regulation of anti-apoptotic proteins like Bcl-xL and Mcl-1, resulting in survival and resistance to apoptotic stimuli induced by chemotherapeutic drugs. (2) The MAPK pathway is activated via SHP-2, Shc, Grb2, Sos, Ras, Raf, Mek or via Gab and Src Family Kinases. (3) The PI3K/Akt pathway leads to the phosphorylation and inactivation of various anti-apoptotic proteins e.g. BAD, caspase-9, GSK3β and FKHR. Furthermore Akt phosphorylation leads to the activation of NFκB. NFκB

induces the transcription of pro-survival/anti-apoptotic mediators, for instance IL-6 itself, cell adhesion molecules, Bcl-xL, IAPs and cyclin D1. Cross talk between the PI3K/Akt pathway and the MAPK pathway is known to occure. (4) The activation of SFKs by CD45 leads to the activation of PLCγ_2, Ca^{2+} release form the ER and the activation of PKC-β [109; 121–123; 141; 167; 284]. Taken together, IL-6 pushes the equilibrium between survival/proliferation and apoptosis/cell death toward survival and proliferation.

1.4.7. Cytokines and resistance to chemotherapy

IL-6 and IGF-1 are known to protect MM cells from drug-induced apoptosis by signalling via the PI3K/Akt and MAPK pathways. IL-6 and IGF-1 both protect myeloma cells against glucocorticoid induced apoptosis [45; 263; 406]. Glucocorticoids especially dexamethasone (Dex) are used in standard chemotherapeutic regimes in patients. However, the mechanism how these cytokines confer to drug resistance is not fully understood. Apart from various cytokines, cell-cell contacts and cell adhesion molecules lead to the activation of pathways which result in survival and proliferation. However a generally accepted model, integrating the different stimuli and signalling pathways with respect to spatial and temporal distribution is not yet available.

1.5. Thesis proposal

The role of the multifunctional cytokine IL-6 as the major growth factor for multiple myeloma cells is supported by clinical data, transgenic mouse models and signalling studies (Section 1.4). SFKs are potential intracellular targets for blocking IL-6 signalling (Sections 1.1 and 1.3). Recently, the Hck binding region of gp130 was mapped to positions 771-811 and was termed acidic domain (AD) [323]. Aims of this thesis are:

(1) To identify the minimal interaction region between gp130 and the SFK Hck.

(2) To characterize the cellular effects of a lipopetide (peptide 18AD), derived from the identified interaction region, on myeloma cells.

(3) To elucidate the molecular basis for the biological effects of peptide 18AD.

(4) To generate novel more potent lipopeptides and to charaterize the biological effects of these peptides on myeloma cells.

2. Materials and Methods

2.1. Materials

2.1.1. Equipment

- -80°C Freezer, Heraeus, Hanau, Germany
- 0.22 μm sterile filters, Millipore, Bedford, MA, USA
- 40 μm sterile cell strainers, BD Biosciences
- Automatic pipets, Gilson, Middleton, WI, USA
- Cell counting chambers, Neubauer, Germany
- Cell freezing containers, Nalgene, Neerijse, Belgium
- Centrifuges, Eppendorf, Hamburg, Germany
- CO_2 Incubators, WTB Binder, Tuttlingen, Germany
- Confocal Microskope, Leica Microsystems, Wetzlar, Germany
- Electrophoresis cells and blotting systems, Biorad, Hercules,CA, USA
- Flow cytometers, Coulter EPICS XL-4, Beckman Coulter GmbH, Krefeld, Germany, FACSScan, BD Biosciences, Heidelberg, Germany
- Heating blocks, Techne, Cambridge, UK
- Laminar flow hoods, BDK, Sonnenbuehl, Germany
- Liquid nitrogen tank, Cryoson, Schoellkrippen, German
- Microscopes, Zeiss, Oberkochen, Leica Microsystems, Wetzlar, Germany
- Modular Flow cytometer (MoFlo), Cytomation, Fort Collins,USA
- pH-meter, WTW, Weilheim, Germany
- Spectrophotometer, Eppendorf, Hamburg, Germany
- Sterile cryotube vials, Nunc, Roskilde, Denmark
- Sterile tissue culture plastic pipets, tubes, dishes, flasks and cell scrapers, Sarstedt, Newton, USA
- Thermocycler, Perkin Elmer, Norwalk, USA
- Vacuum driven disposable filtration systems, Millipore, Bedford,MA, USA
- Vortex, Heidolph, Kelheim, Germany
- Water bath, Koettermann, Haenigsen, Germany

2.1.2. Reagents

- 1-Ethyl-3-(3-dimethylaminopropyl)-carbodiimide (EDAC), Molecular Probes, Leek, The Netherlands
- 2-Mercaptoethanol, Merck, Darmstatdt, Germany
- 5-(Aminoacetamido)fluorescein, Molecular Probes, Leek, The Netherlands
- 40 % Acrylamide-Bis (37,5:1) stock solution, Serva Electrophoresis GmbH, Germany
- Agarose (electrophoresis grade), Sigma-Aldrich Chemie GmbH, Steinheim, Germany
- Ammonium Persulfate, Bio-rad, Hercules, CA, USA
- Amprep C-18 columns, Amersham Biosciences, Freiburg, Germany
- Annexin-V-PE Apoptosis detection kit, BD Pharmingen, San Diego, USA
- BCA Protein assay reagent kit, Pierce, Rockford, IL, USA
- Calcium chloride, Sigma-Aldrich Chemie GmbH, Steinheim, Germany
- Cy5-NHS, Amersham Biosciences, Freiburg, Germany
- DNA isolation and purification kits, Qiagen, Hilden, Germany
- ECLWestern Blotting Detection System, Amersham Biosciences, Buckinghamshire, England, UK
- EDTA, Sigma-Aldrich Chemie GmbH, Steinheim, Germany
- Effectene Transfection Reagent, Qiagen, Hilden, Germany
- Ethanol, Merck, Darmstatdt, Germany
- Ethidium Bromide (10 mg/ml), Sigma-Aldrich Chemie GmbH, Steinheim, Germany
- Gelatine, Merck, Darmstatdt, Germany
- Glycerol, Merck, Darmstatdt, Germany
- Glycine, Merck, Darmstatdt, Germany
- High performance chemiluminescence film, Amersham Biosciences, Buckinghamshire, England, UK
- Immobilon-P PVDF Transfer Membrane, Millipore, Bedford, MA, USA
- Isopropanol, Merck, Darmstatdt, Germany
- LB medium, Invitrogen, Karlsruhe, Germahy
- Lipofectamine 2000, Transfection Reagent, Invitrogen, Carlsbad, California, USA
- Luria agar, Gibco, Eggenstein, Germany
- Methanol, Merck, Darmstatdt, Germany
- Mycoplasma detection kit for conventional PCR, Minerva Biolabs, Berlin, Germany
- N-hydroxysulfoscuccinimide (NHS), Molecular Probes, Leek, The Netherlands
- Nonidet P-40, ICN Biomedicals, Aurora, Ohio, USA
- Phosphatase inhibitor cocktail II for tyrosine protein phosphatases, acid and

alkaline Phosphatases, Sigma, Saint Louis,USA
- Ponceau S, Sigma-Aldrich Chemie GmbH, Steinheim, Germany
- Primers, Metabion, Martinsried, Germany
- Protease inhibitor cocktail, Sigma, Saint Louis, Missouri, USA
- Protein A/G-Agarose, Roche, Mannheim, Germany
- Purified recombinant murine erythropoietin (EPO), Roche, Mannheim, Germany
- Purified recombinant murine IL-3, Biosource International, Nivelles, Belgium
- Purified recombinant human IL-6, RnD Systems, Wiesbaden, Germany
- Purified recombinante soluble human TRAIL, (SuperkillerTRAIL^{TM}), Alexis Corporation, Lausen, Swizerland
- Restriction endonucleases and DNA modifying enzymes, New England Biolabs, Beverly, MA, USA
- SDS (electrophoresis grade), Merck, Darmstatdt, Germany
- SDS-PAGE loading buffer Roti Load (4X concentrate), Roth, Karlsruhe, Germany
- SDS-PAGE Molecular Weight Standarts, MBI-Fermentas, St. Leon-Rot, Germany
- Silver Nitrate, Merck, Darmstatdt, Germany
- Skim Milk Powder (blotting grade), Roth, Karlsruhe, Germany
- Sodium Orthovanadate, Sigma-Aldrich Chemie GmbH, Steinheim, Germany
- TEMED, Roth, Karlsruhe, Germany
- Tween 20, Sigma-Aldrich Chemie GmbH, Steinheim, Germany
- Vybrant Lipid Raft Labeling Kit, Molecular Probes, Leek, The Netherlands

2.1.3. Peptides

- P1: Myr-VPSVQVFSRSESTQPLLDSE-$CONH_2$
- P2: Myr-RSESTQPLLDSEERP-$CONH_2$
- P4: Myr-LLDSEERPEDLQLVD-$CONH_2$
- P5: Myr-ERPEDLQLVDHVDGGDGILPR-$CONH_2$
- P6: Myr-EDLQLVDHVDGG-$CONH_2$
- P7: Myr-HVDGGDGILPR-$CONH_2$
- 18AD: Myr-TQPLLDSEERPEDLQLVD-$CONH_2$
- 18nm: TQPLLDSEERPEDLQLVD-$CONH_2$
- 18sc: Myr-DRQESLVPLTEQLDPELD-$CONH_2$
- 18AD-bio: Bio-SGSGCTQPLLDSEERPEDLQLVD-$CONH_2$
- 18sc-bio: Bio-SGSGCDRQESLVPLTEQLDPELD-$CONH_2$
- 8AD: Myr-SEERPEDL-$CONH_2$
- 8sc: Myr-LESDPERE-$CONH_2$

- 0B: Myr-ktqPLLDSEERPEDLQlvd-$CONH_2$
- 1A: Myr-ktqPLLASAARPAALQlvd-$CONH_2$
- 1Asc-01: Myr-klaDAPVSLTPALQAQalr-$CONH_2$
- 1Asc-03: Myr-klsTAPAVDLPQRAAAlrl-$CONH_2$
- 1Abio: Myr-k(C6bio)-tqPLLASAARPAALQlvd-$CONH_2$
- 1Asc-01bio: Myr-k(C6bio)laDAPVSLTPALQAQalr-$CONH_2$
- SH2-bio: bio-SGSGC-EPQpYEEIPIYL-$CONH_2$

C-terminally amidated peptides (purity >95 %) were synthesized by Fmoc solid phase peptide synthesis and purified by reverse phase high performance liquid chromatography (HPLC) partly as custom syntheses by Clonestar Ltd. (Bristol, UK) and GeneMed Synthesis Inc. (South San Francisco, CA, USA). The myristoyl modification was at the N-terminus. Identity and purity were confirmed by HPLC-mass spectroscopy. 100 mM stock solutions of the peptides were prepared in DMSO and stored at -20°C for up to one year. For pull down assays with peptide 18AD N-terminally biotinylated peptides were synthesized that contained the N-terminal linker sequence SGSGC [333]. The sequnence of the SH2-binding control peptide was taken from [198].

2.1.4. Plasmids

Vector	Insert	Origin
pApuro	-	Dr. S. Corey, Pitsburgh, USA
pApuro	Hck wt	Dr. S. Corey, Pitsburgh, USA
pCDNA3.1^{TM}/His(-)A	-	Invitrogen, Karlsruhe, Germany
pCDNA3.1^{TM}/His(-)A	Hck wt	Dr. O. Mitina, University of Munich
pCDNA3.1^{TM}/His(-)A	Hck Y501F	Dr. O. Mitina, University of Munich
pCDNA3.1^{TM}/His(-)A	Hck K269R	Dr. O. Mitina, University of Munich
pCDNA3.1^{TM}/His(-)A	Eg	Dr. M. Schaeffer, CreRlux, Munich
pCDNA3.1^{TM}/His(-)A	Eg_del41AD	Dr. M. Schaeffer, CreRlux, Munich
pCDNA3.1^{TM}/His(-)A	Eg_del18AD	constructed by PCR mutagenesis
pCDNA3.1^{TM}/His(-)A	Eg_del8AD	constructed by PCR mutagenesis
pCDNA6/V5-HisA	-	Invitrogen, Karlsruhe, Germany
pCDNA6/V5-HisA	Eg	Dr. M. Schaeffer, CreRlux, Munich
pCDNA6/V5-HisA	Eg_del41AD	Dr. M. Schaeffer, CreRlux, Munich

Vector	Insert	Origin
pCDNA6/V5-HisA	Eg_del18AD	cloned from pCDNA3.1^{TM}/His(-)A Eg_del18AD via EcoRI/BamHI restriction sites into pCDNA6/V5-HisA Eg
pCDNA6/V5-HisA	Eg_del8AD	cloned from pCDNA3.1^{TM}/His(-)A Eg_del18AD via EcoRI/BamHI restriction sites into pCDNA6/V5-HisA Eg
pMSCV-IRES-EGFP	-	Dr. R. Van Etten, Boston, MA, USA
pMSCV-IRES-EGFP	Hck wt	Dr. O. Mitina, University of Munich
pMSCV-IRES-EGFP	Hck Y501F	Dr. O. Mitina, University of Munich
pMSCV-IRES-EGFP	Hck K269R	Dr. O. Mitina, University of Munich
pCDNA3 GFP	-	Dr. K. Foster, University of Munich
pMCV-ecopac	-	Dr. R. Van Etten, Boston, MA, USA

Table 2.1. | **Plasmids.**

2.1.5. Primers

- Eg_del18ADfw: 5'-TTC TCA AGA TCC GAG TCT CAT GTA GAT GGC GGT GAT-3'
- Eg_del18ADrev: 5'-ATC ACC GCC ATC TAC ATG AGA CTC GGA TCT TGA GAA-3'
- Eg_del8ADfw: 5'-ACC CAG CCC TTG TTA GAT CAA TTA GTA GAT CAT GTA-3'
- Eg_del8ADrev: 5'-TAC ATG ATC TAC TAA TTG ATC TAA CAA GGG CTG GGT-3'
- EcosfP: 5'-CTG ACC GCT AGC GAA TTC ACT TTT ACT ACC-3'
- EcosfP2: 5-AGC GAA TTC ACT TTT ACT ACC-3'
- BamafP: 5'-GGT ACC GAG CTC GGA TCC CTG AGG CAT GTA GCC-3'
- BamafP2: 5'-GGA TCC CTG AGG CAT GTA GCC-3'

2.1.6. Antibodies

Specificity	Type	Supplier, No.
Antigene		
Actin	rabbit polyclonal	Sigma, St.Louis, USA, A5060
β-tubulin (H235)	rabbit polyclonal	Santa Cruz Biotechnology, Santa Cruz, CA, USA, sc-9104
c-Src (N-16)	rabbit polyclonal	Santa Cruz Biotechnology, Santa Cruz, CA, USA, sc-19
c-Src (B-12)	mouse monoclonal	Santa Cruz Biotechnology, Santa Cruz, CA, USA, sc-8056
cl.-Caspase-3 (Asp175)	rabbit polyclonal	Cell Signaling Technology, Beverly, MA,USA, 9661
cl.-PARP (Asp214)	rabbit polyclonal	Cell Signaling Technology, Beverly, MA, USA, 9541
Fyn (FYN3)	rabbit polyclonal	Santa Cruz Biotechnology, Santa Cruz, CA, USA, sc-16
Fyn (15)	mouse monoclonal	Santa Cruz Biotechnology, Santa Cruz, CA, USA, sc-435
GFP	rabbit polyclonal	Invitrogen, Karlsruhe, Germany, A11122
gp130 (M20)	rabbit polyclonal	Santa Cruz Biotechnology, Santa Cruz, CA, USA, sc-656
Hck (N30)	rabbit polyclonal	Santa Cruz Biotechnology, Santa Cruz, CA, USA, sc-72
Hck(h)	mouse monoclonal	BD Biosciences, San Jose, CA, USA, H28520
Hck(m) (M28)	goat polyclonal	Santa Cruz Biotechnology, Santa Cruz, CA, USA, sc-1428
Lyn (44)	rabbit polyclonal	Santa Cruz Biotechnology, Santa Cruz, CA, USA, sc-15
Lyn	mouse monoclonal	BD Biosciences, San Jose, CA, USA, L05620
PARP (H250)	rabbit polyclonal	Santa Cruz Biotechnology, Santa Cruz, CA, USA, sc-7156
STAT3 (C20)	rabbit polyclonal	Santa Cruz Biotechnology, Santa Cruz, CA, USA, sc-482
Tag-specific		
c-myc(9E10)	mouse monoclonal	Roche, Mannheim, Germany, 11667149001

Specificity	Type	Supplier, No.
V5	mouse monoclonal	Invitrogen, Karlsruhe, Germany, R960-25
V5-HRP	mouse monoclonal, HRP-conjugate, Invitrogen, Karlsruhe, Germany, R961-25	
phosohorylated Epitopes		
phosho-Akt (Ser 473)	rabbit polyclonal	Cell Signaling Technology, Beverly, MA, USA, 9271
phosho-Erk1/2 (Thr 202/Tyr 204)	rabbit polyclonal	Cell Signaling Technology, Beverly, MA, USA, 9101
phosho-GSK-3α/β (Ser 21/9)	rabbit polyclonal	Cell Signaling Technology, Beverly, MA, USA, 9331
phospho-p38 (Thr 180/Tyr 182)	rabbit polyclonal	Cell Signaling Technology, Beverly, MA, USA, 9211
phospho-Src-Family (Tyr 416)	rabbit polyclonal	Cell Signaling Technology, Beverly, MA, USA, 2101
phospho-STAT3 (Tyr 705)	rabbit polyclonal	Cell Signaling Technology, Beverly, MA, USA, 9131
phosph-Tyr (PY99)	mouse monoclonal	Santa Cruz Biotechnology, Santa Cruz, CA, USA, sc-7020
phosph-Tyr (PY20-HRP)	mouse monoclonal, HRP-conjugate	Santa Cruz Biotechnology, Santa Cruz, CA, USA, sc-508
phosph-Tyr (4G10))	mouse monoclonal	Upstate, Charlottesville,VA, USA, 05-321
Isotype controls		
mouse IgG	mouse	Santa Cruz Biotechnology, Santa Cruz, CA, USA, sc-2025
rabbit IgG	rabbit	Santa Cruz Biotechnology, Santa Cruz, CA, USA, sc-2027
IgG_{2a}	mouse monoclonal	Dianova GmbH, Hamburg, Germany, DLN-05804
Secondary Detection		
Anti-mouse IgG	HRP-conjugated, sheep	Amersham Biosciences, Buckinghamshire,UK, NA931V
Anti-rabbit IgG	HRP-conjugated, donkey	Amersham Biosciences, Buckinghamshire,UK, NA9340V

Specificity	Type	Supplier, No.
Anti-rabbit-Cy3	Cy-3-conjugated, goat	Dianova GmbH, Hamburg, Germany, 107-165-142

Table 2.2. | **Antibodies.**

2.1.7. Bacterial strains

- DH5α, gift of Dr. A. Obermeier, Sirenade AG, Martinsried, Germany
- XL-1 Blue, Stratagene La Jolla, USA
- XL-10 Gold, Strategene, La Jolla, USA

2.1.8. Mammalian cell lines

Name	Disease	Description
7TD1	MM	murine, IL-6-dependent hybridoma cell line, [383], from DSMZ ACC 23, RPMI 1640 with 5 % FBS, 5 pM rh IL-6 and 50 μM 2-mercaptoethanol
INA-6	MM	human, IL-6-dependent myeloma, [35], from M. Gramatski, Christian Albrecht University, Kiel, Germany, RPMI 1640 with 10 % FBS, 5 pM rh IL-6 and 50 μM 2-mercaptoethanol
MM1.S	MM	human, IL-6-independent myeloma, [109], from ST Rosen, Northwestern University, Chicago,IL, USA, RPMI 1640 with 10 % FBS
HL-60	AML	human, c-myc gene amplification, from K. Spiekermann, KKG-Leukemia, GSF, Munich, Germany, DSMZ ACC 3, RPMI 1640 with 10 % FBS, [58]
Kasumi	AML	human, ETO-AML1 fusion, from K. Spiekermann, KKG-Leukemia, GSF, Munich, Germany, DSMZ ACC 220, RPMI 1640 with 10 % FBS, [81]
Mono-Mac-6 (MM6)	AML	human, MLL-AF9, from K. Spiekermann, KKG-Leukemia, GSF, Munich, Germany, DSMZ ACC 124, RPMI 1640 with 10 % FBS, [153]
MOLM	AML	human,Flt3 ITD mutation from K. Spiekermann, KKG-Leukemia, GSF, Munich, Germany, RPMI 1640 with 10 % FBS, [93]

Name	Disease	Description
MV4-11	AML	human, Flt3 ITD mutation, from K. Spiekermann, KKG-Leukemia, GSF, Munich, Germany, RPMI 1640 with 10 % FBS, [93]
Jurkat	T-ALL	human, from M. Dryling, KKG-Leukemia, GSF, Munich, Germany, DSMZ ACC 282, RPMI 1640 with 10 % FBS, [330]
U937	Lymphoma	human, from S. Bohlander, KKG-Leukemia, GSF, Munich, Germany, DSMZ ACC 5, RPMI 1640 with 10 % FBS, [365]
Granta-519	MCL	human, from M. Dryling, KKG-Leukemia, GSF, Munich, Germany, DSMZ ACC 342, RPMI 1640 with 20 % FBS, [80]
HBL-2	MCL	human, from M. Dryling, KKG-Leukemia, GSF, Munich, Germany, DSMZ ACC 342, RPMI 1640 with 20 % FBS, [80]
JEKO-1	MCL	human, from M. Dryling, KKG-Leukemia, GSF, Munich, Germany, DSMZ ACC 553, RPMI 1640 with 20 % FBS, [80]
NCEB-1	MCL	human, from M. Dryling, KKG-Leukemia, GSF, Munich, Germany, DSMZ, RPMI 1640 with 20 % FBS, [80]
Rec-1	MCL	human, from M. Dryling, KKG-Leukemia, GSF, Munich, Germany, DSMZ ACC 584, RPMI 1640 with 20 % FBS, [80]
Ba/F3	Pro B-cells	murine, IL-3-dependent, from M. Showers, Dana-Farber Cancer Institute, Bosten, MA, USA, RPMI 1640 with 10% FBS and 10 % WEHI-3B supernatent
Baf-EH	Pro B-cells	murine, IL-3-dependent or EPO-dependent, double transfectant of the cell line Ba/F3 with chimeric EPOR-gp130 and Hck, grown under selection by 8 μg/ml blasticidin and 5 μg/ml puromycin,RPMI 1640 with 10 % FBS and 10 % WEHI-3B suppernatent or rmEPO 8 U/ml [323]
HEK 293	Embryonic kidney	human, adenovirus (Ad5) transformed, DSMZ ACC 305, DMEM with 10 % FBS, [108]
COS-7	Kidney	african green monkey, SV 40 transformed, DSMZ ACC 60, DMEM with 10 % FBS, [105]

Name	Disease	Description
MCF-7	Breast cancer	human, from I. Jeremias, GSF, Munich, Germany, DSMZ ACC 115, RPMI 1640 with 10 % FBS, [358]
U373	Glioblastoma	human, from H. Erhardt GSF, Munich, Germany, DMEM with 10 % FBS,
A-498 (A34)	Renal carcinoma	human, from H. Erhardt,GSF, Munich, Germany, DSMZ ACC 55, RPMI 1640 with 10 % FBS, [102]
MEF	Embryonic fibroblast	murine, from A. Vollmer, Ludwig Maximilian University, Munich, Germany, DMEM with 10 % FBS,
Kelly	Neuroblastoma	human, from I. Jeremias, GSF, Munich, Germany, DSMZ ACC 355, RPMI 1640 with 10 % FBS, [334]

Table 2.3. | **Cell lines.**

2.2. Methods

2.2.1. Molecular biological techniques

2.2.1.1. Cultivation of bacteria

Bacteria a grown in LB-medium or on LB-plates at 37°C.

LB-medium/plates (High salt cond.)	*LB-medium/plates (Low salt cond.)*
1 % Trypton (w/v)	*1 % Trypton (w/v)*
0,5 % Yeast Extract (w/v)	*0,5 % Yeast Extract (w/v)*
1 % NaCl (w/v)	*0,5 % NaCl(w/v)*
1,5 % Agar (for plates)	*1,5 % Agar (for plates)*

Antibiotics were used according to the resistance present on the plasmids.

- Kanamycin 25 μg/ml
- Ampicilin 50-100 μg/ml
- Zeocin 25 μg/ml, low salt LB

2.2.1.2. Production of recombinant DNA plasmids

Production of DNA fragments of interest and their insertion into plasmid DNA is the first step in the generation of multiple copies of a plasmid DNA carrying the

gene/fragment of interest.

Digestion of plasmid DNA with restriction endonucleases Restriction endonucleases recognize short DNA sequences and cleave doublestranded DNA at specific sites within or adjacent to the recognition sequence. For effective cleavage, the enzyme is added to the DNA in the appropriate reaction conditions according to enzyme manufacturer's instructions.

Ligation T4 DNA Ligase catalyzes the formation of phosphodiester bonds between juxtaposed 5'-phosphate and and 3'-hydroxyl termini in duplex DNA. To join restriction fragments , DNA was dissolved in 1X T4 DNA Ligase reaction buffer and incubated with 40 U/μl of T4 DNA Ligase at 16°C for 3 h. Ligation mixture was used directly to transform competent E. coli.

Ligase-Buffer
50 mM Tris-HCl, pH 7.5
10 mM $MgCl_2$
10 mM DTT
1 mM ATP
25 μg/ml BSA

Amplification of DNA fragments by PCR PCR was used to amplify DNA fragments necessary for production of recombinant DNA plasmids. Optimal parameters for the PCR reaction, such as primer annealing temperature, elongation temperature and time were chosen individually for each reaction.

PCR Reaction Mixture
0,2 μM Primer (each)
50 μM dNTPs (each)
100 ng Template DNA
1x Polymerase buffer
1U Polymerase
Sterile PCR water

Generation of deletion constructs by PCR mutagenesis Initially, in two independent PCR reactions two deletion fragments, left and right from the deletion site that carry the deletion and overlap at the deletion site were generated. The second PCR combined both fragments.

First PCR	*Second PCR*
5 min 95°C	*5 min 95°C*
$\left\{ \begin{array}{l} 0.5\ min\ 95°C \\ 1\ min\ 55°C \\ 1\ min\ 72°C \end{array} \right\}$ *30 cycles*	$\left\{ \begin{array}{l} 0.5\ min\ 95°C \\ 1\ min\ 65°C \\ 1\ min\ 72°C \end{array} \right\}$ *30 cycles*
5 min 72°C	*5 min 72°C*
(1A) Primers:Eg_ del18ADfw and BamafP *(1B) Primers:Eg_ del18ADrev and EcosfP*	*(2A) Primers: EcosfP and BamafP*
5 µl of the two first PCRs were mixed and used as template for the second PCR	

Purification of DNA fragments after enzymatic reactions QIAquick PCR Purification kit and QIAquick Gel Extraction kit were used to purify DNA fragments after enzymatic reactions and agarose gel electrophoresis. In both kits spin-columns with silica membranes are used. At high concentration of chaotropic salts and optimal pH, DNA adsorbs to silica membranes while contaminants pass through. DNA is then eluted from the columns using sterile water.

Generation of competent bacteria High concentrations of certain divalent ions makes a small fraction of cells permeable to foreign DNA by a mechanism not yet understood. Bacteria that incorporated plasmid DNA, which carries antibiotic resistance gene, are selected by plating the cells on dishes containing nutrient, agar and appropriate antibiotic.

TfbI-Buffer	*TfbII-Buffer*
30 mM KOAc	*10 mM Na-MOPS*
50 mM $MnCl_2$	*10 mM KCl*
100 mM $CaCl_2$	*5 mM* $CaCl_2$
15 % Glycerin	*15 % Glycerin*

Cells were grown over night on LB-$MgCl_2$-plates, a single colony was picked and inoculated over night in 10 ml liquid culture at 37°C in LB-$MgCl_2$-medium. The culture was diluted 1:10 in LB-$MgCl_2$-medium and the bacteria were grown with shaking at 200 rpm until cell densities reached an OD_{600} of 0,5-0,9. The cells were harvested and transfered to pre-chilled 50 ml tubes, left on ice for 5-10 min and centrifuged for 5-10 min at 4°C with 1000-3000xg (depending on the strain). The cell pellet was resuspended in 10 ml of ice cold $CaCl_2$ solution. Cells were

then centrifuged for 5 min at 1100xg, 4°C. Each cell pellet (of 50 ml culture) was resuspended in 15 ml of ice cold TbfI buffer and left on ice for 10-15 min DH5α and XL-10 and 30 min for XL-1 blue. Cells were pelleted by centrifugation for 5-10 min at 3000xg, 4°C. Each cell pellet was resuspended in 4-8 ml (2-4 ml XL-10) of ice cold TbfII buffer. 100 μl cells were dispensed into prechilled sterile 0.5 ml tubes and frozen immediately in liquid Nitrogen and stored at -80°C.

Transformation of Bacteria Competent Bacteria were thawed on ice immediately before use. Plasmid DNA (1-10 ng) or 10 μl of the ligation reaction was added to one vial of bacteria. (For competet XL-1 blue 2 μl β-mercaptoethanol was added before the addition of DNA. Cells were left on ice for 10 min (DH5α) or 30 min (XL-1 Blue). Heat shock was performed in a water bath for 45-60 sec. Cells were put on ice for 1-2 min. 500 μl pre-warmed SOC-medium was added to the cells and they were grown (shaking) for 45-60 min at 37°C. Cells were pelleted by centrifugation and plated.

SOC-Medium
2 % Trypton (w/v)
0,5 % Yeast Extract(w/v)
0,05 % NaCl (w/v)
pH to 7.0, sterilized by autoclaving
10 mM $MgCl_2$ (sterile, v/v)
10 mM $MgSO_4$ (sterile, v/v)
20 mM Glucose (sterile, v/v)

2.2.2. Manipulating mammalian cells

2.2.2.1. Transfection of plasmid DNA into mammalian cells

Calcium phosphate method In this approach precipitate containing calcium phosphate and DNA is formed by mixing HEPES buffered saline solution (HBS) with a solution containing calcium chloride and DNA. The precipitate adheres to the surface of the cells and is taken up by the cells via yet unknown mechanism.

HBS-Buffer
50 mM Hepes
280 mM NaCl
*1.5 mM NaP**
filter sterilized

*pH is adjusted with NaOH to 7.2. *NaP is 1:1 mixture of equal molar amounts of Na_2HPO_4 and NaH_2PO_4. pH range of HBS solution optimal for transfection is very narrow. Therefore, 5 aliquots of HBS solution with pH ranging from 6.6 to 7.8 with the step of 0.3 were prepared and tested using pCDNA3 GFP for the highest transfection effciency.*

$CaCl_2$ Solution
250 mM $CaCl_2$
filter sterilized

250 mM $CaCl_2$ Solution was prepared shortly before transfection by diluting 2.5 M $CaCl_2$ stock solution using sterile endotoxin-tested water (Sigma, USA).

The day before transfection HEK 293 cells were seeded at 1.7x10^6 cells per 60 mm plate. 5-10 μg of DNA was diluted in 119 μl of 250 mM $CaCl_2$ solution. Components were mixed by vortexing briefly at low speed. 119 μl of HBS the solution was added dropwise to DNA/ $CaCl_2$ mixture and tubes were vortexed immediately for 3-4 sec at low speed. Culture medium was changed to 4 ml of fresh medium and DNA/ $CaCl_2$/ HBS mixture was added to the cells dropwise within two minutes after addition of HBS buffer. 12-24 h after the transfection, culture medium was changed to 4 ml of fresh medium. 36-48 h after transfections cells were either lysed or supernatant containing recombinant retrovirus was harvested.

Lipofection Kationic lipids from complexes with negatively charged plasmid DNA, which can pass the plasma membrane of mammalian cells. HEK 293 and Cos7 cells were transfected with Lipofectamine 2000 or Effecten.

Using Lipofectamie 2000: Cells were seeded in 6 well plates the day before transfection to reach 80-90 % confluence at the day of transfection. 4 μg plasmid-DNA and 10 μl Lipofectamine 2000 were mixed with 250 μl pre-warmed serum and antibiotic free medium, respectively . After 5 min incubation at room temperature, the two solutions are carefully combined and incubated for 20 min. Immediately prior to the addition of the DNA-lipid complexes, the medium was exchanged to 1 ml fresh pre-warmed medium containing serum. The DNA-lipid complexes were added drop wise to the cells while shaking the plate carefully. After 6 h the medium was exchanged. Protein expression of the transfected constructs was analyzed 24-48 h after transfection.

Using Effecten: Cells were seeded in 6 well plates the day before transfection to reach 60-80 % confluence at the day of transfection. 1 μg of plasmid DNA was diluted in 100 μl of buffer EC and 6 μl Enhancer solution was added. The mixture was vortexed and incubated for 5 min at room temperature. 7 μl of Effecten

reagent was added, vortexed for 10 sec and incubated at room temperature for 10 min. The medium was aspirated from the cells and 2 ml fresh medium with reduced glucose (1.5 g/l instead of 4.0 g/l) was added to the cells. The DNA-lipid complexes were added drop wise to the cells while shaking the plate carefully. After 6 h the medium was exchanged. Protein expression of the transfected constructs was analyzed 24-48 h after transfection.

2.2.2.2. Retroviral transduction

Production of recombinant retrovirus Recombinant replication-incompetent retroviruses have been generated by co-transfecting HEK-293 cells with the packaging vector (ecopac) and the retroviral vector pMSCV IRES EGFP. The packaging vector carries retroviral *gag*, *pol* and *env* genes that are required for replication of retrovirus. Retroviral vector carries the gene of interest,$\Psi+$ packaging signal and LTRs, which encode most of the viral control elements including promoter, enchancer, the polyadenylation signal and the integration signal. HEK-293 cells were co-transfected with ecopac and appropriated retroviral vector using calcium phosphate method. 10 μg of retroviral vector and 5 μg of ecopac were usually used per transfection of 80-90 % confluent cells in 60 mm dishes. 12 h after the transfection, medium was changed to 3 ml of fresh medium. Supernatant, containing recombinant retrovirus was harvested 36-48 h after the transfection, aliquoted and stored at -80°C.

To generate cell lines, in which most cells have single proviruses, infections effciency was kept at 10 % or lower. To normalize between different viral stocks, 7TD1 cells were infected with serial dilutions of retrovirus. Infection effciency was measured 36-48 h after the infection by FACS analysis of GFP expression. Dilutions, at which infection eciency was 10 % or less were used for infection. To generate 7TD1-derivative cell lines, the cells were incubated with the retrovirus in the presence of polycations (Polybrene).

Polybrene Solution
800 μg/ml of Polybrene in H_2O filter sterilized

$5x10^4$ 7TD1 cells per infection were resuspended in 250 μl Medium, in 24-well plate. 16 μg/ml (2x final concentration) of polybrene and the appropriate amount of virus was added to the cells and mixed. After 3-5 h, 1.5 ml of fresh medium was then added to the cells. GFP-expressing retrovirus-transduced cells were selected by flow-cytometric cell sorting on a modular flow cytometer 48 h after infection.

2.2.3. Analysis of mammalian cells

2.2.3.1. Proliferation assays

Trypan blue exclusion assay Determination of living cell densities by microscopic cell counting after trypan blue staining. Dying cells lose the integrity of the plasma membrane. These cells can be detected using exclusion dyes such as trypan blue. Trypan blue stains only those cells, which have lost the membrane integrity, leaving cells with intact plasma membrane unstained.

2,5-5x10^5 per ml of Baf-B03 or BaF-EH cells, wt 7TD1 cells, or polyclonal retrovirally transduced 7TD1 populations were seeded in 96 well plates, respectively. For the analysis of growth kinetics, 1-2x10^5 per ml INA-6, MM1S and 7TD1 cells were seeded in 24 well plates. Two days prior to these experiments, cells were seeded in equal concentrations into tissue culture flasks. All assays were performed with PBS-washed cells in the growth media of 7TD1 or BaF-EH cells without antibiotic selection. Factor-dependent cell lines were stimulated with 8 U/ml of rmEpo, 5 U/ml of rmIL-3, or 80 pg/ml (7TD1) to 1 ng/ml (INA-6) rhIL-6, as applicable and unless indicated otherwise. After the incubation for 72 h or 96 h at 37°C, the proliferation was assessed by microscopic cell counting after trypan blue staining. For growth kinetics cells were counted every 12-24 h.

Cell Screen assay Determination of cellular proliferation by automated microscopic cell counting and density determination. Cells were cultivated and seeded in 96 well plates as described above. Peptides were diluted in medium and added to the cells. When different concentrations of peptide were assessed, the concentration of the vehicle DMSO was adjusted to the maximal concentration. The proliferation was assayed every 12-24 h by microscopic cell counting. (Cell Screen). To calculate the rate of proliferation at different peptide concentrations, growth curves were generated from the average of triplicates from each experiment and growth rates were calculated by linear interpolation. To compare the effects of the different peptide concentrations on the different cell lines, the growth rate of vehicle treated cells from each cell line was used as the reference value and set to 100 %.

2.2.3.2. Viability assay

Suspension cells: Cellular viability of suspension cells can be determined by analyzing the light scattering of the cells. Life cells are bigger and less granular

than dead cells. These differences can be determined by forward/sideward scatter (FSC/SSC) analysis in the flow cytometer. 36-48 h after peptide addition, when the proliferation assay was terminated, FSC/SSC-analysis was performed. From vehicle treated cells, the amount of living cells was taken as a reference value and set to 100 %.

Adherent cells: The viability of adherent cells can not be determined by analyzing size and granularity of the cells. Similar to trypan blue, the fluorescent dyes propidiumiodid (PI) and 7-aminoactinomycin (7-AAD) are impermeable for living cells at 4°C, while they stain dying and dead cells. The amount of stained and unstained cells can be determined by FACS analysis.

0.5-2x10^5 cells/ml per 96 well were seeded and the cells were incubated over night to allow attachment. The following day, medium was exchanged against medium containing peptides or vehicle. After 48 h cells were detached with 20 μl Trypsin-EDTA and washed with and resuspended in PBS. PI or 7-AAD was added and the cell suspension was incubated for 15 min on ice prior to FACS analysis.

IC_{50} values were calculated by linear interpolation. Error bars indicate standard errors of the means from triplicates. Statistical significance was determined by two-tailed Student's T-test.

2.2.4. Apoptosis measurement

Annexin-V-staining In normal cells phosphatydilserine is present in the inner leaflet of the plasma membrane, while outer leaflet contains mostly neutral phospholipids. However, as cells undergo apoptosis, loss of asymmetry in the plasma membrane phospholipids occurs. The amount of phosphatidylserine in the outer leaflet of the membrane increases. Annexin-V is a calcilum-dependent phospholipid binding protein, that has a great affinity for phosphatidylserine. Therefore, Annexin-V binds to the surface of apoptotic, but not normal cells. In late stage apoptotic cells and necrotic cells the membrane integrity is destroyed and Annexin-V can enter such cells and bind phosphatidylserine in the inner inner leaflet of cells. To discriminate between apoptotic and necrotic cells, staining with the vital dye 7-Amino-actinomycin (7-AAD) was performed in parallel to Annexin-V labeling. Cells were washed twice with PBS and resuspended in 100 μl freshly prepared Binding Buffer 2 μl of Annexin-V-PE or Annexin-V-FITC and 2 μl of 7-AAD was added to the cells. After 15 min incubation in the dark, 400 μl Binding-Buffer was added and FACS analysis was performed immediately, 5x10^4 cells were analysed for each sample.

Binding-Buffer
0.1 M Hepes, pH 7.4
1.4 M NaCl
25 mM $CaCl_2$
sterile

Cleavage of apoptosis specific substrate proteins Westernblot technique with antibodies which detect cleaved substrate protein fragments was used (Table 2.2).

2.2.4.1. Cell cycle analysis

Propidiumiodid (PI) is a DNA intercalating agent, which interacts stochiometrically with the cellular DNA. PI can be used to analyze the different cell cycle phase using flow cytometry techniques, because it interacts stochiometrically with cellular DNA. The DNA of cells from the G1-phase binds only half of the PI than that of cells from the G2-phase. DNA from S-phase cells binds more PI than DNA from G1-phase cells but less than that of G2-phase cells. To avoid the interaction between PI and RNA, staining is performed in the presence of RNAse.

Prior to FACS-Analysis, 2,5x10^4 cells were washed with PBS and fixed with 80 % Ethanol in PBS for 1 h to overnight. Cells were washed with PBS twice, resuspended in PI buffer and incubated for 30 min at 37°C in the dark.

PI-Buffer
0,1 % Citrat
10 µg/ml RNAse A
10 µg/ml Propidiumiodid (PI)

2.2.4.2. Peptide incorporation

100 µM of each fluorescence-labelled peptide derivative was added to the growth medium of 7TD1 cells and incubated at 37 °C for 15 minutes. After thorough washing and protease treatment to degrade attached labelled peptide, the percentage of fluorescent cells was determined by FACS analysis.

2.2.5. Immunofluorescence (IF) analysis

Immunofluorescence techniques allow to analyze the localisation of proteins and provide insight in the spacio-temporal nature of cellular processes.

Detection of cellular proteins Adherent cells: HEK 293 or Cos7 cells were seeded on glass cover slips (CS, 50x24 mm) in 6 well plates and transfected with the respective constructs, 24-36 h after transfection IF analyses were started.

Suspension cells: CS were put in 6 well plates, coated with poly lysine for 15 min at 37°C and washed 3 times with PBS. 2-3x10^5 cells/ml INA-6 cells were treated with peptides, washed several times with PBS and 1.5 ml of the cell suspension was filled in the well containing the coated CS. Cells were allowed to attach to the CS for 15 min at 37°C.

Adherent and suspension cells: After wasing with PBS for 1-3 times, cells were fixed for 15 min with 3.7 % PFA at room temperature. Cells were incubated for 5 min in neutralization solution to stop the fixation reaction. To permeabilize the cells, Saponin containing permeabiliation solution is added and the cells are permeabilized for 5 min. To avoid unspecific antibody reaction, the fixed and permeabilized cells are incubated in blocking solution for 1 h in a humified chamber. To detect the proteins of interest, 4 μg/ml primary antibody is diluted in antibody diluent. Per CS 150-200 μl were added drop wise on the cells until the whole CS is covered with the antibody solution. Cells are incubated for 1 h at RT or over night at 4°C in a humified chamber. After 3 times washing with PBS for 10 min cells were incubated with the fluorophore conjugated secondary antibody or Alexa-488 conjugated avdin (1:200 in antibody diluents) for 1 h in the dark in a humified chamber. After 3 times washing with PBS, DNA was stained with DAPI (1:10000 in antibody diluents) for 10 min at room temperature in a humified chamber in the dark. CS were washed 2-4 with PBS. Superfrost slides were covered with 1-2 trops of vectorshield mounting medium and CS were sealed on the slides using nail polish. Slides were stored at 4°C in the dark and analyzed by epi- and or confocal fluorescence microscopy (modified from [316]). For confocal images a Leica TCS SRII system was used. The optical magnification was x630. the digital zoom of the microscope software was used to visualise individual cells. Images of optical sections (512 x 512 pixels) were digitally recorded. The resulting images were processed using Image J.

Lipid raft staining of suspension cells For co-staining of lipid rafts with peptides in INA-6 cells, cells were treated with peptide, washed several times with

PBS and were incubated with choleratoxin-B (CTX-B) 1 μg/ml for 10 min at 4°C after 2 washing steps with PBS CTX-B labeled lipid rafts were crosslinked using an anti-CTX-B antibody from rabbit (1:200 dilution in PBS) for 15 min at °4C and washed 2 times with PBS, prior to attachment on polylysine coated CS and fixation. Lipid rafts were visualised using an anti-rabbit-Cy3 conjugate antibody.

Fixation	*Neutralization*	*Permeabilisation*
3,7 % Paraformaldehyd freshly prepared in PBS	*100 nM Glycin in PBS*	*20 mM Glycin 0.1 % Saponin (w/v) in PBS*

Blocking	*Antibody diluents*
10 % FBS (heat inactivated) 0.1 % Saponin in PBS	*1.5 % BSA 0.1 % Saponin in PBS*

Permeabilisation with Saponin is reversible this is why 0.1 % Saponin is present in the antibody solution.

2.2.6. Analysing proteins

2.2.6.1. Factor stimulation and cellular lysis

2x10^7 suspension cells or one 60 mm dish transfected HEK293 cells per sample were starved by serum deprivation for 16-20 h. Stimulation by 1 ng IL-6/ml or 10 U Epo was performed for 1-15 min in 1 ml of medium at 37°C. Suspension cells were diluted immediately in 14 ml ice cold PBS containing 1 mM sodiumorthovanadate (phosphatase inhibitor) and washed with PBS (1 mM sodiumorthovanadate). Detergents and high salt concentration in the lysis buffer destroy the integrity of cellular membrans and solubizle proteins, which proteins are solubilzed dependend on the composition of the lysis buffer. Membranes and nonsolubilized proteins are precipitated by centrifugation. To prevent proteolyis, cellular lysis is performed on ice using ice cold reagents, EDTA is added to chelate divalent ions that are essential for metalloproteases and protease inhibitors are included in the lysis buffer. To maintain the phopsphorylation status of phosphoproteins, after factor stimulation, phosphate inhibitors are added to the lysis buffer.

Lysis-Buffer
20 mM Tris-HCl, pH 8.0
150 mM NaCl
10 % Glycerol
1 % NP-40
10 mM EDTA, pH 8.0
filter sterilized

Protease and phosphatase inhibitor cocktails were added freshly before cell lysis at 1:100 (v/v) dilution.

10 μl of ice cold lysis buffer per 1x10 ^{6} cells was added and the cells. They were incubated for 30 min on ice, vortexing for 3 sec every 5 min.

Aherent cells were immediately put on ice and washed twice with ice cold PBS containing 1 mM sodiumorthovanadate. 200 μl of ice cold lysis buffer per 60 mm was added to the cells and the cells were scraped of the plate and incubated on ice as described for suspension cells. Lysates were centrifuged at 20000xg for 15 min at 4°C to precipitate cellular debris. Lysates were used immediately for IP or Western blot or frozen at -80°C.

2.2.6.2. Protein concentration determination

The BCA Protein Assay Reagent kit, Pierce, USA, was used to measure protein concentration in cellular lysates. BCA method combines the reduction of Cu^{2+} to Cu^{1+} by proteins in an alkaline medium and selective colorimetric detection of the cuprous cation (Cu^{1+}) with a reagent containing bicinchoninic acid (BCA). The purple-colored reaction product of this assay is formed by the chelation of two molecules of BCA with one cuprous cation. This complex has a strong absorbance at 562 nm that is nearly linear with increasing protein concentrations.

2 μl of protein lysates were diluted in 98 μl of water. Protein standards for calibration were prepared by diluting 0, 5, 15 and 30 μg of bovine serum albumin (BSA) from 2 mg/ml stock solution in water to the final volume of 100 μl. Working BCA reagent was prepared freshly by mixing reagent A (containing bicinchoninic acid, sodium carbonate, sodium bicarbonate and sodium tartrate in 0.1M sodium hydroxide) and reagent B (containing 4 % cupric sulfate) from the kit at the ratio of 1:50 (v./v.). 900 μl of working reagent was added to protein samples diluted in water and components were mixed by inverting the tubes 3-4 times. Tubes were placed in 65°C water bath for 5 min. Tubes were allowed to cool down at room temperature for about 10 min. 562 nm absorbance of all samples was measured

using a spectrophotometer. Standard curve was prepared by plotting standard absorbance measurements against their protein concentrations. Equation of a linear fit curve was used to calculate protein concentration in each sample.

2.2.6.3. Immunoprecipitation

For each sample 30 μl of swollen protein A-or G-agarose suspension were pre-incubated with 1-3 μg of antibody at room temperature for 10 min. 200 μl of pre-cleared lysate containing 500 μg of protein were added to the antibody-coated protein-A or G-agarose and incubated for 1 h to over night at 4°C on an overhead rotator. Protein A- or G-immuno-complexes were pelleted by centrifugation at 1000xg at 4°C for 15 sec and washed 3 times with ice-cold IP wash buffer. After being boiled in 4 x sample buffer, the agarose beads were pelleted, and the eluates were analyzed by Western blotting.

IP Wash-Buffer
Lysis buffer with 0.1 % NP-40

Peptide competition assay For peptide competition analyses up to 150 nmol of peptide was added to the IP reaction of a lysate taken from HEK 293 cells which overexpress Hck wt in a volume of 200 μl an incubated for 3 h at 4°C. Pull downs were performed as described for immunoprecipitation using streptavidin-agarose.

Immunokomplex-kinase-assays PBS washed cells were deprived from IL-6 for 20 h. 1x10^6 cells/ml were incubated presence of 1 ng/ml IL-6 und 100 μM peptides for 1 h at 37°C. Cells were washed in PBS with 1 mM sodiumorthovanadate and lysed. Precipitation of the kinases was performed as described in: Wesern blot analysis and IP. Prior to the phosphorylation reaction, the IPs were washed once with Kinase-Assay Puffer . The kinase reaction was started by the addition 100 μM freshly prepared ATP-solution und 20 μg acid inactivated rabbit muscle enolase, as a substrate for SFKs. After 15 min incubation at 30°C the reaction was stopped by boiling the beads in 4x sample buffer.

Kinase Assay-Buffer
50mM Tris HCl pH 7.2
10mM $MgCl_2$
2mM DTT
0.01 % Tween 20
filter sterilized

2.2.6.4. SDS-PAGE

Separation of proteins by denaturing discontinuous polyacrylamide gel electrophoresis (PAGE). Proteins in the mixture from cell lysates are denatured by heating in the presence of 2-mercaptoethanol and SDS. Denatured polypeptides bind SDS and become negatively charged. The amount of bound SDS within the range of a certain molecular weight proportional to the molecular weight of a polypeptide, and is independent of its sequence. Therefore proteins and protein subunits are separated according to their size during migration through the pores in the gel matrix in response to an electrical field.

Protein samples for electrophoresis were prepared by dissolving a mixture of proteins in 4x-SDS-PAGE loading buffer, and heating up the samples at100°C for 5 minutes. Separation gels with the following dimensions were used: thickness 1.0 mm, length 7.3 cm and width 8.3 cm. Solutions for casting one 10 % separating and one stacking 7 % gel:

Solutions	*Stacking gel*	*Separating gel*
H_2O	*2.5 ml*	*2.075 ml*
40 % Acrylamide/Bisacrylamid	*1.25 ml*	*0.33 ml*
1.5 M Tris (pH 8.8)	*1.25 ml*	-
1.0 M Tris (pH 6.8)	-	*0.825 ml*
10 % SDS	*50 µl*	*33 µl*
10 % APS	*16.65 µl*	*17 µl*
TEMED	*7.0 µl*	*3.3 µl*

Proteins were separated at 120 V until the dye front has left the separation gel.

2.2.6.5. Western blot

Analysis of proteins on PVDF membrane by immunoblotting. Proteins are transferred to PVDF membrane using wet blotting technology. Specific antibodies are used to identify proteins transferred to PVDF membrane. First, membrane

is immersed in blocking buffer to fill all protein binding sites with non-reactive protein. Then the membrane is incubated in a solution containing antibody directed against the antigen(s) in the protein to be detected. Primary antibody bound to the protein of interest are recognized by secondary antibody conjugated with horseradish peroxidase (HRP). The complex containing the antigen, primary antibody and secondary antibody- horseradish peroxidase conjugate is detected by chemiluminecsent visualization using ECL detection system (Amersham Biosciences).

PVDF membranes were blocked in the blocking solution either for 1 h at room temperature or overnight at 4°C. G-NET blocking solution was used with phosphoprotein-specific antibodies and corresponding secondary antibodies, while milk blocking or BSA solution was used with all other antibodies. After blocking, membranes were transferred to the containers with primary antibody in 1 % milk blocking solution, 1 % BSA blocking solution or G-NET solution and incubated for either 1 h at room temperature or overnight at 4°C. After incubation with primary antibodies, membranes were washed 3 times for 10 minutes each time with TBS-T buffer. Washed membranes were transferred to the containers with secondary antibody-HRP conjugates in 1 % milk, 1 % BSA solution or G-NET solution and incubated for 30-60 min at room temperature. Blots were then washed 3 times for 10 minutes each time with TBS-T buffer the last wash was performed with TBS buffer. Excess of buffer was drained using tissue paper and 2 ml of freshly prepared ECL developing solution was added per blot. Membranes were incubated with ECL solution for 1 minute with slow rocking. Excess of ECL solution was drained using tissue paper. Membranes were exposed to Hyperfilm (Amersham Biosciences).

Transfer-Buffer	*TBS-T-Buffer*	*NET-Buffer, 10X*
250 mM Tris	*10 mM Tris-HCl, pH 8.0*	*0.5 M Tris, pH 7.5*
200 mM Glycine	*150 mM NaCl*	*1.5 M NaCl*
20 % Methanol	*0.01 % Tween*	*0.05 M EDTA, pH 8.0*
		0.5 % Triton X-100

Milk-Blocking	*BSA-Blocking*	*G-NET-Blocking**
5 % (w./v.) non-fat dry milk in TBS-T buffer	*BSA (Fraction V) in TBS-T buffer*	*2.5 %gelatine in 10xNET-Buffer*

**G-NET-Blocking was brought to boiling. The solution was then mixed using magnetic stir bar until it became clear. The volume was adjusted to 1000 ml with water.*

The public domain program Image J was used for determinations of signal strengths by densitometry.

2.2.7. Chemical peptide labeling

Labeling of carboxl groups In order to label peptide 18AD at available carboxyl groups, a ten-fold molar excess of each of the following three components, 5-(aminoacetamido)fluorescein, 1-ethyl-3-(3-dimethylaminopropyl)-carbodiimide - (EDAC) and N-hydroxyscuccinimide (NHS) was added to 1 mg of the peptide (0.45 μmol) in 0.1 M sodium phosphate buffer, pH 7.4. After two hours reaction at room temperature in the dark [107; 137]. The mixture was passed through a C18 cartridge (Amprep).

Labeling of amino groups Cy5-labelled peptide 18ADnm was prepared by reacting its accessible aminoend with Cy5-NHS. According to manufacturer´s instructions Cy5-NHS-ester (1 mg) was dissolved in 500 μl DMS0 and added to peptide 18nm (1 mg in 500 μl DMS0) the mixture was roled over night in the dark at room temperature, for the last two hours 20 μl triethylamin was added. Die mixture was purified with a C18 cartrigdge (Amprep).

Purification with C18 cartridges Sample buffer was mixed with sample (1:4). The column was activated using 4 bed volumes activating solution and equilibrated using 4 bed volumes wash solution. The sample was loaded on the column, to ensure complete binding the flow through was recovered and loaded on the column again. This step was repeated until the entire sample was loaded on the column. Subsequently the column was washed with 6 bed volumes wash solution. The sample was eluted with elution buffer in two steps. Eluates were dryed using a vacuum evaporator.

Sample-Buffer	*Activating Solution*	*Wash Solution*	*Elution-Buffer*
2 % (v./v.) TFA *20 % ACN*	*50 % Methanol*	*0.5 %TFA* *5 % ACN*	*70 % ACN*

2.2.7.1. Statistical Analysis

If not indicated differently, mean values and standard deviations are shown. Statistical significance is determined by two-tailed students t-test.

3. Results

The role of the multifunctional cytokine IL-6 as the major growth factor for multiple myeloma cells is supported by clinical data, transgenic mouse models and signalling studies (Section 1.4). SFKs are potential intracellular targets for blocking IL-6 signalling (Sections 1.1 and 1.3). Recently, the Hck binding region of gp130 was mapped to positions 771-811 and was termed acidic domain (AD) [323]. Aims of this thesis are to identify and characterise the minimal interaction region between gp130 and the SFK Hck. Initially a set of membrane-permeant peptides, representing overlapping fragments of the AD is used to refine the Hck binding site on gp130. The biological effects of the peptide, representing the Hck binding side are analysed in human and murine, IL-6-dependent and IL-6-independent myeloma cells. The molecular basis for the biological effects of the identified peptide are elucidated, using different experimental systems.

3.1. Peptide screen - Identification of an 18mer

To find out the minimal domain within the intracellular part of gp130, that is required for the interaction with SFKs and for the transduction of proliferation signals, a peptide-based functional screening assay is used to detect effects on growth and survival of 7TD1 cells. 7TD1 is a IL-6-dependent mouse hybridoma cell line, which is derived from the mouse myeloma cell line SP2 [383] and frequently used for IL-6 bioassays [214; 335]. A set of seven overlapping peptides is derived from the previously defined 41 aa Hck-binding region (Figure 3.1). The peptide sequences are chemically synthesized with a myristoyl moiety attached to their N-termini in order to enable them to cross cell membranes. Their capability to inhibit IL-6 dependent growth of 7TD1 cells is monitored by observing the cell densities reached in the presence of 40 pg IL-6/ml and after addition of 50 or 100 μM of the individual peptide sequences (Figure 3.1). Among the tested peptides, the 18mer sequence of P3 comprising aa 783-800 of gp130 shows the biggest inhibitory effect at both peptide doses. Therefore P3, that contained six acidic residues, is selected for further studies and termed peptide 18AD. To determine the specific role of the sequence context, a myristoylated peptide with an identical aa composition but

arbitrarily scrambled sequence, peptide 18sc, which is expected to have similar physicochemical properties, is used as a control. The effects of both peptides on 7TD1 cells are compared. In the presence of 100 μM of peptide 18AD, 7TD1 cells stimulated with IL-6 attain only about 25 % of the cell densities obtained with IL-6 alone or in the presence of the control peptide 18sc (Figure 3.2).

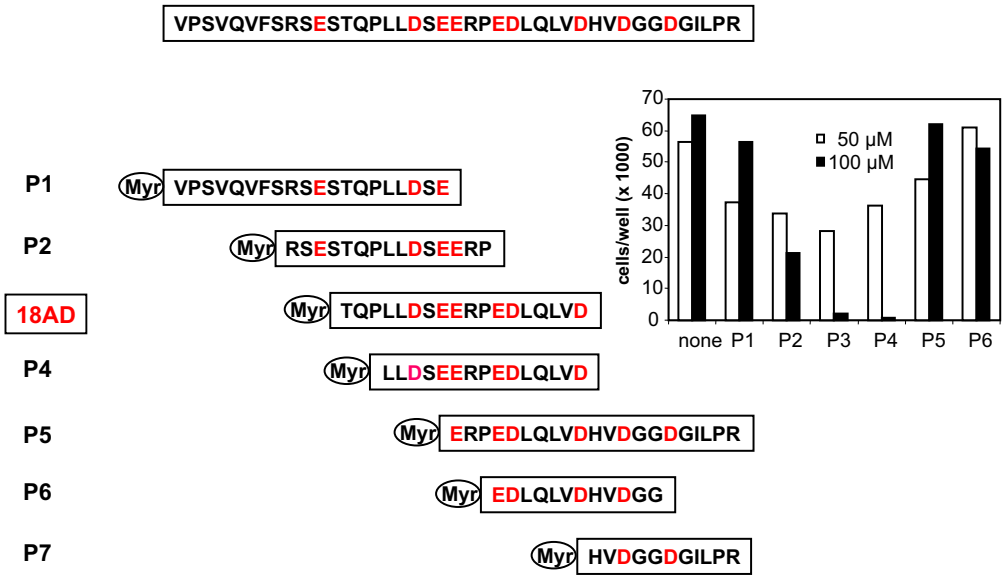

Figure 3.1. | **Peptide screen.** The acidic domain (AD) of gp130 and the sequences of peptides P1-P7, which were synthesised in order to facilitate more precise mapping of the AD. Insert: Inhibitory potency of the different peptides in a functional assay. The results were kindly provided by Dr. R. Tavares-Krause.

3.2. Cellular uptake of myristoylated peptide

Strategies to deliver peptides to the cytoplasm include conjugation to membrane penetrating sequences, fatty acids [2; 86] or hydrophobic fluorescence dyes [23]. Since Hck is a SFK carrying a N-terminal myristoyl moiety, this fatty acid modification is chosen to render peptides cell membrane-permeant. Whereas classical ligands bind to the extracellular surface of their cognate receptors, cell-penetrating peptides, e.g. so-called pepducins [66], need to be used for disrupting intracellular protein-protein interactions, which are e.g. important for G protein-coupled receptor signalling. Membrane penetrating peptides were also used for blocking the transduction of proliferation signals via the MAPKs JNK [26] or ERK [181]. Cellular uptake of the tested peptide sequences is a prerequisite for their efficacy

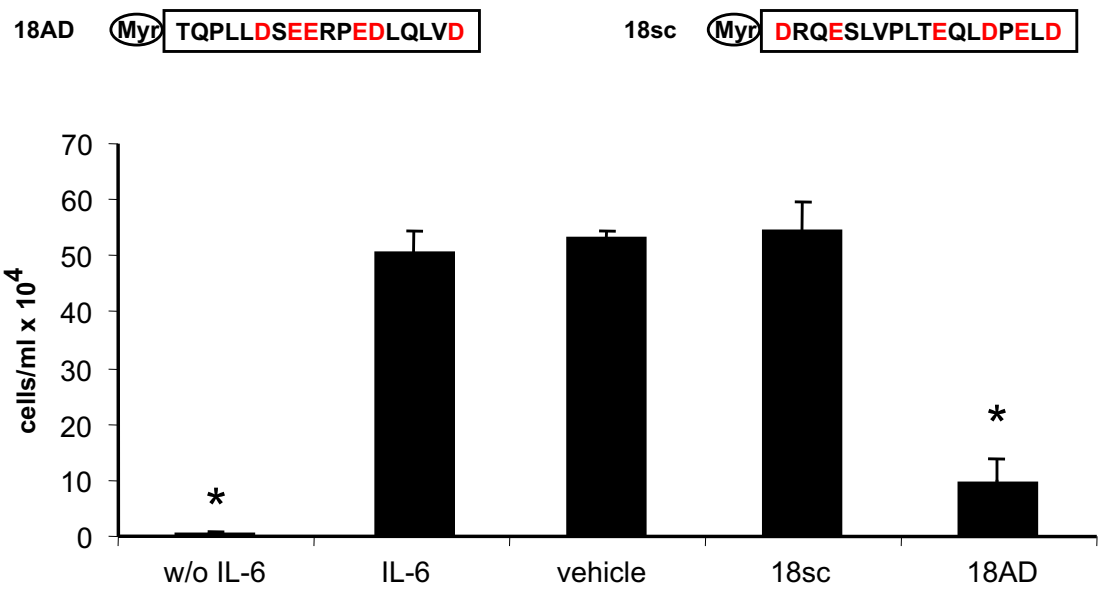

Figure 3.2. | **Peptide 18AD.** Effects of peptides 18AD and 18sc on the IL-6-dependent growth of 7TD1 cells. One 100 μM peptides are used with 0.1 % DMSO as vehicle.* p<0,001.

in influencing intracellular events. The wide use of acylation for peptide delivery in general and myristoylation in particular makes it likely that also the present peptides enters into the cytoplasm. For additionally testing this assumption 100 μM of fluorescence-labelled derivatives of peptide 18AD and its non-myristoylated equivalent are added to suspensions of 7TD1 cells. During flow-cytometric analysis viable cells are gated according to light scattering. Virtually all viable cells treated with fluoresceine-labelled peptide 18AD are stained with the label, whereas only 5 % exhibit fluorescence after treatment with Cy5-labelled peptide 18ADnm (Figure 3.3a). Despite thorough washing, staining of 7TD1 cells by fluorescein-labelled peptide 18AD may also be explained by myristoylated peptide attaching to the outer side of the plasma membrane. Differential up-take of myristoylated and non-myristoylated peptides is supported by their contrasting staining behaviour. In addition an equal concentration of peptide 18ADnm, which lacks the N-terminal myristoyl moiety, does not result in the growth inhibition found with peptide 18AD (Figure 3.3b), proving that only the myristoylated form is taken up into the cytoplasm and that the uptake is a prerequisite for the functionality of the peptide.

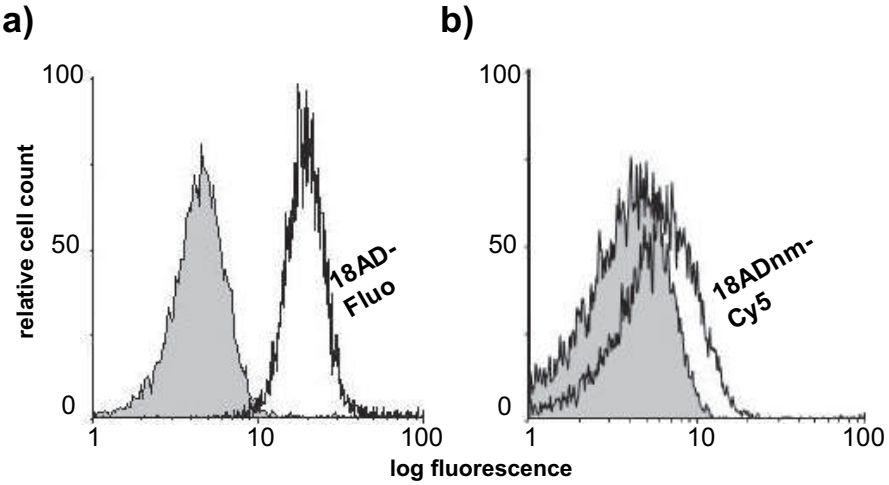

Figure 3.3. | **Uptake.** Populations of viable 7TD1 cells are analysed by fluorescence-activated cell sorter (FACS) either untreated (grey) or after treatment with fluoresceine-labelled peptide 18AD (18AD-Fluo) or its Cy5-labelled unmyristoylated equivalent (18ADnm-Cy5).

3.3. Biological effects of peptide 18AD

Biological effects of peptide 18AD are analysed in human and murine myeloma cell lines.

3.3.1. Effects on proliferation

3.3.1.1. Growth kinetics

The effects of peptide 18AD on the growth kinetics of human and murine, IL-6 -dependent and independent myeloma cells are analysed by proliferation studies. The effects of peptide 18AD and peptide 18sc on the growth kinetics of the human myeloma cell lines, INA-6 and MM1.S, and the murine hybridoma cell line 7TD1 are assessed. While 7TD1 and INA-6 cells are IL-6-dependent, MM1.S cells grow factor independently. Reduced proliferation rates of the two IL-6 -dependent cell lines 7TD1 and INA-6, which are treated with 100 μM peptide 18AD, become apparent after 36-48 h. In 7TD1 cells, the growth curves of peptide 18AD-treated and IL-6-depleted cells are comparable. Both treatments lead to a reduced proliferation rate (Figure 3.4a). The cells fulfill only one doubling cycle within 48 h. DMSO-treated control cultures attain limiting cell densities, so that viable cell numbers cannot increase propotionally and the assay system becomes unstable.

Under the culture conditions used here, these thresholds are reached 48-60 hours after peptide addition. In INA-6 cells, growth-factor depletion and peptide 18AD treatment lead to an entire block of proliferation (Figure 3.4b). While, in INA-6 cells, the amount of living cells treated with peptide 18AD stays nearly constant during 72 h of treatment, IL-6 withdrawal leads to a clear reduction of living cells in the culture after 48 h. In both cell lines, treatment with peptide 18sc results in the same growth kinetics as observerd in solvent controls. As for the treatment with peptide 18AD, the results in IL-6 dependent cell lines are contrasted by the growth curves of the cell line MM1.S, where peptide 18AD does not show any inhibitory effect (Figure 3.4c).

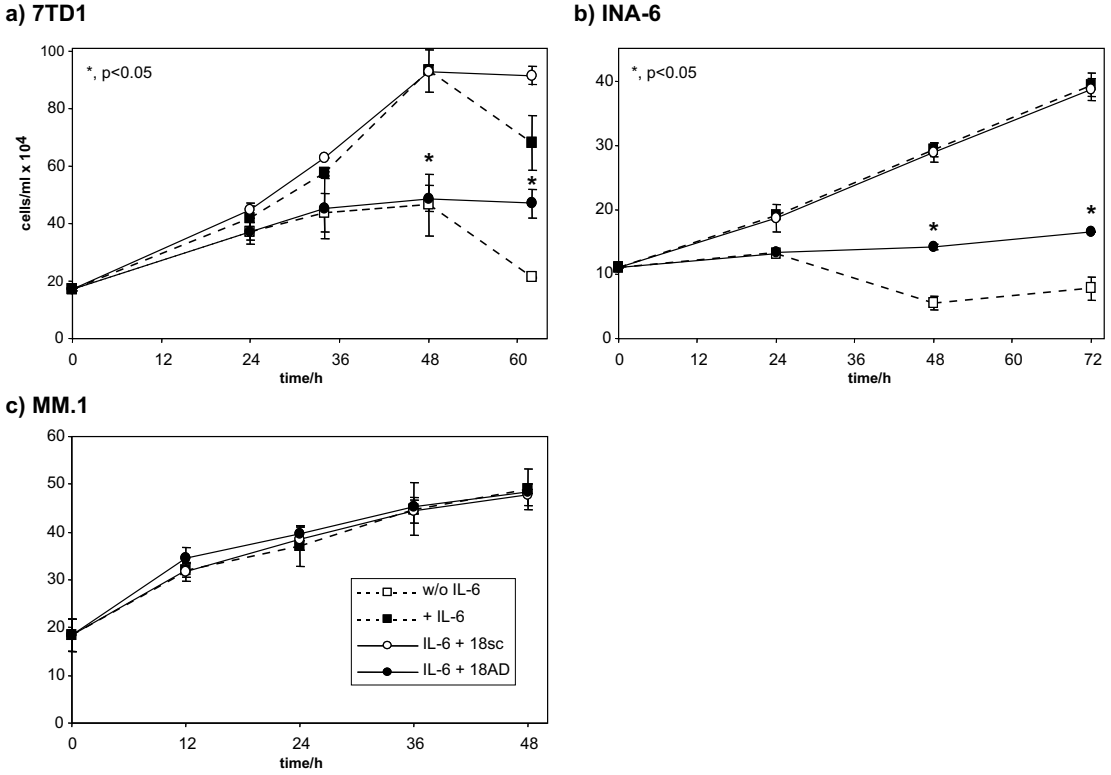

Figure 3.4. | **Growth kinetics of myeloma cell lines in the presence of peptide 18AD.** Time courses of cell densities of murine 7TD1 cells a.) and the human myeloma cell lines INA6 b.) and MM1.S c.) were determined by trypan blue exclusion.

3.3.1.2. Specificity

The inhibitory effect of peptide 18AD on the growth and survival of 7TD1 cells is compared with its effect on the IL-6-independent mouse hybridoma cell line, OKT1

(Figure 3.5a). IL-6-dependent growth of 7TD1 cells is inhibited by peptide 18AD, but neither by the 18sc or 18ADnm control peptides. In contrast, the growth of OKT1 cells, which reaches higher cell densities than 7TD1 cells, is not affected by any of the tested peptides. The impact of peptide 18AD on Epo-dependent growth of Baf/B03 cells overexpressing chimeric EpoR-gp130 (Eg) and Hck (Baf-EH cells) is analysed. Since the concept of an Hck-binding region has been derived from observations of cloned chimeric EpoR-gp130 [323], the impact of peptides 18AD and 18sc on Baf/B03 cells overexpressing Hck and chimeric EpoR-gp130 is investigated. The growth of Baf/B03 cells is known to be IL-3-dependent. Growth induction by Epo is observed in the genetically engineered derivative cell line, but not in the parent cell line. Peptide 18AD inhibits erythropoietin-dependent growth of Baf-EH cells, whereas their IL-3-dependent growth is considerably less influenced by peptide 18AD (Figure 3.5b). The inhibition by peptide 18AD as compared to peptide 18sc and non-myristoylated peptide 18AD even becomes apparent without counting cells just by inspection of medium acidification and cell sediments after prolonged incubation (data not shown).

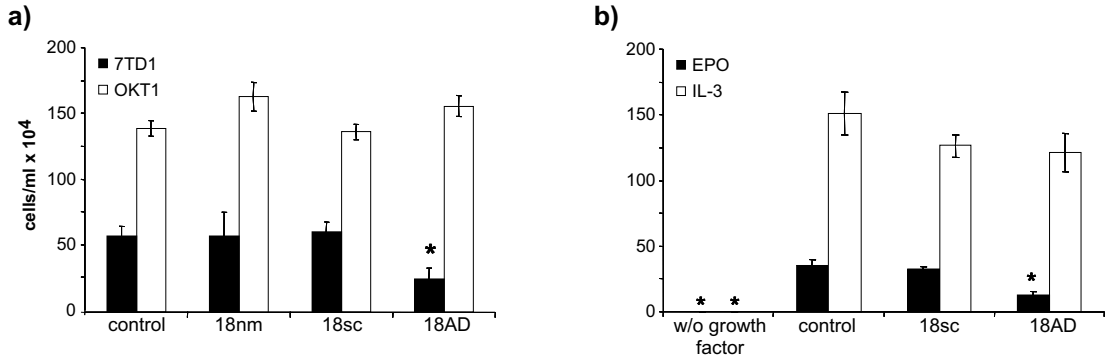

Figure 3.5. | **Specificity.** a.) 7TD1 and IL-6-indepentdent OKT1 cells are treated with 50 μM of peptide 18AD or 18sc or solvent control (0.05 % DMSO). b.) Effects of 50 μM of the indicated peptides on the densities of Baf-EH cells grown in the presence of either IL-3 or Epo.

3.3.1.3. Dose dependency

The peptide 18AD concentration inhibiting 50 % (IC_{50}) is about 30 μM, whereas peptide 18sc does not have any dose-dependent inhibitory effect (Figure 3.6a). In the examined dose range, peptide 18AD invariably results in a stronger inhibition of IL-6-dependent cell growth than an equal concentration of the control, peptide

18sc. Peptide doses of 20 and 40 μM are chosen to assess the influence of IL-6 concentration on peptide effects (Figure 3.6b). At a concentration of 40 μM, peptide 18AD blocks IL-6-dependent growth of 7TD1 cells at all IL-6 concentrations tested. In the presence of 20 μM peptide 18AD or 18sc, increasing IL-6 concentrations in the medium in a range up to 160 pg/ml lead to a rise in the cell densities attained. Peptide 18AD inhibited proliferation of Baf-EH cells with an apparent IC_{50} of about 25 μM, whereas peptide 18sc did not have any dose-dependent inhibitory effect (Figure 3.6c).

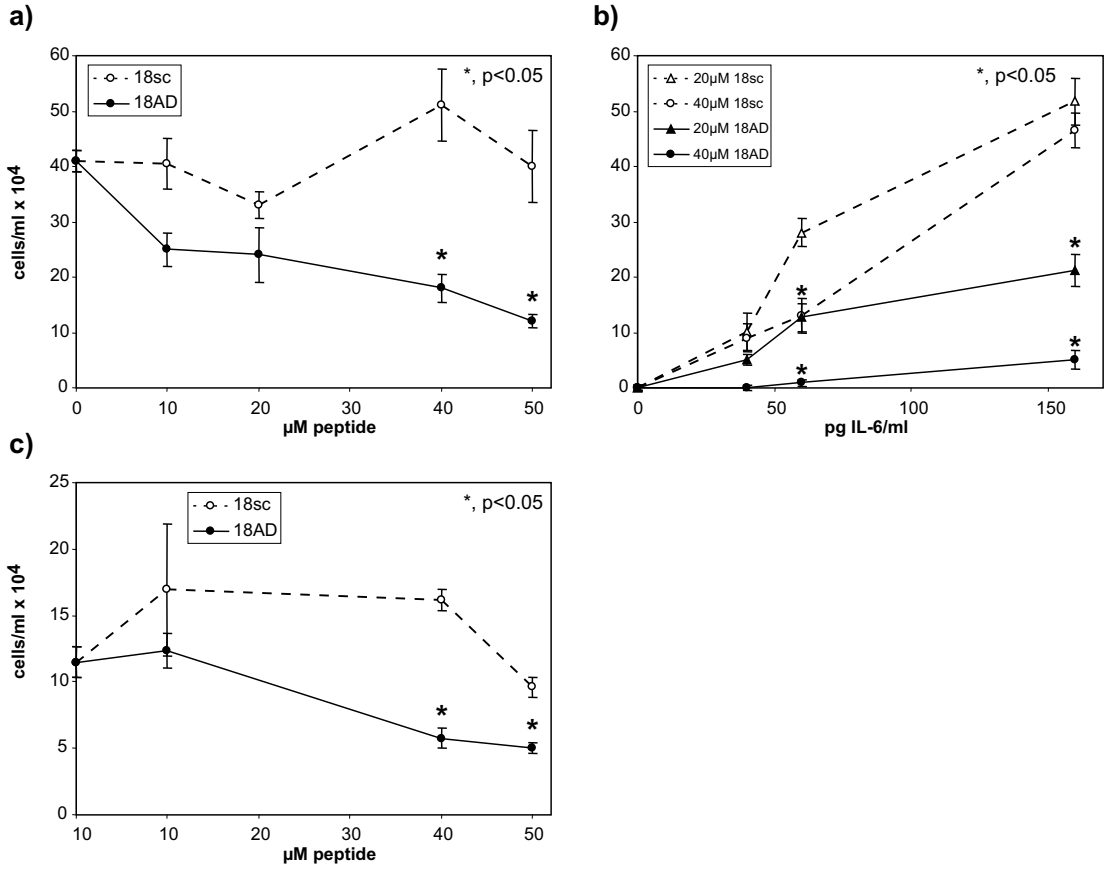

Figure 3.6. | **Dose dependency of peptides 18AD and 18sc.** The influence of 18mer peptide dose a.) and of IL-6 concentration b.) on the IL-6-dependent increase of 7TD1 cell number. c.) Influence of peptide concentration on the Epo-dependent growth of BaF-EH cells. The number of viable cells after 3 days incubation is shown.

3.3.2. Apoptosis induction

Annexin-V-binding to phosphatidylserine indicates disruption of the plasma membrane asymmetry and which is an early marker for apoptosis. IL-6 depletion in INA-6 cells leads to the induction of apoptosis ([35] and Figure 3.7). 7TD1 and INA-6 cells are supplemented with IL-6, and treated with 100 μM peptide 18AD, peptide 18sc or DMSO. As a control the cells are deprived of IL-6. Cells are stained with annexin-V-PE which binds to phosphatidylserine in the outer leaflet of the membrane. Between 5 % and 10 % of the cells from both cell lines are annexin-V-positive at the onset of the experiment, varying between individual experiments (Figure 3.7a,c).

21 % of 7TD1 cells, which are treated for 36 h with peptide 18AD, are annexin-V-positive. IL-6-deprived 7TD1 cells display 20 % annexin-V-positive cells at the same time point. 7TD1 cells which are incubated with peptide 18sc or IL-6 and DMSO, do not show increased levels of annexin-V-positive cells (Figure 3.7a). Treatment times longer than 48 h lead to an increase of annexin-V-positive cells in DMSO and peptide 18sc treated samples, because threshold levels of cell densities in the cultures are reached. In INA-6 cells, the presence of peptide 18AD leads to 27 %, IL-6 withdrawal to 48 % annexin-V-positive cells, at 48 h incubation time. As in 7TD1 cells, the amount of annexin-V-positive cells from peptide 18sc and DMSO treated cells does not change significantly (Figure 3.7c). In Figures 3.7b,d ratios of peptide treated cells to DMSO treated cells are shown. Compared to control treated cells, the part of annexin-V-positive cells is doubled by the treatment with peptide 18AD in both cell lines tested. While in 7TD1 cells the ratio of peptide 18AD treated cells and IL-6-deprived cells is comparable, the withdrawal of IL-6 from INA-6 cells leads to a 3,7-fold increase in annexin-V-positive cells compared to control cultures.

To gain insight into the kinetics of peptide 18AD induced apoptosis, the induction of apoptosis in 7TD1 and INA-6 cells is monitored over a period of 48 h in 7TD1 and 72 h in INA-6 cells (Figure 3.8). Samples are analysed every 12-24 h. In 7TD1 cells treated with peptide 18AD an increase in the population of annexin-V-single-positive cells can be observed as early as 20 h after the addition of the peptide (Figure 3.8a). While in IL-6-deprived 7TD1 cells, the beginning of apoptosis is characterised by an increase of the annexin-V-, 7AAD-double-positive population observed 20 h to 48 h after growth factor withdrawal (Figure 3.8c). A population that moved from a state of annexin-V-single-positive, at earlier time points, to a state of annexin-V-, 7AAD-double-positive, at later time points, could be observed, in some of the experiments as a result of the withdrawal of IL-6. With 3-6 %, however, the absolute amount of viable annexin-V-positive cells is rather low

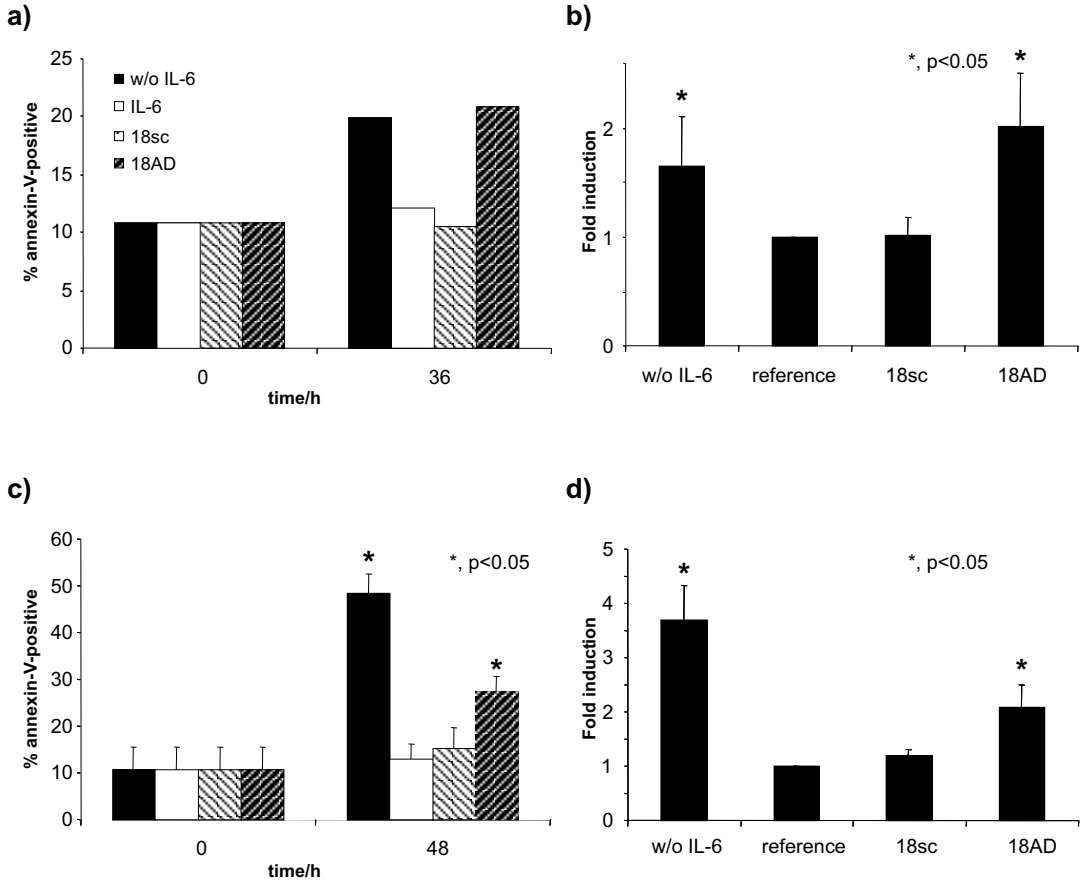

Figure 3.7. | **Apotosis induction.** Annexin-V-positive 7TD1 a.) and c.) INA-6 cells after treatment with 100 μM peptide 18AD or 18sc or after IL-6 starvation, One representative experiment per cell line is shown. To determine the ratios of apoptosis induction, percentages of annexin-V-positive cells within the total population are compared to reference cultures grown for equal periods in the presence of IL-6 without peptides. For 7TD1 b.) or INA-6 d.) cells. Data are derived from at least three independent experiments.

during the whole course of the experiment. The withdrawal of IL-6 from INA-6 cells leads to an increase of annexin-V-single-positive cells in the first 24 h to 48 h of the experiment followed by an increase in the double positive population 48-72 h after the beginning of the experiment. Peptide 18AD treated cells follow comparable kinetics, however the withdrawal of IL-6 is more efficient to induce apoptosis than the addition of peptide 18AD (Figure 3.8b,d). Treatment with the control peptide 18sc or with DMSO could not induce apoptosis in both cell lines tested.

Proliferation assays are done in parallel to each annexin-V-assay (Figure 3.8e,f). Peptide 18AD appears to influence proliferation as well as apoptosis. Also the

time course of peptide effects on these read outs is comparable.

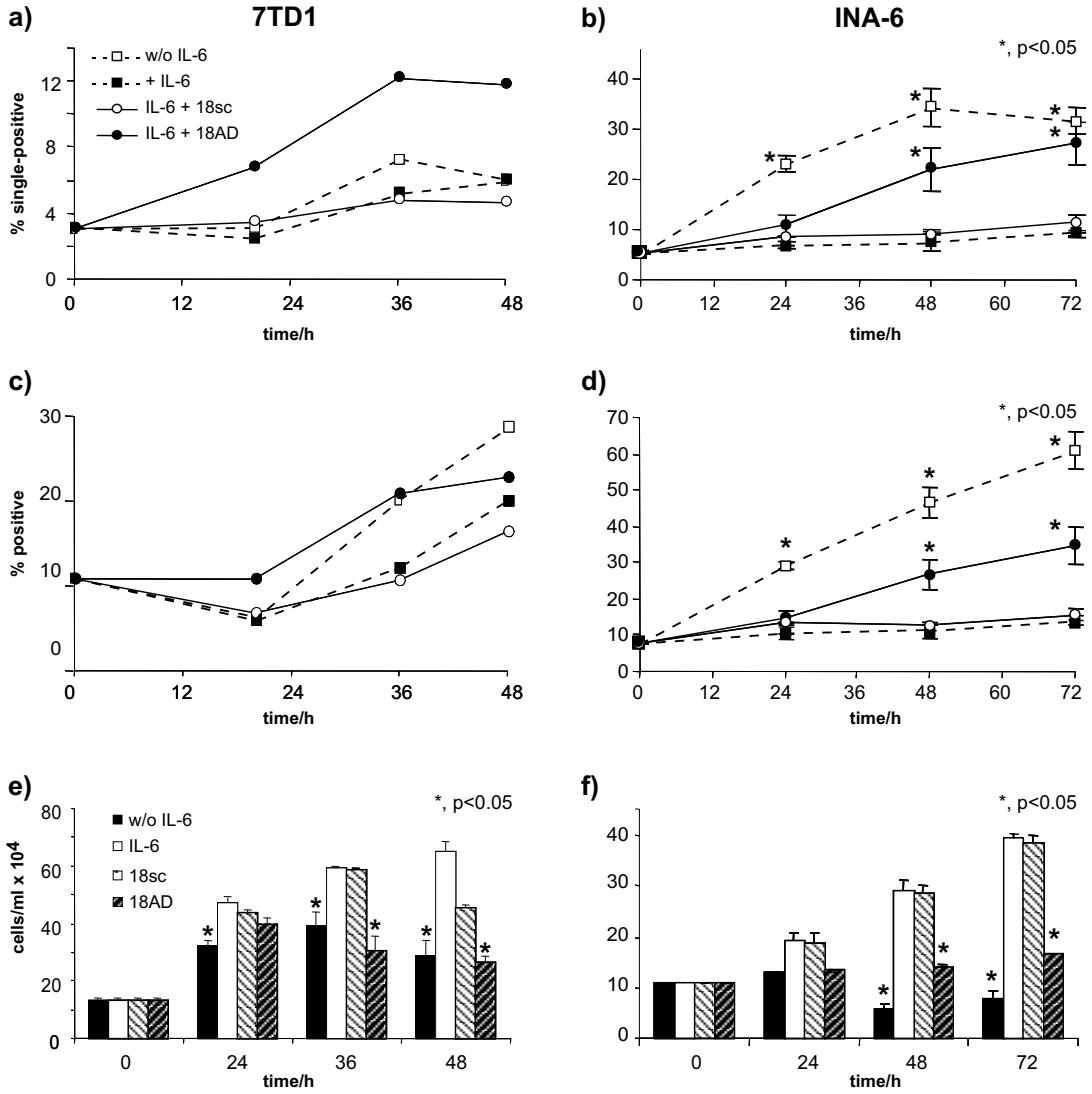

Figure 3.8. | **Kinetics of apotosis induction.** 7TD1 and INA-6 cells are treated with 100 μM peptide 18AD, peptide 18sc, 0.1 %DMSO (as a control) or are deprived of IL-6 for the timecourse of the experiment. The percentage of annexin-V-single-positve a.) 7TD1 and b.) INA-6 cells is shown. In c.) and d.) the percentage of annexin-V-positive derived from the total population is displayed for 7TD1 and INA-6 cells, respectively. Results from proliferation assays performed in parallel to the apotosis assays are shown for e.) 7TD1 and f.) INA-6 cells.

3.3.3. Effects on cell cycle

7TD1, MM1.S and INA-6 cells are incubated with 50 μM of peptides 18AD and 18sc. Samples are taken at various time points between 4 h and 100 h of peptide treatment and cells are stained with the DNA-binding dye, propidiumiodid, which interacts stochiometrically with DNA. The different cell cycle phases are visualised by FACS-analysis. As shown in figure 3.9a the withdrawal of IL-6 induces a G1-arrest in the cell cycle of 7TD1 cells. In the cell cycle profile, shown in figure 3.9a, the G1-arrest becomes visible after 20 h IL-6 depletion. The analysis of the changes of the part of S-phase cells in the cell cycle shows (Figure 3.9b), that the amount of cells in the S-phase decreases during the course of the experiment. The beginning of this decrease in S-phase-cells could be detected after 20 h of IL-6 depletion. Neither the cell cycle profile nor the part of cell in the S-phase of the cell cycle are changed significantly by the treatment with peptide 18AD or peptide 18sc. However, a transient decrease in S-phase cells can be observed after 20 h of treatment with peptide 18AD. The proliferation assay, which has been performed in parallel, clearly shows the inhibitory effect of peptide 18AD on proliferation (Figure 3.9b).

As described in 3.3.1.1 and shown in figure 3.4, MM1.S cells grow IL-6-independently. However, the cell cycle profile and the S-phase-analysis of MM1.S cells treated with 100ng/ml IL-6 show an increase of cells in the S-phase. The presence of peptides 18AD or 18sc has no effect on the cell cycle of MM1.S cells at the tested time points. The growth characteristics of MM1.S cells are not significantly changed by the treatment with peptide 18AD (Figure 3.9c,d).

The cell cycle profile of INA-6 cells is, as for 7TD1 cells, characterised by a high content of cells in the S-phase of the cell cycle. The withdrawal of IL-6 leads to a G1-arrest in these cells. Compared to 7TD1 cells the decrease of cells in the S-phase of the cell cycle, as an answer to factor depletion, is less pronounced. Like in 7TD1 cells, a peptide induced change in the cell cycle is not detectable. However, there is a transient decrease in S-phase cells, treated with peptide 18AD, detectable 16 h after the beginning of the treatment. The growth inhibitory effect of peptide 18AD on INA-6 cells is detectable in the proliferation assays performed in parallel. Since the cell populations used in the described assays are not synchronized, the results reflect effects on the average distribution of the cells cycle phases over the entire population in the culture tested. Transient, but not significant effects of peptide 18AD on the cell cycle of 7TD1 and INA-6 cells after 16-20 h of peptide treatment can be observed.

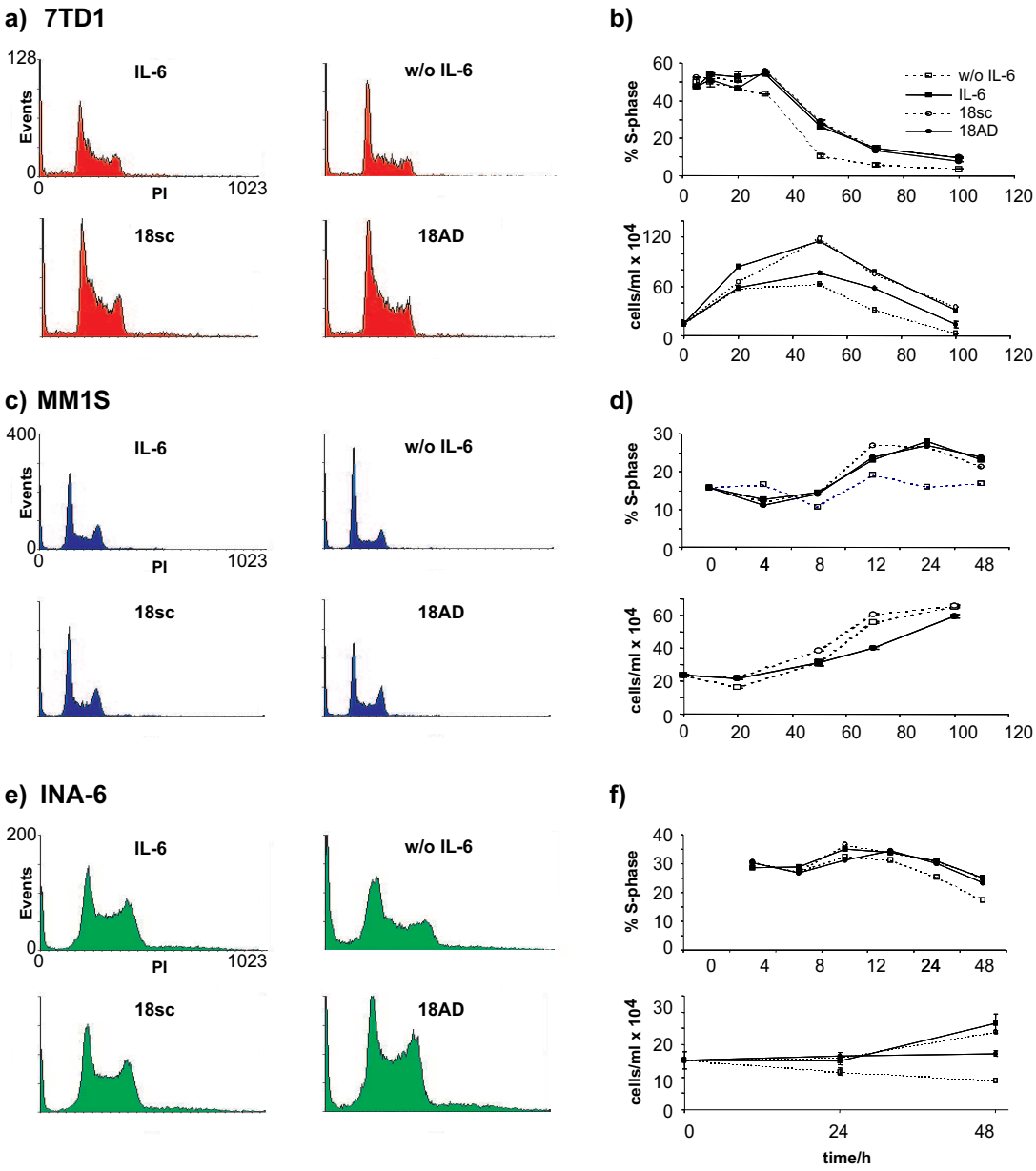

Figure 3.9. | **Cell cycle.** Cell cycle profiles of myeloma cells treated with 50 μM peptides, 0.05 %DMSO or IL-6 depletion. a.) 7TD1 cells are treated for 30 h without or in the presence of 120 pg IL-6/ml. b.) MM1.S cells after 48 h treatment (100 ng/ml IL-6). c.) INA-6 cells after 48 h treatment (1 ng/ml IL-6). The percentage of cells in the S-phase of the cell cycle was determined and the kinetic of the S-phase is shown in the upper graphs of b.) for 7TD1, d.) for MM1.S. and f.) for INA-6 cells. The lower graphs show the proliferation assays, which have been performed in parallel.

3.4. Molecular effects of peptide 18AD

3.4.1. Inhibition of the association between gp130 and Hck

The peptides are designed, based on the hypothesis that they compete with gp130 for binding to SFKs e.g. Hck on a molecular level. The biological data presented in section 3.3 show a link between gp130-dependent proliferation and the effects of peptide 18AD. To investigate the molecular mechanism of action of the gp130-derived peptide 18AD, different experimental systems and conditions are applied.

3.4.1.1. Peptide effects on 7TD1 cells expressing native levels of gp130 and SFKs

In 7TD1 cells, the effect of the addition of 100 μM of the myristoylated and nonmyristoylated peptide 18AD on the association of gp130 and Hck is examined. Peptides are either added to intact cells or to whole cell lysates (Figure 3.10).

Binding of Hck to gp130 is hardly detectable in starved 7TD1 cells, but yields a co-IP band upon addition of 1 ng IL-6/ml to the growth medium for 15 minutes prior to lysis. If added to suspensions of IL-6-stimulated 7TD1 cells, peptide 18AD reduces the co-IP signal, whereas peptide 18ADnm has no effect. The lack of disruption of the Hck-gp130-association by peptide 18ADnm added to intact cells is in agreement with the observations, that the nonmyristoylated peptide in contrast to its myristoylated equivalent does not stain intact 7TD1 cells (Figure 3.3) or inhibits IL-6-dependent proliferation (Figure 3.5). When added to 7TD1 lysates, peptide 18ADnm is more efficient in reducing co-IP signals than the identical sequence with myristoyl tag. To assess, which peptide concentrations are necessary for displacing Hck from gp130, the unmyristoylated sequence is added to 7TD1 lysates (Figure 3.11).

At concentrations above 50 μM, addition of peptide 18ADnm to lysates of IL-6 treated 7TD1 cells clearly inhibits the co-precipitation of gp130 with Hck.

3.4.1.2. Effects of peptide 18AD in cell systems overexpressing gp130 and Hck

In order to improve the detection of co-IP signals and thus to enhance the evidence for the disruption of Hck-gp130 binding, HEK 293 cells, which transiently overexpress the two binding partners, EpoR-gp130 and human Hck, are applied (Figure

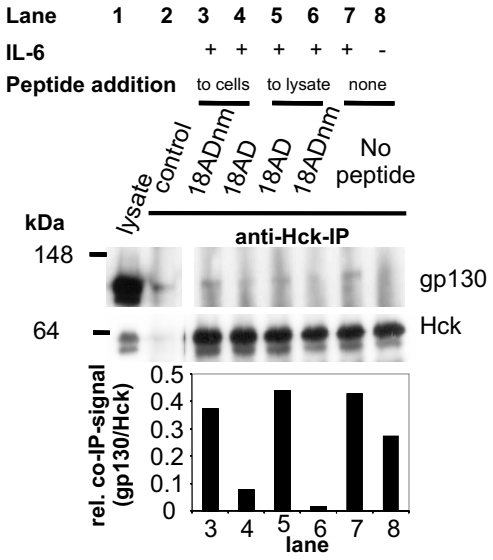

Figure 3.10. | **Dissruption of Hck binding to gp130 by peptide 18AD.** 100 μM peptides are either added to suspensions of IL-6-stimulated 7TD1 cells before lysis or directly to 7TD1 lysates. An anti-mHck-antibody is used for IP. The co-IP-signal is detected with an anti-gp130-antibody. Control bots for Hck IP are developed with anti-hHck-antibody. Relative stengths of co-IP signals are indicated as ratios of densitometer readings.

3.12). Co-precipitations of Hck with EpoR-gp130 in the presence of peptide 18AD, peptide 18sc or DMSO as a vehicle control are analysed. The presence of 150 nmol of peptide 18AD disrupts the association of the two overexpressed proteins, Hck and EpoR-gp130, whereas the control peptide 18 sc does not disturb the association. Compared to peptide 18sc, the presence of 150 nmol peptide 18AD reduces the strength of the interaction between the two binding partners by more than 50 %. In contrast to IL-6 stimulation in 7TD1 cells, addition of 10U Epo/ml for 15 min does not increase the binding of Hck and EpoR-gp130.

3.4.1.3. Interaction of peptide 18AD with Hck

At native protein levels as well as at overexpression levels, peptide 18AD is able to reduce the interaction between gp130 and Hck. Peptide pull down assays are done to demonstrate, that peptide 18AD is able to interact with the SFK Hck. For the affinity pull-downs overexpressed human Hck from HEK 293 lysates is pulled down with chemically synthesized biotinylated peptides 18AD, 18sc and

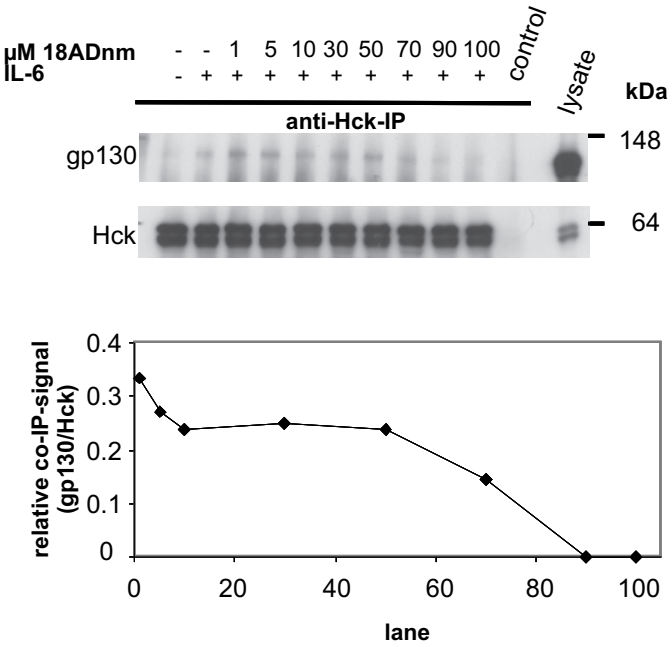

Figure 3.11. | **Concentration-dependent disruption.** Determination of the minmal concentration of peptid 18ADnm that disprupts binding of Hck to gp130. The anti mHck-antibody used for IP is omitted in the control sample. The co-IP-signal is detected with an anti-gp130-antibody. Control bots for Hck expression and IP are developed with anti-hHck-antibody. Relative strengths of co-IP signals are indicated as ratios of densitometer readings.

a SH2-binding peptide, using streptavidin beads (Figure 3.13). The binding of Hck to the peptide coated beads is analysed by Western Blot. Peptide 18AD-bio and the positive control peptide SH2-bio precipitated greater amounts of Hck than peptide 18sc-bio or control assays without peptide, confirming the binding of peptide 18AD to Hck. Most of the SFK present in the lysates is, however, retained after the pull-down (not shown).

3.4.2. Partial deletions of the acidic domain in gp130

The peptides are generated based on a 41 amino acid region in gp130, the AD. Gp130 carrying this deletion has lost the ability to bind the SFK Hck. From the evidence shown here it can be assumed, that peptide 18AD which is derived from the AD, is able to interfere with the interaction between receptor and kinase. In order to find out whether a deletion, of the 18 amino acids corresponding to the sequence of peptide 18AD, in gp130, would have comparable effects, a deletion mu-

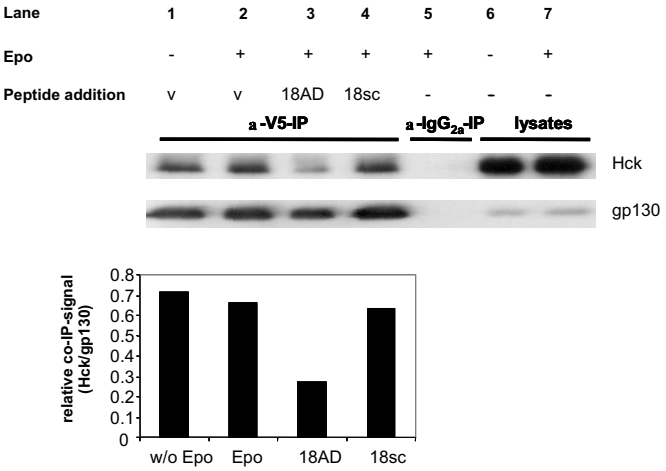

Figure 3.12. | **Disruption of the association of the overexpressed proteins Hck and Eg by peptide 18AD.** Using an anti-V5-antibody, EpoR-g130 ís immunoprecipitated from lysates of transiently transfected HEK 293 cells and analysed for co-precipitated Hck in the presence of 150 nmol peptide 18AD or 18sc or an equivalent amount of vehicle (v), with 25 μg of cell lysates as control for equal expression of EpoR-g130 and Hck in non-simulated cells and in cells which are stimulated with 10U/ml Epo.

tant of EpoR-gp130 (Eg) is generated. Co-immunoprecipitations of Hck and Eg or Eg_del18AD are performed in lysates from HEK 293 cells which overexpress Hck and the respective receptor mutant. The co-immunoprecipitation shows that Hck can still precipitate the mutant receptor. However, less receptor (~60 % of the Eg IP) is precipitated in comparison to the wild type (wt) receptor. The result probably underestimates the effect, because in the lysates of cells which are transfected with Eg_del18AD the expression of the receptor is 1.6 times higher than in the cells which are transfected with the Eg-receptor. This can be concluded from the observed difference in immunoblot signals and from the fact, that equal amounts of total protein are used for the co-IPs. The expression of Hck is comparable in both lysates. A faint band can be seen in co-IPs from lysates which do not express Hck. This band shows unspecific binding of Eg to protein G beads.

3.4.3. SFK activity

As shown in section 3.4.1.1 for native expression levels of Hck and gp130, binding of these two proteins to each other depends on receptor stimulation by IL-6. *Hallek et al., 1997* were able to show that SFKs become activated by IL-6 stimulation in myeloma cell lines. *Schaeffer et al., 2001* showed that the deletion of the acidic

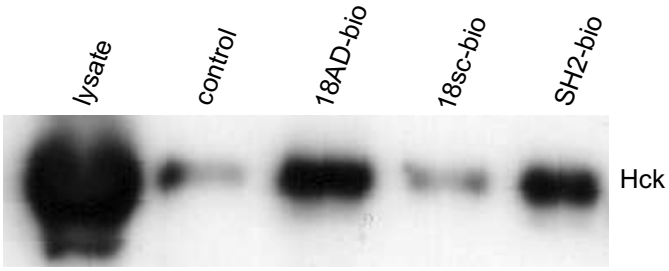

Figure 3.13. | **Peptide pull down.** For affinity pull-down analysis, lysates of HEK 293 cells transiently transfected with Hck are incubated with 150 nmol of peptides 18AD-bio, 18sc-bio or SH2-bio for 3 h. Pull down assays using streptavidin beads are performed and analysed for attached Hck.

domain, inhibited the activation of the SFK, Hck. To find out if peptide 18AD has an effect on SFK activity, immunocomplex kinase assays are performed (Figure 3.15). Hck, Lyn, Fyn and c-Src are precipitated from INA-6 cells, which are treated with 100 μM peptides and stimulated with IL-6 prior to the assay. The activation of the SFKs Hck, Lyn and Fyn is detected in IL-6-stimulated INA-6 cells by increased autophosphorylation of the kinase. Upon treatment with peptide 18AD but not 18sc the tyrosine phosphorylation levels in IPs of Hck, Lyn and Fyn are reduced. To verify, that the effects on autophosphorylation are due to an inhibition of the kinase activity, the phosphorylation of the substrate enolase, is analysed as well. In immunocomplex kinase assays of Hck, Lyn and Fyn from peptide 18AD treated cells, the phosphorylation level of the substrate is comparable to the phosphorylation level of the substrate from unstimulated cells. Preparations from peptide 18sc treated cells show an increased substrate-phosphorylation, which is comparable to control treated cells. Ubiquitously expressed c-Src neither shows increased autophosphorylation nor increased substrate-phosphorylation in response to IL-6 stimulation Peptide 18AD, but not peptide 18sc is able to inhibit IL-6-induced activation of the SFKs Hck, Lyn and Fyn.

3.4.4. Downstream signalling

Signalling from the hexameric IL-6 receptor complex requires the recruitment of cytoplasmic tyrosine kinases and proceeds via at least four major pathways: the JAK/STAT pathway and the Ras/MAPK signalling cascade, the PI3-Kinase pathway and the SFK pathway (Section 1.3.4.5). 7TD1 cells are analysed for activation of STAT3, Erk 1/2 and Akt in response to IL-6 stimulation using antibodies, which are specific for the phosphorylated, active forms of the molecules. Unfortunately neihter Erk 1/2 nor Akt phosphorylation can be detected with these antibodies

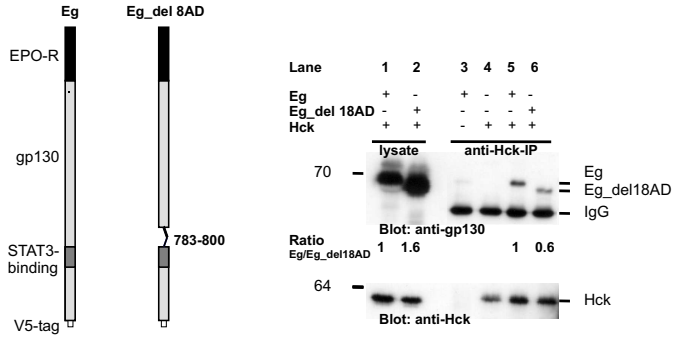

Figure 3.14. | **18AD deletion mutant.** HEK 293 cells are co-transfected with Eg or Eg_del18AD and Hck. The expression of the individual proteins is shown in lanes 1 and 2. Immunoprecipitations (lanes 3-6) are performed with an anti-hHck antibody. The binding of the Eg-receptors is shown with an anti-gp130 antibody (upper blot). Lysates from cells expressing Eg or Hck alone are used as controls (lanes 3 and 4), lanes 5 and 6 show the co-precipitation of Eg and Eg_del18AD, respectively. Ratios are determined from densitometer readings. The blot was stripped and reprobed with an anti-Hck-antibody to show equal expression and IP of Hck.

(not shown). For INA-6 cells a mutation in the N-ras gene is described [35], which leads to constitutive active Erk 1/2. Moreover Akt-phosphorylation could not be detected in INA-6 (Figure 3.17). In conclusion, both cell lines, which show biological responses to peptide 18AD treatment, are not the optimal systems to investigate the effects of peptide 18AD on IL-6-induced downstream signal transduction. Apart from the effect on SFK-activation, STAT3 is the only downstream signalling molecule which is analysed for its phosphorylation status in the presence of peptide 18AD in response to IL-6 stimulation in 7TD1 and INA-6 cells. While STAT3 phosphorylation is not changed by the presence of peptide 18AD in 7TD1 cells and in Epo-stimulated Baf-EH cells (Figure 3.16), reduced phosphorylation of STAT3 is detected in INA-6 cells (Figure 3.17). Although MM1.S cells are IL-6-independent and no biological effects of peptide 18AD are detected, they are especially useful for the analysis of IL-6 induced signalling pathway, because the major downstream molecules of the IL-6 pathway can be analysed in these cells.

3.4.4.1. Phosphomultiplex analysis

Using multiplex technology, it is theoretically possible to analyse the phosphorylation status of 100 different proteins from one lysate at the same time. Here, bead-based multiplex assays are used to simultaneously detect phosphorylation of 8 different phosphoproteins, ATF2, JNK, STAT3, Akt, GSK3a/b, Erk1/2, p38

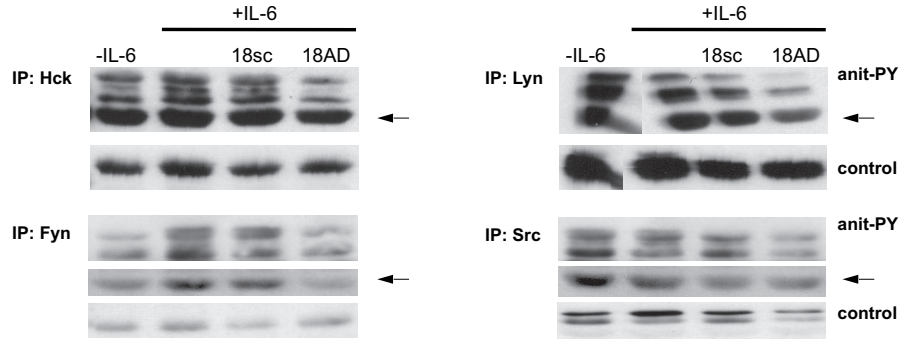

Figure 3.15. | **Effects on SFK ativity.** SFK activities in INA-6 cells after IL-6 treatment in the presence of 100 μM peptide 18AD or 18sc are determined by immunocomplex kinase assay. Arrows point at externally added enolase. Phosphorylation of enolase is detected together with autophosphorylation of respective SFKs using an anti-phospho-Tyr-antibody. As a control for equal IP of the kinases, blots are stripped and reprobed with antibodies specific for the respective kinase.

and IκBα, in whole cell lysates of MM1.S cells. To induce protein-phosphorylation, cells are stimulated with IL-6 for 15 min prior to lysis. IL-6 stimulation in MM1.S cells induces phosphorylation of ATF2, JNK, STAT3, Akt and to a minor extent of GSK3a/b, Erk1/2 and p38. IκBα is not phosphorylated (Figure 3.18b, black columns and data not shown). The same lysates which are used for the phosphomultiplex are analysed by Western Blot using antibodies that detect only the phosphorylated forms of Erk1/2, Akt, Stat3, GSK3a/b, and p38. The stimulation of MM1.S cells with IL-6 leads to an increased phosphorylation of GSK3a/b, STAT3, p38, Akt and Erk1/2 which is detected by Western Blot analysis (Figure 3.18a). In addition, phosphomultiplex analysis shows the phosphorylation of

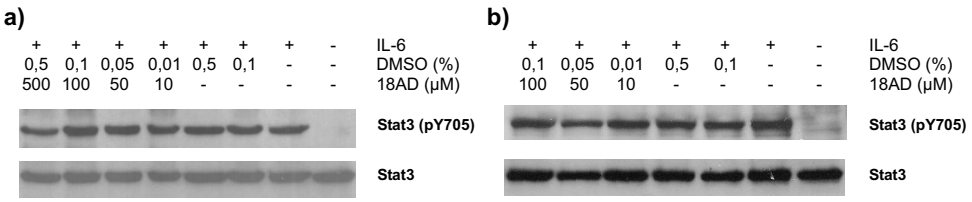

Figure 3.16. | **Effects on STAT3 phosphorylation.** 7TD1 and Baf-EH cells are treated with different concentrations of peptide 18AD and the phosphorylation status of Tyr 705 in STAT3 is determined and compared with the immuno-detection of STAT3 expression levels.

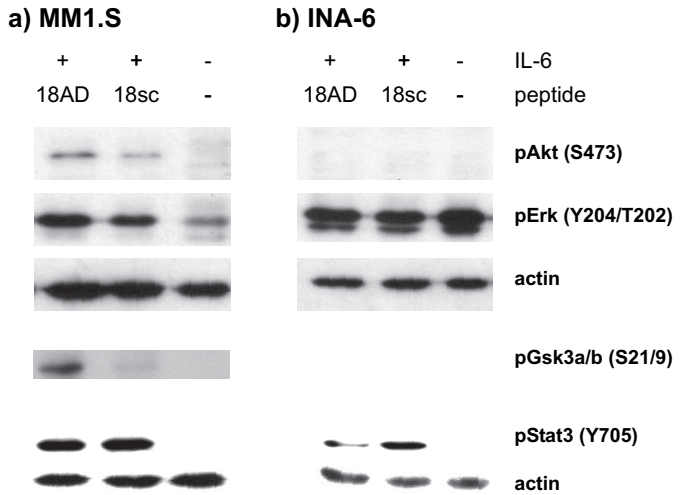

Figure 3.17. | **Effects on downstream signalling molecules.**The effects of peptide 18AD and peptide 18sc on the phosphorylation of the downstream signalling molecules Akt, Erk1/2, GSK3a/b and STAT3 are analysed in MM1.S and INA-6 cells. Cells are starved over night, treated with 100 μM peptides for 1 h and stimulated with 1 ng/ml IL-6 for 15 min prior to lysis.

ATF2 and JNK in response to IL-6 stimulation. An induction of phosphorylation of IκBα is not detected (not shown).

Band intensities with and without IL-6 stimulation are compared densitrometrically in order to calculate the ratios of phosphorylation levels (Figure 3.18a). To validate the data generated in the phosphomultiplex experiment, the ratios of the signals from stimulated vs. non-stimulated cells in the two different types of experiments, Western Blot and phosphomultiplex, are compared (Figure 3.18b). Comparing both techniques, Western Blot is more sensitive for detection small changes in phosphorylation than phosphomultiplex, however the advantage of the phosphomultiplex assay is the possibility to investigate the phosphorylation of more than one protein at the same time. This is why a phosphomultiplex-assay is used to investigate the effects of peptide 18AD treatment on IL-6 signalling in MM1.S cells. No significant differences between MM1.S cells which are treated with 50 μ to 500 μM peptide AD and peptide sc are detectable using multiplex technology. To find out whether this is due to low sensitivity of the multiplex assay, lysates from MM.1S cells treated with 100 μM peptide 18AD are subjected to Western Blot analysis. In the western blot analysis a small increase in GSK-3a/b and Akt phosphorylation is detected. After longer treatment times with peptide 18AD, the phosphorylation of Akt is reduced. Erk 1/2 and STAT3 phosphorylation of peptide 18AD and peptide 18sc treated cells are comparable (Figure 3.17a).

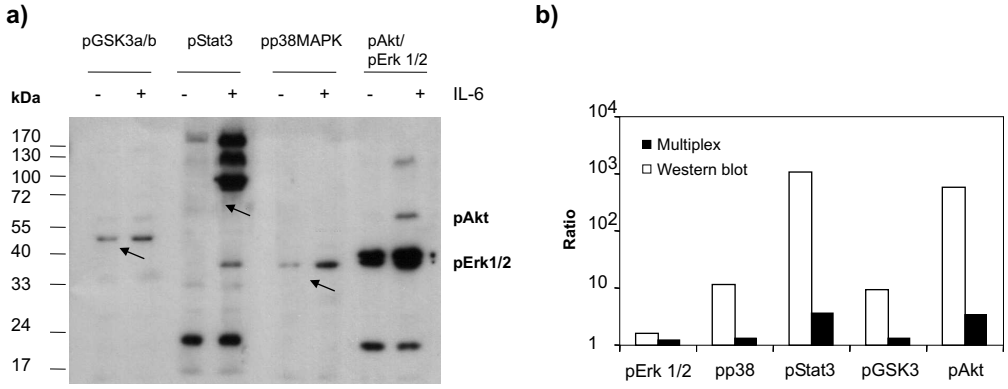

Figure 3.18. | **Western Blot analysis of phosphorylated signalling molecules in MM1.S cells.**

3.5. Hck activity and the IL-6-dependent growth of 7TD1 cells

To demonstrate the role of SFK for IL-6-signalling in 7TD1 cells, wild type (wt) or constitutively active (Y501F) or inactive mutants (K269R) of human Hck are transduced into 7TD1 cells, which express native levels of mouse Hck. Sorted, polyclonal cell populations are examined in proliferation assays using several doses of IL-6 in order to investigate the influence of overexpressed Hck mutants on IL-6-dependence (Figure 3.19a). The IL-6 requirement of 7TD1/Hck-Y501F cells can not be distinguished from that of controls expressing GFP alone. The cell densities of 7TD1/Hck-K269R in response to IL-6 reach a threshold at about $6x10^5$ cells per ml, while cells expressing GFP alone or together with Hck-Y501F grow up to densities of 10^6 cells per ml. Thus, proliferation of 7TD1/Hck-K269R cells in response to IL-6 is decreased compared to the controls, demonstrating that an excess of transduced kinase-inactive Hck disturbs the contribution of intrinsic mouse Hck to the IL-6-dependent growth of 7TD1 cells. Despite equal GFP expression, about four-fold lower expression of the human Hck-Y501F or Hck-wt gene products is detected on Western Blots than of the correspondent kinase-inactive mutant (Figure 3.19b). This difference in expression levels, however, does not affect the conclusion of dominant negative effects, since the changes occurred relative to controls expressing either only intrinsic mouse Hck or additionally human catalytically

active Hck.

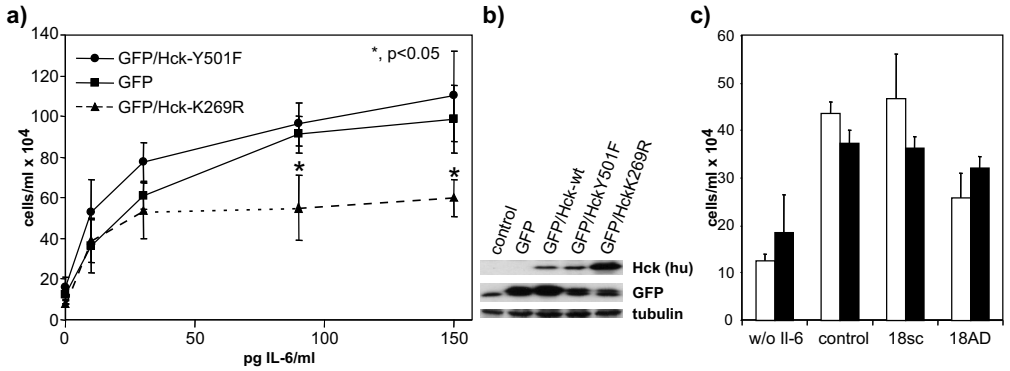

Figure 3.19. | **Role of Hck in IL-6-induced proliferation.** a.) Cell counts of 7TD1 cells transduced with GFP alone, Hck-Y501F or HckK269R at the indicated IL-6 concentrations are obtained after three days. b.) Expression levels of GFP, human Hck and β-tubulin in lysates if 7TD1 cells an the retrovirus-transduced derivatives applied for analyses of IL-6 requirement an tyrosine phosphorylation. c.) Combined effects of retrovirally introduced catalytically inactive Hck and 100 μM peptide 18AD on the number of 7TD1 cells in the presence of 80 pg IL-6/ml. GFP transduced 7TF1 cells (white bares), GPF/HckK269R transduced (black bares).

Since addition of peptide 18AD and the expression of inactive Hck both inhibit the IL-6-dependent increase of 7TD1 cell numbers, the combined effect of these treatments on cell numbers in order to determine the role of SFK activity in IL-6-mediated survival signalling and its inhibition by peptide 18AD is analysed (Figure 3.19c). The cell numbers attained by 7TD1 cells expressing Hck-K269R or treated with peptide 18AD in the presence of IL-6 are significantly lower than those of cells expressing GFP only treated with peptide 18sc. In cells expressing catalytically inactive Hck, treatment with peptide 18AD does not lead to a significant further reduction of cell numbers, demonstrating a considerable contribution of SFK activity to the inhibitory mechanism of peptide 18AD. To further investigate the role of Hck in IL-6 signalling, the tyrosine phosphorylation profiles in retrovirus-transduced 7TD1 cells expressing GFP alone or additionally Hck-wt or Hck-K269R are compared (Figure 3.20). Following IP by two anti-PY antibodies and immunodetection by a third directly labelled anti-PY-antibody, increases of the tyrosine phosphorylation intensities during one and five minutes of IL-6 treatment are considerably weaker in the 7TD1 derivative expressing Hck-K269R, confirming the dominant negative effect of the catalytically inactive Hck mutant. STAT3 phosphorylation is induced upon IL-6 addition to 7TD1 cells independently of additional overexpressed Hck-K269R, which is in line with the observation that peptide 18AD does not disturb the induction of STAT3 phosphorylation upon IL-6

induction in 7TD1 cells (Figure 3.16).

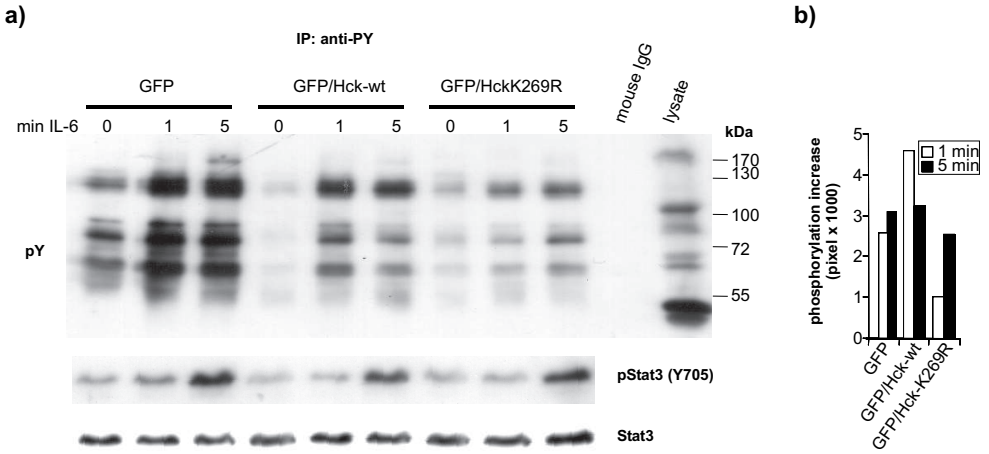

Figure 3.20. | **Role of Hck in IL-6-induced tyrosine phosphorylation.** a.) Lysates of transduced 7TD1 cells treated with 1ng IL-6/ml for the indicated time periods are analysed for global tyrosine phosphorylation and for PY at position 705 of STAT3, which is reprobed with an anti-STAT3-antibody after stripping. b.) Densitometric evaluation of the global PY signals in a.) reveal that the increase in phosphorylation after 1 and 5 min are reduced by expression of human Hck-K269R.

3.5.1. From 18mer to 8mer

Binding studies using degenerated peptide libraries were used to postulate a consensus substrate sequence for cytoplasmatic tyrosine kinase and SH2-domainbinding sites [355]. Comparing the consensus sequence with the sequence of gp130 the homology at the acidic domain, this becomes obvious (Figure 3.21). However in gp130 the central tyrosine or phospho-tyrosine residue which would make the sequence to a kinase or SH2-domain-substrate sequence, is missing. *Songyang and Cantley, 1995* could show that the acidic amino acids surrounding the tyrosine are essential for substrate recognition, because they are responsible for the majority of ionic interactions. The hypothesis that the sequence in gp130 could be a pseudo-substrate-sequence suggests itself.

The acidic core region of peptide 18AD resembles a consensus substrate sequence for tyrosine kinases postulated by [355; 357]. Taking this into account, the effects of peptide 18AD should be mainly due to the acidic sequence DSEERPEDL. This is tested by using another deletion mutant of the receptor Eg_del8AD for co-immunoprecipition (Figure 3.22a).

position:	-4	-3	-2	-1	0	+1	+2	+3
consensus:	E/D	E/D	E/D/G/A	I/V/L	Y	E/G/D	E/D	I/L/V/F
gp130:	S	E	E	R	P	E	D	L

Figure 3.21. | **Consensus sequence.** Comparison of SFK consensus substrate and SH2-ligand sequences with a motive from the gp130 acidic domain. Perfectly matching aa are shown in red, conservative replacements in yellow, and mismatches in black.

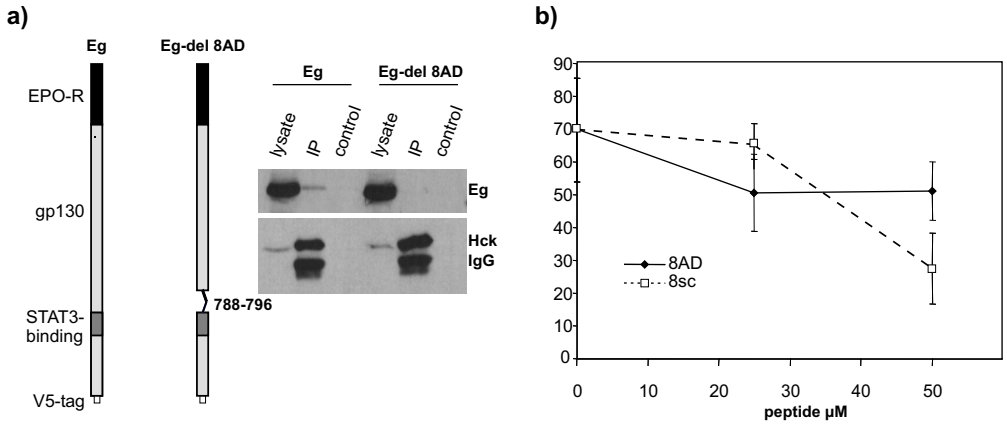

Figure 3.22. | **Eg_del8AD and peptide 8AD.** a.) Scheme of the Eg receptor and the Eg_del8AD mutant receptor constructs. Co-immunoprecipitations from Cos7 cells overexpressing Eg or Eg_del8AD together with human Hck. Hck was precipitated with and anti-Hck-antibody, the receptors were detected with an anti-V5-antibody. Control reactions were performed without an anti-Hck-antibody. b.) Proliferation assays in 7TD1 cells using 25-50 μM peptide 8AD or 8sc.

In addition, the effects of a myrstoylated peptide corresponding to the 8 aa deletion, peptide 8AD on the proliferation of 7TD1 cells is assayed. (Figure 3.22b). While co-immunoprecipitations show that the Eg_del8AD does no longer precipitate with Hck, proliferation assays in the presence of different concentrations of peptide 8AD and peptide 8sc do not indicate a differential inhibition of cell growth.

3.6. A novel lipopeptide inhibiting myeloma growth

3.6.1. Design of peptide sequences for structure function analysis

To find out which amino acids within peptide 18AD are responsible for its effects, the peptide was shortened form 18 to 8 amino acids, based on the high homology to a predicted consensus substrate sequence. However the results from co-immunoprecipitation with a deletion mutant of the receptor (Eg_del8AD) and proliferation assays using peptide 8AD and a scrambled version of the peptide, peptide 8sc are contradictory. While the deletion mutant does not bind to the kinase Hck, the effects of peptide 8AD are very similar to peptide 8sc (Section 3.5.1). At least two explanations for these findings are possible. Peptide 8AD is significantly shorter than peptide 18AD. It is possible that it can not interfere with the interaction site of Hck and gp130 because it is sterically hindered. Based on the homology between the peptide and the consensus sequence, the negatively charged amino acids within the sequence are thought to be responsible for the effects. The problem with a scrambled control peptide for peptide 8AD becomes obvious by looking at the sequence. Four out of eight amino acids are negatively charged. It is hardly possible to arrange these four amino acids in a way that the entire sequence differs significantly from the original one, without getting an accumulation of negatively charged residues. To circumvent this problem the experimental settings are changed. A "reverse alanine scan" is designed. Initially a peptide is synthesised where all acidic amino acids are changed to alanine. This peptide is intended to serve as a negative control. Subsequently the acidic amino acids should be reintroduced into this peptide, until the original effect on myeloma cells is restored. As a read out the proliferation and induction of cell death are analysed. The new peptides have two additional characteristics. the first difference is a lysine residue at the N-terminus of the peptide (between the myrisoyl moiety and the actual sequence). This lysine residue provides a free primary amine which can be used in chemical crosslinking reactions, to covalently link fluorescence markers or tags like biotin to the peptide. These modifications allow localisation studies of the peptides. The second difference is the exchange of natural L-amino acids to the non-natural D-isomers. Peptides composed of D-isomers are less easily cleaved by endogenous proteases and peptidases [97; 168; 405] and increase the half life of the peptides inside the cell. The original peptide 18AD modified in this respect was termed peptide 0B, the peptide which has alanine instead of the acidic residues is termed peptide 1A (Figure 3.23). The results shown below, however, contrast

with these theoretical expectations.

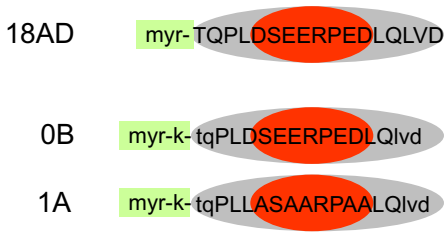

Figure 3.23. | **Peptides used to assess the functional significance of acidic residues in the gp130-derived peptide 18AD.** The homology region with SFK substrates at the peptide core is highlighted in red. Peptides 0B and 1A contain an N-terminal lysine residue for chemical coupling. D-isomers of the amino acids are printed in lower case letters. The acidic residues in peptide 0B were replaced for alanine in peptide 1A.

3.6.2. Effects of an alanine rich lipopeptide sequence on the proliferation of myeloma cells

Unexpectedly, the number of living cells in peptide 1A treated samples is reduces more than 90 fold, compared to DMSO treated cells. Cell number reduction of peptide 18AD and peptide 0B are comparable. At a peptide concentration of 60 μM peptide 1A is at least 25 fold more potent in reducing the number of living cells than peptide 18AD or peptide 0B (Figure 3.24).

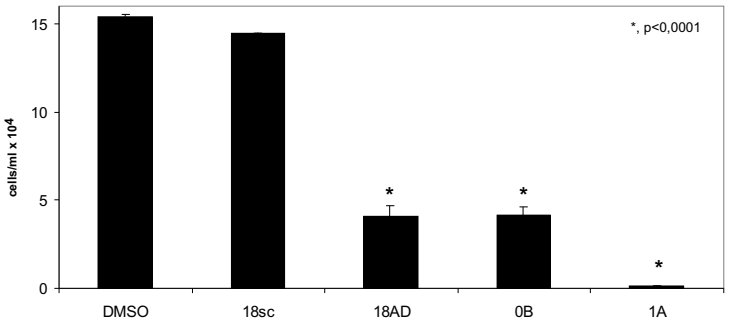

Figure 3.24. | **Effects of peptide 18AD, 18sc, 0B and 1A on cell growth.** Number of living INA-6 cells in the presence of 60 μM peptide 18AD, 18sc, 0B or 1A after 36 h of peptide treatment. Means and SD of two independent experiments are shown. Triplicate measurements were performed for each experiment. Cell numbers were determined by trypan blue exclusion.

The initially planed reverse alanine scan can not be continued because the planed negative control of the scan, peptide 1A, is a far more effective inhibitor of myeloma cell growth than the original one, peptide 18AD. Therefore the cellular effects and the molecular basis of peptide 1A are studied further in this thesis.

3.6.2.1. Growth kinetics of peptide 1A treated myeloma cells

Proliferations is monitored in the presence of 50 μM peptide 1A, peptide 0B or DMSO. The anti-proliferative effect of peptide 1A becomes visible in the growth curves within the first 24 h of treatment. Using the microscopic cell screen method, the inhibitory effect of peptide 0B on INA-6 cells is hardly visible (Figure 3.25).

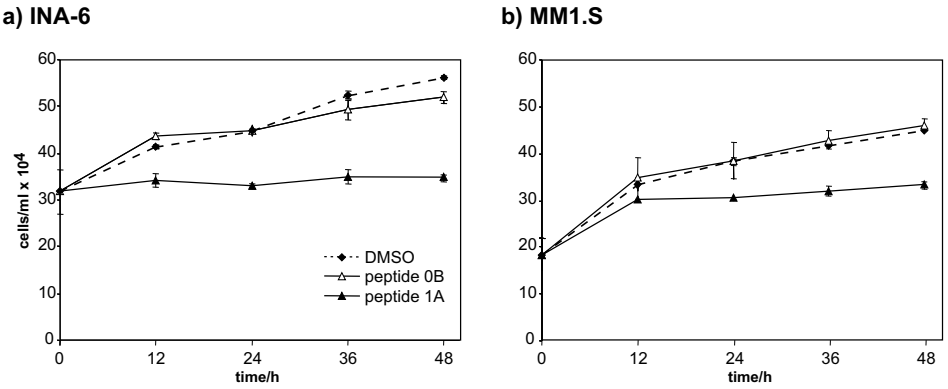

Figure 3.25. | **Growth kinetics of peptide 1A treated myeloma cells.** a.) INA-6 and b.) MM1.S cells are seeded with a density of 2-3x10^5 cells/ml and proliferations is monitored in the presence of 50 μM peptide 1A, peptide 0B or DMSO by microscopic cell screen measurements. Means and SD of triplicate experiments are show.

3.6.3. Effects of an alanine rich lipopeptide sequence on the viability of myeloma cells

Concentration dependent effects of peptide 1A on cellular viability are assayed in human IL-6-dependent INA-6 cells, IL-6-independent MM1.S cells, murine IL-6-dependent 7TD1 cells and Baf-EH cells. Baf-EH cells have a rendered cytokine dependency. In contrast to the native Baf/B03 cells which are IL-3-dependent, Baf-EH cells can grow either IL-3- or Epo-dependent. In Epo-dependent growing Baf-EH cells the proliferative stimulus is transduced via the two ectopically expressed proteins, EpoR-gp130-receptor and human Hck. Cells are treated for 48 h with

0-80 μM peptide or DMSO. Peptide effects are evaluated by FSC/SSC-analysis (Figure 3.26a).

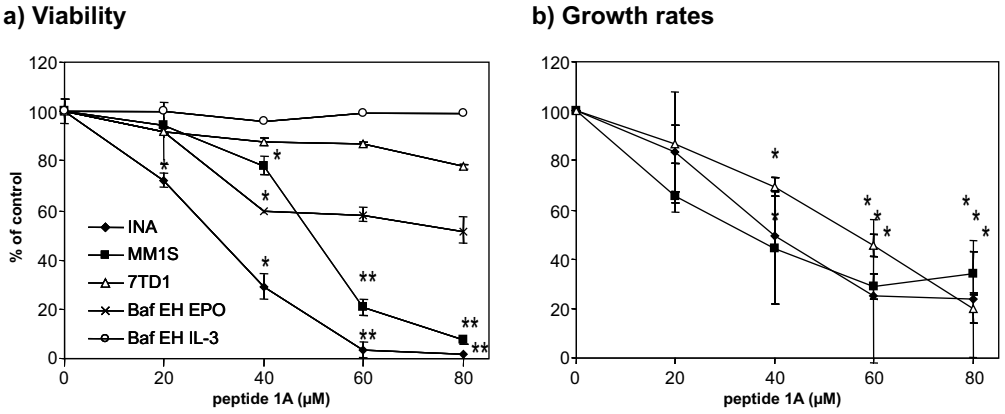

Figure 3.26. | **Effects of peptide 1A on cellular viability of B-cell lines.** The myeloma cell lines INA-6, MM1.S, 7TD1 and Baf-EH cells are seeded at a density of $0.5x10^5$ cells/ml and treated with the indicated concentrations of peptide 1A. The growth medium is supplemented with 1ng/ml and 125pg/ml of IL-6 for INA-6 and 7TD1 cells, respectively, and with 10 % WEHI-conditioned culture supernatend as a source for IL-3 or with 8U/ml mEpo for Baf-EH cells. Experiments are performed in triplicates and averages and standard deviations are shwon a.) Peptide induced cell death is monitored by FSC/SSC-Analysis 48 h after peptide addition and expressed as percentages of viable cells relative to DMSO-treated controls. A representative experiment is shown: *p$\leq$ 0.001 and **p$\leq$ 0.00001. b.) Proliferation of the same cell lines is monitored for 48 h in the presence of peptide 1A. Growth rates relative to DMSO-treated controls are shown. N=3.

In both human myeloma cell lines, INA-6 and MM1.S, the amount of living cells decreases with increasing concentration of peptide added. From this observation it can be concluded, that the effect of peptide 1A on myeloma cells is dose-dependent. The IC_{50} is 31$\pm$3 μM for INA-6 cells and 48$\pm$7 μM for MM1.S cells. The IC_{50}s are calculated from three different experiments. The dose-dependent effect of the peptide on the viability of 7TD1 cells can be detected with higher concentrations of peptide, only. While the peptide shows no effect on IL-3-dependent growing Baf-EH cells, it has some effect on Epo-dependent growing Baf-EH cells.

Concentration dependent effects on cellular proliferation are analysed. INA-6, MM1.S and 7TD1 cells are treated with 0-80 μM of peptide 1A. The proliferation is monitored for 48 h by counting the total number of cells. Growth rates for the different peptide concentrations are calculated from the obtained growth curves (see methods section for calculations). To compare the effects of the different peptide concentrations on the different cell lines, the growth rates of DMSO treated

cells are set to 100 %, respectively (Figure 3.26b). INA-6, MM1.S and 7TD1 cells proliferate less in the presence of increasing concentrations of peptide 1A. The IC_{50}s are 40±1 μM, for INA cells, 36±7 μM for MM1.S cells and 57±4 μM for 7TD1 cells. While the effects on cellular viability of 7TD1 cells can only be detected at higher peptide concentrations, Figure 3.26b shows that peptide 1A inhibited proliferation of 7TD1 cells in a concentration dependent way.

3.6.4. Sequence specificity

Because the effects of peptide 1A are unexpected, new control peptides have to be designed to find out if the effects seen with peptide 1A are sequence specific. For that purpose two new peptides peptide sc-01 and sc-03 are synthesised. Both control peptides have the same amino acid composition as peptide 1A but the primary sequence is arbitrarily scrambled. The sequences are shown in figure 3.27. The advantages of these controls are the similar physicochemical properties of the three peptides.

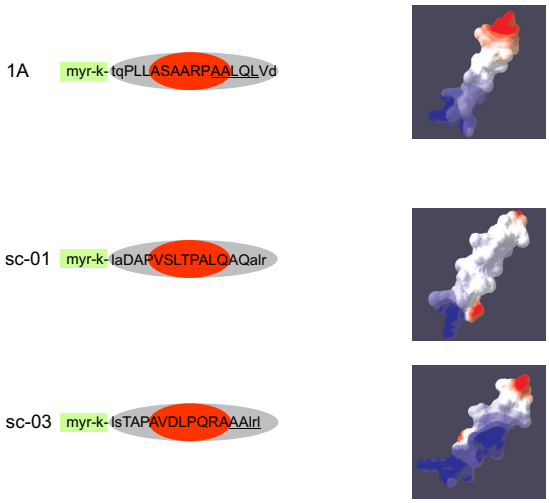

Figure 3.27. | **Sequences and structures of peptides 1A, sc-01 and sc-03.** Sequences and computed 3D-structures of peptides 1A, sc-01 and sc-03. Structures are shown without lipid modification, based on secondary structure predictions. Visualization and calculation of the electrostatic potentials are done with the program SwissPDB-Viewer.

The major difference between the two newly designed control sequences is the distribution of charges within the peptides. Peptide sc-01 is more neutral in the middle of the sequence than peptide 1A. In peptide sc-03 a region of 5 residues in the primary sequence is identical or homologous to peptide 1A. Comparing the

entire peptide sequences of peptide sc-03 with peptide 1A the charge distribution is different between these two peptides. Computed structures with electrostatic potentials of the peptides are shown in figure 3.27.

3.6.5. Concentration dependent effects - peptide 1A vs. control peptides sc-01 and sc-02

An initial evaluation of the effects of the three different peptides is done in INA-6 und MM1.S cells.

Dose-dependent effects of peptide 1A compared to peptides sc-01 and sc-03 are assessed. Peptide concentrations between 10 μM to 120 μM are used. The cells are treated for 48 h with the peptides. The percentage of viable cells is determined. Figure 3.28 shows the concentration-dependent effects of peptide 1A compared to peptides sc-01 and sc-03. While peptides 1A and sc-03 show concentration-dependent effects on cellular viability of INA-6 cells, no such effect is visible with peptide sc-01. The effects on MM1.S cells are comparable. The IC_{50} of peptide 1A in INA-6 cells is ~31 μM which is comparable with the IC_{50} from previous experiments. For peptide sc-03 the IC_{50} is ~69 μM.

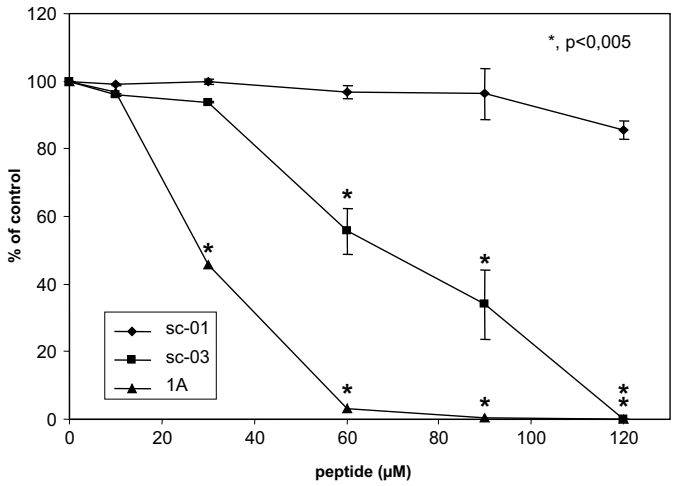

Figure 3.28. | **Dose-dependent effects of peptides 1A, sc-01 and sc-03.** INA-6 cells are treated with up to 120 μM of peptides 1A, sc-01 and sc-03 for 48 h. The percentages of viable cells, determined by FSC/SSC analysis is shown, as percentages of control (DMSO) treated cells. Average percentages of 2-11 measurements obtained in several repetitions of experiments with triplicate cultures.

3.6.6. Mechanism of peptide 1A induced cell death

Annexin-V-binding to phosphatidylserine shows the disruption of the plasma membrane asymmetry which is an early marker for apoptosis. IL-6 depletion in INA-6 cells leads to the induction of apoptosis. INA-6 cells are supplemented with IL-6 and treated with 50 μM peptide 1A or peptide 0B. As a control the cells are deprived of IL-6. 26.4 % of INA-6 cells incubated in the presence of IL-6 alone or 30.1 % of the cells kept with IL-6 and 50 μM peptide 0B are annexin-V-positive. 85.5 % of the IL-6-deprived INA-6 cells and 83.4 % of the cells incubated with IL-6 and peptide 1A are annexin-V-positive. Peptide 1A strongly induces exposure of phosphatidylserine in the outer leaflet of the plasma membrane compared to peptide 0B (Figure 3.29).

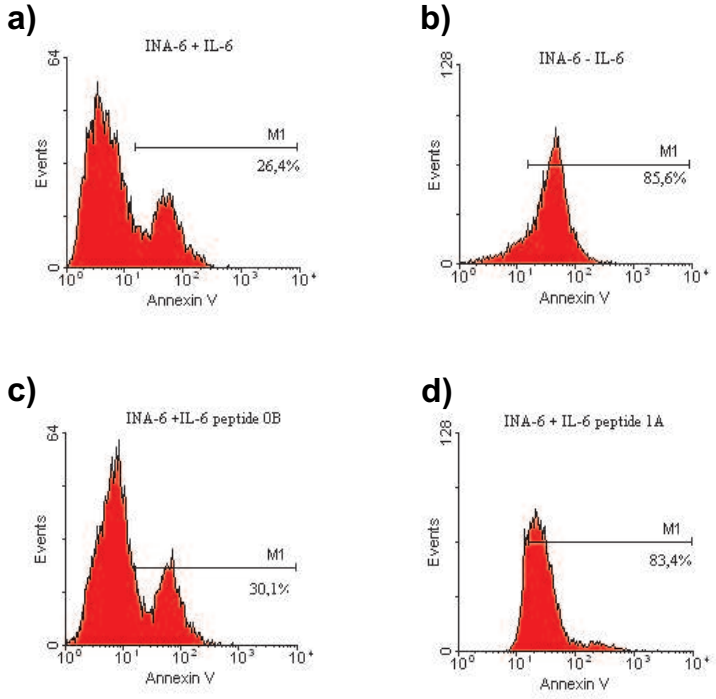

Figure 3.29. | **Peptide 1A-induced disruption of PM asymmetry.** Annexin-V-staining of INA-6 cells grown in the presence a.) or absence b.) of IL-6, or treated with 50 μM of peptides 0B c.) or 1A d.) in the presence of IL-6 for 48 h.

INA-6 cells are treated for 8 h with 40 μM or 80 μM peptide 1A. Aliquots are taken after 2 h, 4 h and 8 h, cells are double-stained with annexin-V and 7AAD. In the presence of 80 μM peptid 1A as early as 2 h after peptide addition, the percentage of total annexin-V-positive cells increased remarkably from 26 % to

68 %. This increase comprises annexin-V single-positive as well as annexin-V- and 7AAD double-positive cells. During the following hours the annexin-V single-positive population becomes double-positive. With 40 μM peptide 1A only a transient increase of annexin-V-positive cells is found (Figure 3.30a).

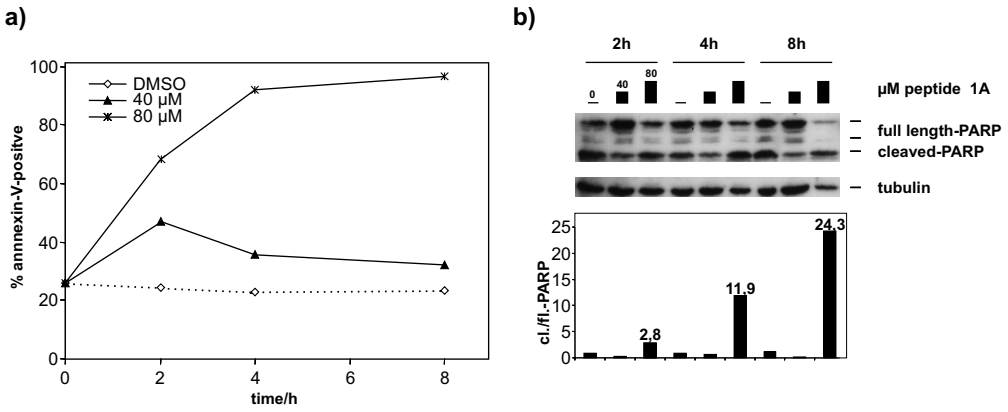

Figure 3.30. | **Apoptosis induction by peptide 1A.** a.) The percentage of annexin-V-positive cells is monitored in INA-6 cells treated for 2 h, 4 h and 8 h with 0.08 % DMSO or with 40 μM or 80 μM peptide 1A, respectively. b.) At all time points, cell samples are lysed, equalized for protein amounts and analysed for PARP cleavage and tubulin expression by Western Blot. The ratio of cleaved to full-length PARP is calculated from densitometry data generated from the Western Blot shown.

Apart from the disruption of plasma membrane asymmetry, caspase activity is a marker for apoptosis. PARP is a substrate of caspase-3 and is cleaved when cells undergo apoptosis. The ratio of cleaved- to full-length-PARP increases more than 20-fold during 8 h of treatment with 80 μM of peptide 1A. However, this effect is caused by an increase of cleaved-PARP mainly during the first 4 h of the treatment, followed by a decrease in full-length protein after longer incubation time. Although equal amounts of protein are loaded, the amount of β-tubulin in the lysates decreases during the time of peptide treatment (Figure 3.30b).

To investigate the molecular effects of apoptosis induction by peptide 1A, INA-6 and MM1.S cells are treated with Trail (Tumor necrosis factor related apoptosis inducing ligand) or with peptide 1A to induce cell death. The effects of peptide treatment on caspase-3 activation is analysed. In addition it is assessed if the pan-caspase inhibitor Z-VAD (Z-VAD-fmk) or the growth factor IL-6 can modulate peptide 1A induced caspase activation. As a positive control, cells are treated with Trail. Trail induced caspase activation can be inhibited by pre-incubation of the cells with Z-VAD. The presence of an excess of IL-6 can not protect the cells against Trail-induced apoptosis. Trail-treated cells can be used as positive controls,

Z-VAD and Trail treated cells can be used as negative controls to investigate the effects of peptide 1A on caspase activation. In the experiment the activation of caspase-3 and the cleavage of PARP are analysed. To finde out if caspase-3 is one of the mediators which participates in the mechanism of peptide 1A-induced cell death, cells are treated for 1 h with 50 μM Z-VAD or DMSO as a control before they are incubated with 60 μM peptide 1A. In addition an excess of IL-6 (2 ng/ml) is added to the cells to find out whether IL-6 can inhibit peptide-induced caspase activation. Figure 3.31 shows induction of caspase-3 activation in INA-6 and MM1.S. The active (cleaved) form of caspase-3 is characterised by a double band at 17 kDA. In cells which are pre-treated with Z-VAD, the cleaved form of caspase-3 is hardly detectable. In INA-6 cells some active caspase-3 can be seen in control cells. An antibody directed against the cleaved form of PARP shows that PARP-cleavage can be induced by Trail or peptide 1A treatment and that the caspase inhibitor Z-VAD can inhibit the cleavage induced by Trail or peptide 1A in both cell lines tested. Incubation of INA-6 cells with peptide 1A leads to activation of caspase-3 and digestion of PARP by caspase-3. The peptide-induced activation of caspase-3 can be blocked by pre-treatment of the cells with Z-VAD. MM1.S cells show similar results. In comparison to INA-6 cells, DMSO treated MM1.S cells show less basal caspase-3 activation and less PARP cleavage. The addition of IL-6 can neither prevent Trail- nor peptide 1A-induced activation of caspase-3 and subsequent PARP cleavage. While the amount of cleaved PARP is comparable in Trail and peptide treated cells, the amount of active caspase-3 is higher in Trail treated cells. This could indicate that different proteases are activated by peptide 1A. While INA-6 cells are already lysed after 3 h incubation with peptide 1A or Trail, MM1.S. are lysed after 16 h. The control staining with an anti-β-tubulin-antibody reveals that the treatment with Trail leads to the proteolytic digestion of β-tubulin. Peptide 1A treatment does not show such an effect on β-tubulin in the experiment shown here.

In parallel to the above described experiment, aliquots are taken after 3 h peptide 1A or Trail treatment and the cellular viability is analysed.

In Trail treated MM1.S cells 35 % more dead cells can be found than in Z-VAD + Trail treated cells. In peptide 1A treated cells 26 % more dead cells are detected, compared to peptide 1A + Z-VAD treated cells (Figure 3.32).

The effect of peptide 1A on the cells can also be visualised by light microscopy. INA-6 cells are treated for 3 h with DMSO or 60 μM peptide 1A. Changes in cellular morphology like loss of membrane integrity, cellular shrinkage and clump formation are found (Figure 3.33).

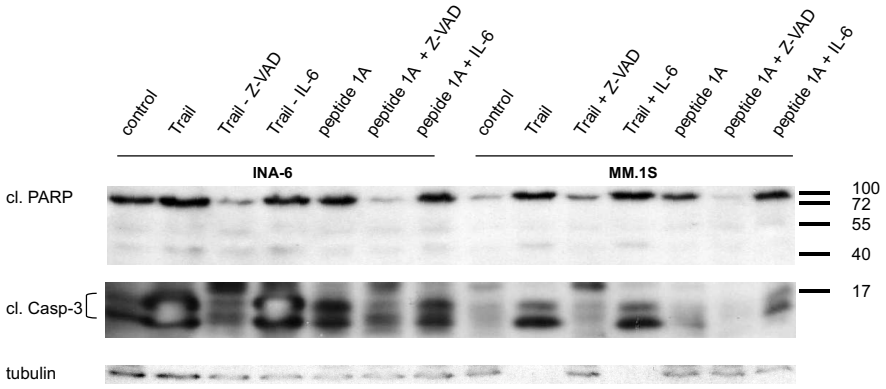

Figure 3.31. | **Peptide 1A-induced caspase-3 activation.** INA-6 and MM1.S cells are treated with peptide 1A or Trail alone or in combination with Z-VAD or IL-6. The activation of caspase-3 is analysed by western blot using an antibody which recognizes the active, cleaved form of caspase-3. Cleaved PARP is detected with a specific antibody against the cleaved form of the enzyme. Beta-tubulin is used as the loading control.

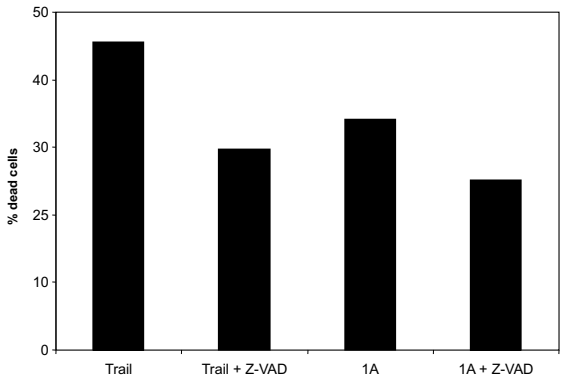

Figure 3.32. | **Caspase inhibition in MM1.S cells.** FSC/SSC analysis of peptide 1A and Trail treated cells in the presence or absence of the caspase inhibitor Z-VAD.

3.6.7. Effects of peptide 1A on the distribution of cell cycle phases

Many chemotherapeutic substances have effects on the progression of the cell cycle. Various mechanisms are known that inhibit proper cell division and can finally lead to cell death. DNA intercalating agents (anthracyclines), inhibitors of replication (topoisomerase II inhibitors, e.g. etoposide) or inhibitors of mitosis (vinca alkaloid or taxanes) are commonly used in standard chemotherapy. The effects of peptide 1A on the cell cycle of INA-6 cells are investigated. The DNA of the cells is stained with propidiumiodid and FSC/SSC analyses are performed in parallel (Figure

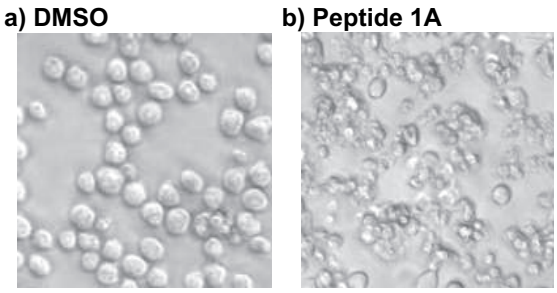

Figure 3.33. | **Phase contrast images of peptide 1A- and control-treated INA-6 cells.** Cells are treated for 3 h with a.) 0.08 % DMSO or b.) 80 μM peptide 1A.

3.34).

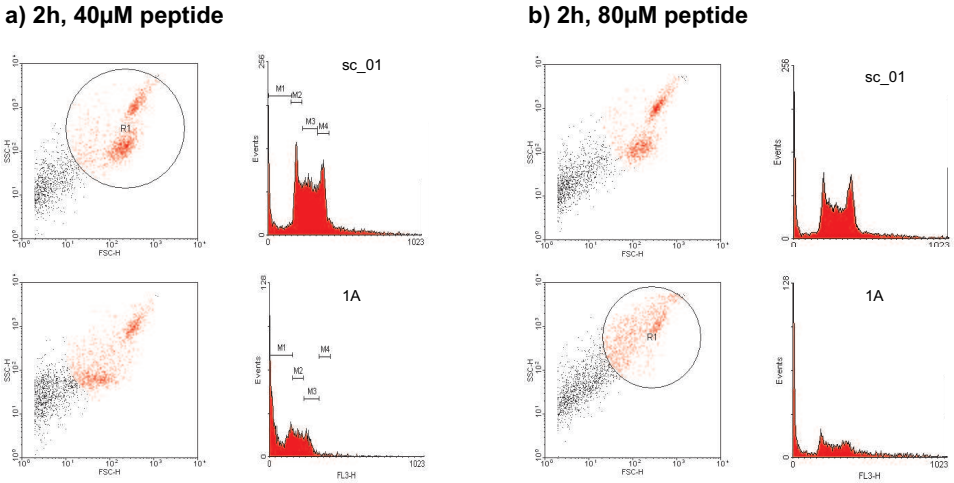

Figure 3.34. | **Cell cycle analysis.** FSC/SSC analysis as well as PI-staining of INA-6 cells, treated for a.) 2 h with 40 μM or b.) 2 h with 80 μM peptide 1A or peptide sc-01.

The population of intact nuclei is significantly reduced after 2 h treatment with 40 μM peptide 1A compared to cells treated with peptide sc-01. The G0-phase, which shows fragmented DNA is increased. After treatment with 80 μM peptide 1A only very few intact nuclei are visible in the FSC/SSC plot. The treatment with 40 μM peptide 1A for 2 h leads to a reduction of all cell cycle phases in comparison to peptide sc-01 and peptide sc-03 treated cells. Using 80 μM peptides the effect is more pronounced, as shown in figure 3.35. The treatment with 40 μM to 80 μM peptide 1A interferes with cell cycle progression and inhibits proper cell division. A cell cycle arrest in one of the phases is not detectable at the peptide concentrations tested.

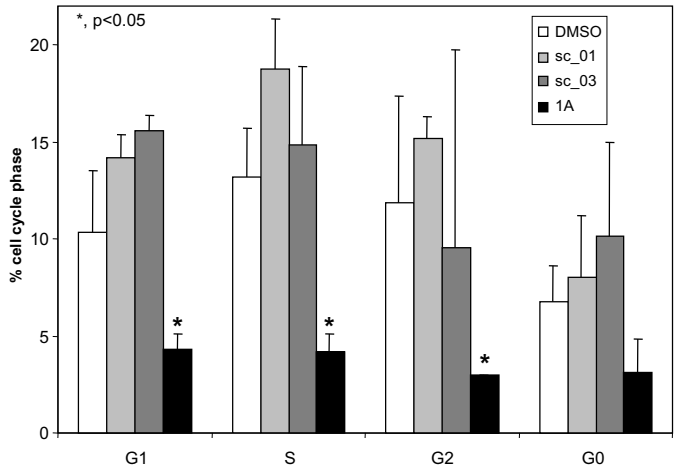

Figure 3.35. | **Distribution of cell cycle phases after peptide treatment.** The effects of the different peptides 1A, sc-01 and sc-03 on the cell cycle phases are analysed. INA-6 cells are incubated for 2 h with 80 μ peptide 1A, peptide sc-01, peptide sc-03 or 0.2 % DMSO. The different phases of the cell cycle are determinded from the histograms of the PI-stainings.

3.6.8. Subcellular localisation of externally administered peptide 1A

To analyse the localisation of peptide 1A inside the cell, a biotin moiety is covalently linked to the ϵ-amino-group of the N-terminal lysine residue of peptide 1A and sc-01. A linker of six carbon-atoms separates the biotin from the peptide. Peptide 1A and peptide sc-01 are biotinylated in that way. The biotinylated peptides are termed peptide 1Abio and peptide sc-01bio. Using fluorescence-labeled avidin or streptavidin the peptide can be visualised.

INA-6 cells are incubated for 1 h with peptide 1Abio and peptide sc-01bio. The localisation of the peptides is visualised by confocal microscopy. Peptides are stained with Alexa-488-labeled avidin (green), nuclei are stained with DAPI (blue). In some experiments the plasma membrane is visualised by lipid raft staining (red) using choleratoxin-B (CTX-B).

Figure 3.36 shows INA-6 cells which are treated for 1 h with peptide 1A. The intensity of the the peptide signal (green) is variable. Four different cells with varying signal intensities are shown. The cell at the very left side did not take up any peptide, while the other cells show more pronounced green areas. Both cells in the middle show green signals mainly in the cytoplasm. The distribution of the signal is not homogeneous. The cell at the very right side shows a diffuse

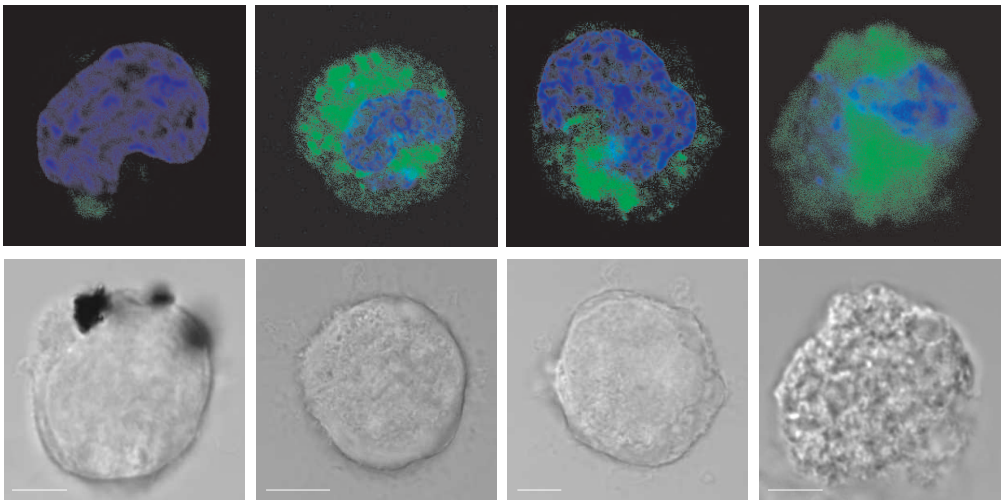

Figure 3.36. | **Localisation of peptide 1Abio.** INA-6 cells are incubated with 80 μM peptide 1Abio, the peptide is visulalized with Alexa-488-labeled avidin (green), the nuclei are stained with DAPI. The lower part shows interference contrast pictures of the respective cells. Scale bar 5 μm.

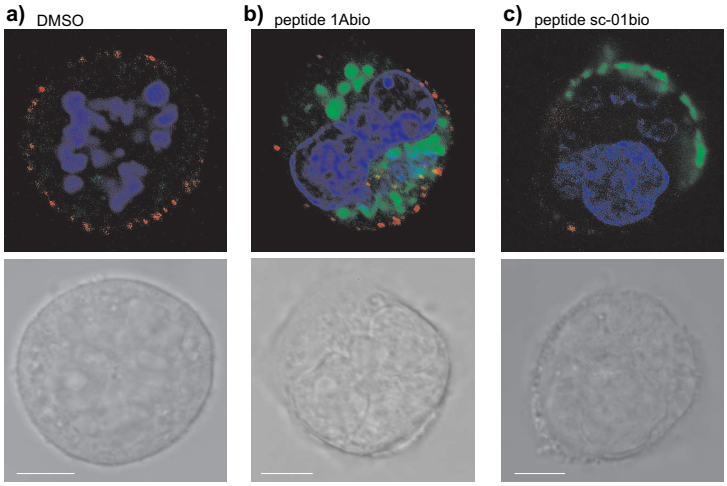

Figure 3.37. | **Co-localisation of peptides with lipid rafts.** The cells are incubated with a.) DMSO, b.) 80 μM peptide 1Abio or c.) peptide sc-01bio. Peptides are visualised with Alexa-488-labeled avidin (green), nuclei with DAPI (blue) and lipid rafts with Cy3 (red). The lower part shows interference contrast pictures of the respective cells, scale bar 5 μm.

distribution of the green areas. Looking at the interference contrast pictures of the respective cells, it becomes clear that the cell at the very right side is very granular, a sign for cell death. In addition co-localisation of the peptides with

lipid rafts is investigated.

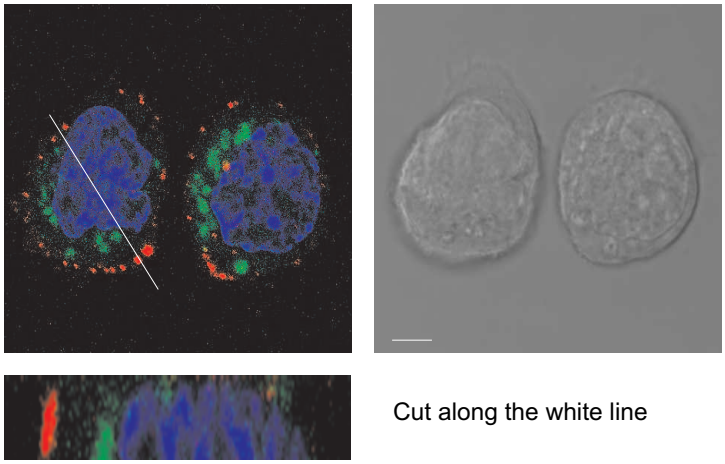

Figure 3.38. | **Co-localistion of peptide 1Abio with lipid rafts.** The cells are incubated with 80 μM peptide 1Abio, the peptide is visualised with Alexa-488-labeled avidin (green), the nuclei are stained with DAPI and lipid rafts with Cy3 (red). The right side shows interference contrast pictures of the respective cells. A cut through the cell along the white line is show. Scale bar 5 μm.

Figures 3.38 and 3.37 show INA-6 cells, which are treated for 1 h with DMSO, peptide 1Abio or peptide sc-01bio. In addition lipid rafts are stained with CTX-B. DMSO treated cells show a clear lipid raft staining. As expected the cells are only very faintly green, this background can be attributed to cellular biotin.

In peptide 1Abio treated cells co-localisation between peptide and lipid rafts is only rarely detected. The peptide seems to be inside the cell. The cut through the cell shown in figure 3.38 underlines this finding. Peptide sc-01bio seems to be predominantly localized at the plasma membrane, the lipid raft staining is hardly detectable in these cells. After 1 h of peptide 1A treatment the peptide is not localized inside the nucleus.

3.6.9. Effects of peptide 1A on IL-6-induced signalling

INA-6 and MM1.S cells are stimulated with IL-6 in the presence of different concentrations of peptide 1A. The effects on downstream signalling molecules which are known to be essential for the anti-apoptotic and pro-prolifeative effects of IL-6 are analysed.

Compared to DMSO-treated controls, INA-6 cells treated with 60 μM peptide 1A have a reduced global tyrosine-phosphorylation profile (Figure 3.39). In the pres-

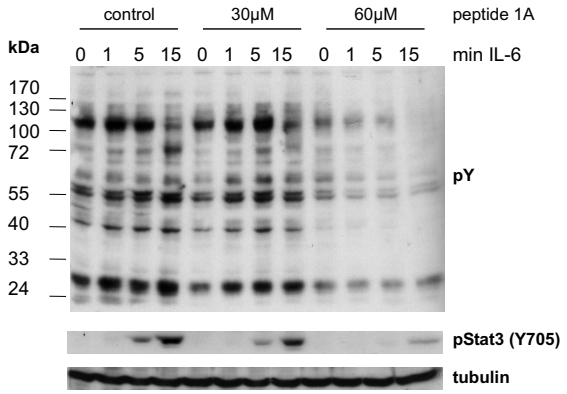

Figure 3.39. | **Inhibition of IL-6-induced signalling in INA-6 cells by peptide 1A.** Prior to lysis cells are deprived of serum for 16 h to reduce background phosphorylation, treated for 2 h either with 0.06 % DMSO, or with 30 or 60 μM of peptide 1A and stimulated for the indicated periods with 1 ng/ml IL-6. Global tyrosine phosphorylation and STAT3 phosphorylation is shown. As a a control for equal loading β-tubulin is shown.

ence of 60 μM peptide 1A, the stimulation with IL-6 does not show the typical increase in phosphorylation of several IL-6-induced proteins. One key-player in the signal transduction from the stimulated IL-6 receptor to the nucleus is STAT3 phosphorylated at tyrosine 705. IL-6-induced STAT3 activation is already impaired by treatment with 30 μM peptide 1A. By treatment with 60 μM peptide 1A tyrosine phosphorylation of STAT3 is blocked almost completely (Figure 3.39). Similarly, in MM1.S cells stimulated with IL-6 for 1-15 min, the IL-6-induced phosphorylation of Akt and Erk1/2 is impaired by treatment with 60 μM peptide 1A (Figure 3.40).

Basal phosphorylation of the MAPK-Family members Erk1/2 and p38 is reduced in INA-6 cells which are kept in the presence of peptide 1A concentrations higher than 40 μM. Minor effects can be seen on STAT3 phosphorylation (Figure 3.41).

Basal as well as IL-6-induced phosphorylation of signalling molecules is impaired in the two human multiple myeloma cell lines INA-6 and MM1.S by peptide 1A concentrations above 30-40 μM.

3.6.10. Celltype specificity of peptide 1A

The ability of peptide 1A to kill neoplastic cells is analysed in 24 different cell lines. The cell lines are derived from human mantle cell lymphoma (MCL), other

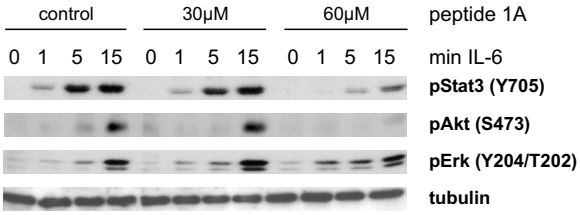

Figure 3.40. | **Inhibition of IL-6-induced signalling in MM1.S cells by peptide 1A.** Prior to lysis, cells are deprived of serum for 16 h, treated for 2 h either with 0.06 % DMSO, or with 30 or 60 μM of peptide 1A and stimulated for the indicated periods with 1 ng/ml IL-6. STAT3, Akt and Erk1/2 phosphorylation in MM1.S cell-lysates is shown. As a a control for equal loading β-tubulin is shown.

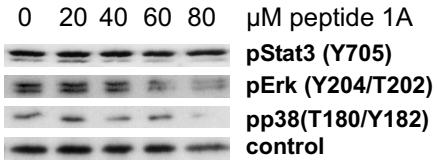

Figure 3.41. | **Effects on basal phosphorylation levels.** INA-6 cells, cultured in the presence of 1 ng/ml IL-6, are left untreated or treated for 2 h either with 0.08 % DMSO or with 20, 40,60 or 80 μ peptide 1A and lysed. The phosphorylation of STAT3, Erk1/2 and p38 is analysed.

lymphomas, acute myeloid leukemia (AML), T-cell acute lyphocytic leukemia (T-ALL) and multiple myeloma. In addition, the IL-3-dependent pro-B-cells Ba/F3, the Epo-dependent Baf-EH and the IL-6-dependent hybridoma cells 7TD1 from murine origin are analysed for their sensitivity to the peptide.

Cells are treated for 48 h with 50 μM peptide 1A, peptide 0B or DMSO, respectively. The percentages of viable cells is determined by FSC/SSC-analysis and annexin-V-staining. As shown in figure 3.42 the human myeloma cell lines INA-6 and MM1.S are most sensitive to peptide 1A treatment. Only 6,6 % of INA-6 and 23,3 % of MM1.S cells are not killed by the peptide. Less pronounced effects are seen in, MM-6, NCEB and in Epo-dependent growing Baf-EH cells.

In addition the effects of peptide 1A on cellular viability of cells, which are derived from solid tumors and on cells which are not derived from tumor tissue are analysed (Figure 3.43). The mammary carcinoma cell line, MCF-7, the glioblastoma/asterocytoma cell line, U373, the renal cell carcinoma cell line, A34, and the neuroblastoma cell line, Kelly, are used as tumor-derived, adherently growing cell lines. Human embryonic kidney cells, HEK 293, and mouse embryonic fibroblasts,

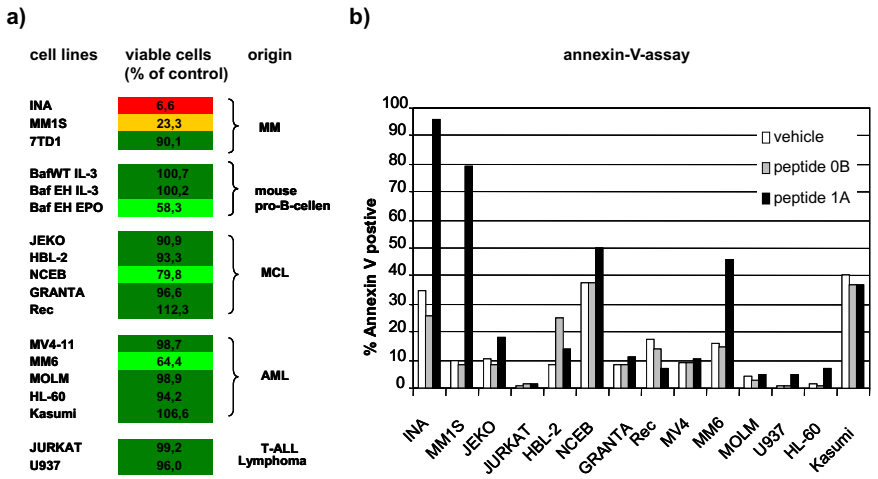

Figure 3.42. | **Effects of peptide 1A on a panel of hematopoetic cell lines.** Cell lines are treated with 50 μM of peptides or DMSO for 48 h, respectively. a.) The percentage of viable, annexin-V-negative cells, relative to DMSO-treated controls, is shown. Color codes are defined according to treatment effects. Shades of red indicate high, shades of green low efficacy of peptide 1A. b.) Typical annexin-V-binding assay of cell lines, as a source of the compilation shown in a).

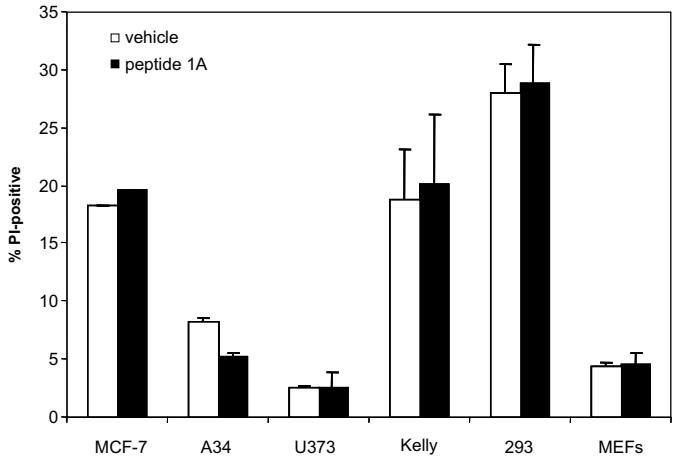

Figure 3.43. | **Effects of peptide 1A on different cell types.** Cell lines derived from solid tumor and non-tumor tissue are treated with 60 μM peptide 1A or 0.06 % DMSO for 48 h. The uptake of PI in the cells is measured by FACS. The percentage of PI-positive cells is shown. N=3.

MEF, represent non-tumor cells. The latter two cell lines are used to assess potential side effects and general toxicity of the peptide. The cells are stained with PI and analysed by FACS. PI can only enter cells with a destroyed plasma membrane.

The peptide has no effects on the viability of the cell lines tested. It should be mentioned that the medium requirements of the assayed cell lines are different.

4. Discussion

The results of this thesis are divided into two major parts. In the first part the SFK interaction and activation region of the signal transducing subunit of the IL-6-receptor, gp130, is narrowed down from 41 to 8 amino acids. A peptide that carries 18 amino acids of this acidic receptor sequence (peptide 18AD) is used to block the receptor-kinase interaction. The biological and molecular effects of peptide 18AD are characterized [129].

To identify single amino acids within the inhibitory peptide sequence a "reverse alanine scan" was employed. Unexpected results changed the direction of the project and led to the identification of peptide 1A, a novel substance with anti-myleloma activities, which is characterized in the second part of the thesis [130].

4.1. Peptide 18AD

The first part of the thesis deals with the N-terminally myristoylated peptide 18AD, the sequence of which is derived from a Hck binding and activating region of gp130. Peptide 18AD is shown to specifically inhibit IL-6-dependent proliferation of MM cells. The inhibitory sequence is identified by a peptide-based functional screening assay. For this purpose, a set of seven overlapping peptides is derived from the AD (Figure 3.1).

4.1.1. Specificity of peptide-induced growth inhibition

The relevance and specificity of the growth inhibition observed in IL-6-dependent MM cell line is supported by the following evidence. (1) Unspecific effects of the peptide sequence can be excluded because an arbitrarily scrambled peptide sequence is included as a control in all experiments (Figure 3.2). (2) Myristoylated peptides actually reach their intracellular site of action. This is shown in two different ways: (a) Fluorescence-labelled peptide 18AD, but not its non-myristoylated equivalent, selectively stained target cells (Figure 3.3). (b) The inhibitory action of

the peptide on factor-dependent growth of 7TD1 depends on the myristoyl modification (Figure 3.5a). (3) The effects of peptide 18AD on 7TD1 cells are reproduced in the IL-6-dependent human myeloma cell line, INA-6 (Figure 3.4b), and in BaF-EH cells overexpressing Hck and chimeric EpoR-gp130. Since the response of Baf-EH cells to Epo is due to overexpressed EpoR-gp130 and Hck molecules, the observed inhibition by peptide 18AD of Epo-dependent proliferation (Figures 3.5b, 3.6c) supports a model, which assumes that peptide 18AD blocks the interaction between gp130 and Hck and thus interrupts proliferation and survival signals. (4) Unspecific cytotoxic effects of peptide 18AD are excluded by the lack of growth inhibition in the IL-6-independent murine hybridoma and human myeloma cell lines OKT1 (Figure 3.5a) and MM1.S (Figure 3.4c). In addition, peptide 18AD does not influence IL-3-dependent growth of wilde type or genetically engineered Ba/F3 cells significantly more than the control peptide 18sc (Figure 3.5b).

The effects of peptide 18AD on myeloma cells are further characterized by assessing growth kinetics (Figure 3.4), apoptosis induction (Figure 3.7), the kinetics of apoptosis induction (Figure 3.8) and distribution of cell cycle phases (Figure 3.9). For potential clinical applications it is important to note that the inhibition of IL-6-dependent proliferation by peptide 18AD is even stronger in the human myeloma cell line, INA-6, than in 7TD1 cells. The bigger effect of IL-6 withdrawal on all three tested read-outs in INA-6 as compared to 7TD1 cells may be due to the 10-times higher IL-6 requirement of INA-6 cells [35]. Apoptosis induction by peptide 18AD appears to be the prevalent contribution to the IL-6-dependent increase in cell number, since significant inhibition of cell cycle progression by peptide treatment could not be detected. A small decrease in the S-phase of the cell cycle can be observed in 7TD1 and INA-6 cells (Figure 3.9). The distribution of cell cycle phases was only moderately changed by IL-6 deprivation itself as compared e.g. to the IL-10 effects in malignant B1 cells [413]. Proliferation must, however, play a role for the balance between cell division and cell death, since the overall cell numbers still increase in the presence of peptide 18AD.

4.1.2. Mechanism of action of peptide 18AD

The potentially therapeutically important inhibition of IL-6-dependent cell growth by peptide 18AD needs to be reaffirmed by mechanistic observations on the level of protein association in order to prove the starting assumptions, that peptide 18AD blocks the binding of Hck and gp130. As a first prerequisite for disrupting intracellular potein-protein interactions the active peptides, must be taken up into the cytoplasm [66]. Here peptide uptake is achieved by conjugation with the fatty acid myristate, that is a common modification of SFK.

Presumably the inhibition of IL-6-dependent growth and survival occurs, because the interaction between the signal transducing subunit of the IL-6 receptor complex, gp130, and the SFK Hck is disturbed in the presence of the membrane penetrating gp130-derived peptide and/or because Hck activation is inhibited. In 7TD1 cells the binding of Hck to gp130 and its displacement by peptide 18AD by co-IP is shown (Figures 3.10, 3.11). Since co-IP is performed at native expression levels, co-precipitation signals upon IL-6 stimulation are weak, but clearly further reduced upon addition of peptide 18ADnm to lysates or of peptide 18AD to intact cells (Figure 3.10). In 7TD1 lysates, peptide 18ADnm is much more efficient in disrupting the association of gp130 and Hck than peptide 18AD. The lack of disruption by peptide 18AD may be explained by altered distribution and accessibility of the myristoylated peptide in lysates containing traces of detergent. For disrupting the association of gp130 and Hck more than 50 μM of peptide 18ADnm is required (Figure 3.11), whereas often peptide concentrations of 20 μM and below are sufficient for displacing proteins from associations [2; 23; 178; 399], although up to 1 mM was used for disrupting preexisting complexes [287; 367; 378]. The association of Hck and gp130 and its interruption by peptide 18AD are confirmed by peptide competition and affinity pull-down analyses using overexpression of the involved proteins and applying a peptide concentration of 750 μM (Figures 3.12, 3.13). Initially the peptide 18AD is derived from the AD of gp130 based on experiments performed with deletion mutants of the EpoR-gp130. The receptor mutant carrying the deletion of the entire AD was unable to bind the SFK Hck, showed reduced kinase activity and reduced proliferation in response to Epo stimulation [323]. To find out whether a deletion of the 18 amino acids corresponding to the sequence of peptide 18AD has comparable effects, a deletion mutant, Eg_del18AD, is constructed. Co-immunopreciptiations of overexpressed Hck and Eg_del18AD show reduced binding of the mutant compared to the wild type receptor to Hck (Figure 3.14).

At native expression levels peptide 18AD effects are more clearly detected in proliferation assays than in co-IP experiments confirming the suitability of a functional assay for the initial characterisation, but leaving a discrepancy in the size of peptide effects between displacement of Hck from gp130 and growth inhibition. The requirement of additional docking proteins [284] and other mechanisms, e.g. inhibition of protein kinase activity or clustering of membrane proteins in lipid rafts [285] may contribute to the stronger effects of peptide 18AD on proliferation and survival than on protein association.

With an IC_{50} of ~30 μM in the 7TD1 and BaF-EH cell culture models peptide 18AD appears comparable to other inhibitory peptides. Thus, the full apoptosis induction in 7TD1 cells by the IL-6-antagonistic peptide RGKEELD was achieved by concentrations above 30 μM [228]. For myristoylated peptides derived from the

catalytic domains of different protein kinases and used at a concentration of 10 μM the thresholds for a proof of efficacy against cancer cell lines was set at 40 % growth inhibition [260]. The inhibition of Erk phosphorylation by membrane-penetrating MEK1-derived peptides exhibited IC_{50} -values of 10-30 μM [181]. In contrast, inhibition by the somatostatin analogs octreotide or RC-160 of the proliferation of myeloma cell lines [99] or a human oral carcinoma cell line [70], respectively, occurred in the nM concentration range, and the latter peptide was more potent when myristoylated. Also the displacement of cytochrome C from IP3-receptor and caspase inhibition by a BODIPY-conjugated acidic peptide occurred with IC_{50}-values in the nM range [23].

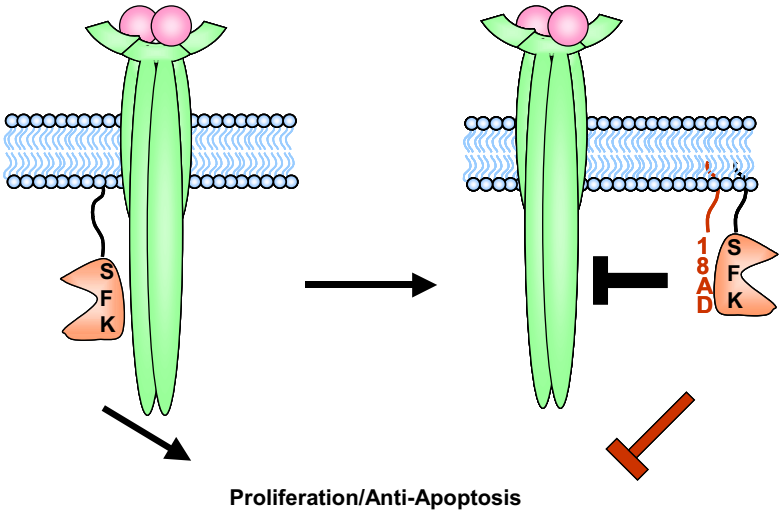

Figure 4.1. | **Peptide 18AD: Model for its mechanistic mode of action.**

4.1.3. Involved signaling pathways

To understand the molecular basis of the peptide-induced block in cell growth and apoptosis, peptide effects on potential signalling pathways downstream of the IL-6 receptor complex are investigated in both the human and murine myeloma model systems (Section 3.4.4.1). Membrane-associated SFKs are known to mediate proliferation and survival signals from a variety of cytokine receptors (Table 1.3). For example p56Lck from the IL-2 receptor [128]. In a similar manner, the SFK Hck was shown to be associated with the AD of gp130 [323]. In MM cell lines IL-6 stimulation increases the activity of Fyn, Hck and Lyn [123]. Here, involvement of SFKs in IL-6-induced signalling pathways in myeloma cells is shown by IL-6-induced activation of several SFKs and by inhibition of this activation by peptide

18AD in INA-6 cells (Figure 3.15). Similarly, expression of kinase-deficient Hck-K269R in 7TD1 cells increased their IL-6-dependence (Figure 3.19a,b) and resulted in lower phosphorylation levels of potential target molecules upon IL-6 stimulation. The combination of the dominant negative effect of Hck-K269R with inhibition by peptide 18AD was not additive (Figure 3.19c). Thus, disruption of gp130-SFK associations and inhibition of SFK activity constitute likely mechanisms explaining the anti-proliferative and pro-apoptotic effects of peptide 18AD (Figure 4.1).

In the murine 7TD1 and Baf-EH cell system, the alternative JAK/STAT-mediated IL-6 signalling pathway was not inhibited by peptide 18AD (Figure 3.16) or catalytically inactive Hck (Figure 3.20) as evidenced by the STAT3 phosphorylation status. However in the human INA-6 cells a reduction of STAT3 phosphorylation upon treatment with 100 μM peptide 18AD can be assessed (Figure 3.17b). This might be a hint for a species or cell typ dependent cross-talk between the JAK/STAT and the SFK-pathways as described in section 1.3.4.3 and figure 1.15. SFKs can play a role in STAT activation in several cytokine, oncogene- and growth factor-induced signalling pathways. For example in the context of signalling from βc, the common signal transducing subunit of the IL-3/IL-5 and GM-CSF receptors, c-Src, is able to phosphorylate and induce nuclear translocation of STAT molecules following IL-3 stimulation [293]. A similar situation is observed in Epo receptor and in Bcr-Abl signalling [162; 185]. Experiments performed in fibroblast show that the SFK Hck directly interacts with STAT3 via its SH3 domain [331].

Here, other signalling pathways which are known to be either downstream of the IL-6 receptor or downstream of SFKs (Figure 1.16) are analysed for their activation (phosphorylation) status after peptide treatment and IL-6 stimulation of IL-6-dependent and independent myeloma cell culture models (Figure 3.17 and 3.18).

Effects on the MAPK family members Erk1/2, p38 and JNK, the PI3-Kinase/Akt pathway, the NFκB and the JAK/STAT are investigated by Western Blot or by using phosphospecific multiplex technology. The deletion of the entire 41aa of the AD led to a reduced Erk1/2 phosphorylation after Epo stimulation in the Baf-EH cell system [323]. However, in 7TD1 cells IL-6 induced Erk1/2 activation could not be detected. For INA-6 cells a mutation of the N-ras gene activates Erk1/2 constitutively. This finding makes it rather unlikely that Erk1/2 activity in INA-6 cells is involved in IL-6-dependent proliferation. In accordance with this, is the observation that the high activity of Erk1/2 could not be blocked by peptide treatment.

Neither Akt nor GSK3a/b phosphorylation could be detected in IL-6 stimulated 7TD1 and INA-6 cells. In these two model cell lines this pathway seams to play a minor role in IL-6-induced prolifieration and in the underlying mechanism of peptide 18AD functions.

Although MM1.S cells did not show any response to peptide 18AD treatment, they are used to find potential downstream signalling molecules which are altered by peptide treatment. The advantage of the MM1.S system is that the major known IL-6-induced signalling molecules can be detected by Western Blot (Figure 3.18a). No difference in the phosphorylation of Erk1/2 and STAT3 are detected in peptide 18AD and peptide 18sc treated cells. Transient and small increases in Akt and GSK3a/b phosphorylation compared to peptide 18sc treated cells can be observed after 1 h peptide 18AD treatment (Figure 3.17a). These finding could not be reproduced using the phospho-multiplex technology because the technique is less sensitive in detecting small changes in phosphorylation levels than the Western Blot technique (Figure 3.18b).

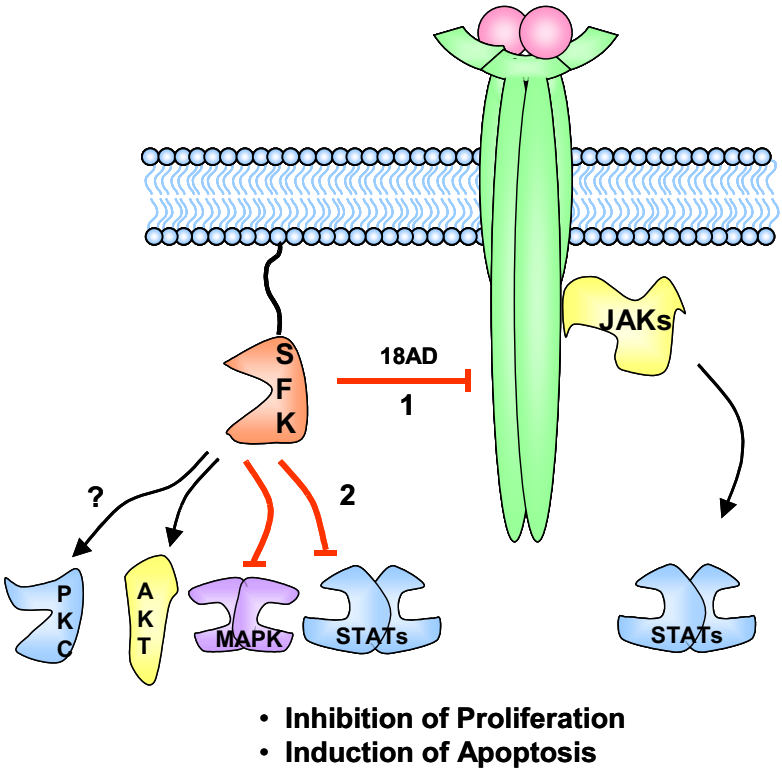

Figure 4.2. | **Peptide 18AD: Model for interference with downstream signalling pathways.** (1) The interaction between SFKs and gp130 and the activity of SFKs are blocked by addition of peptide 18AD or deletion of the AD in gp130. (2) Specific block of signalling pathways downstream of SFKs.

Results from different factor dependent cell lines demonstrate a common mechanism of the molecular peptide effects on SFK activity, but the involved pathways

downstream of the SFKs appear to differ among species and cell lines tested. The results obtained from 7TD1 and Baf-EH cells support a model of independent JAK/STAT and SFK pathways without crosstalk between the respective pathways. Data from INA-6 cells show peptide effects on both pathways and this speaks in favor of a model in which crosstalk takes place. The disturbance of both major survival and proliferation pathways downstream of IL-6 by peptide 18AD in INA-6 cells would explain the high sensitivity of these cells toward peptide treatment.

The effects on many other potential signalling molecules and pathway which are known to be involved in SFK-signalling and in IL-6 signling have not been investigated in this thesis. One candidate pathway is the CD45/SFK-pathway. CD45 activates receptor bound SFKs. The activated SFKs lead to the activation of PLCγ_2, Ca^{2+} release from the ER and the activation of PKC-β. This pathway was shown to be independent of JAK/STAT and SHP-2/Erk1/2 signalling [165; 167]. Recently, an important role of Hck for survival signalling in MM cells was found to consist in mediating the phosphorylation of the docking proteins Gab1 and Gab2 [284]. In epithelial cells devoid of SFK activity, however, signal transduction pathways induced by leukaemia inhibitory factor were fully active [202]. Taken together SFKs are the most prominent target of peptide 18AD in the IL-6 signalling pathways analyzed here. Figure 4.2 summarizes the effects of peptide 18AD on multiple signalling pathways downstream of SFKs.

Recently SFKs have been shown to be involved in other haematological diseases like bcr-abl-induced B-lymphoblastic [153] and chronic lymphocytic [61] leukaemia and identified as targets for small molecule drugs [339]. Interestingly the dual specific Src/Abl inhibitor Dasatinib® is now in clinical trials for MM [54].

4.1.4. Binding motives

Binding studies using degenerated peptide libraries yielded a consensus substrate sequence for cytoplasmatic tyrosine kinase- and SH2-domain-binding sites [355]. This consensus sequence is similar to the acidic domain of gp130 apart from the central tyrosine or phospho-tyrosine. *Songyang and Cantley, 1995* could show that the acidic amino acids surrounding the tyrosine are essential for substrate recognition, because they contribute the majority of ionic interactions (Figure 3.21). Therefore, the acidic core sequence of peptide1 8AD, DSEERPEDL, which resembles the consensus substrate sequence of tyrosine kinases [355; 357] may also be the structrual basis for peptide 18AD effects. This assumption is tested by using another deletion mutant of the receptor Eg_del8AD for co-immunoprecipition (Figure 3.22a) and peptide 8AD for proliferation assays in 7TD1 cells (Figure 3.22b).

While co-immunoprecipitations show that the Eg_del8AD does no longer precipitate with Hck, proliferation assays done with different concentrations of peptide 8AD and the scrambled control peptide, peptide 8sc, do not show a differential inhibition of cell growth.

Motives, similar to the acidic domain, could be found by *in silicio* motive scan analysis [261] in different growth factor, cytokine receptors and signalling molecules. In these analyses the motive is scanned against the amino acid sequence of the complete human proteome. Initially the motives DSEERPEDL and LLDSEERPEDLQLVD are used for the search. In this stringent search four sequence motives matches were found with, the cytoplasmatic domain of the IL-20 receptor alpha chain (IL-20Rα), the signal transducing region of the vascular endothelial growth factor receptor 2 (VEGF-R2), the adapter molecule caspase recruiting domain protein 11 (CARD11,CARMA1) and with the receptor like tyrosine kinase (Ryk) (Figure 4.3). The IL-20 receptor is a type II cytokine and is involved in the signal transduction of cytokines like IL-20, IL-19, IL-24 and IL-26. Moreover the receptor was shown to heterodimerize with the IL-10 receptor beta chain [274; 340]. The receptor tyrosine kinase VEGF-R2 is involved in angiogenesis, is overexpressed in a variety of cancers and is an attractive drug target. Ryk is discussed to be involved in Wnt signalling and may play a role in ovarian cancer [39; 394]. CARMA1 is an adapter molecule which links the innate and adaptive immune response. CARMA1 gets phosphorylated by different isoforms of PKC at several serine residues in response to antigen stimulation of the BCR or the TCR. Interestingly, as in gp130, the serine phosphorylation sites are close to the sequence of the acidic domain derived motive. Together with other adapter molecules e.g. Bcl-10, Malt-1, TRAF2 and TRAF6 which are also involved in the innate immune response downstream of TNFR and toll-like-receptors, CARMA1 is involved in the downstream activation of NFκB and JNK [292].

In a less stringent motif scan, certain amino acides are allowed to take the place of those with similar properties, i.e. for instance the acidic amino acids glutamic acid and aspartic acid may substitute each other. These search reveal additional proteins containing related motives of which at least nine are known to be involved in cellular signalling (Figure 4.3). The cytoplasmatic tails of the cytokine receptor IL-2Rβ and the growth factor receptor HER-2 are among those. HER-2 is well known to be overexpressed in certain breast cancer tumors. Furthermore signalling molecules like Vav-2 or the oncogenic kinase PIM-1 and PIM-3 have such motives. Some molecules of the tumor necrosis factor (TNF) signalling cascade e.g. TNF receptor 1, the adapter molecules TRADD and TRAF7 and RIP kinase contain similar motives.

The results of this thesis show, that a sequence of 8-9 amino acids within gp130

consensus sequences		Position
18AD	LLDSEERPEDLQLVD	786-790
high stringency homology matrices		
IL-20R	HTDSEEGPEEEPSTT	464-478
VEGF-R2	DVEEEEAPEDLYKDF	985-999
CARMA1	SSTSEESPEDSKYFL	477-491
RYK	ALDPEERPKFQQLVQ	577-591
degenerated homology matrices		
IL-2RB	DPYSEEDPDEGVAGA	385-399
PIM-3	LLDWFERPDGFLLVL	109-123
PIM-1	LLDWFERPDSFVLIL	106-120
VAV-2	LSHSAERPERQQLKE	347-361
TRADD	LAESGGSPDVLQMLK	49-63
HER-2	MIDSECRPRFRELVS	960-974
TRAF7	LPEEEEEPEPLVFAE	109-123
TNF-R2	LGSTEEKPLPLGVPD	441-455
RIP	GIEEKFRPFYLSQLE	280-294

Figure 4.3. | **A web based motive scan software [261] is used to identify molecules which share the AD motive.** Initially the motive DSEERPEDL is used as the homology matrix. The enlarged motive LLDSEERPEDLQLVD, revealed the kinase Ryk. The degenerated matrix [X][X][DE][STWQDE][DE][DE][HKR][P][DE][DE][GAVILM][X][X][X][X] led to the identification of the IL-2Rβ motive, the more degenerated matrices [L(GAVILM)][L(GAVILM)][D(DE)][S(STWQ)][E(DE)][E(DE)][R(HKR)][P][E(DE)]-[D(DE)][L(GAVILM)][Q(STWQ)][L(GAVILM)][V(GAVILM)][D(DE)] and [GAVILM][GAVILM][STWQDE][STWQDE][DE][DE][HKR][P][DE][DE][GAVILM]-[STWQ][GAVILM][GAVILM][DE] showed the rest of the identified molecules. All scans are performed with high stringency conditions (only the best 0,2 % of the search are taken into considerations).

with the prevalence of acidic side chains resembles a potential pseudo substrate domain of tyrosine kinase and is responsible for localisation and activation of SFKs in response to receptor stimulation. The identification of sequence motives similar to the acidic domain in gp130 in other cytokine receptors, receptor tyrosine kinases and adapter proteins might suggest a general role of such motives that could consist

in recruiting kinases to signalling complexes that eventually may be activated by ligand stimulation.

In the first part oft this thesis, a specific inhibitory potency of a myristoylated 18mer peptide for IL-6- or Epo-dependent cell growth and survival is demonstrated in several human and murine cell lines. Peptide 18AD is shown to interfere with the interaction of gp130 with the SFK Hck. The IL-6-induced activation of the SFK Hck, Lyn and Fyn is inhibited by peptide 18AD treatment, because of the inhibited interaction between kinase and receptor. Co-immunoprecipitations from overexpressed proteins confirm that the association is mainly due to the interaction between the kinase and the 9 aa spanning pseudosubstrate domain of gp130. Peptide 18AD is expected to prove useful for developing derivatives with possible applications for the treatment of MM, further studies are needed to elucidate its mode of action. The most important questions to further clarify the mechanisms behind the observed effects of peptide 18AD are: How does the peptide block SFK activity? Which domain(s) of the SFKs is/are involved in binding the peptide and the receptor? Are adapter molecules involved? Can acidic domains generally serve as scaffolds for signalling complex formation in other model systems? Which single amino acids are essential for the effects of peptide 18AD and the concept of the acidic domain? Regarding the clinical relevance and applicability, the influence of the bone marrow microenvironment on the peptide effects has to be clarified. The effects of peptide 18AD have to be confirmed on primary patient samples and in a mouse model.

4.2. Peptide 1A

4.2.1. Design of peptide 1A and its effects on myeloma cells

While biochemical co-immuoprecipitation experiments clearly identified the sequence DSEERPEDL of gp130 as the interaction site for the SFK Hck, proliferation assays using a peptide based approach could not be applied successfully, because the peptide of interest as well as the control peptide reduced proliferation (Figure 3.22). Presumably, the high content of acidic amino acids in the short stretch of eight amino acids is responsible for the anti-proliferative effects of the control peptide, peptide 8sc. Based on the homology between the peptide and the above discussed consensus sequence, the negative charged amino acids within the sequence are thought to be responsible for the effects. Four out of eight amino acids in the sequence of peptide 8AD are negatively charged. It is hardly possible to arrange these four amino acids in a way that the entire sequence differs

significantly from the original one, without getting an accumulation of negatively charged residues.

In oder to elucidate the role of glutamic and aspartic acid residues in the acidic domain of gp130, that was discussed above, a peptide-based "reverse alanine scan" is performed. Using this approach, the shortening of the sequence and the accumulation of negatively charged amino acids can be circumvented. The new peptides have two additional characteristics: A lysine residue is introduced at the N-terminus of the peptide between the myrisoyl moiety and the actual sequence. This lysine residue provides a free primary amine which can be used for chemical crosslinking reactions, to covalently link fluorescence markers or tags like biotin to the peptide. These modifications allow localisation studies of the peptides. Moreover positively charged amino acids at the N-termini of peptides are believed to increase permeability of the peptides [367]. To increase the stability of the peptide inside the cell, some of the amino acids flanking the core-region are exchanged form the natural L-amino acids to the non-natural D-isomers. Peptides composed of D-isomers show better resistance against cleavage by endogenous proteases and peptidases [97; 168; 405] and increase the half life of the peptides inside the cell. Two peptides are synthesised initially: The original peptide 18AD is modified as described above and termed peptide 0B, and peptide 1A, which contains alanine instead of the acidic residues in the core sequence (Figure 3.23). The initial comparison of the effects of both new peptides on the proliferation and viability of human and murine MM cells reveal unexpected results. Peptide 1A, the peptide, designed as a negative control peptide, shows significant growth inhibition and induction of cell death (Figures 3.24, 3.26). IC_{50}s determined from viability assays are 31±3 μM for INA-6 cells and 48±7 μM for MM1.S cells. On 7TD1 cells, effects are seen with higher concentrations only and are more pronounced on cell growth than on viability. The inhibitory potency of peptide 1A on the proliferation of INA-6 and MM1.S cells is in the same range as for apoptosis induction. The inhibitory effects of peptide 0B which corresponds to peptide 18AD but contains D-amino acids and the N-terminal lysine residue, are comparable to the effects of peptide 18AD.

Myeloma cells treated with peptide 1A die very efficiently during the first three to four hours after peptide addition (Figure 3.33) and peptide 1A preferentially acts on myeloma cells while cells from leukaemia and lymphoma as well as cells from solid tumours or of non tumour origin remain unaffected (Figures 3.42, 3.43). The nature of this effect is investigated in the second part of this thesis.

To verify the sequence specificity of the observed effect, two additional scrambled control peptides are generated. Both control peptides, peptide sc-01 and peptide sc-03 have the same amino acid composition as peptide 1A, but the amino

acid sequence is arbitrarily scrambled. However, the control peptides differ in their charge distribution within the sequence. This is also reflected by the hypothetical structures and electrostatic potentials of the peptides (Figure 3.27). Moreover, in peptide sc-03 a region of five residues in the primary sequence is identical/homologous to the sequence of peptide 1A. The most impressive effect of peptide 1A is its ability to induce cell death in myeloma cells. To validate the effects of control peptides, the viability assay with the most sensitive cell line, INA-6, is chosen. Peptide 1A and peptide sc-03 show concentration dependent effects on cellular viability of INA-6 cells, no such effect is visible with peptide sc-01 (Figure 3.28). For peptide sc-03 the IC_{50} is in the micromolar range but significantly higher than that of peptide 1A. Potentially the sequence AALRL of peptide sc-03, which is very similar to AALQL of peptide 1A, is responsible for the effects of peptide sc-03. Taken together, these data suggest that the effects seen with peptide 1A are sequence specific.

4.2.2. Mechanism of apoptosis induction

To elucidate the effects of peptide 1A, the mechanism of peptide 1A induced cell death is investigated. Does peptide 1A lyse the cells by perforation of the plasma membrane and mainly lead to a necrotic cell death or does it induce apoptosis in the treated cells? One hallmark of apoptotic cell death is the disruption of plasma membrane asymmetry. In a normal eurkaryotic cell, phospholipids are distributed asymmetrically between the outer and the inner leaflet of the plasma membrane. During the early events of apoptosis, phosphatidylserine which is mainly found in the inner leaflet of the membrane is found at the outer leaflet. Annexin-V, a molecule which specifically interacts with phosphatidylserine, is used for the detection of phosphatidylserine at the outer surface of the dying cell. Treatment of INA-6 cells with 50 μM peptide 1A for 48 h leads 83,4 % annexin-V-postive cells (Figure 3.29). IL-6 depletion for the same period of time leads to a comparable amount of annexin-V-positive cells. This result can be interpreted as a first hint for the induction of apoptosis by the peptide. However, a scenario where peptide 1A disrupts the plasma membrane and lyses the cells could probably also lead to detectable amounts of annexin-V-bound phosphatidylserine molecules. Therefore, peptide 1A treated INA-6 cells are tested for annexin-V-positive cells in combination with the analysis of PARP cleavage by Western Blot. The cleavage of nuclear poly (ADP-ribose) polymerase (PARP) is another common marker for apoptotic cell death. The enzyme PARP appears to be involved in DNA-repair in response to environmental stress [322]. The human 116 kDA protein is one of the main targets of the effector caspases-3 and -7 in vivo [101; 370]. PARP is cleaved into two pieces of 24 kDA and 89 kDA. This event occurs in the late phase of apoptotic

cell death. The cells become annexin-V-positive rapidly after peptide 1A addition (Figure 3.30). As early as two hours after the addition of peptide 1A to INA-6 cells, approximately 70 % of the cells bind annexin-V. At this time, the ratios of cleaved vs. full-lenght PARP is only slightly increased. Longer treatment periods increase the ratio of cleaved vs. full-length PARP, resulting in 20 times more cleaved PARP than full-length PARP after 20 h treamtent with peptide 1A (Figure 3.30b). The expression of the house keeping protein β-tubulin, however decreases as well after 8 hours as a result of cell death. Both, annexin-V-binding and PARP cleavage, suggest apoptosis as the mode of action of peptide 1A in myeloma cells. In the same line of evidence, treatment with peptide 1A leads to cleavage and activation of caspase-3. Peptide 1A induced caspase-3 activation and PARP cleavage are inhibited by pre-treatment of the cells with the pan-caspase inhibitor Z-VAD-fmk (Figure 3.31). On a functional level, Z-VAD-fmk pre-treatment protected MM1.S cells from peptide 1A induced cell death (Figure 3.32). As a positive control for these experiments, cells are treated in parallel with TRAIL a member of the TNF-receptor superfamily, which is known to induce apoptosis in many tumour cells via the formation of a DISC complex. TRAIL stimulation eventually induces caspase-3 activation and PARP cleavage [183]. The ability of peptide 1A to induce proteolytic cleavage of caspase-3 into the two active fragments (17 and 19 kDA) of the caspase is not very strong in comparison with TRAIL-induced activation of caspase-3. On the other hand, the amount of cleaved PARP is comparable for these substances (Figure 3.31). Most likely peptide 1A activates different effector caspases e.g. caspase-7 to execute apoptosis and cleave substrates like PARP [199].

4.2.3. Effects on cell cycle phases

Many chemotherapeutic substances have effects on the progression of the cell cycle by various mechanisms that inhibit proper cell division and finally lead to cell death. The effects of peptide 1A on the cell cycle of INA-6 cells are investigated. Figures 3.34 and 3.35 show that peptide 1A interferes with all phases of the cell cycle. Further analyses are necessary to define the detailed effects on the different phases of the cell cycle.

4.2.4. Subcellular localisation

Since little is known about potential targets of peptide 1A, it is of interest where the peptide is localized and acts within the target cell. Is it at the surface, in the cytoplasm, inside organells like mitochondria, the ER-membrane or lumen, the nucleus or in other compartments. To learn something about the localisation of

the peptide, a peptide which is covalently linked to biotin at the ϵ-amino-group of the N-terminal lysine residue is used for immunofluorescence detection with dye-conjugated avidin. The biotin is separated from the peptide with a C6-linker. After 1 h treatment time, peptide 1A is mainly distributed unevenly within the cytoplasm of INA-6 cells (Figure 3.36). Counterstaining of the plasma membrane for GM1 using labeled CTX-B demonstrates that peptide 1A is not localized at the cytoplasmic membrane. Moreover, after 1 h the peptide cannot be detected inside the nucleus of the cells (Figure 3.38). Interestingly the control peptide, peptide sc-01-bio is, after the same treatment time, localized close to the membrane (Figure 3.37). Experiments are ongoing to further define the localisation and processing of peptide 1A. The different localisations of peptide 1A and its control, peptide sc-01 maybe explained by the active uptake and processing of peptide 1A, while peptide sc-01 stays unaffected at the membrane. However this assumption has to be verified by additional experiments.

4.2.5. Interference with signalling pathways

The investigation of the mode of action of peptide 1A, apart from its localisation comprises its effects on key signalling pathways. Because IL-6 is one of the major growth and survival factors in MM, peptide effects on downstream signalling molecules of the IL-6 signalling pathway are investigated as described in detail in section 1.3 and discussed above in the context of the effects seen with peptide 18AD. In INA-6 cells, treatment with 60 μM peptide 1A effects IL-6-induced tyrosine phosphorylation in general and STAT3 tyrosine phosphorylation in particular (Figure 3.39).

Major survival and proliferation promonting signalling pathways downstream of the IL-6 receptor are impaired by peptide 1A treatment. In MM1.S cells treated with peptide 1A, the IL-6-induced phosphorylation of STAT3 and Akt are significantly inhibited. Erk1/2 phosphorylation in response to IL-6 stimulation is slightly reduced after peptide treatment (Figure 3.40). Moreover constitutive phosphorylation of signalling molecules of the MAPK family members Erk1/2 and p38 is impaired in peptide 1A treated INA-6 cells at peptide concentrations above 40 μM (Figure 3.41).

4.2.6. Conclusions and outlook

Peptide 1A is a novel peptide-based, sequence and cell typ specific anti-myeloma agent with an IC_{50} of 30-40 μM. Peptide 1A shows, as tested so far, no effects on

cells derived from non-tumors tissue or tumor cells of various origins other than multiple myeloma. Peptide 1A kills myeloma cells by the induction of apoptosis and severely disturbs cell cycle progression. Major survival pathways downstream of the cytokine IL-6, like the STAT3, PI3K/Akt and the MAPK pathway, are inhibited in peptide 1A treated cells. After a treatment time of 1 h the biotinylated version of the peptide is localised in defined regions of the cytoplasm of myeloma cells.

Taking into account the observed cellular and molecular effects of peptide 1A, it is difficult to define a model for the mechanism of action of this peptide, especially because the molecular targets of the peptide are still unknown. Experiments to identify target molecules are going on. Initial peptide pull-down experiments revealed a first potential target molecule with 60 kDA in size which has to be confirmed and identified by mass spectrometry. Some of the results found with peptide 1A in myeloma cells resemble the results described in a publication from *Podar et al., 2006* These authors could show that cholesterol rich caveolae are essential for myeloma cell survival. Cholesterol depletion led to impaired signalling downstream of the IL-6 and IGF-1 receptor because lipid rafts can no longer support proper formation of receptor complexes. The membrane proximal signalling pathways like the PI3K/Akt, the JAK/STAT or the SFK pathway were inhibited. Cytoplasmatic components of downstream components of the signalling pathways were less effected [285]. These findings are in accordance with results obtained after treatment with peptide 1A. Membrane proximal signalling seems to be more affected than more distal signalling events. So far the effects of peptide 1A are investigated only in the context of IL-6 signalling. However, the effects of peptide treatment on signalling events downstream of other important myeloma growth and survival factors like IGF-1 or SCF or others need to be analysed in additional experiments to clarify if the effects seen with peptide 1A are specific for IL-6-dependent signalling process or if they are seen with other factors as well. If the latter is the case, one could speculate about a target which is essential for most receptor transmitted signalling events. Such a mechanism is likely, because peptide 1A does not exclusively induce cell death in IL-6-dependent myeloma cells but also in factor independent cells. It has to be investigated if lipid rafts are properly formed in the presence of peptide 1A and if membrane proximal signalling molecules like SFKs or PI3K are still localised correctly into lipid raft structures. Other similarities with the data shown by *Podar et al., 2006* are the effects on cellular viability and the entirely impaired cell cycle profile seen with the cholesterol depletion agent β-cyclodexrin. The localisation studies with peptide 1A show, that the distribution of the glycosphingolipid GM1, which is often found in lipid rafts is not changed in response to treatment with the biotinylated peptide 1A. CTX-B specifically interacts with GM1 on the membrane and permits labeling of

raft regions. Thus peptide 1A does not seem to influence the existence of lipid rafts. However, GM1 staining provides no information about peptide effects on protein distribution at the plasma membrane. Agents like β-cyclodexrin or lovastatin change the distribution of proteins in the lipid-rafts, but the lipid GM1 is still localised in these structures [297; 404]. The results from the localisation studies speak against a lytic mechanism of action of the peptide. The lines of evidence discussed above, show some similarities with the effects seen by *Podar et al., 2006* after disruption of the protein composition of lipid rafts by cholesterol depletion. Another class of anti-cancer agents which acts at the plasmamembrane are Alkyl-lysophospholipids. They were shown to induce recruitment of death receptors into lipid rafts and activate death receptor signalling independent of ligand stimulation in myeloma cells [96]. Such a mechanism of apoptosis induction could also be responsible for peptide 1A-induced cell death.

Various points of action of peptide 1A are possible with the results obtained so far: (1) Peptide 1A could compete for cell surface receptor binding with cytokines e.g. IL-6. (2) It could interfere with proper receptor assembly or (3) correct association of downstream signalling complexes. (4) Peptide 1A could inactivate upstream kinases like JAKs, SFKs or PI3K or activate phosphatases or other proteins which are responsible to turn signals "off" like the family of SOCS and PIAS proteins. (5) As described above it could activate death receptor signalling and DISC formation. (6) Peptide 1A could induce ER-stress which would also lead to impaired signalling and induction of apoptosis. Figure 4.4 summarizes some possible points of action of peptide 1A. Potential effects of peptide 1A on protein composition of lipid rafts are speculative and have to be investigated further.

Regarding the mechanism of action of peptide 1A the identification of the target molecule(s) of peptide 1A is essential. Two scenarios are possible: (1) The target(s) is/are known for multiple myeloma or other diseases. As a consequence, mechanisms are known and the effects of peptide 1A can be explained by the characteristics of the target(s). If so, peptide 1A has to be compared to other substances targeting the same molecule(s) to find out whether it is superior to theses substances or not. (2) The target(s) is/are unknown. In that case, the quality of the target(s) has to be validated experimentally e.g. by knock-out and overexpression of the identified target molecule(s). Knowing the target molecule(s) will guide experiments clarifying the described peptide effects on signalling, localisation, cell cycle and apoptosis.

Clinical relevance and applicability of a peptide based therapy have to be confirmed in *in vitro* experiments with patient samples and in *in vivo* experiments using a nude [387] mouse model in which subcutaneous tumor growth is monitored or a NOD/SCID [245; 393] mouse model in which tumor burden is analyzed by whole

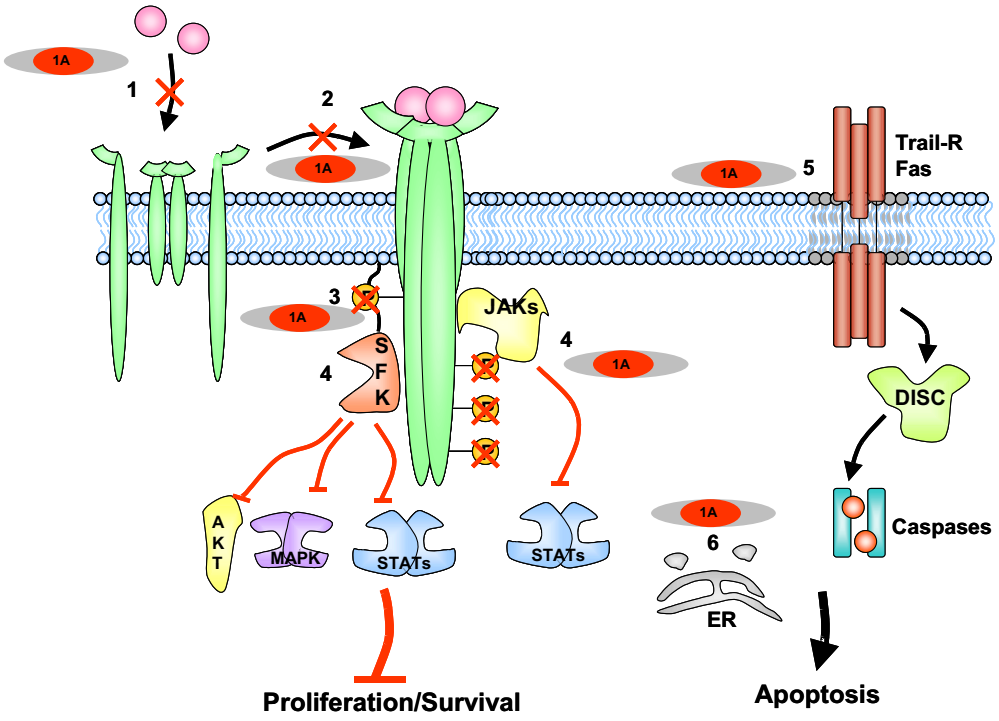

Figure 4.4. | **Potential targets of peptide 1A.**

body imaging.

4.3. Peptide applications in signalling therapies

4.3.1. Therapeutic antibodies, gene and immunotherapies

For decades surgical removal of solid tumors and bone marrow transplantation for some haematopoietic malignancies are the only potential curative therapies available for cancer treatment. The development of novel curative non-invasive therapies against cancer is urgently needed. Antibody therapy is one of the most recent accomplishments of modern, biology-based medicine. Humanized antibodies against more than 10 different target molecules at the surface of malignant cells are approved for clinical use in the EU [92]. Rituximab (MabThera®) should be mentioned as the first therpeutic antibody, approved in 1997 by the FDA. It targets the CD20 antigene. CD20 is expressed on the surface of mature B-cells. Rituximab is used in combination therapy with chemotherapy against agressive Non-Hodgkin-lymphomas. Since 2006 it has been also used in the therapy of

rheumatoid arthritis. Other target molecules of therapeutic antibodies are for example the anti-EGFR antibody (Cetuximab/Erbitux®) used in treatments of epithelial cancers e.g. colon carcinoma, non small cell lung cancer (NSCLC) or head and neck cancer or the anti-HER2/neu-receptor antibody (Herceptin®), which is used in breast cancer therapy. The greatest setback in antibody-based therapies was the first human clinical test for an anti CD-28 antibody TGN1412 in March 2006. Six out of 13 healthy male volunteers suffered from multiple organ dysfunction after treatment [389]. CD28 is expressed on T-cells. For T-cell activation, co-stimulation in addition to TCR stimulation is necessary. In pre-clinical tests, TGN1412 was shown to be a superagonist, which activates T-cells without the need of TCR-ligation [225]. TGN1412 was intended to be used in therapy for B cell chronic lymphocytic leukemia (B-CLL) and rheumatoid arthritis. Applying antibody-based therapy regimes, complete remission is found, but cure is rare; drug resistance occurs and patients suffer from relapse [351]. Major disadvantages of antibody therapy are the limitation of their action to surface proteins or soluble factors because the size of the antibody excludes penetration of cells. In addition elaborate re-engineering is required to minimize immunogenicity.

Gene therapeutic approaches target tumor cells by using viruses as transducers to specifically infect tumor cells and express proteins which are either frequently mutated in cancer e.g. p53 [294], or express proteins involved in the immune response, e.g. CD40L on CLL cells [236]. Initial results looked promising but deaths associated with viral therapy put virotherapy on hold [385].

Immunotherapeutic approaches challenge the immune system to recognize and destroy the tumor cells specifically. Individualized therapies, as well as general tumor associated antigen therapies are tested in clinical trails [54]. The concept of tumor vaccination is an additional promising approach in cancer therapy and prevention. The first "cancer-vaccine" against human papilloma virus (HPV) has been approved in Europe in 2006 [149]. Certain HPV variants are known to cause cervical cancer. However this is a vaccine against the virus causing the neoplasm, not a vaccination against tumor associated antigens.

The complex mechanism of protein-protein interactions in the living cell and its malfunctions are known to be involved in the development and manifestation of cancer and many other diseases. To date mainly enzymatic activities are targets for targeted cancer therapy with small molecule inhibitors. For haematopoietic malignancies the success of Imatinib mesylate (Gleevec®, STI 571), a specific inhibitor for the tyrosine kinase bcr-abl, is the prime example for targeted cancer therapy with a small molecule inhibitor. For non-hematopoetic malignancies the EGFR inhibitor Gefitinib (Iressa®) has to mentioned. Both small molecules target the ATP-binding pocket of the kinase. Targeting the ATP binding pocket to

generate protein kinase inhibitors is common. However this approach has some intrinsic limitations. The ATP binding pocket is highly conserved among kinases [230]. Inhibitors which compete with ATP for binding to the ATP binding pocket of a specific kinase often lack specificity [93]. Moreover, because ATP is the only source of cellular energy, the intracellular ATP concentration is high. Therefore high inhibitor concentrations are required for cellular and *in vivo* activities [210].

4.3.2. Targeting protein-protein interactions and kinases

Only a few inhibitors that inhibit crucial protein protein interactions are available. A few examples are outlined below. Rapamycin is a lipophilic macrolid which was isolated from *Streptomyces hygroscopicus* indigenous to Easter Island (known as Rapa Nui) [384]. It inhibits downstream signalling from the mammalian target of rapamycin (mTOR) proteins [290], that functions in a signalling pathway to promote tumor growth. These evolutionarily conserved protein kinases coordinate the balance between protein synthesis and protein degradation in response to nutrient quality and quantity. Rapamycin binds to the FK-506 binding protein FKBP12 and the rapamycin/FKBP12 complex then binds to mTOR and prevents interaction of mTOR with target proteins in this signalling pathway [312; 313]. The anti-apoptotic protein Bcl-2 (B-cell lymphoma-2) is overexpressed in many different tumors types. Bcl-2 is therefore an attractive drug target. However it exerts its function mainly by protein-protein interaction and not by an enzymatic activity. The main function of the anti-apoptotic members of the Bcl-2 family is to sequester pro-apoptotic molecules of the Bcl-2 family like BAK or BAX or the BH3-only proteins BIM and BID [206].

Medicinal chemistry improves and seems to divide into two major directions: On the one hand by the selection of appropriate small molecules which can block important protein-protein interactions using computer-aided drug design (CAAD) [424] on the other hand by rebuilding of interaction surfaces, generating stable secondary structure elements like α-helices or β-sheets [392]. One excellent example is the peptidiomimetic approach to inhibit the interaction of Bcl-2 with the pro-apoptocic members of the family. For this interaction an α-helix in the anti-apoptotic interaction partner is responsible for the interaction with Bcl-2. A peptide derived from the α- helix of BID was successfully locked in its secondary structure by introducing al-hydrocarbon staples. This "stapled" peptide was able to cross the cell membrane and showed anti tumor activity in a human leukemic xenograft mouse model [393]. Recently stapled peptides were applied to restore native levels of the tumor suppressor p53 and to kill cancer cells by reactivating the p53 pathway [16].

Peptides have been used for decades as *in vitro* inhibitors for enzymatic actives, and to identify and characterize protein-protein interaction sites. If they can be reduced to a few amino acids, they can serve as lead compounds for inhibitor development.

4.3.3. Therapeutic application of intracellular peptides

Peptides themselves have some intrinsic limitations for clinical applications. Usually they are unable to enter cells without modifications. They are extremely sensitive to degradation by proteases and peptidases which are present, as part of the innate immune system, in all body fluids, as well as inside the potential target cells. In addition, peptide stability inside the cells depends on the cell type and the peptide itself [272]. Nevertheless peptides are used in a wide variety of applications. Methods are developing which seem to overcome most of these limitations. Lipid modifications and C-terminal amidations [69; 260; 402], as well as the use of the non-natural D-amino acids instead of the natural L-amino acids stabilizes the peptides and makes them resistant to proteolysis [97; 168; 405]. Membrane permeability can be achieved by addition of lipid modifications or by the addition of a so called cell penetrating peptide (CPP) sequence. The best studied examples for CPPs are the antennapedia protein from *Drosophila*, the VP22 from Herpes simplex and the Tat protein from HIV. Their common feature is a high arginine content and the resulting poly-cationic nature. CPPs were shown to be able to penetrate the cell membrane by macropinocytosis and cross the nuclear envelope [388], while lipid-modified peptides are localized in the cytoplasm [106]. Peptides are also used for tumour cell imaging. In an elegant study *Jiang et al., 2004* fused a poly-cationic sequence for cellular penetration with a polyanionic sequence divided by a matrix-metalloproteinase (MMP) cleavage sequence. In the absence of MMP-2 or -9 the peptide stayed in an uncleaved state and did not enter the cell, because the CPP sequence was shielded by ionic interactions with the polyanionic amino acid residues. In the presence of MMP-2 or -9, which are well known to be overexpressed by tumors, the peptide became cleaved and could enter the cells. A fluorescence dye attached to the peptide enabled in vivo visualization of xenograft tumor cells in mice [168]. The use of peptides to deliver a certain cargo to the cells and to the nucleus is extended to the delivery of peptide-conjugated PNA, which target chromosomal DNA [152] and to si-RNA transduction [237]. For the special interest of modulation of intracellular protein-protein interactions, peptides are shown to be versatile multifunctional tools, which specifically can target a cell of interest, deliver their cargo inside this cell and influence specific protein-protein interactions in this cell. Two examples should be mentioned here: P53-activating peptides and cyclin-dependent kinase 2 antagonist peptides were

successfully targeted to chemokine receptor 4 (CXC4) overexpressing cells [352]. A Stat-3-blocking peptide was targeted to ErbB2 positive breast cancer cells and showed anti-tumor activity in mouse tumor xenografts [367]. As shown in this thesis and discussed above, peptides are excellent tools to target altered and deregulated protein-protein interactions or interactions of hyperactive pathways, e.g. the IL-6 pathway, in diseases like rheumatoid arthritis or multiple myeloma. Peptides can also be used to reactivate hypoactive pathways e.g. the pathways downstream of death stimuli involving Bcl-2 family proteins or the inactivation of transcription factors like the tumor supressor p53. Peptides play an important role for the development of more specific, more effective and individualized therapies and the improvement of diagnostic tools.

5. Summary

The pleiotropic cytokine interleukin-6 (IL-6) is one of the major growth factors for multiple myeloma cells. Our group has previously shown that IL-6 induces the activation of Src family kinases Hck, Lyn and Fyn and that Hck is associated with the IL-6-receptor beta chain (gp130) via an acidic domain in gp130.

In the first part of this thesis the acidic domain is narrowed down from 41 to 18 amino acids by a peptide-based functional screening assay. A derivative of the acidic domain, an 18mer lipopeptide, peptide 18AD, is charaterised on the cellular and molecular level. IL-6-dependent growth of human and murine myeloma cells is inhibited with an IC_{50} of 25-30 μM by the addition of peptide 18AD to the growth medium. These cells remain unaffected by treatment with a control peptide with scrambled sequence (18sc). Furthermore, growth of IL-6-independent myeloma cells is not inhibited by peptide 18AD. In IL-6-dependent cells, peptide 18AD causes the same degree of apoptosis induction as IL-6 deprivation.

On the molecular level it is shown by peptide competition assays that the association of Hck and gp130 is inhibited by peptide 18AD in a concentration dependent way. Peptide 18AD blocked the IL-6-induced activity of the Src family kinases Hck, Lyn and Fyn. Results from different factor-dependent cell lines demonstrate a common mechanism of the molecular peptide effects on Src family kinase activity, but the involved pathways downstream of the kinases appear to differ among species and cell lines tested. Treatment of human IL-6-dependent myeloma cells with peptide 18AD reduced the activating tyrosine phosphorylation of the signal transducer and activator of transcription 3 (STAT3), while STAT3 activation remains unaffected in murine cells. The Co-immunoprecipitations from different overexpressed receptor-deletionmutants and Hck confirms that the association is mainly due to the interaction between the kinase and a 9 amino acids spanning region within the acidic domain which carries the highest accumulation of acidic residues.

Apparently, a sequence of 8-9 amino acids within gp130 with the prevalence of acidic side chains resembles a potential pseudosubstrate domain of tyrosine kinases and is responsible for localisation and activation of Src family kinases in response to receptor stimulation. The identification of sequence motives similar to the

acidic domain of gp130 in other cytokine receptors, receptor tyrosine kinases and adapter proteins by an *in silicio* motive scan might suggest a general role of such motives. This could be the efficient recruitment of cytoplasmic kinases to signalling complexes at the time of ligand stimulation. Here, the importance of the acidic domain-kinase interaction for the IL-6-signaling pathway is shown by the growth-inhibiting effect of peptide 18AD on myeloma cells.

In the second part, a novel sequence and celltype-specific anti-myeloma agent, peptide 1A, is characterised. It was initially designed as the negative control for a "reverse alanine scan" to define the role of the acidic residues within the sequence of peptide 18AD. Unexpectedly it turned out to be at least a 25-fold more potent growth inhibitor of myeloma cells than peptide 18AD. Similar molecular bases of the observed effects of peptide 18AD and peptide 1A are very unlikely, because in contrast to peptide 18AD, peptide 1A efficiently kills IL-6-independent myeloma cells as well. Moreover, an excess of IL-6 fails to rescue the cells from peptide 1A-induced cell death. Peptide 1A shows, as tested so far, no effects on cells derived from non-tumor tissue or tumor cells of various origins other than multiple myeloma. Peptide 1A specifically kills myeloma cells by the induction of apoptosis and severely disturbs cell cycle progression. Apoptotic cell death induction by peptide 1A is shown by peptide 1A-induced caspase-3 activation and the cleavage of PARP, a substrate of effector caspases. Peptide-induced cell death can partly be inhibited by co-treatment with the pan-caspase inhibitor ZVAD-fmk. Major survival pathways like the STAT3, PI3K/Akt and the MAPK pathway are inhibited in peptide 1A treated cells. If a biotinylated version of the peptide is added to the growth medium, it is incorporated into human myeloma cells and localised in defined regions of the cytoplasm of myeloma cells. Here some of the molecular mechanisms of peptide 1A-induced cell death are elucidated. However, the direct molecular target(s) are still unknown.

Despite the potential difference in the molecular mechanisms, both peptides 18AD and 1A are expected to prove useful for developing derivatives with possible applications for the treatment of multiple myeloma.

A. Appendix

A.1. Abbreviations

Abl	Abelson kinase
Akt	Protein kinase B, derived from oncogene carrying retrovirus AKT8
ATP	Adenosinetriphosphate
BAD	Bcl-xL/Bcl-2 associated death promotor
BAX	Bcl-2 associated X protein
Bcl-2	B-cell lymphoma-2
Bcl-10	B-cell lymphoma-10
Bcl-xL	B-cell lymphoma-xL
BCR	B-cell receptor
Blk	B lymphoid tyrosine kinase
BLNK	B-cell linker protein
BID	BH3-interacting domain death agonist
BIM	Bcl-2-like protein 11
CARMA1	Adapter molecule caspase recruiting domain protein 11
Cbp/PAG	Csk binding protein/ predominantly associated with glucolipid enriched membranes
c-Cbl	Casitas B-lineage lymphoma
CD	Catalyic domain
CDK	Cyclin-dependent kinases
CHK	CSK homologous kinase
CSK	C-terminal Src kinase
EGF	Epidermal growth factor
EGFR	Epidermal growth factor receptor
EPO	Erythropoietin
Erk	Extracellular signal-regulated kinase
FcRXY	Fc-ReceptorXY bind to the Fc region (fragment cyristalizable) of an antibody
FGF	Fibroblast growth factor

FGFR	Fibroblast growth factor receptor
Fgr	Feline Gardner Rasheed viral oncogene homolog
FKBP12	FK-506 binding protein
Fyn	Src/yes related novel gene
G-CSF	Granulocyte-colony stimulation factor
GM-CSF	Granulocyte-macrophage-colony stimulation factor
GPXY	Glycoprotein XY
Grb2	Growth factor receptor-bound protein 2
Hck	Hematopoietic cell kinase
HER-2	
HGF	Hepatocyte growth factor
HGFR	Hepatocyte growth factor receptor
IAPs	Inhibitors of apoptosis
IGF-1	Insulin-like grwoth factor-1
IgH	Immunoglobulin heavy chain
IP3-R	Inositol-3-phosphate receptor
ITAM	Immunoreceptor tyrosine-based activation motive
ITIM	Immunoreceptor tyrosine-based inhibitory motive
JNK	c-Jun-N-terminal kinase
LAT	Linker for activation of T-cells
Lck	Lymphocyte specific protein tyrosine kinase
Lyn	Yamaguchi sarcoma viral (v-yes-1) homolog
Malt-1	Mucosa-associated lymphoid tissue lymphoma translocation gene 1
MAPK	Mitogene-activated kinase
Mcl-1	Myeloid derived member of the Bcl family
MD	Molecular dynamics
MEK	MAP/Erk kinase kinase
mTOR	mammalian target of rapamycin
Myc	Avian myelocytomatosis viral oncogene homolog
NF-*kappa*B	Nuclear factor *kappa*-B
P53	Tumorsuppressor
PDGF	Platelet derived growth factor
PDGFR	Platelet derived growth factor Receptor
PH-domain	Pleckstrin homology domain
PI3K	Phospho-inositiol-3-kinase
PIM-1,3	Proto-oncogene serine/threonine-protein kinase. PIM-1,3
PIR-B	Paired Ig-like receptor

PP1	4-Amino-5-(4-methylphenyl)-7-(t-butyl)pyrazolo[3,4-d]- pyrimidine
PP2	4-Amino-5-(4-chlorophenyl)-7-(t-butyl)pyrazolo[3,4-d]- pyrimidine
PTK	Protein-tyrosine-kinase
PTP	Protein tyrosine phosphatase
Pyk-2	Related adhesion focal kinase
Rac	Ras-related C3 Botulinum toxin substrate
Raf	v-Raf murine leukemia viral oncogene homolog
Ras	Rat sarcoma viral homologue (H-Ras, K-Ras ,N-Ras)
Rho	Ras homologue
RIP	Receptor-interacting ser/thr kinase
RTK	Receptor-tyrosine-kinase
Ryk	Receptor like tyrosine kinase
SFK	Src-family-kinase
SH2	Src homology domain 2
SH3	Src homology domain 3
Shc	Src homologous and collagen protein
SHIP-1	SH2-containing inositol 5-phosphatase
SHP-1	SH2 domain-containing PTP-1
SHP-2	SH2 domain-containing PTP-2
SJIA	Systemic Juvenil Idiopatic Arthritis
SLP-76	SH2 domain-containing leukocyte protein of 76 kDa
Src	Avian sarcoma (Schmidt Ruppin A-2) viral oncogene
Syk	Spleen Tyrosine kinase
TCR	T-cell receptor
TGF-β	Transformingr growth factor-β
TKB	Tyrosine kinase binding domain
TNF-α	Tumor necrosis factor-α
TRADD	TNF-receptor associated death domain protein
TRAF-2,6,7	TNF-receptor associated factor-2,6,7
Vav	Guanine nucleotide exchange factor
VEGF	Vascular-endothelial growth factor
VEGFR	Vascular-endothelial growth factor receptor
Yes	Yamaguchi sarcoma viral oncogene
Yrk	Yes-related kinase
Zap- 70	70 kDa Zeta-Associated Protein

Bibliography

[1] T. Adachi, K. Pazdrak, S. Stafford, and R. Alam. The mapping of the lyn kinase binding site of the common b subunit of il-3/granulocyte-macrophage colony stimulation factor/il-5 receptor. *J Immunol*, 162:1496–1501, 1999.

[2] T. Adachi, S. Stafford, S. Sur, and R. Alam. A novel lyn-binding peptide inhibitor blocks eosinophil differentiation, survival, and airway eosinophilic inflammation. *J Immunol*, 163(2):939–46, 1999.

[3] S. Ahn, J. Kim, C. L. Lucaveche, M. C. Reedy, L. M. Luttrell, R. J. Lefkowitz, and Y. Daaka. Src-dependent tyrosine phosphorylation regulates dynamin self-assembly and ligand-induced endocytosis of the epidermal growth factor receptor. *J Biol Chem*, 277(29):26642–51, 2002.

[4] K. Alexandropoulos and D. Baltimore. Coordinate activation of c-src by sh3- and sh2-binding sites on a novel p130cas-related protein, sin. *Genes Dev*, 10(11):1341–55, 1996.

[5] L. Alland, S. M. Peseckis, R. E. Atherton, L. Berthiaume, and M. D. Resh. Dual myristylation and palmitylation of src family member p59fyn affects subcellular localization. *J Biol Chem*, 269(24):16701–5, 1994.

[6] G. Alonso, M. Koegl, N. Mazurenko, and S. A. Courtneidge. Sequence requirements for binding of src family tyrosine kinases to activated growth factor receptors. *J Biol Chem*, 270(17):9840–8, 1995.

[7] O. Alper and E. T. Bowden. Novel insights into c-src. *Curr Pharm Des*, 11(9):1119–30, 2005.

[8] D. Anderson, C. A. Koch, L. Grey, C. Ellis, M. F. Moran, and T. Pawson. Binding of sh2 domains of phospholipase c gamma 1, gap, and src to activated growth factor receptors. *Science*, 250(4983):979–82, 1990.

[9] A. J. Ashcroft, F. E. Davies, and G. J. Morgan. Aetiology of bone disease and the role of bisphosphonates in multiple myeloma. *Lancet Oncol*, 4(5):284–92, 2003.

[10] G. C. Astaldi, M. C. Janssen, P. Lansdorp, C. Willems, W. P. Zeijlemaker, and F. Oosterhof. Human endothelial culture supernatant (hecs): a growth factor for hybridomas. *J Immunol*, 125(4):1411–4, 1980.

[11] T. Atsumi, K. Ishihara, D. Kamimura, H. Ikushima, T. Ohtani, S. Hirota, H. Kobayashi, S. J. Park, Y. Saeki, Y. Kitamura, and T. Hirano. A point mutation of tyr-759 in interleukin 6 family cytokine receptor subunit gp130 causes autoimmune arthritis. *J Exp Med*, 196(7):979–90, 2002.

[12] R. Bataille, M. Jourdan, X. G. Zhang, and B. Klein. Serum levels of interleukin 6, a potent myeloma cell growth factor, as a reflect of disease severity in plasma cell dyscrasias. *J Clin Invest*, 84(6):2008–11, 1989.

[13] S. Becker, B. Groner, and C. W. Muller. Three-dimensional structure of the stat3beta homodimer bound to dna. *Nature*, 394(6689):145–51, 1998.

[14] I. Behrmann, T. Smyczek, P. C. Heinrich, H. Schmitz-Van de Leur, W. Komyod, B. Giese, G. Muller-Newen, S. Haan, and C. Haan. Janus kinase (jak) subcellular localization revisited: The exclusive membrane localization of endogenous janus kinase 1 by cytokine receptor interaction uncovers the jakmiddle dotreceptor complex to be equivalent to a receptor tyrosine kinase. *J. Biol. Chem.*, 279(34):35486–35493, 2004.

[15] E. Bergamin, J. Wu, and S. R. Hubbard. Structural basis for phosphotyrosine recognition by suppressor of cytokine signaling-3. *Structure*, 14(8):1285–92, 2006.

[16] F. Bernal, A. F. Tyler, S. J. Korsmeyer, L. D. Walensky, and G. L. Verdine. Reactivation of the p53 tumor suppressor pathway by a stapled p53 peptide. *J Am Chem Soc*, 129(9):2456–7, 2007.

[17] S. Bezieau, H. Avet-Loiseau, J. P. Moisan, and R. Bataille. Activating ras mutations in patients with plasma-cell disorders: a reappraisal. *Blood*, 100(3):1101–2; author reply 1103, 2002.

[18] A. S. Bhatt, H. Erdjument-Bromage, P. Tempst, C. S. Craik, and M. M. Moasser. Adhesion signaling by a novel mitotic substrate of src kinases. *Oncogene*, 24(34):5333–43, 2005.

[19] J. S. Biscardi, M. C. Maa, D. A. Tice, M. E. Cox, T. H. Leu, and S. J. Parsons. c-src-mediated phosphorylation of the epidermal growth factor receptor on tyr845 and tyr1101 is associated with modulation of receptor function. *J Biol Chem*, 274(12):8335–43, 1999.

[20] J. S. Biscardi, D. A. Tice, and S. J. Parsons. c-src, receptor tyrosine kinases, and human cancer. *Adv Cancer Res*, 76:61–119, 1999.

[21] J. D. Bjorge, A. Jakymiw, and D. J. Fujita. Selected glimpses into the activation and function of src kinase. *Oncogene*, 19(49):5620–35, 2000.

[22] P. Blume-Jensen and T. Hunter. Oncogenic kinase signalling. *Nature*, 411(6835):355–65, 2001.

[23] D. Boehning, D. B. van Rossum, R. L. Patterson, and S. H. Snyder. A peptide inhibitor of cytochrome c/inositol 1,4,5-trisphosphate receptor binding blocks intrinsic and extrinsic cell death pathways. *Proc Natl Acad Sci U S A*, 102(5):1466–71, 2005.

[24] T. J. Boggon, Y. Li, P. W. Manley, and M. J. Eck. Crystal structure of the jak3 kinase domain in complex with a staurosporine analog. *Blood*, 106(3):996–1002, 2005.

[25] J. B. Bolen, P. A. Thompson, E. Eiseman, and I. D. Horak. Expression and interactions of the src family of tyrosine protein kinases in t lymphocytes. *Adv Cancer Res*, 57:103–49, 1991.

[26] C. Bonny, A. Oberson, S. Negri, C. Sauser, and D. F. Schorderet. Cell-permeable peptide inhibitors of jnk: novel blockers of beta-cell death. *Diabetes*, 50(1):77–82, 2001.

[27] M. J. Boulanger, D. C. Chow, E. E. Brevnova, and K. C. Garcia. Hexameric structure and assembly of the interleukin-6/il-6 alpha-receptor/gp130 complex. *Science*, 300(5628):2101–4, 2003.

[28] T. Boulton, N. Stahl, and G. Yancopoulos. Ciliary neurotrophic factor/leukemia inhibitory factor/interleukin 6/oncostatin m family of cytokines induces tyrosine phosphorylation of a common set of proteins overlapping those induced by other cytokines and growth factors. *J Biol Chem*, 269(15):11648–55, 1994.

[29] P. A. Bromann, H. Korkaya, and S. A. Courtneidge. The interplay between src family kinases and receptor tyrosine kinases. *Oncogene*, 23(48):7957–68, 2004.

[30] J. F. Bromberg, M. H. Wrzeszczynska, G. Devgan, Y. Zhao, R. G. Pestell, C. Albanese, and J. Darnell, J. E. Stat3 as an oncogene. *Cell*, 98(3):295–303, 1999.

[31] L. M. Brown, M. S. Linet, R. S. Greenberg, D. T. Silverman, R. B. Hayes, G. M. Swanson, A. G. Schwartz, J. B. Schoenberg, L. M. Pottern, and J. F. Fraumeni, Jr. Multiple myeloma and family history of cancer among blacks and whites in the u.s. *Cancer*, 85(11):2385–2390, 1999.

[32] M. T. Brown and J. A. Cooper. Regulation, substrates and functions of src. *Biochim Biophys Acta*, 1287(2-3):121–49, 1996.

[33] J. S. Brugge and R. L. Erikson. Identification of a transformation-specific antigen induced by an avian sarcoma virus. *Nature*, 269(5626):346–8, 1977.

[34] A. N. Bullock, J. E. Debreczeni, A. M. Edwards, M. Sundstrom, and S. Knapp. Crystal structure of the socs2-elongin c-elongin b complex defines a prototypical socs box ubiquitin ligase. *Proceedings of the National Academy of Sciences of the United States of America*, 103(20):7637–42, 2006.

[35] R. Burger, A. Guenther, F. Bakker, M. Schmalzing, S. Bernand, W. Baum, B. Duerr, G. M. Hocke, H. Steininger, E. Gebhart, and M. Gramatzki. Gp130 and ras mediated signaling in human plasma cell line ina-6: a cytokine-regulated tumor model for plasmacytoma. *Hematol J*, 2(1):42–53, 2001.

[36] G. Burnett and E. P. Kennedy. The enzymatic phosphorylation of proteins. *J. Biol. Chem.*, 211(2):969–980, 1954.

[37] E. A. Burton, S. Hunter, S. C. Wu, and S. M. Anderson. Binding of src-like kinases to the beta-subunit of the interleukin-3 receptor. *J Biol Chem*, 272(26):16189–95, 1997.

[38] C. A. Buser, C. T. Sigal, M. D. Resh, and S. McLaughlin. Membrane binding of myristylated peptides corresponding to the nh2 terminus of src. *Biochemistry*, 33(44):13093–101, 1994.

[39] K. M. Cadigan and Y. I. Liu. Wnt signaling: complexity at the surface. *J Cell Sci*, 119(Pt 3):395–402, 2006.

[40] A. B. Cantor and S. H. Orkin. Hematopoietic development: a balancing act. *Curr Opin Genet Dev*, 11(5):513–9, 2001.

[41] S. Carreno, M.-E. Gouze, S. Schaak, L. J. Emorine, and I. Maridonneau-Parini. Lack of palmitoylation redirects p59hck from the plasma membrane to p61hck-positive lysosomes. *J. Biol. Chem.*, 275(46):36223–36229, 2000.

[42] C. A. Cartwright, M. P. Kamps, A. I. Meisler, J. M. Pipas, and W. Eckhart. pp60c-src activation in human colon carcinoma. *J Clin Invest*, 83(6):2025–33, 1989.

[43] V. W. Chan, C. A. Lowell, and A. L. DeFranco. Defective negative regulation of antigen receptor signaling in lyn-deficient b lymphocytes. *Curr Biol*, 8(10):545–53, 1998.

[44] V. W. Chan, F. Meng, P. Soriano, A. L. DeFranco, and C. A. Lowell. Characterization of the b lymphocyte populations in lyn-deficient mice and the

role of lyn in signal initiation and down-regulation. *Immunity*, 7(1):69–81, 1997.

[45] D. Chauhan, P. Pandey, T. Hideshima, S. Treon, N. Raje, F. E. Davies, Y. Shima, Y. T. Tai, S. Rosen, S. Avraham, S. Kharbanda, and K. C. Anderson. Shp2 mediates the protective effect of interleukin-6 against dexamethasone-induced apoptosis in multiple myeloma cells. *J Biol Chem*, 275(36):27845–50., 2000.

[46] D. Chauhan, H. Uchiyama, Y. Akbarali, M. Urashima, K. Yamamoto, T. A. Libermann, and K. C. Anderson. Multiple myeloma cell adhesion-induced interleukin-6 expression in bone marrow stromal cells involves activation of nf-kappa b. *Blood*, 87(3):1104–12, 1996.

[47] X. Chen, U. Vinkemeier, Y. Zhao, D. Jeruzalmi, J. Darnell, J. E., and J. Kuriyan. Crystal structure of a tyrosine phosphorylated stat-1 dimer bound to dna. *Cell*, 93(5):827–39, 1998.

[48] H. C. Cheng, C. M. Litwin, D. M. Hwang, and J. H. Wang. Structural basis of specific and efficient phosphorylation of peptides derived from p34cdc2 by a pp60src-related protein tyrosine kinase. *J. Biol. Chem.*, 266(27):17919–17925, 1991.

[49] M. Chesi, P. L. Bergsagel, and W. M. Kuehl. The enigma of ectopic expression of fgfr3 in multiple myeloma: a critical initiating event or just a target for mutational activation during tumor progression. *Curr Opin Hematol*, 9(4):288–93, 2002.

[50] G. G. Chiang and B. M. Sefton. Phosphorylation of a src kinase at the autophosphorylation site in the absence of src kinase activity. *J. Biol. Chem.*, 275(9):6055–6058, 2000.

[51] Y.-P. Chong, T. D. Mulhern, H.-J. Zhu, D. J. Fujita, J. D. Bjorge, J.-P. Tantiongco, N. Sotirellis, D. S. S. Lio, G. Scholz, and H.-C. Cheng. A novel non-catalytic mechanism employed by the c-terminal src-homologous kinase to inhibit src-family kinase activity. *J. Biol. Chem.*, 279(20):20752–20766, 2004.

[52] D.-c. Chow, L. Brevnova, X.-l. He, M. M. Martick, A. Bankovich, and K. C. Garcia. A structural template for gp130-cytokine signaling assemblies. *Biochimica et Biophysica Acta (BBA) - Molecular Cell Research*, 1592(3):225–235, 2002.

[53] C. D. Chung, J. Liao, B. Liu, X. Rao, P. Jay, P. Berta, and K. Shuai. Specific

inhibition of stat3 signal transduction by pias3. *Science*, 278(5344):1803–5, 1997.

[54] ClinicalTrails.gov. searched for immunotherapy.

[55] M. S. Collett, J. S. Brugge, and R. L. Erikson. Characterization of a normal avian cell protein related to the avian sarcoma virus transforming gene product. *Cell*, 15(4):1363–9, 1978.

[56] M. S. Collett, E. Erikson, and R. L. Erikson. Structural analysis of the avian sarcoma virus transforming protein: sites of phosphorylation. *J Virol*, 29(2):770–81, 1979.

[57] M. S. Collett, E. Erikson, A. F. Purchio, J. S. Brugge, and R. L. Erikson. A normal cell protein similar in structure and function to the avian sarcoma virus transforming gene product. *Proc Natl Acad Sci U S A*, 76(7):3159–63, 1979.

[58] S. J. Collins, R. C. Gallo, and R. E. Gallagher. Continuous growth and differentiation of human myeloid leukaemic cells in suspension culture. *Nature*, 270(5635):347–9, 1977.

[59] S. N. Constantinescu, L. J. Huang, H. Nam, and H. F. Lodish. The erythropoietin receptor cytosolic juxtamembrane domain contains an essential, precisely oriented, hydrophobic motif. *Mol Cell*, 7(2):377–85, 2001.

[60] J. Content, L. De Wit, P. Poupart, G. Opdenakker, J. Van Damme, and A. Billiau. Induction of a 26-kda-protein mrna in human cells treated with an interleukin-1-related, leukocyte-derived factor. *Eur J Biochem*, 152(2):253–7, 1985.

[61] A. Contri, A. M. Brunati, L. Trentin, A. Cabrelle, M. Miorin, L. Cesaro, L. A. Pinna, R. Zambello, G. Semenzato, and A. Donella-Deana. Chronic lymphocytic leukemia b cells contain anomalous lyn tyrosine kinase, a putative contribution to defective apoptosis. *J Clin Invest*, 115(2):369–78, 2005.

[62] J. A. Cooper, F. S. Esch, S. S. Taylor, and T. Hunter. Phosphorylation sites in enolase and lactate dehydrogenase utilized by tyrosine protein kinases in vivo and in vitro. *J Biol Chem*, 259(12):7835–41, 1984.

[63] J. A. Cooper and B. Howell. The when and how of src regulation. *Cell*, 73(6):1051–4, 1993.

[64] S. J. Corey and S. M. Anderson. Src-related protein tyrosine kinases in hematopoiesis. *Blood*, 93(1):1–14, 1999.

[65] S. A. Courtneidge, A. D. Levinson, and J. M. Bishop. The protein encoded by the transforming gene of avian sarcoma virus (pp60src) and a homologous protein in normal cells (pp60proto-src) are associated with the plasma membrane. *Proc Natl Acad Sci U S A*, 77(7):3783–7, 1980.

[66] L. Covic, A. L. Gresser, J. Talavera, S. Swift, and A. Kuliopulos. Activation and inhibition of g protein-coupled receptors by cell-penetrating membrane-tethered peptides. *Proc Natl Acad Sci U S A*, 99(2):643–8, 2002.

[67] N. Dainiak. Hematologic consequences of exposure to ionizing radiation. *Experimental Hematology*, 30(6):513–528, 2002.

[68] B. Dankbar, T. Pador, R. Leo, B. Feldmann, M. Kropff, R. Mensters, H. Serve, W. Berdel, and J. Kienast. Vascular endothelial growth factor and interleukin-6 in paracrine tumor-stromal cell interactions in multiple myeloma. *Blood*, 95(8):2630–2636, 2000.

[69] P. Dasgupta, A. Singh, and R. Mukherjee. N-terminal acylation of somatostatin analog with long chain fatty acids enhances its stability and anti-proliferative activity in human breast adenocarcinoma cells. *Biol Pharm Bull*, 25(1):29–36, 2002.

[70] P. Dasgupta, A. T. Singh, and R. Mukherjee. Lipophilization of somatostatin analog rc-160 with long chain fatty acid improves its anti-proliferative activity on human oral carcinoma cells in vitro. *Life Sci*, 66(17):1557–70, 2000.

[71] G. Davey Smith, J. D. Neaton, D. Wentworth, R. Stamler, and J. Stamler. Mortality differences between black and white men in the usa: contribution of income and other risk factors among men screened for the mrfit. mrfit research group. multiple risk factor intervention trial. *Lancet*, 351(9107):934–9, 1998.

[72] D. Davidson, L. M. L. Chow, and A. Veillette. Chk, a csk family tyrosine protein kinase, exhibits csk-like activity in fibroblasts, but not in an antigen-specific t-cell line. *J. Biol. Chem.*, 272(2):1355–1362, 1997.

[73] F. E. Davies, A. M. Dring, C. Li, A. C. Rawstron, M. A. Shammas, S. M. O'Connor, J. A. L. Fenton, T. Hideshima, D. Chauhan, I. T. Tai, E. Robinson, D. Auclair, K. Rees, D. Gonzalez, A. J. Ashcroft, R. Dasgupta, C. Mitsiades, N. Mitsiades, L. B. Chen, W. H. Wong, N. C. Munshi, G. J. Morgan, and K. C. Anderson. Insights into the multistep transformation of mgus to myeloma using microarray expression analysis. *Blood*, 102(13):4504–4511, 2003.

[74] P. De Sepulveda, S. Ilangumaran, and R. Rottapel. Suppressor of cytokine signaling-1 inhibits vav function through protein degradation. *J Biol Chem*, 275(19):14005–8, 2000.

[75] A. L. DeFranco, V. W. Chan, and C. A. Lowell. Positive and negative roles of the tyrosine kinase lyn in b cell function. *Semin Immunol*, 10(4):299–307, 1998.

[76] J. DeVos, T. Thykjaer, K. Tarte, M. Ensslen, P. Raynaud, G. Requirand, F. Pellet, V. Pantesco, T. Reme, M. Jourdan, J. Rossi, T. Orntoft, and B. Klein. Comparison of gene expression profiling between malignant and normal plasma cells with oligonucleotide arrays. *Oncogene*, 21(44):6848–57, 2002.

[77] I. Dikic. Mechanisms controlling egf receptor endocytosis and degradation. *Biochem Soc Trans*, 31(Pt 6):1178–81, 2003.

[78] E. Dittrich, C. R. Haft, L. Muys, P. C. Heinrich, and L. Graeve. A di-leucine motif and an upstream serine in the interleukin-6 (il-6) signal transducer gp130 mediate ligand-induced endocytosis and down-regulation of the il-6 receptor. *J Biol Chem*, 271(10):5487–94, 1996.

[79] J. A. Doumanov, M. Daubrawa, H. Unden, and L. Graeve. Identification of a basolateral sorting signal within the cytoplasmic domain of the interleukin-6 signal transducer gp130. *Cell Signal*, 18(8):1140–6, 2006.

[80] H. G. Drexler and R. A. MacLeod. Malignant hematopoietic cell lines: in vitro models for the study of mantle cell lymphoma. *Leuk Res*, 26(9):781–7, 2002.

[81] H. G. Drexler, R. A. MacLeod, A. Borkhardt, and J. W. Janssen. Recurrent chromosomal translocations and fusion genes in leukemia-lymphoma cell lines. *Leukemia*, 9(3):480–500, 1995.

[82] H. G. Drexler and Y. Matsuo. Malignant hematopoietic cell lines: in vitro models for the study of multiple myeloma and plasma cell leukemia. *Leuk Res*, 24(8):681–703, 2000.

[83] B. G. Durie. Concise review of disease and treamtent options. *International Myeloma Foundation*, 2006.

[84] M. J. Eck, S. E. Shoelson, and S. C. Harrison. Recognition of a high-affinity phosphotyrosyl peptide by the src homology-2 domain of p56lck. *Nature*, 362(6415):87–91, 1993.

[85] W. Eckhart, M. A. Hutchinson, and T. Hunter. An activity phosphorylating tyrosine in polyoma t antigen immunoprecipitates. *Cell*, 18(4):925–33, 1979.

[86] T. Eichholtz, D. B. de Bont, J. de Widt, R. M. Liskamp, and H. L. Ploegh. A myristoylated pseudosubstrate peptide, a novel protein kinase c inhibitor. *J Biol Chem*, 268(3):1982–6, 1993.

[87] C. Ellis, F. Kasmi, P. Ganju, E. Walls, G. Panayotou, and A. D. Reith. A juxtamembrane autophosphorylation site in the eph family receptor tyrosine kinase, sek, mediates high affinity interaction with p59fyn. *Oncogene*, 12(8):1727–36, 1996.

[88] M. Encinas, R. J. Crowder, J. Milbrandt, and J. Johnson, E. M. Tyrosine 981, a novel ret autophosphorylation site, binds c-src to mediate neuronal survival. *J Biol Chem*, 279(18):18262–9, 2004.

[89] M. Ernst, D. P. Gearing, and A. R. Dunn. Functional and biochemical association of hck with the lif/il-6 receptor signal transducing subunit gp130 in embryonic stem cells. *Embo J*, 13(7):1574–84, 1994.

[90] M. Ernst and B. J. Jenkins. Acquiring signalling specificity from the cytokine receptor gp130. *Trends Genet*, 20(1):23–32, 2004.

[91] M. Ernst, A. Oates, and A. R. Dunn. Gp130-mediated signal transduction in embryonic stem cells involves activation of jak and ras/mitogen-activated protein kinase pathways. *J Biol Chem*, 271(47):30136–43, 1996.

[92] EU. http://ec.europa.eu/enterprise/pharmaceuticals/register/alfregister.htm -adressed september 07. 2007.

[93] M. A. Fabian, r. Biggs, W. H., D. K. Treiber, C. E. Atteridge, M. D. Azimioara, M. G. Benedetti, T. A. Carter, P. Ciceri, P. T. Edeen, M. Floyd, J. M. Ford, M. Galvin, J. L. Gerlach, R. M. Grotzfeld, S. Herrgard, D. E. Insko, M. A. Insko, A. G. Lai, J. M. Lelias, S. A. Mehta, Z. V. Milanov, A. M. Velasco, L. M. Wodicka, H. K. Patel, P. P. Zarrinkar, and D. J. Lockhart. A small molecule-kinase interaction map for clinical kinase inhibitors. *Nat Biotechnol*, 23(3):329–36, 2005.

[94] R. Fonseca, B. Barlogie, R. Bataille, C. Bastard, P. L. Bergsagel, M. Chesi, F. E. Davies, J. Drach, P. R. Greipp, I. R. Kirsch, W. M. Kuehl, J. M. Hernandez, S. Minvielle, L. M. Pilarski, J. Shaughnessy, John D., A. K. Stewart, and H. Avet-Loiseau. Genetics and cytogenetics of multiple myeloma: A workshop report. *Cancer Res*, 64(4):1546–1558, 2004.

[95] M. C. Frame. Src in cancer: deregulation and consequences for cell behaviour. *Biochim Biophys Acta*, 1602(2):114–30, 2002.

[96] C. Gajate and F. Mollinedo. Edelfosine and perifosine induce selective apoptosis in multiple myeloma by recruitment of death receptors and downstream signaling molecules into lipid rafts. *Blood*, 109(2):711–719, 2007.

[97] S. T. Gammon, V. M. Villalobos, J. L. Prior, V. Sharma, and D. Piwnica-Worms. Quantitative analysis of permeation peptide complexes labeled with technetium-99m: chiral and sequence-specific effects on net cell uptake. *Bioconjug Chem*, 14(2):368–76, 2003.

[98] J. Gauldie, C. Richards, D. Harnish, P. Lansdorp, and H. Baumann. Interferon beta 2/b-cell stimulatory factor type 2 shares identity with monocyte-derived hepatocyte-stimulating factor and regulates the major acute phase protein response in liver cells. *Proceedings of the National Academy of Sciences of the United States of America*, 84(20):7251–5, 1987.

[99] P. Georgii-Hemming, T. Stromberg, E. T. Janson, M. Stridsberg, H. J. Wiklund, and K. Nilsson. The somatostatin analog octreotide inhibits growth of interleukin-6 (il-6)-dependent and il-6-independent human multiple myeloma cell lines. *Blood*, 93(5):1724–31, 1999.

[100] P. Georgii-Hemming, H. J. Wiklund, O. Ljunggren, and K. Nilsson. Insulin-like growth factor i is a growth and survival factor in human multiple myeloma cell lines. *Blood*, 88(6):2250–8, 1996.

[101] M. Germain, E. B. Affar, D. D'Amours, V. M. Dixit, G. S. Salvesen, and G. G. Poirier. Cleavage of automodified poly(adp-ribose) polymerase during apoptosis. evidence for involvement of caspase-7. *J. Biol. Chem.*, 274(40):28379–28384, 1999.

[102] D. J. Giard, S. A. Aaronson, G. J. Todaro, P. Arnstein, J. H. Kersey, H. Dosik, and W. P. Parks. In vitro cultivation of human tumors: establishment of cell lines derived from a series of solid tumors. *J Natl Cancer Inst*, 51(5):1417–23, 1973.

[103] R. M. Gibson, W. P. Schiemann, L. B. Prichard, J. M. Reno, L. H. Ericsson, and N. M. Nathanson. Phosphorylation of human gp130 at ser-782 adjacent to the di-leucine internalization motif. effects on expression and signaling. *J Biol Chem*, 275(29):22574–22582, 2000.

[104] B. Giese, C. Roderburg, M. Sommerauer, S. B. Wortmann, S. Metz, P. C. Heinrich, and G. Muller-Newen. Dimerization of the cytokine receptors gp130 and lifr analysed in single cells. *J Cell Sci*, 118(21):5129–5140, 2005.

[105] Y. Gluzman. Sv40-transformed simian cells support the replication of early sv40 mutants. *Cell*, 23(1):175–82, 1981.

[106] M. Goldenberg-Furmanov, I. Stein, E. Pikarsky, H. Rubin, S. Kasem, M. Wygoda, I. Weinstein, H. Reuveni, and S. A. Ben-Sasson. Lyn is a target gene for prostate cancer: sequence-based inhibition induces regression of human tumor xenografts. *Cancer Res*, 64(3):1058–66, 2004.

[107] Z. Grabarek and J. Gergely. Zero-length crosslinking procedure with the use of active esters. *Analytical Biochemistry*, 185(1):131–135, 1990.

[108] F. L. Graham, J. Smiley, W. C. Russell, and R. Nairn. Characteristics of a human cell line transformed by dna from human adenovirus type 5. *J Gen Virol*, 36(1):59–74, 1977.

[109] S. Greenstein, N. L. Krett, Y. Kurosawa, C. Ma, D. Chauhan, T. Hideshima, K. C. Anderson, and S. T. Rosen. Characterization of the mm.1 human multiple myeloma (mm) cell lines: a model system to elucidate the characteristics, behavior, and signaling of steroid-sensitive and -resistant mm cells. *Exp Hematol*, 31(4):271–82, 2003.

[110] J. S. Greiser, C. Stross, P. C. Heinrich, I. Behrmann, and H. M. Hermanns. Orientational constraints of the gp130 intracellular juxtamembrane domain for signaling. *J Biol Chem*, 277(30):26959–26965, 2002.

[111] J. Grotzinger. Molecular mechanisms of cytokine receptor activation. *Biochim Biophys Acta*, 1592(3):215–23, 2002.

[112] T. Groves, P. Smiley, M. P. Cooke, K. Forbush, R. M. Perlmutter, and C. J. Guidos. Fyn can partially substitute for lck in t lymphocyte development. *Immunity*, 5(5):417–28, 1996.

[113] H. Gu and B. G. Neel. The "gab" in signal transduction. *Trends in Cell Biology*, 13(3):122–30, 2003.

[114] H. Gu, J. C. Pratt, S. J. Burakoff, and B. G. Neel. Cloning of p97/gab2, the major shp2-binding protein in hematopoietic cells, reveals a novel pathway for cytokine-induced gene activation. *Mol Cell*, 2(6):729–40, 1998.

[115] A. C. Guappone and D. C. Flynn. The integrity of the sh3 binding motif of afap-110 is required to facilitate tyrosine phosphorylation by, and stable complex formation with, src. *Mol Cell Biochem*, 175(1-2):243–52, 1997.

[116] C. T. Guy, S. K. Muthuswamy, R. D. Cardiff, P. Soriano, and W. J. Muller. Activation of the c-src tyrosine kinase is required for the induction of mammary tumors in transgenic mice. *Genes Dev*, 8(1):23–32, 1994.

[117] C. Haan, H. Hermanns, P. Heinrich, and I. Behrmann. A single amino acid substitution (trp(666)–>ala) in the interbox1/2 region of the interleukin-6

signal transducer gp130 abrogates binding of jak1, and dominantly impairs signal transduction. *Biochem J*, 349(Pt 1):261–6, 2000.

[118] C. Haan, S. Kreis, C. Margue, and I. Behrmann. Jaks and cytokine receptors–an intimate relationship. *Biochem Pharmacol*, 72(11):1538–46, 2006.

[119] S. Haan, M. Kortylewski, I. Behrmann, W. Muller-Esterl, P. C. Heinrich, and F. Schaper. Cytoplasmic stat proteins associate prior to activation. *Biochem J*, 345 Pt 3:417–21, 2000.

[120] Y. Hakak and G. S. Martin. Ubiquitin-dependent degradation of active src. *Curr Biol*, 9(18):1039–42, 1999.

[121] M. Hallek. Tyrosine kinases and phosphatases in hematopietic growth factor signaling. In H. F. Mertelsmann R., editor, *Hematopoietic Growth Factors in Clinical Application*, pages 10–48. Marcel Dekker Inc., New York, 1995.

[122] M. Hallek, L. P. Bergsagel, and K. C. Anderson. Multiple myeloma: increasing evidence for a multistep transformation process. *Blood*, 91(1):3–21, 1998.

[123] M. Hallek, C. Neumann, M. Schaffer, S. Danhauser-Riedl, N. von Bubnoff, G. de Vos, B. J. Druker, K. Yasukawa, J. D. Griffin, and B. Emmerich. Signal transduction of interleukin-6 involves tyrosine phosphorylation of multiple cytosolic proteins and activation of src-family kinases fyn, hck, and lyn in multiple myeloma cell lines. *Exp Hematol*, 25(13):1367–77, 1997.

[124] J. H. Han, S. J. Choi, N. Kurihara, M. Koide, Y. Oba, and G. D. Roodman. Macrophage inflammatory protein-1alpha is an osteoclastogenic factor in myeloma that is independent of receptor activator of nuclear factor kappab ligand. *Blood*, 97(11):3349–53, 2001.

[125] H. Hanafusa, C. C. Halpern, D. L. Buchhagen, and S. Kawai. Recovery of avian sarcoma virus from tumors induced by transformation-defective mutants. *J Exp Med*, 146(6):1735–47, 1977.

[126] K. W. Harder, N. P. Moller, J. W. Peacock, and F. R. Jirik. Protein-tyrosine phosphatase alpha regulates src family kinases and alters cell-substratum adhesion. *J Biol Chem*, 273(48):31890–900, 1998.

[127] K. F. Harris, I. Shoji, E. M. Cooper, S. Kumar, H. Oda, and P. M. Howley. Ubiquitin-mediated degradation of active src tyrosine kinase. *Proc Natl Acad Sci U S A*, 96(24):13738–43, 1999.

[128] M. Hatakeyama, T. Kono, N. Kobayashi, A. Kawahara, S. D. Levin, R. M. Perlmutter, and T. Taniguchi. Interaction of the il-2 receptor with the src-family kinase p56lck: identification of novel intermolecular association. *Science*, 252(5012):1523–8, 1991.

[129] A. Hausherr, R. Tavares, M. Schaffer, A. Obermeier, C. Miksch, O. Mitina, J. Ellwart, M. Hallek, and G. Krause. Inhibition of il-6-dependent growth of myeloma cells by an acidic peptide repressing the gp130-mediated activation of src family kinases. *Oncogene*, 26(34):4987–98, 2007.

[130] A. Hausherr-Bohn, G. Krause, and M. Hallek. Peptides for treating multiple myeloma. Patent No. 2008113597, 2008.

[131] T. Hayashi, T. Hideshima, and K. C. Anderson. Novel therapies for multiple myeloma. *Br J Haematol*, 120(1):10–7, 2003.

[132] L. A. Hazlehurst, R. F. Argilagos, M. Emmons, D. Boulware, C. A. Beam, D. M. Sullivan, and W. S. Dalton. Cell adhesion to fibronectin (cam-dr) influences acquired mitoxantrone resistance in u937 cells. *Cancer Res*, 66(4):2338–45, 2006.

[133] L. A. Hazlehurst, J. S. Damiano, I. Buyuksal, W. J. Pledger, and W. S. Dalton. Adhesion to fibronectin via beta1 integrins regulates p27kip1 levels and contributes to cell adhesion mediated drug resistance (cam-dr). *Oncogene*, 19(38):4319–27, 2000.

[134] P. C. Heinrich, I. Behrmann, S. Haan, H. M. Hermanns, G. Muller-Newen, and F. Schaper. Principles of interleukin (il)-6-type cytokine signalling and its regulation. *Biochem J*, 374(Pt 1):1–20, 2003.

[135] P. C. Heinrich, I. Behrmann, G. Muller-Newen, F. Schaper, and L. Graeve. Interleukin-6-type cytokine signalling through the gp130/jak/stat pathway. *Biochem J*, 334 (Pt 2):297–314, 1998.

[136] H. M. Hermanns, G. Muller-Newen, P. C. Heinrich, and S. Haan. Bow to your partner for signaling. *Nat Struct Mol Biol*, 12(6):476–8, 2005.

[137] G. Hermanson. Bioconjugate techniques. *Academic Press*, 1996.

[138] M. L. Hibbs, K. W. Harder, J. Armes, N. Kountouri, C. Quilici, F. Casagranda, A. R. Dunn, and D. M. Tarlinton. Sustained activation of lyn tyrosine kinase in vivo leads to autoimmunity. *J Exp Med*, 196(12):1593–604, 2002.

[139] M. L. Hibbs, D. M. Tarlinton, J. Armes, D. Grail, G. Hodgson, R. Maglitto, S. A. Stacker, and A. R. Dunn. Multiple defects in the immune system of

lyn-deficient mice, culminating in autoimmune disease. *Cell*, 83(2):301–11, 1995.

[140] T. Hideshima and K. Anderson. Molecular mechanisms of novel therapeutic approaches for multiple myeloma. *Nat Rev Cancer*, 2(12):927–37, 2002.

[141] T. Hideshima, P. L. Bergsagel, W. M. Kuehl, and K. C. Anderson. Advances in biology of multiple myeloma: clinical applications. *Blood*, 104(3):607–618, 2004.

[142] T. Hideshima, D. Chauhan, T. Hayashi, M. Akiyama, N. Mitsiades, C. Mitsiades, K. Podar, N. C. Munshi, P. G. Richardson, and K. C. Anderson. Proteasome inhibitor ps-341 abrogates il-6 triggered signaling cascades via caspase-dependent downregulation of gp130 in multiple myeloma. *Oncogene*, 22(52):8386–93, 2003.

[143] T. Hideshima, D. Chauhan, R. Schlossman, P. Richardson, and K. Anderson. The role of tumor necrosis factor a in the pathophysiology of human multiple myeloma: therapeutic applications. *Oncogene*, 20:4519–4527, 2001.

[144] T. Hirano, T. Teranishi, B. Lin, and K. Onoue. Human helper t cell factor(s). iv. demonstration of a human late-acting b cell differentiation factor acting on staphylococcus aureus cowan i-stimulated b cells. *J Immunol*, 133(2):798–802, 1984.

[145] T. Hirano, T. Teranishi, and K. Onoue. Human helper t cell factor(s). iii. characterization of b cell differentiation factor i (bcdf i). *J Immunol*, 132(1):229–34, 1984.

[146] T. Hirano, T. Teranishi, H. Toba, N. Sakaguchi, T. Fukukawa, and I. Tsuyuguchi. Human helper t cell factor(s) (thf). i. partial purification and characterization. *J Immunol*, 126(2):517–22, 1981.

[147] K. Hoebe, E. Janssen, and B. Beutler. The interface between innate and adaptive immunity. *Nat Immunol*, 5(10):971–4, 2004.

[148] P. Hof, S. Pluskey, S. Dhe-Paganon, M. Eck, and S. Shoelson. Crystal structure of the tyrosine phosphatase shp-2. *Cell*, 92(February 20):441–450, 1998.

[149] K. Honey. Hpv vaccine gets a shot in the arm. *J Clin Invest*, 116(12):3087, 2006.

[150] K. Horikawa, H. Nishizumi, H. Umemori, S. Aizawa, K. Takatsu, and T. Yamamoto. Distinctive roles of fyn and lyn in igd- and igm-mediated signaling. *Int Immunol*, 11(9):1441–9, 1999.

[151] C. J. Howlett and S. M. Robbins. Membrane-anchored cbl suppresses hck protein-tyrosine kinase mediated cellular transformation. *Oncogene*, 21(11):1707–16, 2002.

[152] J. Hu and D. R. Corey. Inhibiting gene expression with peptide nucleic acid (pna)–peptide conjugates that target chromosomal dna. *Biochemistry*, 46(25):7581–9, 2007.

[153] Y. Hu, Y. Liu, S. Pelletier, E. Buchdunger, M. Warmuth, D. Fabbro, M. Hallek, R. A. Van Etten, and S. Li. Requirement of src kinases lyn, hck and fgr for bcr-abl1-induced b-lymphoblastic leukemia but not chronic myeloid leukemia. *Nat Genet*, 36(5):453–61, 2004.

[154] S. R. Hubbard. Src autoinhibition: let us count the ways. *Nat Struct Biol*, 6(8):711–4, 1999.

[155] S. R. Hubbard. Protein tyrosine kinases: autoregulation and small-molecule inhibition. *Curr Opin Struct Biol*, 12(6):735–41, 2002.

[156] T. Hunter. Protein phosphorylated by the rsv transforming function. *Cell*, 22(3):647–8, 1980.

[157] T. Hunter and B. M. Sefton. Transforming gene product of rous sarcoma virus phosphorylates tyrosine. *Proc Natl Acad Sci U S A*, 77(3):1311–5, 1980.

[158] J. N. Ihle. Cytokine receptor signalling. *Nature*, 377(6550):591–4, 1995.

[159] J. N. Ihle, B. A. Witthuhn, F. W. Quelle, K. Yamamoto, and O. Silvennoinen. Signaling through the hematopoietic cytokine receptors. *Annu Rev Immunol*, 13:369–98, 1995.

[160] A. Imamoto and P. Soriano. Disruption of the csk gene, encoding a negative regulator of src family tyrosine kinases, leads to neural tube defects and embryonic lethality in mice. *Cell*, 73(6):1117–24, 1993.

[161] P. F. Infante. Benzene exposure and multiple myeloma: A detailed meta-analysis of benzene cohort studies. *Ann NY Acad Sci*, 1076(1):90–109, 2006.

[162] E. Ingley and S. P. Klinken. Cross-regulation of jak and src kinases. *Growth Factors*, 24(1):89–95, 2006.

[163] R. B. Irby, W. Mao, D. Coppola, J. Kang, J. M. Loubeau, W. Trudeau, R. Karl, D. J. Fujita, R. Jove, and T. J. Yeatman. Activating src mutation in a subset of advanced human colon cancers. *Nat Genet*, 21(2):187–90, 1999.

[164] R. B. Irby and T. J. Yeatman. Role of src expression and activation in human cancer. *Oncogene*, 19(49):5636–42, 2000.

[165] H. Ishikawa, N. Tsuyama, S. Abroun, S. Liu, F. J. Li, K. Otsuyama, X. Zheng, and M. M. Kawano. Interleukin-6, cd45 and the src-kinases in myeloma cell proliferation. *Leuk Lymphoma*, 44(9):1477–81, 2003.

[166] H. Ishikawa, N. Tsuyama, S. Abroun, S. Liu, F.-J. Li, O. Taniguchi, and M. M. Kawano. Requirements of src family kinase activity associated with cd45 for myeloma cell proliferation by interleukin-6. *Blood*, 99(6):2172–2178, 2002.

[167] H. Ishikawa, N. Tsuyama, M. Obata, and M. M. Kawano. Mitogenic signals initiated via interleukin-6 receptor complexes in cooperation with other transmembrane molecules in myelomas. *J Clin Exp Hematopathol*, 45:55–66, 2006.

[168] T. Jiang, E. S. Olson, Q. T. Nguyen, M. Roy, P. A. Jennings, and R. Y. Tsien. Tumor imaging by means of proteolytic activation of cell-penetrating peptides. *Proc Natl Acad Sci U S A*, 101(51):17867–72, 2004.

[169] L. N. Johnson, M. E. Noble, and D. J. Owen. Active and inactive protein kinases: structural basis for regulation. *Cell*, 85(2):149–58, 1996.

[170] S. A. Jones. Directing transition from innate to acquired immunity: defining a role for il-6. *J Immunol*, 175(6):3463–8, 2005.

[171] T. Jostock, J. Mullberg, S. Ozbek, R. Atreya, G. Blinn, N. Voltz, M. Fischer, M. F. Neurath, and S. Rose-John. Soluble gp130 is the natural inhibitor of soluble interleukin-6 receptor transsignaling responses. *Eur J Biochem*, 268(1):160–7, 2001.

[172] R. Jove and H. Hanafusa. Cell transformation by the viral src oncogene. *Annu Rev Cell Biol*, 3:31–56, 1987.

[173] K. J. Kallen. The role of transsignalling via the agonistic soluble il-6 receptor in human diseases. *Biochim Biophys Acta*, 1592(3):323–43, 2002.

[174] D. Kamimura, K. Ishihara, and T. Hirano. Il-6 signal transduction and its physiological roles: the signal orchestration model. *Rev Physiol Biochem Pharmacol*, 149:1–38, 2003.

[175] M. P. Kamps, J. E. Buss, and B. M. Sefton. Rous sarcoma virus transforming protein lacking myristic acid phosphorylates known polypeptide substrates without inducing transformation. *Cell*, 45(1):105–12, 1986.

[176] M. P. Kamps and B. M. Sefton. Neither arginine nor histidine can carry out the function of lysine-295 in the atp-binding site of p60src. *Mol Cell Biol*, 6(3):751–7, 1986.

[177] T. Kamura, S. Sato, D. Haque, L. Liu, J. Kaelin, W. G., R. C. Conaway, and J. W. Conaway. The elongin bc complex interacts with the conserved socs-box motif present in members of the socs, ras, wd-40 repeat, and ankyrin repeat families. *Genes Dev*, 12(24):3872–81, 1998.

[178] C. Kardinal, B. Konkol, A. Schulz, G. Posern, H. Lin, K. Adermann, M. Eulitz, Z. Estrov, M. Talpaz, R. B. Arlinghaus, and S. M. Feller. Cell-penetrating sh3 domain blocker peptides inhibit proliferation of primary blast cells from cml patients. *Faseb J*, 14(11):1529–38, 2000.

[179] R. E. Karess, W. S. Hayward, and H. Hanafusa. Cellular information in the genome of recovered avian sarcoma virus directs the synthesis of transforming protein. *Proc Natl Acad Sci U S A*, 76(7):3154–8, 1979.

[180] M. Kawabuchi, Y. Satomi, T. Takao, Y. Shimonishi, S. Nada, K. Nagai, A. Tarakhovsky, and M. Okada. Transmembrane phosphoprotein cbp regulates the activities of src-family tyrosine kinases. *Nature*, 404(6781):999–1003, 2000.

[181] B. R. Kelemen, K. Hsiao, and S. A. Goueli. Selective in vivo inhibition of mitogen-activated protein kinase activation using cell-permeable peptides. *J Biol Chem*, 277(10):8741–8, 2002.

[182] M. Kim, T. Tezuka, K. Tanaka, and T. Yamamoto. Cbl-c suppresses v-src-induced transformation through ubiquitin-dependent protein degradation. *Oncogene*, 23(9):1645–55, 2004.

[183] F. C. Kimberley and G. R. Screaton. Following a trail: update on a ligand and its five receptors. *Cell Res*, 14(5):359–72, 2004.

[184] T. Kishimoto, T. Taga, and S. Akira. Cytokine signal transduction. *Cell*, 76(2), 1994.

[185] A. Klejman, S. J. Schreiner, M. Nieborowska-Skorska, A. Slupianek, M. Wilson, T. E. Smithgall, and T. Skorski. The src family kinase hck couples bcr/abl to stat5 activation in myeloid leukemia cells. *Embo J*, 21(21):5766–74, 2002.

[186] R. A. Klinghoffer, C. Sachsenmaier, J. A. Cooper, and P. Soriano. Src family kinases are required for integrin but not pdgfr signal transduction. *Embo J*, 18(9):2459–71, 1999.

[187] B. Knoll and U. Drescher. Src family kinases are involved in epha receptor-mediated retinal axon guidance. *J. Neurosci.*, 24(28):6248–6257, 2004.

[188] N. Kobayashi, T. Kono, M. Hatakeyama, Y. Minami, T. Miyazaki, R. M. Perlmutter, and T. Taniguchi. Functional coupling of the src-family protein tyrosine kinases p59fyn and p53/56lyn with the interleukin 2 receptor: implications for redundancy and pleiotropism in cytokine signal transduction. *Proc Natl Acad Sci U S A*, 90(9):4201–5, 1993.

[189] N. Kotaja, U. Karvonen, O. A. Janne, and J. J. Palvimo. Pias proteins modulate transcription factors by functioning as sumo-1 ligases. *Mol Cell Biol*, 22(14):5222–34, 2002.

[190] R. Kralovics, F. Passamonti, A. S. Buser, S.-S. Teo, R. Tiedt, J. R. Passweg, A. Tichelli, M. Cazzola, and R. C. Skoda. A gain-of-function mutation of jak2 in myeloproliferative disorders. *N Engl J Med*, 352(17):1779–1790, 2005.

[191] G. Krause, A. Hausherr, and M. Hallek. Src kinases in hematopoetic malignancies. *Manuscript in preparation*, 2009.

[192] D. L. Krebs and D. J. Hilton. Socs proteins: negative regulators of cytokine signaling. *Stem Cells*, 19(5):378–87, 2001.

[193] W. M. Kuehl and P. L. Bergsagel. Multiple myeloma: evolving genetic events and host interactions. *Nat Rev Cancer*, 2(3):175–87, 2002.

[194] R. Kuppers. Mechanisms of b-cell lymphoma pathogenesis. *Nat Rev Cancer*, 5(4):251–62, 2005.

[195] T. Kurosaki. Regulation of b cell fates by bcr signaling components. *Curr Opin Immunol*, 14(3):341–7, 2002.

[196] R. A. Kyle and S. V. Rajkumar. Monoclonal gammopathies of undetermined significance. *Rev Clin Exp Hematol*, 6(3):225–52, 2002.

[197] R. A. Kyle and S. V. Rajkumar. Multiple myeloma. *N Engl J Med*, 351(18):1860–1873, 2004.

[198] M. LaFevre-Bernt, F. Sicheri, A. Pico, M. Porter, J. Kuriyan, and W. T. Miller. Intramolecular regulatory interactions in the src family kinase hck probed by mutagenesis of a conserved tryptophan residue. *J Biol Chem*, 273(48):32129–34, 1998.

[199] S. A. Lakhani, A. Masud, K. Kuida, J. Porter, George A., C. J. Booth, W. Z. Mehal, I. Inayat, and R. A. Flavell. Caspases 3 and 7: Key mediators of mitochondrial events of apoptosis. *Science*, 311(5762):847–851, 2006.

[200] K. S. Lam, J. Wu, and Q. Lou. Identification and characterization of a novel synthetic peptide substrate specific for src-family protein tyrosine kinases. *Int J Pept Protein Res*, 45(6):587–92, 1995.

[201] T. H. Landowski, N. E. Olashaw, D. Agrawal, and W. S. Dalton. Cell adhesion-mediated drug resistance (cam-dr) is associated with activation of nf-kappa b (relb/p50) in myeloma cells. *Oncogene*, 22(16):2417–21, 2003.

[202] G. S. Laszlo and N. M. Nathanson. Src family kinase-independent signal transduction and gene induction by leukemia inhibitory factor. *J Biol Chem*, 278(30):27750–7, 2003.

[203] S. Latour and A. Veillette. Proximal protein tyrosine kinases in immunoreceptor signaling. *Curr Opin Immunol*, 13(3):299–306, 2001.

[204] U. Lehmann, J. Schmitz, M. Weissenbach, R. M. Sobota, M. Hortner, K. Friederichs, I. Behrmann, W. Tsiaris, A. Sasaki, J. Schneider-Mergener, A. Yoshimura, B. G. Neel, P. C. Heinrich, and F. Schaper. Shp2 and socs3 contribute to y759-dependent attenuation of il-6-signaling through gp130. *J Biol Chem*, page M210552200, 2002.

[205] J. Lennartsson, P. Blume-Jensen, M. Hermanson, E. Ponten, M. Carlberg, and L. Ronnstrand. Phosphorylation of shc by src family kinases is necessary for stem cell factor receptor/c-kit mediated activation of the ras/map kinase pathway and c-fos induction. *Oncogene*, 18(40):5546–53, 1999.

[206] A. Letai. Restoring cancer's death sentence. *Cancer Cell*, 10(5):343–5, 2006.

[207] P. A. Levene and C. L. Alsberg. The cleavage products of vitellin. *J. Biol. Chem.*, 2(1):127–133, 1906.

[208] A. D. Levinson, H. Oppermann, L. Levintow, H. E. Varmus, and J. M. Bishop. Evidence that the transforming gene of avian sarcoma virus encodes a protein kinase associated with a phosphoprotein. *Cell*, 15(2):561–72, 1978.

[209] A. D. Levinson, H. Oppermann, H. E. Varmus, and J. M. Bishop. The purified product of the transforming gene of avian sarcoma virus phosphorylates tyrosine. *J. Biol. Chem.*, 255(24):11973–11980, 1980.

[210] A. Levitzki and E. Mishani. Tyrphostins and other tyrosine kinase inhibitors. *Annu Rev Biochem*, 75:93–109, 2006.

[211] S. Li, J. Couet, and M. P. Lisanti. Src tyrosine kinases, galpha subunits, and h-ras share a common membrane-anchored scaffolding protein, caveolin. caveolin binding negatively regulates the auto-activation of src tyrosine kinases. *J. Biol. Chem.*, 271(46):29182–29190, 1996.

[212] X. Liang, A. Nazarian, H. Erdjument-Bromage, W. Bornmann, P. Tempst, and M. D. Resh. Heterogeneous fatty acylation of src family kinases with

polyunsaturated fatty acids regulates raft localization and signal transduction. *J. Biol. Chem*, 276(33):30987–30994, 2001.

[213] B. Liu, J. Liao, X. Rao, S. A. Kushner, C. D. Chung, D. D. Chang, and K. Shuai. Inhibition of stat1-mediated gene activation by pias1. *Proceedings of the National Academy of Sciences of the United States of America*, 95(18):10626–31, 1998.

[214] J. Liu, H. Li, N. de Tribolet, R. Jaufeerally, M. F. Hamou, and E. G. Van Meir. Il-6 stimulates growth and inhibits constitutive, protein synthesis-independent apoptosis of murine b-cell hybridoma 7td1. *Cell Immunol*, 155(2):428–35, 1994.

[215] S. Liu, H. Ishikawa, N. Tsuyama, F. J. Li, S. Abroun, K. I. Otsuyama, X. Zheng, Z. Ma, Y. Maki, M. S. Iqbal, M. Obata, and M. M. Kawano. Increased susceptibility to apoptosis in cd45(+) myeloma cells accompanied by the increased expression of vdac1. *Oncogene*, 25(3):419–29, 2006.

[216] O. Livnah, E. A. Stura, S. A. Middleton, D. L. Johnson, L. K. Jolliffe, and I. A. Wilson. Crystallographic evidence for preformed dimers of erythropoietin receptor before ligand activation. *Science*, 283(5404):987–90, 1999.

[217] Q. Lou, M. E. Leftwich, and K. S. Lam. Identification of giywhhy as a novel peptide substrate for human p60c-src protein tyrosine kinase. *Bioorg Med Chem*, 4(5):677–82, 1996.

[218] C. A. Lowell. Src-family kinases: rheostats of immune cell signaling. *Mol Immunol*, 41(6-7):631–43, 2004.

[219] C. A. Lowell, L. Fumagalli, and G. Berton. Deficiency of src family kinases p59/61hck and p58c-fgr results in defective adhesion-dependent neutrophil functions. *J. Cell. Biol.*, 133(4):895–910, 1996.

[220] C. A. Lowell and P. Soriano. Knockouts of src-family kinases: stiff bones, wimpy t cells, and bad memories. *Genes Dev*, 10(15):1845–57, 1996.

[221] C. A. Lowell, P. Soriano, and H. E. Varmus. Functional overlap in the src gene family: inactivation of hck and fgr impairs natural immunity. *Genes Dev*, 8(4):387–98, 1994.

[222] C. Lütticken, U. M. Wegenka, J. Yuan, J. Buschmann, C. Schindler, A. Ziemiecki, A. G. Harpur, A. F. Wilks, K. Yasukawa, T. Taga, and et al. Association of transcription factor aprf and protein kinase jak1 with the interleukin-6 signal transducer gp130. *Science*, 263(5143):89–92, 1994.

[223] W. Lu, D. Gong, D. Bar-Sagi, and P. A. Cole. Site-specific incorporation of a phosphotyrosine mimetic reveals a role for tyrosine phosphorylation of shp-2 in cell signaling. *Mol Cell*, 8(4):759–69, 2001.

[224] F. Luciano, J. E. Ricci, and P. Auberger. Cleavage of fyn and lyn in their n-terminal unique regions during induction of apoptosis: a new mechanism for src kinase regulation. *Oncogene*, 20(36):4935–41, 2001.

[225] F. Luhder, Y. Huang, K. M. Dennehy, C. Guntermann, I. Muller, E. Winkler, T. Kerkau, S. Ikemizu, S. J. Davis, T. Hanke, and T. Hunig. Topological requirements and signaling properties of t cell-activating, anti-cd28 antibody superagonists. *J Exp Med*, 197(8):955–66, 2003.

[226] K. E. Lukong and S. Richard. Sam68, the kh domain-containing superstar. *Biochim Biophys Acta*, 1653(2):73–86, 2003.

[227] M. S. Mahmoud, H. Ishikawa, R. Fujii, and M. M. Kawano. Induction of cd45 expression and proliferation in u-266 myeloma cell line by interleukin-6. *Blood*, 92(10):3887–97, 1998.

[228] R. Manfredini, E. Tenedini, M. Siena, E. Tagliafico, M. Montanari, A. Grande, T. Zanocco-Marani, C. Poligani, R. Zini, C. Gemelli, A. Bergamaschi, T. Vignudelli, F. De Rienzo, P. G. De Benedetti, M. C. Menziani, and S. Ferrari. Development of an il-6 antagonist peptide that induces apoptosis in 7td1 cells. *Peptides*, 24(8):1207–20, 2003.

[229] G. Manning, G. D. Plowman, T. Hunter, and S. Sudarsanam. Evolution of protein kinase signaling from yeast to man. *Trends Biochem Sci*, 27(10):514–20, 2002.

[230] G. Manning, D. B. Whyte, R. Martinez, T. Hunter, and S. Sudarsanam. The protein kinase complement of the human genome. *Science*, 298(5600):1912–34, 2002.

[231] W. Mao, R. Irby, D. Coppola, L. Fu, M. Wloch, J. Turner, H. Yu, R. Garcia, R. Jove, and T. J. Yeatman. Activation of c-src by receptor tyrosine kinases in human colon cancer cells with high metastatic potential. *Oncogene*, 15(25):3083–90, 1997.

[232] A. Martens, J. Bode, P. Heinrich, and L. Graeve. The cytoplasmic domain of the interleukin-6 receptor gp80 mediates its basolateral sorting in polarized madin-darby canine kidney cells. *J Cell Sci*, 113(Pt):3593–3602, 2000.

[233] G. S. Martin. The hunting of the src. *Nat Rev Mol Cell Biol*, 2(6):467–75, 2001.

[234] B. J. Mayer and D. Baltimore. Mutagenic analysis of the roles of sh2 and sh3 domains in regulation of the abl tyrosine kinase. *Mol Cell Biol*, 14(5):2883–94, 1994.

[235] B. J. Mayer and M. J. Eck. Sh3 domains. minding your p's and q's. *Curr Biol*, 5(4):364–7, 1995.

[236] C. Mayr, D. M. Kofler, H. Buning, D. Bund, M. Hallek, and C. M. Wendtner. Transduction of cll cells by cd40 ligand enhances an antigen-specific immune recognition by autologous t cells. *Blood*, 106(9):3223–6, 2005.

[237] B. R. Meade and S. F. Dowdy. Exogenous sirna delivery using peptide transduction domains/cell penetrating peptides. *Adv Drug Deliv Rev*, 59(2-3):134–40, 2007.

[238] T. Meyer, A. Begitt, I. Lodige, M. van Rossum, and U. Vinkemeier. Constitutive and ifn-gamma-induced nuclear import of stat1 proceed through independent pathways. *Embo J*, 21(3):344–54, 2002.

[239] T. Meyer, K. Gavenis, and U. Vinkemeier. Cell type-specific and tyrosine phosphorylation-independent nuclear presence of stat1 and stat3. *Exp Cell Res*, 272(1):45–55, 2002.

[240] D. S. Michaud, K. Augustsson, E. B. Rimm, M. J. Stampfer, W. C. Willet, and E. Giovannucci. A prospective study on intake of animal products and risk of prostate cancer. *Cancer Causes Control*, 12(6):557–67, 2001.

[241] W. T. Miller. Determinants of substrate recognition in nonreceptor tyrosine kinases. *Acc Chem Res*, 36(6):393–400, 2003.

[242] L. H. Milocco, J. A. Haslam, J. Rosen, and H. M. Seidel. Design of conditionally active stats: insights into stat activation and gene regulatory function. *Mol Cell Biol*, 19(4):2913–20, 1999.

[243] O. Mitina, M. Warmuth, G. Krause, M. Hallek, and A. Obermeier. Src family tyrosine kinases phosphorylate flt3 on juxtamembrane tyrosines and interfere with receptor maturation in a kinase-dependent manner. *Ann Hematol*, 86(11):777–85, 2007.

[244] C. S. Mitsiades, N. Mitsiades, N. C. Munshi, and K. C. Anderson. Focus on multiple myeloma. *Cancer Cell*, 6(5):439–444, 2004.

[245] C. S. Mitsiades, N. S. Mitsiades, C. J. McMullan, V. Poulaki, R. Shringarpure, M. Akiyama, T. Hideshima, D. Chauhan, M. Joseph, T. A. Libermann, C. García-Echeverría, M. A. Pearson, F. Hofmann, K. C. Anderson, and A. L. Kung. Inhibition of the insulin-like growth factor receptor-

1 tyrosine kinase activity as a therapeutic strategy for multiple myeloma, other hematologic malignancies, and solid tumors. *Cancer Cell*, 5(3):221–230, 2004.

[246] I. Moarefi, M. LaFevre-Bernt, F. Sicheri, M. Huse, C. H. Lee, J. Kuriyan, and W. T. Miller. Activation of the src-family tyrosine kinase hck by sh3 domain displacement. *Nature*, 385(6617):650–3, 1997.

[247] A. S. Mohamed, K. A. Rivas-Plata, J. R. Kraas, S. M. Saleh, and S. L. Swope. Src-class kinases act within the agrin/musk pathway to regulate acetylcholine receptor phosphorylation, cytoskeletal anchoring, and clustering. *J Neurosci*, 21(11):3806–18, 2001.

[248] M. F. Moran, C. A. Koch, D. Anderson, C. Ellis, L. England, G. S. Martin, and T. Pawson. Src homology region 2 domains direct protein-protein interactions in signal transduction. *Proc Natl Acad Sci U S A*, 87(21):8622–6, 1990.

[249] G. Muller-Newen. The cytokine receptor gp130: faithfully promiscuous. *Sci STKE*, 2003(201):PE40, 2003.

[250] G. Muller-Newen, A. Kuster, U. Hemmann, R. Keul, U. Horsten, A. Martens, L. Graeve, J. Wijdenes, and P. C. Heinrich. Soluble il-6 receptor potentiates the antagonistic activity of soluble gp130 on il-6 responses. *J Immunol*, 161(11):6347–6355, 1998.

[251] M. Murakami, M. Narazaki, M. Hibi, H. Yawata, K. Yasukawa, M. Hamaguchi, T. Taga, and T. Kishimoto. Critical cytoplasmic region of the interleukin 6 signal transducer gp130 is conserved in the cytokine receptor family. *Proceedings of the National Academy of Sciences of the United States of America*, 88(24):11349–53, 1991.

[252] U. myeloma forum. Diagnosis and management of multiple myeloma. *British Journal of Haematology*, 115(3):522–540, 2001.

[253] S. Nada, M. Okada, A. MacAuley, J. A. Cooper, and H. Nakagawa. Cloning of a complementary dna for a protein-tyrosine kinase that specifically phosphorylates a negative regulatory site of p60c-src. *Nature*, 351(6321):69–72, 1991.

[254] S. Nada, T. Yagi, H. Takeda, T. Tokunaga, H. Nakagawa, Y. Ikawa, M. Okada, and S. Aizawa. Constitutive activation of src family kinases in mouse embryos that lack csk. *Cell*, 73(6):1125–35, 1993.

[255] S. A. Nair, M. H. Kim, S. D. Warren, S. Choi, Z. Songyang, L. C. Cantley,

and D. G. Hangauer. Identification of efficient pentapeptide substrates for the tyrosine kinase pp60c-src. *J Med Chem*, 38(21):4276–83, 1995.

[256] M. Narazaki, M. Fujimoto, T. Matsumoto, Y. Morita, H. Saito, T. Kajita, K. Yoshizaki, T. Naka, and T. Kishimoto. Three distinct domains of ssi-1/socs-1/jab protein are required for its suppression of interleukin 6 signaling. *Proceedings of the National Academy of Sciences of the United States of America*, 95(22):13130–4, 1998.

[257] M. Narazaki, K. Yasukawa, T. Saito, Y. Ohsugi, H. Fukui, Y. Koishihara, G. D. Yancopoulos, T. Taga, and T. Kishimoto. Soluble forms of the interleukin-6 signal-transducing receptor component gp130 in human serum possessing a potential to inhibit signals through membrane-anchored gp130. *Blood*, 82(4):1120–6, 1993.

[258] S. E. Nicholson, D. De Souza, L. J. Fabri, J. Corbin, T. A. Willson, J. G. Zhang, A. Silva, M. Asimakis, A. Farley, A. D. Nash, D. Metcalf, D. J. Hilton, N. A. Nicola, and M. Baca. Suppressor of cytokine signaling-3 preferentially binds to the shp-2-binding site on the shared cytokine receptor subunit gp130. *Proceedings of the National Academy of Sciences of the United States of America*, 97(12):6493–8, 2000.

[259] N. Nishimoto and T. Kishimoto. Interleukin 6: from bench to bedside. *Nat Clin Pract Rheumatol*, 2(11):619–26, 2006.

[260] M. Y. Niv, H. Rubin, J. Cohen, L. Tsirulnikov, T. Licht, A. Peretzman-Shemer, E. Cna'an, A. Tartakovsky, I. Stein, S. Albeck, I. Weinstein, M. Goldenberg-Furmanov, D. Tobi, E. Cohen, M. Laster, S. A. Ben-Sasson, and H. Reuveni. Sequence-based design of kinase inhibitors applicable for therapeutics and target identification. *J. Biol. Chem.*, 279(2):1242–1255, 2004.

[261] J. C. Obenauer, L. C. Cantley, and M. B. Yaffe. Scansite 2.0: Proteome-wide prediction of cell signaling interactions using short sequence motifs. *Nucleic Acids Res*, 31(13):3635–41, 2003.

[262] M. Ogawa. Differentiation and proliferation of hematopoietic stem cells. *Blood*, 81(11):2844–53, 1993.

[263] M. Ogawa, T. Nishiura, K. Oritani, H. Yoshida, M. Yoshimura, Y. Okajima, J. Ishikawa, K. Hashimoto, I. Matsumura, Y. Tomiyama, and Y. Matsuzawa. Cytokines prevent dexamethasone-induced apoptosis via the activation of mitogen-activated protein kinase and phosphatidylinositol 3-kinase pathways in a new multiple myeloma cell line. *Cancer Res*, 60(15):4262–4269, 2000.

[264] T. Ohtani, K. Ishihara, T. Atsumi, K. Nishida, T. Miyata, S. Itoh, M. Narimatsu, H. Maeda, T. Fukada, M. Itoh, H. Okano, and T. Hirano. Dissection of signaling cascades through gp130 in vivo: reciprocal roles for stat3- and shp2-mediated signals in immune responses. *Immunity*, 12:95–105, 2000.

[265] M. Okada, S. Nada, Y. Yamanashi, T. Yamamoto, and H. Nakagawa. Csk: a protein-tyrosine kinase involved in regulation of src family kinases. *J. Biol. Chem*, 266(36):24249–52, 1991.

[266] H. Oppermann, A. D. Levinson, H. E. Varmus, L. Levintow, and J. M. Bishop. Uninfected vertebrate cells contain a protein that is closely related to the product of the avian sarcoma virus transforming gene (src). *Proc Natl Acad Sci U S A*, 76(4):1804–8, 1979.

[267] J. J. O'Shea, M. Gadina, and R. D. Schreiber. Cytokine signaling in 2002: new surprises in the jak/stat pathway. *Cell*, 109 Suppl:S121–31, 2002.

[268] J. J. O'Shea, M. Husa, D. Li, S. R. Hofmann, W. Watford, J. L. Roberts, R. H. Buckley, P. Changelian, and F. Candotti. Jak3 and the pathogenesis of severe combined immunodeficiency. *Mol Immunol*, 41(6-7):727–37, 2004.

[269] A. E. Ottenhoff-Kalff, G. Rijksen, E. A. van Beurden, A. Hennipman, A. A. Michels, and G. E. Staal. Characterization of protein tyrosine kinases from human breast cancer: involvement of the c-src oncogene product. *Cancer Res*, 52(17):4773–8, 1992.

[270] E. Ozkirimli and C. B. Post. Src kinase activation: A switched electrostatic network. *Protein Sci*, 15(5):1051–62, 2006.

[271] E. H. Palacios and A. Weiss. Function of the src-family kinases, lck and fyn, in t-cell development and activation. *Oncogene*, 23(48):7990–8000, 2004.

[272] C. Palm, M. Jayamanne, M. Kjellander, and M. Hallbrink. Peptide degradation is a critical determinant for cell-penetrating peptide uptake. *Biochim Biophys Acta*, 1768(7):1769–76, 2007.

[273] G. Paonessa, R. Graziani, A. De Serio, R. Savino, L. Ciapponi, A. Lahm, S. A. L., C. Toniatti, and G. Ciliberto. Two distinct and independent sites on il-6 trigger gp 130 dimer formation and signalling. *Embo J*, 14(9):1942–1951, 1995.

[274] J. Parrish-Novak, W. Xu, T. Brender, L. Yao, C. Jones, J. West, C. Brandt, L. Jelinek, K. Madden, P. A. McKernan, D. C. Foster, S. Jaspers, and Y. A. Chandrasekher. Interleukins 19, 20, and 24 signal through two distinct receptor complexes. differences in receptor-ligand interactions mediate unique biological functions. *J Biol Chem*, 277(49):47517–23, 2002.

[275] R. F. Paulson and A. Bernstein. Receptor tyrosine kinases and the regulation of hematopoiesis. *Semin Immunol*, 7(4):267–77, 1995.

[276] T. Pawson. Protein modules and signalling networks. *Nature*, 373(6515):573–80, 1995.

[277] T. Pawson. Specificity in signal transduction: from phosphotyrosine-sh2 domain interactions to complex cellular systems. *Cell*, 116(2):191–203, 2004.

[278] T. Pawson and J. D. Scott. Protein phosphorylation in signaling–50 years and counting. *Trends Biochem Sci*, 30(6):286–90, 2005.

[279] P. Pellicena, K. R. Stowell, and W. T. Miller. Enhanced phosphorylation of src family kinase substrates containing sh2 domain binding sites. *J Biol Chem*, 273(25):15325–8, 1998.

[280] M. F. M. Percy MC. The v617f jak2 mutation and the myeloproliferative disorders. *Hematological Oncology*, 23(3-4):91–93, 2005.

[281] S. M. Peseckis and M. D. Resh. Fatty acyl transfer by human n-myristyl transferase is dependent upon conserved cysteine and histidine residues. *J Biol Chem*, 269(49):30888–92, 1994.

[282] S. Pflanz, I. Kurth, J. Grotzinger, P. C. Heinrich, and G. Muller-Newen. Two different epitopes of the signal transducer gp130 sequentially cooperate on il-6-induced receptor activation. *J Immunol*, 165(12):7042–7049, 2000.

[283] Podar and Anderson. Caveolin-1 as a potential new therapeutic target in multiple myeloma. *Cancer Letters*, 233(1):10–15, 2006.

[284] K. Podar, G. Mostoslavsky, M. Sattler, Y. T. Tai, T. Hayashi, L. P. Catley, T. Hideshima, R. C. Mulligan, D. Chauhan, and K. C. Anderson. Critical role for hematopoietic cell kinase (hck)-mediated phosphorylation of gab1 and gab2 docking proteins in interleukin 6-induced proliferation and survival of multiple myeloma cells. *J Biol Chem*, 279(20):21658–65, 2004.

[285] K. Podar, Y. T. Tai, C. E. Cole, T. Hideshima, M. Sattler, A. Hamblin, N. Mitsiades, R. L. Schlossman, F. E. Davies, G. J. Morgan, N. C. Munshi, D. Chauhan, and K. C. Anderson. Essential role of caveolae in interleukin-6- and insulin-like growth factor i-triggered akt-1-mediated survival of multiple myeloma cells. *J Biol Chem*, 278(8):5794–801, 2003.

[286] M. Porter, T. Schindler, J. Kuriyan, and W. T. Miller. Reciprocal regulation of hck activity by phosphorylation of tyr527 and tyr416. effect of introducing a high affinity intramolecular sh2 ligand. *J. Biol. Chem.*, 275(4):2721–2726, 2000.

[287] G. Posern, J. Zheng, B. S. Knudsen, C. Kardinal, K. B. Muller, J. Voss, T. Shishido, D. Cowburn, G. Cheng, B. Wang, G. D. Kruh, S. K. Burrell, C. A. Jacobson, D. M. Lenz, T. J. Zamborelli, K. Adermann, H. Hanafusa, and S. M. Feller. Development of highly selective sh3 binding peptides for crk and crkl which disrupt crk-complexes with dock180, sos and c3g. *Oncogene*, 16(15):1903–12, 1998.

[288] R. Ralston and J. M. Bishop. The product of the protooncogene c-src is modified during the cellular response to platelet-derived growth factor. *Proc Natl Acad Sci U S A*, 82(23):7845–9, 1985.

[289] S. G. Rane and E. P. Reddy. Jaks, stats and src kinases in hematopoiesis. *Oncogene*, 21(21):3334–58, 2002.

[290] B. Raught, A. C. Gingras, and N. Sonenberg. The target of rapamycin (tor) proteins. *Proc Natl Acad Sci U S A*, 98(13):7037–44, 2001.

[291] J. V. Ravetch and L. L. Lanier. Immune inhibitory receptors. *Science*, 290(5489):84–9, 2000.

[292] D. J. Rawlings, K. Sommer, and M. E. Moreno-Garcia. The carma1 signalosome links the signalling machinery of adaptive and innate immunity in lymphocytes. *Nat Rev Immunol*, 6(11):799–812, 2006.

[293] E. P. Reddy, A. Korapati, P. Chaturvedi, and S. Rane. Il-3 signaling and the role of src kinases, jaks and stats: a covert liaison unveiled. *Oncogene*, 19(21):2532–47, 2000.

[294] T. Reid, R. Warren, and D. Kirn. Intravascular adenoviral agents in cancer patients: lessons from clinical trials. *Cancer Gene Ther*, 9(12):979–86, 2002.

[295] M. D. Resh. Myristylation and palmitylation of src family members: the fats of the matter. *Cell*, 76(3):411–3, 1994.

[296] M. Reth. Antigen receptor tail clue. *Nature*, 338(6214):383–4, 1989.

[297] D. Ribatti, B. Nico, and A. Vacca. Importance of the bone marrow microenvironment in inducing the angiogenic response in multiple myeloma. *Oncogene*, 25(31):4257–4266, 2006.

[298] J. E. Ricci, L. Maulon, F. Luciano, S. Guerin, A. Livolsi, B. Mari, J. P. Breittmayer, J. F. Peyron, and P. Auberger. Cleavage and relocation of the tyrosine kinase p59fyn during fas-mediated apoptosis in t lymphocytes. *Oncogene*, 18(27):3963–9, 1999.

[299] P. G. Richardson, P. Sonneveld, M. W. Schuster, D. Irwin, E. A. Stadtmauer, T. Facon, J.-L. Harousseau, D. Ben-Yehuda, S. Lonial, H. Goldschmidt, D. Reece, J. F. San-Miguel, J. Blade, M. Boccadoro, J. Cavenagh, W. S. Dalton, A. L. Boral, D. L. Esseltine, J. B. Porter, D. Schenkein, K. C. Anderson, and I. the Assessment of Proteasome Inhibition for Extending Remissions. Bortezomib or high-dose dexamethasone for relapsed multiple myeloma. *N Engl J Med*, 352(24):2487–2498, 2005.

[300] L. Ries, D. Harkins, M. Krapcho, A. Mariotto, B. Miller, E. Feuer, L. Clegg, M. Eisner, M. Horner, N. Howlader, M. Hayat, B. Hankey, and E. B. (eds). Seer cancer statistics review, 1975-2003. *Bethesda, MD, based on November 2005 SEER data submission, posted to the SEER web site, 2006.*, 2003.

[301] S. M. Robbins, N. A. Quintrell, and J. M. Bishop. Myristoylation and differential palmitoylation of the hck protein- tyrosine kinases govern their attachment to membranes and association with caveolae. *Mol. Cell. Biol.*, 15(7):3507–3515, 1995.

[302] D. R. Robinson, Y. M. Wu, and S. F. Lin. The protein tyrosine kinase family of the human genome. *Oncogene*, 19(49):5548–57, 2000.

[303] M. J. Robinson, P. C. Harkins, J. Zhang, R. Baer, J. W. Haycock, M. H. Cobb, and E. J. Goldsmith. Mutation of position 52 in erk2 creates a nonproductive binding mode for adenosine 5'-triphosphate. *Biochemistry*, 35(18):5641–6, 1996.

[304] A. M. Roccaro, T. Hideshima, P. G. Richardson, D. Russo, D. Ribatti, A. Vacca, F. Dammacco, and K. C. Anderson. Bortezomib as an antitumor agent. *Current Pharmaceutical Biotechnology*, 7:441–448, 2006.

[305] S. Roche, S. Fumagalli, and S. A. Courtneidge. Requirement for src family protein tyrosine kinases in g2 for fibroblast cell division. *Science*, 269(5230):1567–9, 1995.

[306] S. Roche, M. Koegl, M. V. Barone, M. F. Roussel, and S. A. Courtneidge. Dna synthesis induced by some but not all growth factors requires src family protein tyrosine kinases. *Mol Cell Biol*, 15(2):1102–9, 1995.

[307] S. Rose-John, J. Scheller, G. Elson, and S. A. Jones. Interleukin-6 biology is coordinated by membrane-bound and soluble receptors: role in inflammation and cancer. *J Leukoc Biol*, 80(2):227–36, 2006.

[308] N. Rosen, J. B. Bolen, A. M. Schwartz, P. Cohen, V. DeSeau, and M. A. Israel. Analysis of pp60c-src protein kinase activity in human tumor cell lines and tissues. *J Biol Chem*, 261(29):13754–9, 1986.

[309] J. Roskoski, R. Src kinase regulation by phosphorylation and dephosphorylation. *Biochem Biophys Res Commun*, 331(1):1–14, 2005.

[310] J. F. Rossi, N. Fegueux, Z. Y. Lu, E. Legouffe, C. Exbrayat, M. C. Bozonnat, R. Navarro, E. Lopez, P. Quittet, J. P. Daures, V. Rouille, T. Kanouni, J. Widjenes, and B. Klein. Optimizing the use of anti-interleukin-6 monoclonal antibody with dexamethasone and 140 mg/m2 of melphalan in multiple myeloma: results of a pilot study including biological aspects. *Bone Marrow Transplant*, 36(9):771–9, 2005.

[311] P. Rous. A transmissible avian neoplasm. (sarcoma of the common fowl) by peyton rous, m.d., experimental medicine for sept. 1, 1910, vol. 12, pp.696-705. *J. Exp. Med.*, 150(4):729–753, 1979.

[312] D. M. Sabatini, H. Erdjument-Bromage, M. Lui, P. Tempst, and S. H. Snyder. Raft1: A mammalian protein that binds to fkbp12 in a rapamycin-dependent fashion and is homologous to yeast tors. *Cell*, 78(1):35–43, 1994.

[313] C. J. Sabers, M. M. Martin, G. J. Brunn, J. M. Williams, F. J. Dumont, G. Wiederrecht, and R. T. Abraham. Isolation of a protein target of the fkbp12-rapamycin complex in mammalian cells. *J. Biol. Chem.*, 270(2):815–822, 1995.

[314] S. Sachdev, L. Bruhn, H. Sieber, A. Pichler, F. Melchior, and R. Grosschedl. Piasy, a nuclear matrix-associated sumo e3 ligase, represses lef1 activity by sequestration into nuclear bodies. *Genes Dev*, 15(23):3088–103, 2001.

[315] K. Saijo, C. Schmedt, I. H. Su, H. Karasuyama, C. A. Lowell, M. Reth, T. Adachi, A. Patke, A. Santana, and A. Tarakhovsky. Essential role of src-family protein tyrosine kinases in nf-kappab activation during b cell development. *Nat Immunol*, 4(3):274–9, 2003.

[316] E. Sandilands, C. Cans, V. J. Fincham, V. G. Brunton, H. Mellor, G. C. Prendergast, J. C. Norman, G. Superti-Furga, and M. C. Frame. Rhob and actin polymerization coordinate src activation with endosome-mediated delivery to the membrane. *Dev Cell*, 7(6):855–69, 2004.

[317] A. Sanjay, W. C. Horne, and R. Baron. The cbl family: ubiquitin ligases regulating signaling by tyrosine kinases. *Sci STKE*, 2001(110):PE40, 2001.

[318] A. Sanjay, A. Houghton, L. Neff, E. DiDomenico, C. Bardelay, E. Antoine, J. Levy, J. Gailit, D. Bowtell, W. C. Horne, and R. Baron. Cbl associates with pyk2 and src to regulate src kinase activity, alpha(v)beta(3) integrin-mediated signaling, cell adhesion, and osteoclast motility. *J Cell Biol*, 152(1):181–95, 2001.

[319] M. Sant, T. Aareleid, F. Berrino, M. Bielska Lasota, P. M. Carli, J. Faivre, P. Grosclaude, G. Hedelin, T. Matsuda, H. Moller, T. Moller, A. Verdecchia, R. Capocaccia, G. Gatta, A. Micheli, M. Santaquilani, P. Roazzi, D. Lisi, and E. W. G. the. Eurocare-3: survival of cancer patients diagnosed 1990-94–results and commentary. *Ann Oncol*, 14(suppl-5):v61–118, 2003.

[320] A. Sasaki, H. Yasukawa, A. Suzuki, S. Kamizono, T. Syoda, I. Kinjyo, M. Sasaki, J. A. Johnston, and A. Yoshimura. Cytokine-inducible sh2 protein-3 (cis3/socs3) inhibits janus tyrosine kinase by binding through the n-terminal kinase inhibitory region as well as sh2 domain. *Genes Cells*, 4(6):339–51, 1999.

[321] J. D. Sato, T. Kawamoto, and T. Okamoto. Cholesterol requirement of p3-x63-ag8 and x63-ag8.653 mouse myeloma cells for growth in vitro. *J. Exp. Med.*, 165(6):1761–1766, 1987.

[322] M. S. Satoh and T. Lindahl. Role of poly(adp-ribose) formation in dna repair. *Nature*, 356(6367):356–358, 1992.

[323] M. Schaeffer, M. Schneiderbauer, S. Weidler, R. Tavares, M. Warmuth, G. de Vos, and M. Hallek. Signaling through a novel domain of gp130 mediates cell proliferation and activation of hck and erk kinases. *Mol Cell Biol*, 21(23):8068–81, 2001.

[324] F. Schaper, C. Gendo, M. Eck, J. Schmitz, C. Grimm, D. Anhuf, and I. M. Kerr. Activation of the protein tyrosine phosphatase shp2 via the interleukin-6 signal transduction receptor protein gp130 requires tyrosine kinase jak1 and limits acute-phase protein expression. *Biochem J*, 335:557–565, 1998.

[325] J. Scheller, N. Ohnesorge, and S. Rose-John. Interleukin-6 trans-signalling in chronic inflammation and cancer. *Scand J Immunol*, 63(5):321–9, 2006.

[326] J. Scheller and S. Rose-John. Interleukin-6 and its receptor: from bench to bedside. *Med Microbiol Immunol (Berl)*, 195(4):173–83, 2006.

[327] W. P. Schiemann, J. L. Bartoe, and N. M. Nathanson. Box 3-independent signaling mechanisms are involved in leukemia inhibitory factor receptor alpha - and gp130-mediated stimulation of mitogen-activated protein kinase. evidence for participation of multiple signaling pathways which converge at ras. *J Biol Chem*, 272(26):16631–16636, 1997.

[328] T. Schindler, F. Sicheri, A. Pico, A. Gazit, A. Levitzki, and J. Kuriyan. Crystal structure of hck in complex with a src family-selective tyrosine kinase inhibitor. *Mol Cell*, 3(5):639–48, 1999.

[329] J. Schmitz, M. Weissenbach, S. Haan, P. C. Heinrich, and F. Schaper. Socs3 exerts its inhibitory function on interleukin-6 signal transduction through the shp2 recruitment site of gp130. *J Biol Chem*, 275(17):12848–56, 2000.

[330] U. Schneider, H. U. Schwenk, and G. Bornkamm. Characterization of ebv-genome negative "null" and "t" cell lines derived from children with acute lymphoblastic leukemia and leukemic transformed non-hodgkin lymphoma. *Int J Cancer*, 19(5):621–6, 1977.

[331] S. J. Schreiner, A. P. Schiavone, and T. E. Smithgall. Activation of stat3 by the src family kinase hck requires a functional sh3 domain. *J Biol Chem*, 277(47):45680–7, 2002.

[332] A. Schroers, O. Hecht, K.-J. Kallen, M. Pachta, S. Rose-John, and J. Grotzinger. Dynamics of the gp130 cytokine complex: A model for assembly on the cellular membrane. *Protein Sci*, 14(3):783–790, 2005.

[333] W. X. Schulze and M. Mann. A novel proteomic screen for peptide-protein interactions. *J Biol Chem*, 279(11):10756–64, 2004.

[334] M. Schwab, K. Alitalo, K. H. Klempnauer, H. E. Varmus, J. M. Bishop, F. Gilbert, G. Brodeur, M. Goldstein, and J. Trent. Amplified dna with limited homology to myc cellular oncogene is shared by human neuroblastoma cell lines and a neuroblastoma tumour. *Nature*, 305(5931):245–8, 1983.

[335] M. Schwabe, G. W. Cox, M. C. Bosco, R. Prohaska, and H. F. Kung. Multiple cytokines inhibit interleukin-6-dependent murine hybridoma/plasmacytoma proliferation. *Cell Immunol*, 168(1):117–21, 1996.

[336] R. Sears, G. Leone, J. DeGregori, and J. R. Nevins. Ras enhances myc protein stability. *Mol Cell*, 3(2):169–79, 1999.

[337] R. Sears, F. Nuckolls, E. Haura, Y. Taya, K. Tamai, and J. R. Nevins. Multiple ras-dependent phosphorylation pathways regulate myc protein stability. *Genes Dev*, 14(19):2501–14, 2000.

[338] B. M. Sefton and T. Hunter. From c-src to v-src, or the case of the missing c terminus. *Cancer Surv*, 5(2):159–72, 1986.

[339] N. P. Shah, C. Tran, F. Y. Lee, P. Chen, D. Norris, and C. L. Sawyers. Overriding imatinib resistance with a novel abl kinase inhibitor. *Science*, 305(5682):399–401, 2004.

[340] F. Sheikh, V. V. Baurin, A. Lewis-Antes, N. K. Shah, S. V. Smirnov, S. Anantha, H. Dickensheets, L. Dumoutier, J. C. Renauld, A. Zdanov, R. P. Donnelly, and S. V. Kotenko. Cutting edge: Il-26 signals through a

novel receptor complex composed of il-20 receptor 1 and il-10 receptor 2. *J Immunol*, 172(4):2006–10, 2004.

[341] A. M. Shenoy-Scaria, D. J. Dietzen, J. Kwong, D. C. Link, and D. M. Lublin. Cysteine3 of src family protein tyrosine kinase determines palmitoylation and localization in caveolae. *J Cell Biol*, 126(2):353–63, 1994.

[342] A. M. Shenoy-Scaria, L. K. Gauen, J. Kwong, A. S. Shaw, and D. M. Lublin. Palmitylation of an amino-terminal cysteine motif of protein tyrosine kinases p56lck and p59fyn mediates interaction with glycosyl-phosphatidylinositol-anchored proteins. *Mol Cell Biol*, 13(10):6385–92, 1993.

[343] Y. Shi, J. Gera, L. Hu, J.-h. Hsu, R. Bookstein, W. Li, and A. Lichtenstein. Enhanced sensitivity of multiple myeloma cells containing pten mutations to cci-779. *Cancer Res*, 62(17):5027–5034, 2002.

[344] F. Sicheri and J. Kuriyan. Structures of src-family tyrosine kinases. *Curr Opin Struct Biol*, 7(6):777–85, 1997.

[345] F. Sicheri, I. Moarefi, and J. Kuriyan. Crystal structure of the src family tyrosine kinase hck. *Nature*, 385(6617):602–9, 1997.

[346] C. T. Sigal, W. Zhou, C. A. Buser, S. McLaughlin, and M. D. Resh. Amino-terminal basic residues of src mediate membrane binding through electrostatic interaction with acidic phospholipids. *Proc Natl Acad Sci U S A*, 91(25):12253–7, 1994.

[347] C. M. Silva. Role of stats as downstream signal transducers in src family kinase-mediated tumorigenesis. *Oncogene*, 23(48):8017–23, 2004.

[348] N. R. Sinclair. Immunoreceptor tyrosine-based inhibitory motifs on activating molecules. *Crit Rev Immunol*, 20(2):89–102, 2000.

[349] G. Skiniotis, M. J. Boulanger, K. C. Garcia, and T. Walz. Signaling conformations of the tall cytokine receptor gp130 when in complex with il-6 and il-6 receptor. *Nat Struct Mol Biol*, 2005.

[350] A. Smith, F. Wisloff, and D. Samson. Guidelines on the diagnosis and management of multiple myeloma 2005. *Br J Haematol*, 132(4):410–51, 2006.

[351] M. R. Smith. Rituximab (monoclonal anti-cd20 antibody): mechanisms of action and resistance. *Oncogene*, 22(47):7359–68, 2003.

[352] E. L. Snyder, C. C. Saenz, C. Denicourt, B. R. Meade, X. S. Cui, I. M. Kaplan, and S. F. Dowdy. Enhanced targeting and killing of tumor cells expressing the cxc chemokine receptor 4 by transducible anticancer peptides. *Cancer Res*, 65(23):10646–50, 2005.

[353] W. Somers, M. Stahl, and J. Seehra. 1.9 a crystal structure of interleukin 6: implications for a novel mode of receptor dimerization and signaling. *Embo J*, 16(5):989–97, 1997.

[354] U. Sommer, C. Schmid, R. M. Sobota, U. Lehmann, N. J. Stevenson, J. A. Johnston, F. Schaper, P. C. Heinrich, and S. Haan. Mechanisms of socs3 phosphorylation upon interleukin-6 stimulation. contributions of src- and receptor-tyrosine kinases. *J Biol Chem*, 280(36):31478–88, 2005.

[355] Z. Songyang and L. C. Cantley. Recognition and specificity in protein tyrosine kinase-mediated signalling. *Trends Biochem Sci*, 20(11):470–5, 1995.

[356] Z. Songyang and L. C. Cantley. Sh2 domain specificity determination using oriented phosphopeptide library. *Methods Enzymol*, 254:523–35, 1995.

[357] Z. Songyang, r. Carraway, K. L., M. J. Eck, S. C. Harrison, R. A. Feldman, M. Mohammadi, J. Schlessinger, S. R. Hubbard, D. P. Smith, C. Eng, and et al. Catalytic specificity of protein-tyrosine kinases is critical for selective signalling. *Nature*, 373(6514):536–9, 1995.

[358] H. D. Soule, J. Vazguez, A. Long, S. Albert, and M. Brennan. A human cell line from a pleural effusion derived from a breast carcinoma. *J Natl Cancer Inst*, 51(5):1409–16, 1973.

[359] N. Stahl, T. Farugella, T. Boulton, N. Ip, S. Davis, B. Witthuhn, F. Quelle, O. Silvennoinen, G. Barberi, S. Pellegrini, J. Ihle, and Y. G.D. Association and activation of jak-tyk kinases by cntf-lif-osm-il-6 b receptor components. *Science*, 263(7 Jan):92–95, 1994.

[360] N. Stahl, T. Farugella, T. Boulton, Z. Zhong, J. J. Darnell, and Y. G.D. Choice of stats and other substrates specyfied by modular tyrosine-based motifs in cytokine receptors. *Science*, 267(3 Mar):1349–1353, 1995.

[361] L. F. Stancato, M. David, C. Carter-Su, A. C. Larner, and W. B. Pratt. Preassociation of stat1 with stat2 and stat3 in separate signalling complexes prior to cytokine stimulation. *J Biol Chem*, 271(8):4134–7, 1996.

[362] R. Starr, T. A. Willson, E. M. Viney, L. J. Murray, J. R. Rayner, B. J. Jenkins, T. J. Gonda, W. S. Alexander, D. Metcalf, N. A. Nicola, and D. J. Hilton. A family of cytokine-inducible inhibitors of signalling. *Nature*, 387(6636):917–21, 1997.

[363] D. Stehelin, H. E. Varmus, J. M. Bishop, and P. K. Vogt. Dna related to the transforming gene(s) of avian sarcoma viruses is present in normal avian dna. *Nature*, 260(5547):170–3, 1976.

[364] M. Sugimura, K. Kobayashi, S. Sagae, Y. Nishioka, S. Ishioka, K. Terasawa, T. Tokino, and R. Kudo. Mutation of the src gene in endometrial carcinoma. *Jpn J Cancer Res*, 91(4):395–8, 2000.

[365] C. Sundstrom and K. Nilsson. Establishment and characterization of a human histiocytic lymphoma cell line (u-937). *Int J Cancer*, 17(5):565–77, 1976.

[366] M. Takahashi-Tezuka, Y. Yoshida, T. Fukada, T. Ohtani, Y. Yamanaka, K. Nishida, K. Nakajima, M. Hibi, and T. Hirano. Gab1 acts as an adapter molecule linking the cytokine receptor gp130 to erk mitogen-activated protein kinase. *Mol Cell Biol*, 18(7):4109–17, 1998.

[367] M. Tan, K. H. Lan, J. Yao, C. H. Lu, M. Sun, C. L. Neal, J. Lu, and D. Yu. Selective inhibition of erbb2-overexpressing breast cancer in vivo by a novel tat-based erbb2-targeting signal transducers and activators of transcription 3-blocking peptide. *Cancer Res*, 66(7):3764–72, 2006.

[368] P. Tassone, P. Neri, R. Burger, R. Savino, M. Shammas, L. Catley, K. Podar, D. Chauhan, S. Masciari, A. Gozzini, P. Tagliaferri, S. Venuta, N. C. Munshi, and K. C. Anderson. Combination therapy with interleukin-6 receptor superantagonist sant7 and dexamethasone induces antitumor effects in a novel scid-hu in vivo model of human multiple myeloma. *Clin Cancer Res*, 11(11):4251–8, 2005.

[369] T. Teranishi, T. Hirano, N. Arima, and K. Onoue. Human helper t cell factor(s) (thf). ii. induction of igg production in b lymphoblastoid cell lines and identification of t cell-replacing factor- (trf) like factor(s). *J Immunol*, 128(4):1903–8, 1982.

[370] M. Tewari, L. T. Quan, K. O'Rourke, S. Desnoyers, Z. Zeng, D. R. Beidler, G. G. Poirier, G. S. Salvesen, and V. M. Dixit. Yama/cpp32[beta], a mammalian homolog of ced-3, is a crma-inhibitable protease that cleaves the death substrate poly(adp-ribose) polymerase. *Cell*, 81(5):801–809, 1995.

[371] S. Thiel, H. Dahmen, A. Martens, G. Muller-Newen, F. Schaper, P. C. Heinrich, and L. Graeve. Constitutive internalization and association with adaptor protein-2 of the interleukin-6 signal transducer gp130. *FEBS Lett*, 441(2):231–4, 1998.

[372] J. W. Thomas, B. Ellis, R. J. Boerner, W. B. Knight, n. White, G. C., and M. D. Schaller. Sh2- and sh3-mediated interactions between focal adhesion kinase and src. *J Biol Chem*, 273(1):577–83, 1998.

[373] S. M. Thomas and J. S. Brugge. Cellular functions regulated by src family kinases. *Annu Rev Cell Dev Biol*, 13:513–609, 1997.

[374] D. A. Tice, J. S. Biscardi, A. L. Nickles, and S. J. Parsons. Mechanism of biological synergy between cellular src and epidermal growth factor receptor. *Proc Natl Acad Sci U S A*, 96(4):1415–20, 1999.

[375] J. Toshima, K. Ohashi, S. Iwashita, and K. Mizuno. Autophosphorylation activity and association with src family kinase of sky receptor tyrosine kinase. *Biochem Biophys Res Commun*, 209(2):656–63, 1995.

[376] M. Trikha, R. Corringham, B. Klein, and J. F. Rossi. Targeted anti-interleukin-6 monoclonal antibody therapy for cancer: a review of the rationale and clinical evidence. *Clin Cancer Res*, 9(13):4653–65, 2003.

[377] I. S. Trowbridge, J. F. Collawn, and C. R. Hopkins. Signal-dependent membrane protein trafficking in the endocytic pathway. *Annu Rev Cell Biol*, 9:129–61, 1993.

[378] J. Turkson, D. Ryan, J. S. Kim, Y. Zhang, Z. Chen, E. Haura, A. Laudano, S. Sebti, A. D. Hamilton, and R. Jove. Phosphotyrosyl peptides block stat3-mediated dna binding activity, gene regulation, and cell transformation. *J Biol Chem*, 276(48):45443–55, 2001.

[379] D. Ungureanu, P. Saharinen, I. Junttila, D. J. Hilton, and O. Silvennoinen. Regulation of jak2 through the ubiquitin-proteasome pathway involves phosphorylation of jak2 on y1007 and interaction with socs-1. *Mol Cell Biol*, 22(10):3316–26, 2002.

[380] M. Urashima, A. Ogata, D. Chauhan, M. Hatziyanni, M. B. Vidriales, D. A. Dedera, R. L. Schlossman, and K. C. Anderson. Transforming growth factor-beta1: differential effects on multiple myeloma versus normal b cells. *Blood*, 87(5):1928–38, 1996.

[381] N. S. van Oers, N. Killeen, and A. Weiss. Lck regulates the tyrosine phosphorylation of the t cell receptor subunits and zap-70 in murine thymocytes. *J Exp Med*, 183(3):1053–62, 1996.

[382] N. S. van Oers, B. Lowin-Kropf, D. Finlay, K. Connolly, and A. Weiss. alpha beta t cell development is abolished in mice lacking both lck and fyn protein tyrosine kinases. *Immunity*, 5(5):429–36, 1996.

[383] J. Van Snick, S. Cayphas, A. Vink, C. Uyttenhove, P. G. Coulie, M. R. Rubira, and R. J. Simpson. Purification and nh2-terminal amino acid sequence of a t-cell-derived lymphokine with growth factor activity for b-cell hybrido-

mas. *Proceedings of the National Academy of Sciences of the United States of America*, 83(24):9679–83, 1986.

[384] C. Vezina, A. Kudelski, and S. N. Sehgal. Rapamycin (ay-22,989), a new antifungal antibiotic. i. taxonomy of the producing streptomycete and isolation of the active principle. *J Antibiot (Tokyo)*, 28(10):721–6, 1975.

[385] R. Vile, D. Ando, and D. Kirn. The oncolytic virotherapy treatment platform for cancer: unique biological and biosafety points to consider. *Cancer Gene Ther*, 9(12):1062–7, 2002.

[386] U. Vinkemeier, I. Moarefi, J. Darnell, J. E., and J. Kuriyan. Structure of the amino-terminal protein interaction domain of stat-4. *Science*, 279(5353):1048–52, 1998.

[387] E. P. von Strandmann, H. P. Hansen, K. S. Reiners, R. Schnell, P. Borchmann, S. Merkert, V. R. Simhadri, A. Draube, M. Reiser, I. Purr, M. Hallek, and A. Engert. A novel bispecific protein (ulbp2-bb4) targeting the nkg2d receptor on natural killer (nk) cells and cd138 activates nk cells and has potent antitumor activity against human multiple myeloma in vitro and in vivo. *Blood*, 107(5):1955–1962, 2006.

[388] J. S. Wadia, R. V. Stan, and S. F. Dowdy. Transducible tat-ha fusogenic peptide enhances escape of tat-fusion proteins after lipid raft macropinocytosis. *Nat Med*, 10(3):310–5, 2004.

[389] M. Wadman. London's disastrous drug trial has serious side effects for research. *Nature*, 440(7083):388–389, 2006.

[390] G. Waksman and J. Kuriyan. Structure and specificity of the sh2 domain. *Cell*, 116(2 Suppl):S45–8, 3 p following S48, 2004.

[391] G. Waksman, S. E. Shoelson, N. Pant, D. Cowburn, and J. Kuriyan. Binding of a high affinity phosphotyrosyl peptide to the src sh2 domain: crystal structures of the complexed and peptide-free forms. *Cell*, 72(5):779–90, 1993.

[392] L. D. Walensky. Bcl-2 in the crosshairs: tipping the balance of life and death. *Cell Death Differ*, 13(8):1339–50, 2006.

[393] L. D. Walensky, A. L. Kung, I. Escher, T. J. Malia, S. Barbuto, R. D. Wright, G. Wagner, G. L. Verdine, and S. J. Korsmeyer. Activation of apoptosis in vivo by a hydrocarbon-stapled bh3 helix. *Science*, 305(5689):1466–1470, 2004.

[394] X. C. Wang, R. Katso, R. Butler, A. M. Hanby, R. Poulsom, T. Jones,

D. Sheer, and T. S. Ganesan. H-ryk, an unusual receptor kinase: isolation and analysis of expression in ovarian cancer. *Mol Med*, 2(2):189–203, 1996.

[395] Y. Wang and G. M. Fuller. Phosphorylation and internalization of gp130 occur after il-6 activation of jak2 kinase in hepatocytes. *Mol Biol Cell*, 5(7):819–28, 1994.

[396] L. Ward, G. Howlett, G. Discolo, K. Yasukawa, A. Hammacher, R. Moritz, and R. Simpson. High affinity interleukin-6 receptor is a hexameric complex consisting of two molecules each of interleukin-6, interleukin-6 receptor, and gp- 130. *J. Biol. Chem.*, 269(37):23286–23289, 1994.

[397] L. D. Ward, A. Hammacher, G. Howlett, J. M. Matthews, L. Fabri, R. Moritz, E. Nice, J. Weinstock, and R. Simpson. Influence of interleukin-6 (il-6) dimerization on formation of the high affinity hexameric il-6 receptor complex. *J Biol Chem*, 271(33):20138–44, 1996.

[398] M. F. Ware, D. A. Tice, S. J. Parsons, and D. A. Lauffenburger. Overexpression of cellular src in fibroblasts enhances endocytic internalization of epidermal growth factor receptor. *J Biol Chem*, 272(48):30185–90, 1997.

[399] M. Warmuth, R. Damoiseaux, Y. Liu, D. Fabbro, and N. Gray. Src family kinases: potential targets for the treatment of human cancer and leukemia. *Curr Pharm Des*, 9(25):2043–59, 2003.

[400] M. A. Webster, R. D. Cardiff, and W. J. Muller. Induction of mammary epithelial hyperplasias and mammary tumors in transgenic mice expressing a murine mammary tumor virus/activated c-src fusion gene. *PNAS*, 92(17):7849–7853, 1995.

[401] J. Weissenbach, Y. Chernajovsky, M. Zeevi, L. Shulman, H. Soreq, U. Nir, D. Wallach, M. Perricaudet, P. Tiollais, and M. Revel. Two interferon mrnas in human fibroblasts: in vitro translation and escherichia coli cloning studies. *Proceedings of the National Academy of Sciences of the United States of America*, 77(12):7152–6, 1980.

[402] A. Wettergren, L. Pridal, M. Wojdemann, and J. J. Holst. Amidated and non-amidated glucagon-like peptide-1 (glp-1): non-pancreatic effects (cephalic phase acid secretion) and stability in plasma in humans. *Regul Pept*, 77(1-3):83–7, 1998.

[403] A. Wilde, E. C. Beattie, L. Lem, D. A. Riethof, S. H. Liu, W. C. Mobley, P. Soriano, and F. M. Brodsky. Egf receptor signaling stimulates src kinase phosphorylation of clathrin, influencing clathrin redistribution and egf uptake. *Cell*, 96(5):677–87, 1999.

[404] A. A. Wolf, Y. Fujinaga, and W. I. Lencer. Uncoupling of the cholera toxin-g(m1) ganglioside receptor complex from endocytosis, retrograde golgi trafficking, and downstream signal transduction by depletion of membrane cholesterol. *J Biol Chem*, 277(18):16249–56, 2002.

[405] L. R. Wright, J. B. Rothbard, and P. A. Wender. Guanidinium rich peptide transporters and drug delivery. *Curr Protein Pept Sci*, 4(2):105–24, 2003.

[406] F. Xu, A. Gardner, Y. Tu, P. Michl, D. Prager, and A. Lichtenstein. Multiple myeloma cells are protected against dexamethasone-induced apoptosis by insulin-like growth factors. *Br J Haematol*, 97(2):429–40, 1997.

[407] W. Xu, A. Doshi, M. Lei, M. J. Eck, and S. C. Harrison. Crystal structures of c-src reveal features of its autoinhibitory mechanism. *Mol Cell*, 3(5):629–38, 1999.

[408] W. Xu, S. Harrison, and M. Eck. Three-dimensinonal structure of the tyrosine kinase c-src. *Nature*, 385(13 Feb):595–601, 1997.

[409] Y. Xu, K. W. Harder, N. D. Huntington, M. L. Hibbs, and D. M. Tarlinton. Lyn tyrosine kinase: accentuating the positive and the negative. *Immunity*, 22(1):9–18, 2005.

[410] H. Yamaguchi and W. A. Hendrickson. Structural basis for activation of human lymphocyte kinase lck upon tyrosine phosphorylation. *Nature*, 384(6608):484–9, 1996.

[411] H. Yasui, T. Hideshima, P. G. Richardson, and K. C. Anderson. Novel therapeutic strategies targeting growth factor signalling cascades in multiple myeloma doi:10.1111/j.1365-2141.2005.05860.x. *British Journal of Haematology*, 132(4):385–397, 2006.

[412] H. Yasukawa, H. Misawa, H. Sakamoto, M. Masuhara, A. Sasaki, T. Wakioka, S. Ohtsuka, T. Imaizumi, T. Matsuda, J. N. Ihle, and A. Yoshimura. The jak-binding protein jab inhibits janus tyrosine kinase activity through binding in the activation loop. *Embo J*, 18(5):1309–20, 1999.

[413] S. Yen Chong, Y. C. Lin, J. Czarneski, M. Zhang, F. Coffman, F. Kashanchi, and E. Raveche. Cell cycle effects of il-10 on malignant b-1 cells. *Genes Immun*, 2(5):239–47, 2001.

[414] M. Yokouchi, T. Kondo, A. Sanjay, A. Houghton, A. Yoshimura, S. Komiya, H. Zhang, and R. Baron. Src-catalyzed phosphorylation of c-cbl leads to the interdependent ubiquitination of both proteins. *J. Biol. Chem.*, 276(37):35185–35193, 2001.

[415] N. Yoshio-Hoshino, Y. Adachi, C. Aoki, A. Pereboev, D. T. Curiel, and N. Nishimoto. Establishment of a new interleukin-6 (il-6) receptor inhibitor applicable to the gene therapy for il-6-dependent tumor. *Cancer Res*, 67(3):871–875, 2007.

[416] C. L. Yu, D. J. Meyer, G. S. Campbell, A. C. Larner, C. Carter-Su, J. Schwartz, and R. Jove. Enhanced dna-binding activity of a stat3-related protein in cells transformed by the src oncoprotein. *Science*, 269(5220):81–3, 1995.

[417] H. Yu, J. K. Chen, S. Feng, D. C. Dalgarno, A. W. Brauer, and S. L. Schreiber. Structural basis for the binding of proline-rich peptides to sh3 domains. *Cell*, 76(5):933–45, 1994.

[418] H. Yu, M. K. Rosen, T. B. Shin, C. Seidel-Dugan, J. S. Brugge, and S. L. Schreiber. Solution structure of the sh3 domain of src and identification of its ligand-binding site. *Science*, 258(5088):1665–8, 1992.

[419] R. Zeng, Y. Aoki, M. Yoshida, K. Arai, and S. Watanabe. Stat5b shuttles between cytoplasm and nucleus in a cytokine-dependent and -independent manner. *J Immunol*, 168(9):4567–75, 2002.

[420] F. Zhan, J. Hardin, B. Kordsmeier, K. Bumm, M. Zheng, E. Tian, R. Sanderson, Y. Yang, C. Wilson, M. Zangari, E. Anaissie, C. Morris, F. Muwalla, F. van Rhee, A. Fassas, J. Crowley, G. Tricot, B. Barlogie, and J. Shaughnessy, J. Global gene expression profiling of multiple myeloma, monoclonal gammopathy of undetermined significance, and normal bone marrow plasma cells. *Blood*, 99(5):1745–57, 2002.

[421] J. G. Zhang, A. Farley, S. E. Nicholson, T. A. Willson, L. M. Zugaro, R. J. Simpson, R. L. Moritz, D. Cary, R. Richardson, G. Hausmann, B. J. Kile, S. B. Kent, W. S. Alexander, D. Metcalf, D. J. Hilton, N. A. Nicola, and M. Baca. The conserved socs box motif in suppressors of cytokine signaling binds to elongins b and c and may couple bound proteins to proteasomal degradation. *Proceedings of the National Academy of Sciences of the United States of America*, 96(5):2071–6, 1999.

[422] S. Q. Zhang, W. Yang, M. I. Kontaridis, T. G. Bivona, G. Wen, T. Araki, J. Luo, J. A. Thompson, B. L. Schraven, M. R. Philips, and B. G. Neel. Shp2 regulates src family kinase activity and ras/erk activation by controlling csk recruitment. *Mol Cell*, 13(3):341–55, 2004.

[423] X. M. Zheng, Y. Wang, and C. J. Pallen. Cell transformation and activation of pp60c-src by overexpression of a protein tyrosine phosphatase. *Nature*, 359(6393):336–9, 1992.

[424] S. Zhong, A. T. Macias, and J. MacKerell, A. D. Computational identification of inhibitors of protein-protein interactions. *Curr Top Med Chem*, 7(1):63–82, 2007.

[425] A. H. Zisch, M. S. Kalo, L. D. Chong, and E. B. Pasquale. Complex formation between ephb2 and src requires phosphorylation of tyrosine 611 in the ephb2 juxtamembrane region. *Oncogene*, 16(20):2657–70, 1998.

[426] L. I. Zon. Developmental biology of hematopoiesis. *Blood*, 86(8):2876–91, 1995.

Curriculum Vitae

Personal details	
Name	Amparo Hausherr-Bohn
Date of birth	20. August 1975
Place of birth	Wiesbaden, Germany

Scientific education	
11/1997-08/2002	Biochemistry, University of Regensburg, Germany
04/1997-10/1997	Chemistry, Johnann Wolfgang Goethe University Frankfurt (Main), Germany

Research experience	
06/2006- present	Research Fellow: *"Target Identification and Characterisation of Lipopeptides with Anti-Myeloma Activities*; HelmholtzZentrum München, Medical Clinic I, University of Cologne, Germany; Prof. Dr. M. Hallek, Dr. G. Krause and PD. Dr. Irmela Jeremias
01/2003-06/2007	PhD thesis: *"Cellular and Molecular Characterisation of Novel Lipopeptides with Anti-Myeloma Activities"*; HelmholtzZentrum München, Germany; Prof. Dr. M. Hallek
11/2001-08/2002	Diploma thesis: *"Identification and Characterization of the Promotorregion of Chlamyopsin-4 from Chlamydomonas reinhardtii"*; University of Regensburg, Regensburg, Germany; Prof. Dr. P. Hegemann
08/2001-10/2001	Research assistant: *Purification of codon adapted Renilla Luciferase from E. Coli.*; University of Regensburg, Germany; Prof. Dr. P. Hegemann, Dr. A. Eichler-Stahlberg
08/2000-06/2001	Research assistant: *Role of Phosphodiesterases in the kidney of mice and rats*; University of Regensburg, Germany; Prof. Dr. A. Kurtz, Dr. P. Sandner

Publications and Patents

Journal papers

The role of Src kinases in hematopoietic malignancies, Krause, G., Hausherr-Bohn, A., Veldurthy A., Patz, M. and Hallek M., manuscript in preparation.

Inhibition of IL-6-dependent proliferation of myeloma cells by an acidic peptide blocking the association of gp130 and the Src family kinase Hck. Amparo Hausherr, Rosario Tavares, Joachim Ellwart Christian Mikisch, Axel Obermeier, Michael Schäffer, Michael Hallek, Guenter F. Krause, Oncogene, 26 (34):4987-98,2007.

Monitoring dynamic expression of nuclear genes in Chlamydomonas reinhardtii by using a synthetic luciferase reporter gene. Fuhrmann M, Hausherr A, Ferbitz L, Schodl T, Heitzer M, Hegemann P., Plant Mol Biol., 55(6):869-81, 2004.

Conference papers

Interleukin-6-induced Activities of the Src Family Kinases Hck, Lyn and Fyn in Myeloma Cells is Blocked by an Acidic Peptide. A. Hausherr, R. Tavares, M. Hallek and G.F. Krause, P-122, International Meeting on Targeting the Kinome, Basel, Switzerland, 2006.

An Acidic Peptide Inhibits the Interleukin-6-Induced Activities of the Src Family Kinases Hck, Lyn and Fyn in Myeloma Cells. Amparo Hausherr, Rosario Tavares, Michael Hallek, Guenter F. Krause, Blood 106 (11), [2480], 2005.

The Inhibition of IL-6-Induced Proliferation of Myeloma Cells by an Acidic Peptide Derived form gp130 Depends on the Src-Family-Kinase (SFK) Pathway. A. Hausherr, R. Tavares, M.Schaeffer, M. Hallek and G. Krause, P-73, Dubrovnik Signaling Conference, Croatia, 2004.

IL6-Induced Proliferation of Myeloma Cells Is Inhibited by an Acidic Peptide Derived from the Src-Family Kinase (SFK) Activating Domain of gp130. Amparo Hausherr, Rosario Tavares, Martina Bamberger, Michael Schaeffer, Guenter F. Krause, Michael J. Hallek, Blood 101 (11), p 135, [464], 2003.

Bioluminescence Resonance Energy Transfer as a Tool to Analyze the Interaction of IL-6- receptor and Hck. Hausherr A., Tavares, R., Krause G. and Hallek M., EMBO/EMBL Minisymposium on Modern Methods in Molecular Biology, Heidelberg, Germany, 2003.

Signaling in B-cell Neoplasias A. Hausherr, M. Bamberger, R. Tavares, G. Krause, M. Hallek, CCG-Symposium, GSF, Munich, 2003.

Phosphodiesterase 5 (PDE 5) expression and regulation in the kidney of Dahl rat. Sandner P., Castrop H., Vitzthum H., Hausherr A., Jensen B. L., and Kurtz A. Pflügers Arch-EuroJPhysiol 441, 8, 2001.

Patent

Peptides for Treating Multiple Myeloma, Hausherr-Bohn, A and Krause, G. and Hallek, M., Patent No. 2008113597, 2008.